Enhancing Performance of Electricity Networks through Application of Demand Side Response and Storage Technologies

A thesis submitted to

Imperial College London

For the degree of Doctor of Philosophy

by

Vladimir Stanojević

Department of Electrical and Electronic Engineering

Imperial College London

October 2012

Declaration

This is to certify that:

1. The material contained within this thesis is my own work.

2. No part of the work referred to in this thesis has been presented in support of an application for another degree or qualification in this or any other University.

3. Other work is appropriately referenced.

4. This thesis is less than 100,000 words in length excluding references and any appendices.

Vladimir Stanojević

Abstract

It is broadly trusted that effective scheduling of flexible demand and energy storage operation will offer opportunities for reduced investment in transmission and distribution assets together with the associated lower environmental footprint and avoidance of long delays in connecting renewable generation.

Expected demand migration from transport and heat sectors in few next decades is going to give additional stress to the electricity networks as this load is characterized with relatively low diversity factors restricting the amount of demand growth that can be accommodated into existing networks.

The potential benefits of using Demand Side Response (DSR) and Storage technologies for network applications have not been fully explored due to a lack of rigorous methodology for quantification of the effects of these technologies on network operation and development.

In this context, this work focuses on the investigation of the potential benefits of utilization of DSR, Storage and Electric Vehicles (EV) as potential means for network congestion management and for maximizing the system capability to employ renewable energy sources.

To this purpose, novel methodologies are developed based on a multi-period Optimal Power Flow (OPF), where DSR, Storage and EV are modelled as a part of the optimisation constraints. The proposed optimisation methodologies and techniques are applied to estimate a magnitude of order of potential value of DSR, Storage and EV for alternative development of the electricity systems. Without loss of generality, DSR principle explained is based on a batch of wet appliances (composed by dishwashers, washing machines, and tumble dryers). The benefits are evaluated by comparing scenarios without and with these enabling technologies.

The expected outcome of the research is to identify trends and characteristic conditions in which the enabling technologies are likely to have a high value, and also to determine the key driving factors for the value of these technologies in the context of releasing latent network capacity.

Contents

LIST OF FIGURES 7
LIST OF TABLES 10
LIST OF SYMBOLS 16

CHAPTER 1. INTRODUCTION 21

1.1 TRANSMISSION NETWORK ISSUES ASSOCIATED WITH INTEGRATING NEW FORMS OF GENERATION AND DEMAND 22
1.2 DISTRIBUTION NETWORK ISSUES ASSOCIATED WITH INTEGRATING NEW FORMS OF GENERATION AND DEMAND 23
1.3 DEMAND SIDE RESPONSE 24
1.4 ENERGY STORAGE 28
1.5 ELECTRIC VEHICLES 30
1.6 EXPERIENCE 32
1.7 MOTIVATION FOR THESIS 34
1.7.1 Challenges 35
1.7.2 Objective 36
1.7.3 Research questions 37
1.7.4 Contributions 39
1.7.5 Thesis Structure 40

CHAPTER 2. SMART APPLIANCES AND SHIFTING ALGORITHM 41

2.1 INTRODUCTION 41
2.2 CONSUMER ACCEPTANCE 43
2.3 SHIFTING DEVICES DATA 44
2.4 SHIFTING ALGORITHM 46
2.4.1 Input data to the algorithm 47
2.4.2 Control possibilities pre-processing 49
2.4.3 Generating a list of control actions 49
2.4.4 Control actions applications 50
2.5 MODELLING OF SMART APPLIANCES 50
2.6 SUMMARY 52

CHAPTER 3. VALUE OF STORAGE AND SMART APPLIANCES FOR NETWORK CONGESTION MANAGEMENT IN TRANSMISSION NETWORKS 55

3.1 INTRODUCTION 55
3.2 PROPOSED LINEAR MULTI-PERIOD OPTIMAL POWER FLOW 56
3.2.1 Power Balance Constraints 56
3.2.2 Network constraints 57
3.2.3 Generator constraints 57
3.2.4 Storage Model – Optimal Storage Capacity Allocation 58
3.3 METRICS FOR DSR AND STORAGE VALUE EVALUATION 59
3.3.1 Reduction in the cost of operation 59
3.3.2 Reduction in the wind curtailed in the system 59
3.3.3 Line utilization and Line Loading Duration Curve 59
3.3.4 Value of Smart Appliances and Storage 60
3.4 CASE STUDY 61
3.4.1 Test System 61
3.4.2 Reference case results 63
3.4.3 DSR Results 64
Increase of wind penetration 65

Increase of load 71
Impact of generation flexibility 75
3.4.4 Storage Testing on a DC Model 80
Changes in wind penetration 80
Increase of load 88
Impact of generation flexibility 91
3.5 CONCLUSIONS 93

CHAPTER 4. VALUE OF STORAGE AND SMART APPLIANCES FOR NETWORK CONGESTION MANAGEMENT IN DISTRIBUTION NETWORKS 97

4.1 INTRODUCTION 97
4.2 NON-LINEAR MULTI-PERIOD OPTIMAL POWER FLOW CONSIDERING STORAGE AND DSR 98
4.2.1 Power Balance Constraints 99
4.2.2 Demand Side Response Constrains 101
4.2.3 Network constraints 101
4.2.4 Generator constraints 103
4.3 STORAGE MODEL 104
4.4 SOLUTION METHOD 106
4.5 CASE STUDY 1 107
4.5.1 Test system description – 38 bus radial distribution network 107
4.5.2 Reference Case Results 108
4.5.3 DSR Results 112
4.5.4 Storage Results 121
Specified storage attached at the most distant bus 121
Optimal Storage size and location 125
4.5.5 Economic benefits of Demand Side Response and Energy Storage 127
4.5.6 Network losses reduction with DSR and Storage 129
4.6 CASE STUDY 2 137
4.6.1 Analyzed test system and problem description 137
4.6.2 Solutions to the problem 142
4.7 CONCLUSIONS 146

CHAPTER 5. ELECTRICAL VEHICLES IN ELECTRICITY NETWORKS 149

5.1 INTRODUCTION 149
5.2 BASIC UK TRANSPORT CHARACTERISTICS 150
5.2.1 Number of journeys distances, and start/end times 153
5.3 DISTANCE BANDS AGGREGATION 157
5.3.1 Combinations of two journeys a day 158
5.4 CHARGING STRATEGIES 163
5.4.1 Charging after the first journey finished 163
5.4.2 Charging after the second journey finished 165
5.4.3 Charging after each journey 165
5.4.4 Charging all available time with minimum power 167
5.4.5 Optimal charging 168
5.4.6 Proposed Optimization Problem Formulation 169
5.5 CASE STUDY 171
5.6 CONCLUSION 182

CHAPTER 6. GENERAL CONCLUSIONS AND DISCUSSIONS 185

6.1 ENHANCEMENT OF TRANSMISSION NETWORK PERFORMANCE 185

6.2 ENHANCEMENT OF DISTRIBUTION NETWORK PERFORMANCE 187
6.3 ELECTRIC VEHICLES 189
6.4 FUTURE WORK 190
LITERATURE 193

APPENDIX 1. NODE POWER INJECTIONS 201

APPENDIX 2. DIVERSIFIED CURVE DISAGGREGATING 202

APPENDIX 3. 16 BUS GB TRANSMISSION SYSTEM 203

APPENDIX 4. DISTRIBUTION NETWORKS 225

APPENDIX 5. ELECTRIC VEHICLES 230

List of Figures

Figure 1-1: Typical power range versus discharge times for different storage technologies 29
Figure 1-2: Estimation of worldwide EV and PHEV sales 31
Figure 2-1: Domestic appliances' demand in the UK 42
Figure 2-2: Diversified profiles and operation cycles for washing machine, dish washer and tumble dryer 45
Figure 2-3: Operation cycle for a washing machine with tumble dryer 46
Figure 2-4: Schematic diagram of the shifting algorithm 47
Figure 2-5: Estimated number of appliances vs. starting time 48
Figure 3-1: GB transmission system boundaries (a) and the sixteen bus-bar diagram (b) 62
Figure 3-2: Distribution of wind and total generation capacity (a) and distribution of load (b) on network buses 63
Figure 3-3: Effect of DSR on reduction in wind curtailment 66
Figure 3-4: Effect of DSR on reduction in generation costs 66
Figure 3-5: Effects of DSR on generation adjustment (per technology) 67
Figure 3-6: Reduction in production cost per technology 68
Figure 3-7: DSR effect on reduction in CO_2 emissions 69
Figure 3-8: Average capitalized value of DSR per appliance 70
Figure 3-9: Capitalized value per type of device 70
Figure 3-10: Distribution of wind curtailment on network buses 72
Figure 3-11: Effect of DSR on reduction in wind curtailment as load increases 72
Figure 3-12: DSR impact on Reduction in operation cost as load increases 73
Figure 3-13: DSR impact on reductions in CO_2 emissions vs. load growth 73
Figure 3-14: Production adjustment per generation type, for normal DSR flexibility, 100% DSR penetration 74
Figure 3-15: DSR activity for load growth 74
Figure 3-16: Capitalized value of DSR vs. load growth 75
Figure 3-17: Wind curtailment vs. generation flexibility 76
Figure 3-18: Effect of DSR on reduction in wind curtailment vs. generation flexibility 76
Figure 3-19: Reduction in generation cost vs. generation flexibility 77
Figure 3-20: DSR impact on reduction in the slope of load changes 78
Figure 3-21: Impact of DSR on reduction in CO_2 emissions vs. generation flexibility 79
Figure 3-22: DSR activity vs. generation flexibility 79
Figure 3-23: Capitalized value of DSR vs. generation flexibility 80
Figure 3-24: Effect of Storage on reduction in wind curtailment 81
Figure 3-25: Effect of Storage on reduction in generation costs 81
Figure 3-26: Impact of storage on generation adjustment per technology type 82
Figure 3-27: Storage effect on reduction in CO_2 emissions 83
Figure 3-28: Distribution of storage capacities through network nodes 83
Figure 3-29: Impact of Storage on Line loading factors 84
Figure 3-30: Capitalized value of storage 85
Figure 3-31: Time evaluation of load with and without storage and available wind at the system level 86

Figure 3-32: Storage activity at Bus 1 (20% wind penetration, storage 5GW, 80% efficiency): storage activity follows wind 87
Figure 3-33: Storage activity at Bus 16 87
Figure 3-34: Effect of Storage on reductions in wind curtailment as load increases, wind penetration 30% 88
Figure 3-35: Storage impact on reduction in generation cost as load increases, wind penetration 30% 89
Figure 3-36: Storage impact on reduction in CO_2 emissions as load grows 89
Figure 3-37: Impact of storage on generation adjustment per technology type as load grows 90
Figure 3-38: Capitalized value of Storage vs. load growth 91
Figure 3-39: Effect of Storage on reduction in wind curtailment vs. generation flexibility 91
Figure 3-40: Reduction in generation cost vs. generation flexibility 92
Figure 3-41: Impact of Storage on reduction in CO_2 emissions vs. generation flexibility 92
Figure 3-42: Capitalized value of Storage vs. generation flexibility 93
Figure 4-1: SLP speed of convergence: number of unconverged variables vs. time 107
Figure 4-2: Distribution network 38 bus test system 107
Figure 4-3: Minimal voltage throughout network vs. load growth 109
Figure 4-4: As load increases, under-voltages propagate towards supply point 110
Figure 4-5: Congested lines caused by load growth 111
Figure 4-6: Under-voltages propagation towards supply point when DSR is applied 113
Figure 4-7: Congested lines caused by load growth in case when DSR is applied 114
Figure 4-8: a) voltage in Bus 38; b) apparent power flow through line Bus 1 – Bus 2; c) DSR reduction and payback at system level 116
Figure 4-9: a) DSR activity; b) number of shifted devices 118
Figure 4-10: DSR scheduling of WM1h (a) and DW (b) for the whole network 120
Figure 4-11: Under-voltages propagation towards supply point in case when Storage 200kW, 1.2MWh is installed in Bus 38 122
Figure 4-12: Congested lines and reinforcement schedule caused by load growth in case when given storage is installed in the most distant bus 123
Figure 4-13: voltage in the most distant bus (Bus 38) (a); apparent power flow through the most congested line (Bus 1 – Bus 2) (b); Storage activity (c) 124
Figure 4-14: Congested lines and reinforcement schedule in case of optimal storage location and size 126
Figure 4-15: Voltage in Bus 38: voltage stays above low limit only if Storage is installed at Bus 29 .. 127
Figure 4-16: Dependence of total network losses (middle chart) and voltage (lower chart) on system load (upper chart) 131
Figure 4-17: Net DSR activity 132
Figure 4-18: Total losses in the network with and without DSR when: there is no increase in load (upper chart) and load increases 20% (lower chart) 132
Figure 4-19: Voltage in Bus 38 with and without DSR, for no load increase and for load increase 20% 133
Figure 4-20: Storage (83% efficiency) activity (a); total losses in the network (b) and voltage in Bus 38 (c) 134

Figure 4-21: Storage (100% efficiency) activity (a); total losses in the network (b) and voltage in Bus 38 (c) 136
Figure 4-22: Schematic diagram of Leighton Buzzard 33/11 kV/kV substation 138
Figure 4-23: Loading of transformers T1 and T2 and total load 139
Figure 4-24: Network voltage profile during peak in normal working conditions (12th January 2011 at 18.00) 139
Figure 4-25: Apparent power through line Bus 2 – Bus 3 during outage of Branch 2 140
Figure 4-26: Network voltage profile during peak, in case of Branch 2 outage 141
Figure 4-27: Apparent power through line Bus 2 – Bus 3 during outage of Branch 2 with and without storage (upper chart); lower chart shows storage activities 143
Figure 4-28: Network voltage profile during peak, in case of Branch 2 outage with support of storage 144
Figure 4-29: Apparent power through line Bus 2– Bus 3 during outage of Branch 2 with and without storage (upper chart); storage active power charging and discharging (middle chart); and reactive power compensation (lower chart) 145
Figure 4-30: Network voltage profiles during peak time, in case of Branch 2 outage with storage and reactive power compensation 146
Figure 5-1: Daily journey profiles 153
Figure 5-2: Cumulative percentage of number of journeys and total (maximum) daily mileage 154
Figure 5-3: Distribution of aggregated daily distance (upper band limit) vs. distance range 155
Figure 5-4: Distribution of number of journeys vs. distance range 155
Figure 5-5: Probability of cars being off-road during the day 156
Figure 5-6: Allowed combination of journeys 159
Figure 5-7: An example of eligible combinations of two short journeys 160
Figure 5-8: Charging after 1st journey 163
Figure 5-9: Charging after 2nd journey 165
Figure 5-10: Charging after each journey 166
Figure 5-11: Charging all the standing time with minimum power 167
Figure 5-12: Piece-wise linearization of quadratic generation cost curve 170
Figure 5-13: IEEE 30 bus test system 172
Figure 5-14: Total network load with different charging strategies 175
Figure 5-15: Optimal charging – load is almost flat, and peak is increased about 15% comparing to base load 176
Figure 5-16: Estimated number of vehicles that could not be charged for strategy “charging after first journey” 178
Figure 5-17: Total load (base load + EV) follows the wind (three different days with different wind profiles) 179
Figure 5-18: Wind utilization and total generation by technology 181
Figure 5-19: Complementarities of charging: selected buses (upper chart) and all the busses (lower chart) 182

List of figures in appendices:

Figure A. 2-1: Matrix representation of the linear system equations (1) 202

Figure A. 3-1: Effect of DSR flexibility on reduction in wind curtailment 204
Figure A. 3-2: Effect of DSR flexibility on reduction in generation costs 204
Figure A. 3-3: Effect of DSR flexibility on Generation adjustment 205
Figure A. 3-4: Effect of DSR flexibility on reduction in CO_2 emissions 205
Figure A. 3-5: Effect of DSR flexibility on average capitalized value per appliance 206
Figure A. 3-6: Effect of DSR flexibility on capitalized value per type of device 206
Figure A. 3-7: Effect of DSR flexibility on reduction in wind curtailment as load increases 207
Figure A. 3-8: Effect of DSR flexibility on reduction in generation cost as load increases 207
Figure A. 3-9: Effect of DSR flexibility on reduction in CO_2 emissions as load grows 208
Figure A. 3-10: Effect of DSR flexibility on DSR activity as load grows 208
Figure A. 3-11: Effect of DSR flexibility on average capitalized value as load grows 209
Figure A. 3-12: Effect of DSR flexibility on reductions in CO_2 emissions vs. generation flexibility 209
Figure A. 3-13: Effect of DSR flexibility on DSR activity vs. generation flexibility 210
Figure A. 3-14: Effect of DSR flexibility on average capitalized value of DSR vs. generation flexibility 210
Figure A. 3-15: Effect of Storage efficiency on reduction in wind curtailment 211
Figure A. 3-16: Effect of Storage efficiency on reduction in generation costs 211
Figure A. 3-17: Effect of Storage efficiency on reduction in CO_2 emissions 212
Figure A. 3-18: Effect of Storage efficiency on capitalized value of storage 212
Figure A. 3-19: Effect of Storage efficiency on reduction in wind curtailment as load increases 213
Figure A. 3-20: Effect of Storage efficiency on reduction in generation cost as load increases 214
Figure A. 3-21: Effect of Storage efficiency on reduction in CO_2 emissions as load grows 214
Figure A. 3-22: Effect of Storage efficiency on capitalized value of Storage vs. load growth 215
Figure A. 3-23: Effect of Storage efficiency on reduction in CO_2 emissions vs. generation flexibility 215
Figure A. 3-24: Effect of Storage efficiency on capitalized value of Storage vs. generation flexibility 216
Figure A. 3-25: DSR activity 218
Figure A. 3-26: Snapshots during high wind (hour 6124), wind penetration 20%, base case 220
Figure A. 3-27: Snapshots during high wind (hour 6124), with total installed storage capacity of 5GW, 80% efficiency, wind penetration 20% 222
Figure A. 3-28: Snapshots during peak demand and lower wind (hour 5923), with total installed storage capacity of 5GW, 80% efficiency, wind penetration 20% 224
Figure A. 5-1: Estimated number of vehicles that could not be charged for strategy “charging after second journey” 236

List of tables

Table 2-1: Smart appliances acceptance survey 43
Table 2-2: Summary of device types 44
Table 3-1: Reference case results vs. wind penetration 64
Table 3-2: Smart appliances parameters variations 65
Table 3-3: Wind curtailment for different levels of load 71
Table 3-4: Considered generation flexibility levels 75
Table 3-5: Considered values of total storage capacity and storage efficiency 80
Table 4-1: Main Network Data 108

Table 4-2: Line thermal capacity constraints violation vs. load growth 110
Table 4-3: Summary of device types 112
Table 4-4: Line thermal capacity constraints violation vs. load growth 114
Table 4-5: Details of shifted devices 117
Table 4-6: Storage characteristics 121
Table 4-7: Line thermal capacity constraints violation vs. load growth 122
Table 4-8: Line thermal capacity constraints violation vs. load growth 126
Table 4-9: Comparison of economical benefits of DSR and Storage 128
Table 4-10: Total network losses are reduced due to DSR 133
Table 4-11: Total network losses are reduced due to storage 135
Table 4-12: Total network losses are reduced due to storage 137
Table 4-13: Apparent power flows and active and reactive power losses in the network lines during peak, 12th January 2011 at 18.00 in case of Branch 2 outage 141
Table 4-14: Required energy storage parameters for power flow control 142
Table 4-15: Required energy storage parameters for power flow control with reactive compensation 144
Table 5-1: Sample of original data from NTS database 150
Table 5-2: Daily numbers of journeys and distances (obtained from Table 5-1) 151
Table 5-3: Total daily number of journeys and associated distances (for all categories of journeys) 152
Table 5-4: Basic statistics on the UK transportation (daily) 152
Table 5-5: Number of journeys (in thousands) for given start and end times 153
Table 5-6: Distance band clusters and equivalent distances 157
Table 5-7: Number of short journeys defined by the start and end times (in 1,000) 158
Table 5-8: Data required for optimization 159
Table 5-9: Journey types definition 161
Table 5-10: System data 171
Table 5-11: Generator data 172
Table 5-12: System peak for different charging strategies 176
Table 5-13: Summary of replacement costs 177
Table 5-14: Maximum number of vehicles that could be connected to the network 178

List of tables in appendices:

Table A. 3-1: Distribution of generation installed capacity on network buses and generation types 203
Table A. 3-2: Distribution of generation installed capacity on network buses and generation types 216
Table A. 4-1: Load time series data for case of load growth 0%, 10% and 20% 225
Table A. 4-2: Network branch data and power flows through the branches during peak hour for case 0% load growth 226
Table A. 4-3: Load distribution among buses (in percent) and minimal voltages obtained during peak hour for case 0% load growth 227
Table A. 4-4: Circuit data for Leighton Buzzard Substation network 228
Table A. 4-5: Transformer data for Leighton Buzzard Substation 228
Table A. 4-6: Snapshot of power flows during peak, 12th January 2011 at 18.00 in case of Branch 2 outage (all the load supplied from Branch 1) 229

Table A. 5-1: Daily driven minimal distances (in 1,000 km) for given start and end times 230
Table A. 5-2: Energy (in MWh) required for the minimum driven distances 230
Table A. 5-3: Daily driven maximal distances (in 1,000 km) for given start and end times 230
Table A. 5-4: Energy (in MWh) required for the maximum driven distances 231
Table A. 5-5: Daily driven short distances (≤ 15 miles) defined with start time and end time (in 1,000 km) 231
Table A. 5-6: Daily driven medium distances (15 ÷ 50 miles) defined with start time and end time (in 1,000 km) 231
Table A. 5-7: Daily driven long distances (50+ miles) defined with start time and end time (in 1,000 km) 232
Table A. 5-8: Energy required for short distances (in MWh) 232
Table A. 5-9: Energy required for medium distances (in MWh) 232
Table A. 5-10: Energy required for long distances (in MWh) 233
Table A. 5-11: Number of medium journeys defined by the start and end times (in 1,000) 233
Table A. 5-12: Number of long journeys defined by the start and end times (in 1,000) 233
Table A. 5-13: An example of data ready for optimization 234
Table A. 5-14: Maximal flows through the lines 235

List of Published/Submitted Technical Papers

1. V. Silva, V. Stanojevic, D. Pudjianto, G. Strbac: Benefits of Storage and DSM in Transmission Congestion Management in Systems with High Wind Penetration, 7th International Workshop on Large-Scale Integration of Wind Power into Power Systems as well as on Transmission Networks for Offshore Wind Farms, May 2008, Madrid, Spain.

2. V. Stanojevic, V.Silva, D.Pudjianto, G.Strbac, P. Lang, D.Macleman: Application of storage and Demand Side Management to optimise existing network capacity, 20th International Conference and Exhibition on Electricity Distribution (CIRED), pp.1-4, Prague, June 2009.

3. V. Silva, V. Stanojevic, M. Aunedi, D. Pudjianto and G. Strbac: Smart domestic appliances as enabling technology for demand side integration: modelling, value and drivers, ed. M. Pollit, Cambridge University Press, Cambridge, 2010.

4. D. Pudjianto, C.K. Gan, V. Stanojevic, M. Aunedi, P. Djapic, G. Strbac: Value of integrating Distributed Energy Resources in the UK electricity system, Power and Energy Society (PES) IEEE General Meeting, pp.1-6, Minnesota, July 2010

5. C.K. Gan, M. Aunedi, V. Stanojevic, G. Strbac, D. Openshaw: Investigation of the Impact of Electrifying Transport and Heat Sectors on the UK Distribution Networks, 21st International Conference on Electricity Distribution (CIRED), Germany, June 2011

6. D. Papadaskalopoulos, P. Mancarella, M. Aunedi, V. Stanojevic, G. Strbac: Decentralized Participation of Flexible Demand in Electricity Markets Part II: Application with Electric Vehicles and Heat Pump Systems (*submitted for IEEE Transactions on Power Systems*)

Acknowledgements

I would like to thank to my supervisor, Professor Goran Strbac, for giving me the opportunity and providing a guidance throughout this research work and whose help was indispensable.

Special thanks go to my colleagues and administrative personnel in Control and Power Group, who have always been willing to give me all kinds of support.

Finally, my deepest gratitude goes to my family who encouraged and supported me throughout my PhD.

Узносићу те, Боже мој, Царе мој,
И благосиљаћу Име Твоје до века, и у век века.

(Псалам 145)

I will extol you, my God and King,
And bless Your Name forever and ever.

(Psalm 145)

List of Symbols

The main symbols used throughout this report are defined below. Others will be defined as required in the text.

Sets

G	generators
$\mathbf{G_{BUS}}$	generator buses
$\mathbf{NG_b}$	generators connected to bus b
$\mathbf{N_{BUS}}$	network buses
$\mathbf{N_{BR}}$	network branches
T	optimization horizon
$\mathbf{L_{type}}$	types of devices
$\mathbf{L_{BUS}}$	load buses
$\mathbf{N_{PV}}$	Set of PV buses
$\mathbf{NS_g}$	set of segments for generator g cost function linearization
$\mathbf{S_{BUS}}$	buses where storage may be placed

Indices

g	Index of generators
b	Index of buses
t	Index of time periods
k	appliance group identifier
i_S, i_R	Indices of buses connected with branch i
i	Index of branches
I	start time step of Journey 1
J	end time step of Journey 1
K	start time step of Journey 2
L	end time step of Journey 2
T_1	type of Journey 1 (short, medium or long)
T_2	type of Journey 2 (short, medium or long)
s	index of segments for generator cost function linearization

Variables

$P_g(t)$	production of generator g at time step t [MW]

$Pd_b(t)$	active power demand at bus b at time step t [MW]
$P_{bp}^{branch}(t)$	active power flow through branch branch, connecting buses b and p, at time step t [MW]
$\delta_b(t)$	Voltage phase angle at bus b at time step t [rad]
$load_shed_b(t)$	Involuntary loss of active load at bus b at time step t [MW]
$over_slack_b(t)$	Artificial active load at bus b at time step t, introduced to avoid infeasibility in the solution [MW]
$P_b^{EX}(t)$	power exchange from bus b to all incidental buses p at time step t
$Pd_b^{DSR}(t)$	active demand at bus b at time step t after DSR is applied [MW]
$Pd_b^c(t)$	active demand reduction at bus b at time step t due to DSR [MW]
$Pd_b^p(t)$	active demand payback at bus b at time step t due to DSR [MW]
$Q_shed_b(t)$	Involuntary loss of reactive load at bus b at time step t [Mvar]
$Q_b^{EX}(t)$	Reactive power exchange from bus b to all incidental buses at time step t
$Q_{bp}(t)$	Reactive power flow in branch bp at time step t [Mvar]
$Qd_b(t)$	Reactive power demand at bus b at time step t [Mvar]
$Qd_b^{DSR}(t)$	Reactive demand at bus b at time step t after DSR is applied [Mvar]
$Qd_b^c(t)$	Reactive demand reduction at bus b at time step t due to DSR [Mvar]
$Qd_b^p(t)$	Reactive demand payback at bus b at time step t due to DSR [Mvar]
$Q_g(t)$	Reactive power of generator g at time step t [Mvar]
$Qover_slack_b(t)$	Artificial reactive load at bus b at time step t, introduced to avoid infeasibility in the solution [Mvar]
$V_b(t)$	Voltage magnitude at bus b at time step t [V]
X_{ijkb}	number of type k devices at bus b that were originally expected to start their consumption at time step i and after the optimisation are going to start consumption at time step j
$S_b^d(t)$	power discharged by storage at bus b at time step t [MW]
$S_b^c(t)$	power charged by storage at bus b at time step t [MW]
$ES_b(t)$	Energy stored in storage at bus b at time step t [MWh]
$S_{cap}^{\max}$	total installed storage capacity in the system [MW]
a_i	Off-nominal transformer ratio for branch i

$N_{journey}(t)$ number journeys for each hour of the day

$P_{journey}(t)$ probability of a journey

$N_{journey}^{total}$ total number of journeys during a day

$P_{available}(t)$ Probability that there will be no journeys during hour t

N_{I,J,T_1} the number of T_1 type journeys that start at I and finish at J

Ne_{I,J,T_1}^{K,L,T_2} number of eligible journeys of type T_2 lasting between K and L, for a journey of T_1 type journeys that start at I and finish at J

S_e^{I,J,T_1} sum of all eligible journeys for a given Journey 1

N_{I,J,T_1}^{K,L,T_2} number of vehicles that make one journey of type T_1 between I and J, and another journey of type T_2 between K and L

$E1_{I,J,T_1}^{K,L,T_2}$ energy required by vehicles for Journey 1

$E2_{K,L,T_2}^{I,J,T_1}$ energy required by vehicles for Journey 2

E_{I,J,T_1} total energy consumed by all the vehicles making type T_1 journey between time steps I and J

$Pch_{I,J,T_1}^{K,L,T_2}(ct,b)$ Charging power of all vehicles in bus b making Journey 1 of type T_1 between I and J, and Journey 2 of type T_2 between K and L, during charging time

$P_{ch}^{sum}(t,b)$ Total charging power in bus b at hour t

NT_{ch} Duration of charging period for the battery of a vehicle having one journey of type T_1 between hours I and J, and another journey of type T_2 between hours K and L

NT_1 Duration of charging period for journey 1

NT_2 Duration of charging period for journey 2

$C_g(P_g)$ quadratic cost function of generator g

$charge_shed_b(t)$ curtailed charging power

$e_{s,g}$ elbows of the generator's g segment s

$ec_{s,g}$ costs at elbows point s for generator g

$IC_{s,g}$ generator g incremental cost at segment s

NL_g no load cost of generator g

$Pseg_{s,g}$ Power at segment s of generator g [MW]

Constants

T_h	time horizon length [h]
Δt	time resolution used in simulations (h)

Parameters

c_g	generator g production cost [£/MW]
G_i	Conductance of branch i [S]
B_i	Susceptance of branch i [S]
Ψ	Ratio between reactive and real power
$P_{g,min}$	minimal stable generation of generator g [MW]
$Q_{g,\min}$	Minimal reactive output of generator g [Mvar]
$P_{g,max}$	maximal active output of generator g [MW]
$Q_{g,max}$	Maximal reactive output of generator g [Mvar]
$Ramp_g^{up}$	generator ramping-up rate [MW/h]
$Ramp_g^{down}$	generator ramping-down rate [MW/h]
B_{bp}^{branch}	reciprocal of reactance of branch branch, connecting buses b and p [p.u.]
B_{bp}	element of system matrix **B** at row b and column p [p.u.]
C_{bp}^{branch}	capacity limit of branch branch connecting buses b and p [MW]
S_i^{lim}	Thermal capacity limit of branch i [MVA]
V_{max}	Upper limit for bus voltages [V]
V_{min}	Lower limit for bus voltages [V]
D_{ikb}	number of type k devices available for control at bus b at time step i
$DELAY_k^{MAX}$	max. allowed time for shifting device of type k [h]
d_k	operating cycle length for type k device [h]
p_{ik}	consumption pattern for type k device [W]
s_{ik}	first possible time step where the appliance of type k, starting consumption at time step i, can be shifted to
w_{ik}	number of successive time steps (starting from s_{ik}) which are also possible connection times
c_{LS}	cost of involuntary load shed [£/MW]
c_{OS}	cost of overslack [£/MW]

P_{ch}^{max}	charger's rating power [kW]
η_{ch}	charging cycle efficiency [%]
$a_{1,g}$	no-load cost of generator g [£]
$a_{2,g}$	linear cost coefficient of generator g [£/MW]
$a_{3,g}$	quadratic cost coefficient of generator g [£/MW^2]
$N_{s,g}$	number of segments for generator g cost function linearization

Storage parameters

S_b^{max}	power rating of storage attached at bus b [MW]
c_{sto}^{energy}	cost of installing 1MWh of storage energy capacity [£/MWh]
c_{sto}^{power}	cost of installing 1MW of storage power [£/MW]
ES_b^{max}	maximal energy capacity of storage attached at bus b [MWh]
ES_b^{FIN}	minimal energy in storage attached at bus b at a specific hour of the day [MWh]
η_b	efficiency factor of storage attached at bus b

Metrics

R_{oc}	Reduction in operation costs [£]
R_{wc}	Reduction in wind curtailed [MWh/year]
LF_{branch}	Load factor for branch branch

CHAPTER 1. Introduction

Significant amounts of renewable energy are planned to be connected to power systems world-wide in the near future. This is driven predominantly by environmental commitment. At present, wind power is the main commercially accessible renewable energy resource, and it is envisaged to dominate in the short term, out to 2020. The other sources of renewable energy are expected to contribute more in the medium and long term.

In the UK, according to the Renewable Energy Strategy [1], it is expected that up to 30% of electricity demand will be supplied from renewable generation by 2020 (compared to the 2012 levels of 6.5%). The electricity sector need to be almost completely decarbonised by 2030, in order to meet the target proposed by the UK's Committee on Climate Change with the objective of reducing Greenhouse Gas (GHG) emissions by at least 80% by 2050 relative to 1990 levels. Such a GHG reduction requires not only decarbonisation of electricity but also transport and heat which are likely to require extensive electrification.

Under such conditions, it is expected that operational problems will rise from the following reasons:

- stochastic nature of wind generation,
- geographical location of the wind resource and its distance from load centres
- load growth

One of the main problems regarding stochastic output of wind is that it requires additional generation capacity commitment to maintain security of supply and provide enough reserve. A larger amount of intermittent renewable generation and relatively inflexible nuclear generation in a future decarbonised electricity system is expected. If uncontrollable demand is to be supplied from such a generation mix, then the task of balancing demand and supply will become significantly more challenging. However, this research will not address the balancing problems related to renewable sources.

The position of the resource and their remoteness relative to demand centres, as well as load growth problems are in relation with requirements imposed on the transmission and distribution network infrastructure. The key purpose of a network is to provide reliable and efficient transport of electricity from generation to demand. Therefore, the location of generation relative to demand as well as the amount of power to be transported, are the most important factors driving the design and operation of electricity networks.

The problem will be aggravated as heat and transport is decarbonised. For example, in [2] it was demonstrated that in the UK, the incorporation of Electric Vehicles (EV) and Heat Pumps (HP) could increase electric energy consumption by about 50%, while the system peak would increase by almost twice. This disproportional increase of demand peaks, comparing to the growth in energy demand, will lead to further degradation of the utilisation of generation and network infrastructure.

Thus, the integration of alternative energy sources and migration of new demand to the existing power system will add a significant stress to both transmission and distribution networks. For this reason, the questions regarding operation and design of the transmission and distribution networks in a cost effective manner need to be explored.

1.1 Transmission Network issues associated with integrating new forms of generation and demand

Transmission networks will be significantly affected if the massive onshore and offshore wind resources are to be exploited. The increased penetration of wind energy will displace fossil fuel plants. This will cause control and operational issues in the transmission network:

- Control issues: The flows of power through the present transmission networks are controlled mostly by large generators, i.e. by varying their output. There are two factors that enable this kind of control: first, the impedance of the network is determined by the electrical characteristics of the circuits used; and second, the transmission network operates with fixed topology. However, with the displacement of large generation units, a more significantly active role in the network control will be required from demand side.
- Operational issues: Large scale intermittent generation is mostly available at sites placed remotely from load centres. In most systems, transmission networks have not been designed for this additional transport of energy from the areas where the new wind plants are to be connected, to the demand centres, which are mainly large cities or industrial areas. Moreover, existing fossil fuel plants are usually located closer to large demand centres. This will cause further stress to the transmission system and produce network congestion problems, which will limit the integration of the expected amount of wind power.

For these reasons, solutions to mitigate the congestion in transmission networks need to be explored. Matevosyan in [3] summarizes the following four options to lessen the problem:

- transmission network reinforcement,
- utilise dynamic rating of the available transmission capacity,
- wind-hydro generation coordination and

- wind curtailment.

The network capacity reinforcement is a costly and time consuming solution and is often environmentally and socially constrained. Also, due to the low load factor of wind generation, a MW per MW based transmission network reinforcement will inevitably lead to low utilization of transmission capacity. Dynamic transmission rating methods, which allow short-time overloading of transmission lines during high wind, are proposed in [4], [5] and [6]. This solution may postpone investment in new transmission capacities, but for high wind periods it will lead to wind energy curtailment. Another solution to mitigate transmission congestion problems is through coordination of wind and hydro generation, as proposed in [7]. This solution leads to a significant reduction in wind curtailment and is most beneficial economically and environmentally but it is confined to the system with significant hydro power. Wind curtailment during the periods of high wind when congestion in transmission capacity occurs is also explored as a trade-off to investments in transmission capacity [8]. However, this wastes wind energy which has low running costs and is carbon-free and so this solution should be considered as the last resort.

In addition to the options discussed above, energy storage and Demand Side Response (DSR) can also have a key role in providing additional network capacity to mitigate transmission congestion and to increase the utilisation of transmission circuits, especially in systems such as the GB, where the connection of wind generation is expected to be in the north (Scotland) or off-shore, whilst large demand centres are located in the south and central (England). This option will be investigated in the work presented.

1.2 Distribution Network issues associated with integrating new forms of generation and demand

The historic function of distribution networks in a power system is centred on the fundamental requirements of providing efficient transport of electrical energy from a transmission grid to end customers, whilst maintaining the required standards of security and quality of supply. The network is designed in such a way that sufficient network capacity is available to deal with planned extreme demand conditions. Conventionally, operation of distribution network requires no real time management, as the control problem is resolved through appropriate investment at the network planning stage. This historical passive operation philosophy has now been challenged particularly with the introduction of Distributed Generation (DG). This is because the passive network operation considerably limits the amount of DG that can be connected and it also restricts the amount of demand growth that can be accommodated into the existing networks. Hence, if the passive

operation philosophy is to be maintained, significant network reinforcement will be necessary to accommodate DG and load growth.

To respond to these challenges, efficient integration of DG will require distribution network operators to change their approach to network operation, protection and control from passive to active in order to enhance security of operation, to improve utilisation of the existing network assets and to minimise the need for network reinforcements [9]. Adopting an active approach to distribution network operation and overcoming the obsolete fit and forget paradigm is suggested in [10]. In that work the integration of demand side response with DG into network operation is identified as an important step to the active approach.

Active management means real time active network operation for optimising the utilisation of the existing network capacity, deferring network reinforcement, enhancing security of supply and improving power quality. It can be realized through simultaneous utilization of classical means for network control, such as on-load tap changing transformers, voltage regulators, reactive compensators, etc., optimal network topology, and non-networks solutions, e.g. controllable types of DG. In addition, a spectrum of enabling technologies such as storage and DSR can be used to provide distribution network support services, such as voltage and load flow control. This thesis will describe this approach.

1.3 Demand Side Response

The idea of load management and the potential benefits it could bring to the system operator has been known for many years and utilities have tried to influence the way consumers use electricity. In general, there are three main load management strategies:

- Indirect or conventional load control: the end users themselves take the actions to modify their load profile, based on an agreement (incentive or obligatory) with the utility. The system operator does not have capability to directly control customers' load. Conventional forms of load management almost always specify the number of load reductions that may be requested. Customers sign such contracts because the cost reduction outweighs the occasional and relatively unpredictable loss of production or inconvenience. All kinds of interruptible programs, time of use tariffs[1], dynamic pricing, and in recent years market-based demand side bidding are the examples of indirect load control [11].

[1] Time of use tariffs are different pre-defined prices of electricity, for different blocks of hours. The Economy 7 in the UK is one example.

- Direct Load Control (DLC): a unidirectional communication infrastructure is established between the system operator and customers, who are provided with suitable hardware. Thus, the system operator is able to directly control the load. This kind of control is performed in a relatively abrupt manner as the operator does not know the status of the device being controlled. This potentially may cause more inconveniences to the customers and generate high spikes of power demand.
- Demand Side Response: customers are provided with a bidirectional communication infrastructure and the required hardware, enabling the system operator to control the load. In contrast to DLC, the end user preferences are taken into account, as DSR requires the ability and the willingness to curtail demand on almost a daily basis. DSR redistributes the load but does not reduce the total energy consumed.

The demand side response system presented in this thesis explores the possibilities of new methodologies that can be implemented by two way communication systems, such as the shifting of domestic appliance loads in time and electric vehicles charging. Thermal load control, such as air conditioning and heat pumps are not considered in this research.

Historically, during the last 30 years, utilities and system operators (mainly in the USA) have tried to modify the load profile through one-way communication direct load control methodologies, primarily as a means to minimize system peaks and reduce production costs. There is a plenty of literature on the existing load scheduling algorithms and strategies, e.g. [15], [16], [17], [18] and [19]. In the UK radio-controlled heating load has been researched [20], [21]. In Australia, there have been several DLC programs for peak reduction, mostly focused on air conditioning systems [12]. Common to these approaches is that they all focus mainly on small customers and involve the periodic curtailment of domestic appliances and commercial devices, which possess some kind of thermal inertia, in a relatively aggressive manner. The control actions are centrally calculated and executed, and the end-user's participation is completely passive. Whilst it is relatively easy to implement the DLC program through a one-way communication system, for example with water heaters, it is difficult to maintain the end-users' comfort level, as the system operator has no information about the status of the appliances. As a result, some customers may withdraw from DSR participation. In addition, one-way communication DLC cannot properly control the payback[2] effect generated immediately after demand re-connection. This is caused by the fact that the load control

[2] The payback effect is the increase in power demand due to energy restoration of controlled loads that appears in the period immediately after reconnecting to the system the loads that previously had been disconnected. This phenomenon is mainly related to thermal loads and is a function of the duration of disconnection and load characteristics.

disturbs the natural demand diversity and may create unwanted demand spikes as described in [15], [17] and [69]. And more importantly, actually obtained load reduction is usually less than expected [22]. This can be avoided if more information is available about the status of the load when sending control signals. Two-way communication systems may provide this functionality by enabling the appliances to send status information to the system operator. The system operator can then foresee the amount of load that is managed, as well as the dynamics of curtailment and re-connection, in order to avoid the peaks and network congestion. Moreover, the system operator will know for how long they can postpone the operation of each device, thus minimizing the end-users' discomfort.

Today, many appliances are already equipped with delayed start functions[3] that could be used by consumers to change their starting times in order to take advantage of time-of-use tariffs for example. Smart appliances go beyond this by having more decentralized (automatic) intelligent control that may or may not involve the intervention of the consumer. They are enabled with technologies to allow their interaction with the electricity system. Such interaction can involve directions to modify their operation cycles such as time shifting or interruption for a limited period of time. Such appliances offer comparatively more flexibility preserving the customer's comfort level.

These new technologies offer an opportunity to address wider system concerns, such as managing network congestion problems. However, little attempts have been made so far to this end. It was recognized that two-way communication infrastructure for load control can be effectively used to help distribution automation (DA) [23]. The paper lists the utilities that have implemented DA and DSR programs and concludes that the experience they gained in implementing integrated distribution automation and DSR systems is still limited due to the high cost of DA products and the uncertainty over the DSR programs to be undertaken. Smith in [24] describes a combined feeder and substation control in the future distribution networks, where DA and DSR will be used to even out voltage profiles along the feeder, to improve a power factor and balance phase currents.

The work presented in [25] investigates the benefits of combining new ICT technologies, such as Phasor Measurement Units with flexible load on a simple two bus-bar system. It was demonstrated that load control was capable of mitigating congestion in a tie line between two systems in the presence of highly unpredictable wind generation at one bus. Another attempt is made in [26] where a distributed energy storage and non-critical load is examined, such as electric vehicles, to

[3] This is a function that allows the consumer to postpone the start time by a fixed time period.

increase the network utilization. Even though a full network model is used, a real DSR simulation throughout different network locations was not demonstrated.

References [27] and [28] involve the work that author of the Thesis has done with other part of the Imperial College team on the network congestion managing problem. In these references, a more detailed analysis of DSR and the energy storage potential for increasing network operation flexibility is presented. The papers describe a methodology that reduces congestion costs and that is based on a linear OPF combined with thermal load and energy storage control actions. However, there was a strong motivation for the further work in this area due to:

- In [27] and [28], a simplified storage model was used, where a certain storage capacity was a priory allocated in each bus of the network (in advance, before the optimization started). With that approach, the optimal allocation of storage resources in transmission networks as well as the optimal size and position of the storage in distribution networks could not be determined.

- DSR model used in [27] and [28] is based on thermal load, where DLC approach is used for water heater control. As mentioned above, DLC compromises the end-user comfort which puts in question the large scale acceptance by the customers. Apart from being relatively inflexible, this kind of control may cause high power spikes during load recovery. In this Thesis, a model involving Smart Appliances was implemented and based on DSR, rather than DLC.

- In [27] and [28], the DC-OPF method is used. That method is not capable for voltage control, which is of crucial importance in distribution networks. In this Thesis, both DC and AC OPF methods are demonstrated.

- Model in [27] and [28] was based on a two-step procedure: in the first step, economic dispatching of generators, assuming infinite network capacity, is performed. The second step performs the optimal generator re-dispatching taking into account network constraints. The model presented in this Thesis is an improvement of the previous model since the economic dispatching and network constraints are now incorporated in one step, thus simplifying the model and reducing computational time.

- A novel model for optimal EV charging strategies in congested distribution networks has been developed and implemented.

There are other attempts to address the network congestion management issue. In [29], a model for congestion management in transmission networks is presented. It is based on large customers who are willing to participate in price-incentive schemes. Load is modelled as price-responsive and the linear OPF model was used but the paper failed to address the broad utilization of DSR into electricity networks. An attempt to apply game theory into distribution networks congestion management is presented in [30]. In the proposed 'game', the end users represent the players whose goal is to minimize the electricity price whilst the daily load profiles represent the set of game strategies. The users' preferences regarding the electricity consumption are weighted with the appropriate cost for each time step. A global objective is then obtained through the optimization of the individual users' objectives. The approach is based on classical price-load elasticity and assumes the users themselves set up the criteria which describe their readiness to change the load profile in exchange for lower energy prices. Apart from the problems related with estimation of realistic value for price-load elasticity, the model does not include voltage modelling.

1.4 Energy Storage

The utilities and power system operators have been aware of the value and potential benefits of energy storage applications since the early days of electricity systems. However, due to the high price of battery technology, the practical commercial deployment of energy storage has been confined to large scale hydro-pumped storage (HPS) that have been used for daily load levelling. In Europe, such HPS were introduced as early as 1910s [31]. The first constructions consisted of a pump and a separated generator, and later on reversible pump-generator systems were introduced. However, the building of large hydro-pumped storage plants is limited as they require very specific geological configurations of the terrain. According to EPRI, there is over 127GW of installed HPS capacity world-wide [32]. At present, the largest HPS are in the USA (Bath County Pumped Storage Station with installed power of 3GW), Japan (Kannagawa Hydropower Plant – 2.8GW) and China (Guangdong Pumped Storage Power Station – 2.4GW) [33]. The potential role of large-scale storage gained more attention as significant wind energy penetration began to be considered. As a result, many papers have been published on the utilization of energy storage for various purposes, such as load levelling and standing reserve [35], [36], [37] or system peak shaving [36]. Nowadays, apart from hydro-pumped storage, there is a spectrum of storage technologies under development, such as: battery (of all kinds), fluid-based (compressed air, liquefied air), flywheels, superconducting magnet energy storage and hydrogen-based storage. The rated power of these storage systems ranges from kW to GW, as shown in Figure 1-1. The figure also shows the discharge times and designates possible areas of application for each technology type.

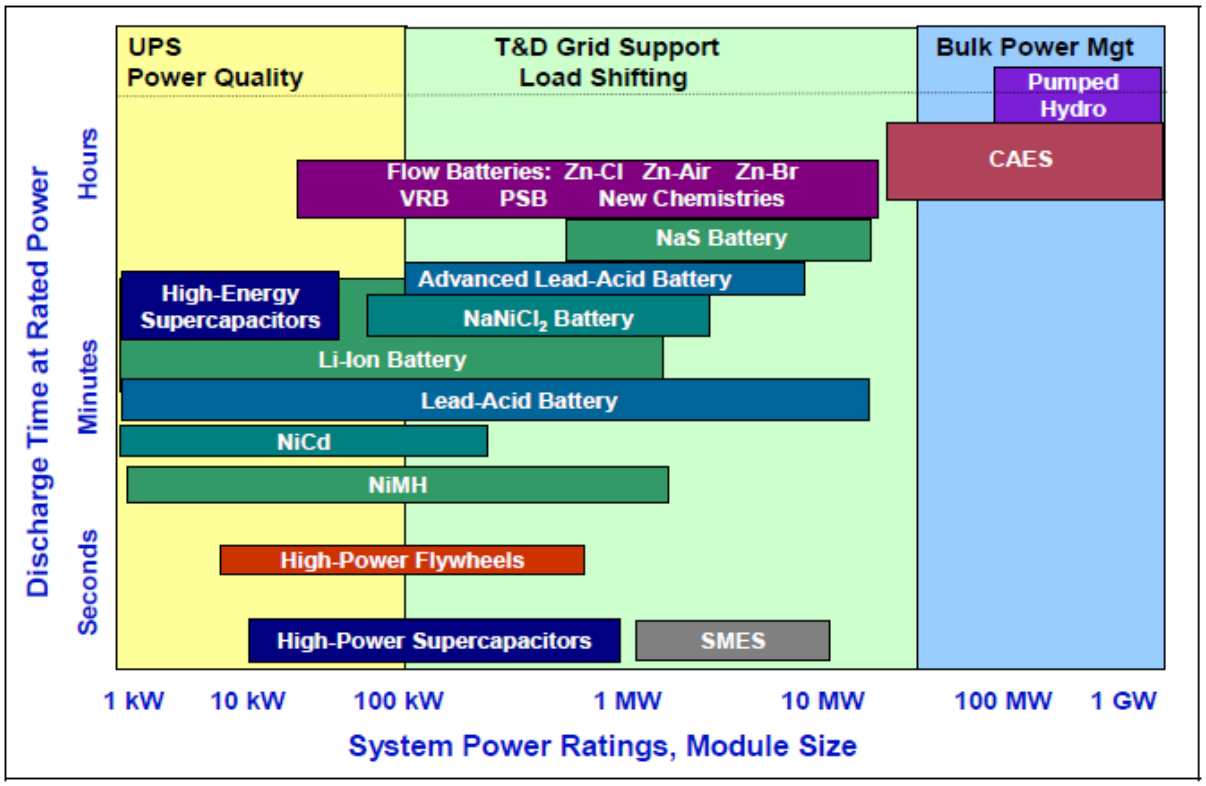


Figure 1-1: Typical power range versus discharge times for different storage technologies (picture taken from EPRI report [38])

As Figure 1-1 illustrates, the range of technologies offers the potential to provide a spectrum of system services, such as: spinning reserve [35], [39], power system stabilization [40], [41], as well as supporting islanded systems [42] and black start [43].

The applications of storage devices on electricity networks have also been investigated in the open literature. In [44], a model is presented to increase transmission line utilization and to assess the value of compressed air energy storage by coordinated dispatch of storage devices and wind generation for different market strategies and different areas in the USA. However, this approach does not assess the value of storage distributed throughout the network, as it is based on the analysis of a single transmission line at which the storage is attached to. In [45] the congestion management problem is solved using a genetic algorithm and combining network and generation re-dispatching based measures, including wind curtailment. The model is non-linear, taking into account $(n-1)$ security criterion. The approach is tested on a realistic transmission network with large penetration of wind energy. However, the main drawback of the model is that it optimizes each time step separately, i.e. there is no inter-temporal relation between the control actions which is of essential importance for energy storage. The application of storage in distribution networks is considered in [46], where a load connected to the grid with two parallel lines is studied. Similar to [44], this approach also does not consider full network operation modelling. The work given in [47]

presents a software planning and operational tool for medium voltage distribution networks capable of determining the optimal size and placement of energy storage. The work is based on a genetic algorithm. Storage is modelled as a bank of several units of different technology types and sizes attached to each bus and the optimization chooses the optimal number of units for each type. However, storage is modelled to run in on/off mode: when it is on, it can charge or discharge only at rated power, which significantly reduces the potential benefits that storage can bring to the system.

From the literature survey above, it may be concluded that there is still a need for a decision making methodology that will evaluate the economic viability of storage in transmission and distribution networks, based on all the potential benefits it may bring to the system, which is one of the motivation for this research.

1.5 Electric Vehicles

The idea of using electric vehicles is almost as old as the automotive industry: with the exception of manually produced cars in the private garages in the middle of 19th century, the first manufactured electric vehicles were on the road in the last quarter of the 19th century, mostly in Great Britain and France [95]. Around that time, an increased interest in electric cars emerged in the USA. Hence the period between the two centuries was the most prosperous for electromotive industry [96]. The reason for the high demand on electric vehicles at that time was traveller's comfort and operational easiness comparing to the other types of vehicles, especially steam ones. In 1899, an electric car named 'La Jamais Contente', produced by a Belgian designer Camille Jénatzy even won a world record for ground speed of 105.8km/h [97]. However electric vehicles became less popular with: massive exploitation of crude oil that significantly reduced the prices of this energy source; invention of electric starter for combustion engines; and the improvement in gear changer made the operation of gasoline vehicles much easier. Price of electric vehicles at that time was about $1,500USA, while Ford offered vehicles in between $500 and $1,000USA [95]. And finally, road building between cities required vehicles to have a higher driving range, which electric cars could not manage. All these reasons meant electric vehicles slowly declined and by WW2, there was almost no electric vehicle on the roads [95]. It was not until 1970s when the international oil crisis hit that the use of electricity for road transport was reconsidered [98], in an attempt to reduce the dependence on imported oil and gas [99]. Since then there has been a considerable research into electric vehicles with the main focus on batteries, which are the main limitations in terms of range, recharging and cost. Further interest in electric vehicles arose in mid 1980s, but this time mostly from scientists as a consequence of growing awareness of global warming [100]. Namely, the scientists began to conclude that human activities were contributing to global warming and in particular Carbon Dioxide (CO_2) was identified

as a major cause. The UN identified that 21% of GHG emissions worldwide come from transportation [101], so the efforts to replace internal combustion engine vehicles with electric has grown since. In addition, there are also concerns with other vehicle emissions and air quality particularly within cities. Exhaust emissions contain various products hazardous to health, such as Carbon Monoxide, Nitrogen Dioxide, Sulphur Dioxide, Benzene, Formaldehyde, Polycyclic hydrocarbons [101]. The situation is especially difficult in large cities where vast numbers of vehicles are concentrated. The World Health Organization set the air quality standard which specifies that concentration of suspended particles (airborne smoke and lead, soot, dust and liquid droplets as a product of fuel combustion) should not exceed 90 $\mu g/m^3$ which is already violated in many cities worldwide [101]. With increasing number of internal combustion vehicles (ICV) produced globally every year, pollution caused by vehicles is likely to continue to increase.

For these reasons, governments in many countries, including the UK, give various incentives to both the automotive industry and to end-buyers to produce, sell and use EV rather than ICV [94]. Consequently, the number of manufactured EVs increases each year, as shown in Figure 1-2 [103].

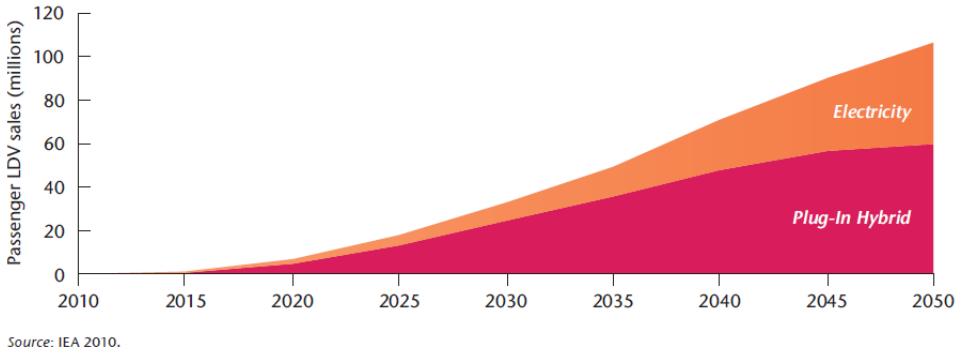


Figure 1-2: Estimation of worldwide EV and PHEV sales (picture taken from IEA report [103])

However, the increase in the number of EVs raises concerns whether the electricity grid is able to supply this additional load. Vehicle-to-grid (V2G) concept, where batteries can be also discharged to support grid operation is suggested in [104] and [112]. As for the UK, recent reports say there is sufficient generating capacity to supply this added load, if charging EV is performed at off-peak periods [107]. The same report states: "The existing national transmission network will be sufficient to cope with the demand from vehicles." On the other hand, increased number of EVs will probably lead to congestion and the need to reinforce distribution networks. To this end, many papers have been published presenting different algorithms for optimal EV charging strategies. For example, a genetic algorithm is used in [105] and a binary particle swarm optimization is applied in [106] to optimize car charging in a parking lot. Papers have been published recently where the impact of EV

on distribution network has been analyzed, such as [108], [109] and [110], but there is still a lack of solutions to manage the vehicles charging once they are connected to the network.

1.6 Experience

In order to address these changes in a cost-effective way whilst achieving maximum utilization of the network assets, a fundamental revision of the way that generation, transmission and distribution systems operate will be required. The scale of this transformation closely follows the advances in Information and Communication Technology (ICT). Power systems, enhanced by ICT are generically called Smart Grids. Smart Grids symbolize a new paradigm for power generation, transmission and distribution where ICT is harnessed to disperse the centralized system control from generation towards demand. As such, the Smart Grid concept may be considered as an innovative metamorphosis of the electric power system as a whole, rather than the transformation of its individual parts, technical or functional. Not surprisingly, the revision of these basic principles of power system design and operation attracts a broad public attention, as this new paradigm will not have only technological effects, but also environmental, economical and social consequences.

There is an intensive world-wide work on transforming power networks to Smart Grids. It is forecasted that the world-wide market for investment in Smart Grids will attract 200 billion USA dollars between 2008 and 2015, including network enhancements and smart metering [48]. Below are listed several recent projects on Smart Grids [49].

In Miami, Florida, there is a USA$200 million project named Energy Smart Miami, led by Florida Power & Light (FPL), with partners GE, Cisco Systems and Silver Spring Networks. In this project, GE supplies one million smart advanced wireless meters to every home and most businesses in Miami-Dade County. With these meters, the FPL customers will be able to reduce their electric bills through demand side response and energy savings (for example, air conditioners will be able to communicate with smart meters to reschedule high-energy functions or switch to a lower-consumption mode) [50].

UK utility Scottish and Southern Energy (SSE) ran a pilot project in Oxfordshire, for which purpose GE smart meters were used. With the help of these meters a community of North Leigh reduced energy consumption by 10%, for which the village received a £20,000 award from SSE. The aim of the project is to identify the most effective methods of influencing consumer behaviour to reduce energy usage to achieve the UK government's goal of 20% CO_2 reduction by 2020 [51].

GE installed 90,000 smart meters for the Swedish utility Gothenburg Energy in Goteborg, Sweden. The meters are based on an economical wireless mesh networking, named ZigBee technology. With

this technology, the utility will have real-time data access and the customers will have information on their actual consumption and ability to adapt their energy usage [52].

Not only the utilities, but also the large manufacturers are competing for Smart Grid funding. The Association of Home Appliance Manufacturers (AHAM), which includes more than 150 members throughout the world, published a White Paper in 2009, where they expressed interest in the development of Smart Grid and surrounding policies, articulating the following three crucial requirements for the Smart Grid's interaction with consumers [53]:

- Pricing must provide incentives to manage energy use more efficiently and enable consumers to save money.
- Communication standards must be open, flexible, secure, and limited in number.
- Consumer choice and privacy must be respected; the consumer is the decision maker.

Whirlpool Corporation, the world's leading manufacturer of major home appliances, will make all the electronically controlled appliances it produces (washing machine, refrigerator, space heater, cloth dryer etc.) capable of receiving and responding to signals from Smart Grids by 2015 [54]. General Electric, another AHAM member, is investing $40 million in the Smart Grid technology centre in Markham, Ontario. The GRID IQ^{TM} Innovation Centre will be developing grid enhancement technologies [55]. GE has also announced its targets to enable net zero energy homes by 2015, where apart from efficient utilization of energy using automated home appliances, residential generation will be used (PV cells, micro wind generation etc.) [56].

All these appliances are designed to minimize user's discomfort while working in smart mode, which is in line with AHAM's vision that Smart Grid concept can and should be met without causing significant disruption or lifestyle changes for the consumer. In order to operate the appliances in smart regime, a communication standard between appliances and Smart Grid is required. Since AHAM is also a standards development organization, accredited by the American National Standards Institute, they support and encourage development of interoperability standards for Smart Grid devices and systems.

Capgemini, Cisco Systems, GE Energy, Hewlett-Packard, Intel and Oracle established the Smart Energy Alliance in 2006. The ultimate goal of the Alliance is to drive transmission and distribution utilities from Smart Grid roadmaps to the real world. In their vision, the networks transformation

challenges could be addressed only through the complete integration of complex communication systems using Internet Protocols [57].

However, there is also an example of political obstacles for Smart Grid concept deployment. The Town Board of Lewisboro, New York, in a debate lasting for 30 minutes declined even to hear a five minute proposal for a project that would make the town a consortium to participate in Demand Side Bidding through energy response using smart appliances [58].

Developments in battery technologies led to commercial applications of energy storage systems. ABB has developed energy storage modules (ESM) up to 2MW, voltage range from 120V to 40.5kV, 50 or 60Hz, single phase or three phase systems. The type of batteries depends on the application and size. They also offer optimal product selection regarding the grid conditions [59].

UK Government offer an incentive named Plug-In Car Grant for electric-vehicles buyers where 25% of the cost of an electric vehicle or up to £5,000 will be granted to the buyers of this type of the car. It is estimated there are about 17,000 hybrid or plug-in EV in London. There are planned about 1,300 publicly accessible charging points for EV to be built in London by 2013. [60]

1.7 Motivation for Thesis

Traditionally, energy storage and DSR have been considered for energy arbitrage while the use of these technologies for unlocking unused network capacity and the provision of system support services have barely been considered.

The potential benefits of using storage and DSR technologies for network applications have not been fully explored because of the lack of rigorous methodology and tools for quantification of the effects of these technologies on network operation and development. This is however a very complex task as the evaluation tools need to be capable of coordinating real time network operation strategies and network investment decisions across a number of possible load and generation development scenarios whilst minimising the overall costs.

In this context, electric vehicles (EV) may be considered as a distributed storage, with special constraints regarding time of charging and required energy. The effect of migration of transport sector to the electricity sector has been explored in many papers at system level, such as load levelling, peak shaving, balancing services etc. However, the real problem that emerges with EV is related with distribution network congestion. Since the problem of optimal EV charging in distribution networks has not been answered, this work will investigate and develop prototype

techniques and algorithms required to support the deployment of EV to assist network operators and developers to maximise the value of EV in a spectrum of practical applications.

1.7.1 Challenges

One of the key challenges of the development of future electricity systems is to ensure cost effective integration of renewable resources and additional demand in the operation of the electricity system without compromising security of supply and power quality. Potential operational problems could emerge at all levels in electricity systems:

- **Generation level**: problem of balancing power and providing reserve, which is a consequence of the intermittent nature of the output of wind generation.
- **Transmission level**: connection of wind generation in remote areas increases the congestion in transmission network thus confining the amount of wind generation that can be connected to the system.
- **Distribution level**: connection of DG and increased electrification of transport and heat sectors at distribution level will lead to additional stress in distribution networks, causing congestion, voltage problems and deteriorating power quality.

Problems arise from the fact that wind generators operate at low load factors and network design is based on peak output conditions which may lead to network overinvestment and suboptimal utilisation of network assets. On the other hand, wind curtailment should be minimized. The situation will deteriorate with high penetration of EV that have a very high peak coincidence factor.

This work will examine in more details the problems at transmission and distribution level.

Challenges in transmission network

To achieve a significant reduction in CO_2 emissions, renewable and other low carbon energy sources must become major contributors to the future electricity power system. The location of these new sources, usually at some distance from the centres of demand and (in the UK) predominantly in off-shore sites, will be of considerable importance in assessing the impacts on the transmission network.

Thus, deployment of significant amount of renewable generation and rapid growth of electricity demand are likely to increase the requirements for transmission in the future. However, this is not balanced with the development in new transmission capacities which is often very slow for various reasons. It is widely recognized that transmission is the biggest long term barrier to significant wind energy expansion, and is already leading to significant challenges for system developers.

Challenges in distribution network

Conventionally, operation of distribution networks requires no real time management, as the real time network control problem is resolved through appropriate investment at the network planning stage. This historical passive operation philosophy has now been challenged particularly with the introduction of Distributed Generation (DG). This is because the passive network operation considerably limits the amount of DG that can be connected. New demand that is supposed to migrate from transport and heat sectors in the next few decades is going to give additional stress to the distribution network since this demand is characterized with relatively low load factors which restricts the amount of demand growth that can be accommodated into the existing networks. Hence, if the passive operation philosophy is to be maintained, significant network reinforcement will be necessary to accommodate DG and load growth.

Another kind of challenge arises from the computational tractability of the results. Namely, as the DSR and EV models are relatively detailed they are not particularly suitable for network optimisation applications. In this context the key challenge will be to reduce the complexity of the models whilst preserving their main characteristics so that these can be incorporated in network control and optimisation algorithms.

1.7.2 Objective

Effective scheduling of responsive demand, storages and EVs will offer opportunities for reduced investment in transmission and distribution equipment together with the associated lower environmental footprint and avoidance of long delays in connecting renewable generation. In this context, this work focuses on the investigation of the potential benefits of utilization of Storage, DSR and EV as potential means for network congestion management and for maximizing the system capability to employ renewable energy sources in systems with constrained capacities.

In order to achieve the above goals, it is necessary to develop novel optimisation methodologies and techniques to estimate the potential value of Storage, DSR and EV for an alternative future development of the electricity system.

Therefore, the outcome of the research is to identify trends and characteristic conditions for which the enabling technologies are likely to have some value, and also the conditions under which this will not be the case.

List of Objectives

1. Develop models for a storage systems, load control and EV charging strategies for network optimisation applications;
2. Assess the feasibility of alternative applications for DSR, storage and EV charging strategies to help address network problems;
3. Develop techniques for the optimisation of active distribution network operation including real time control of storage and load control of devices to help manage network voltage and flow profiles in real time;
4. Develop techniques and methods to determine the optimal size, location, and operating strategy of storage technologies to enhance the utilisation of existing network assets and to minimise future network reinforcement;
5. Quantify and optimise the multiple value streams of the various storage applications, DSR and EV charging strategies

1.7.3 Research questions

The main research questions are:

1. Identify financial benefits that Storage, DSR and additional flexible demand such as Electric Vehicles could have in network optimisation applications. These include:

- deferring new network investment,
- increasing the amount of on and off-shore wind generation that can be connected to the existing network infrastructure,
- increasing the amount of additional demand (specifically, EV) that can be connected to the existing network infrastructure
- relieving voltage constrained power transfer problems,
- relieving congestion in distribution substations,
- enhancing quality and security of supply to critical load customers,
- reducing the requirement for standby and peak generation, and
- corresponding CO_2 reduction.

2. Identify key factors that drive the value of these technologies for network applications, especially for:

- transmission network
- distribution network

Approach:

The approach adopted to answer these questions is to develop and validate models of Storage device, DSR and EV charging strategies that may be relevant for transmission and distribution network operation and development.

This will involve the modelling of storage plant operating regimes and cost drivers specific to individual applications, including battery storage and load control for the management of network power flows and voltages.

DSR does not reduce the total energy consumed, but does redistribute the load, lowering its natural diversity, which can lead to the occurrence of high peaks. This should be avoided and modelling of such phenomenon will be a part of this work.

Increased electrification of road transport for small and medium size cars is expected in next few decades, and the models have to take into account all of the characteristics of this new load, including the behaviour of car owners, availability of charging infrastructure, energy required, battery constraints etc.

Apart from the constraints specific for each enabling technology (Storage, DSR, EV), the model also has to take into account various constraints such as

- power balance constraints,
- network thermal constraints,
- voltage constraints, and
- generation plant constraints.

Assessment of the viability of Storage, DSR and EV technologies and their applications is made from a network operator's perspective. The benefit of these enabling technologies will be established as the difference between the total costs of the traditional, passive network operation based solutions and the costs of the system that includes storage, DSR and EV technologies. The analysis will be performed on various voltage level networks.

On the basis of the case studies, opportunities will be identified and the value of Storage, DSR and EV applications quantified in the context of releasing network capacity. The key driving factors for the value of these technologies for network applications will also be identified.

1.7.4 Contributions

The main contribution of this work is the integration of demand response models in the optimal power flow algorithms and the development of an innovative methodology and appropriate simulation tools for transmission and distribution network operation. The approach is based on a multi-period optimal power flow in which generation outputs (of both conventional and renewable generators) are coordinated with actions of storage and DSR being distributed throughout the network. The detailed list of contributions is as follows:

- Development of mathematical models of different types of loads, such as smart appliances and electrical vehicles to be implemented in network optimization applications.

- Comprehensive assessment of the limitations and advantages of different DSR modelling approaches. This includes an evaluation of the benefits that smart demand control brings compared to the business as usual approach. By this, smart control is assumed to be based on a two way communication and full scheduling of loads, taking into account their characteristics and consumer constraints.

- Development of dedicated demand scheduling algorithms for the optimisation of the benefits of controllable load. These algorithms are suitable for integration into larger system scheduling tools, such as: system demand and generation scheduling, transmission congestion and active distribution network management planning and expansion.

- Development of a tool capable to perform a multi-period optimisation, as Storage, DSR and EV operation require the consideration of time coupling between different periods.

- The full integration of the developed load models and dedicated demand scheduling algorithms into multi-period DC and AC OPF algorithm. This enables to incorporate Storage, DSR and EV operation as part of the optimisation and is the main novelty of the model.

- Quantification of the value of Storage, DSR and EV in the reduction of congestion costs and the increase in the amount of wind integrated by the system for different types of networks (radial and meshed)

- Estimation of the potential for using DG, Storage, DSR and EV to support the development of Smart Grids by resorting to these technologies for load flow control, voltage support and deferral of network reinforcement needs.

1.7.5 Thesis Structure

In order to efficiently present the objectives and the proposed approach discussed above, the thesis is structured as follows:

Chapter 2 gives a detailed description of the smart appliances that operate in limited-duration cycles, such as washing machines, dish washers and tumble dryers. This is supported by a survey of consumer acceptance, which is taken into account when designing the shifting algorithm for the network operation applications.

Chapter 3 presents a methodology developed to identify and quantify the benefits that non-network solutions, such as storage and DSR bring to the operation of transmission networks. A storage model suitable for network applications is developed and together with a model of smart appliances described in previous chapter is implemented in the proposed methodology. The methodology is tested on the UK transmission network with high wind energy penetrations envisioned, and the key factors that drive the value of these technologies are identified.

Chapter 4, based on the methodology developed in the previous chapter, introduces additional constraints and requirements specific to distribution network operation, such as voltage magnitude limits and reactive power flows, making the problem non-linear. A sequential linear programming method is employed for solving this non-linear problem. A model for optimal storage location and sizing is also presented in this chapter. The proposed methodology allows to identify main drivers for the benefits of the enabling technologies in distribution systems and to quantify the values they bring. The models are tested on distribution networks and the improved utilization of the existing network assets is shown.

Chapter 5 presents a novel methodology for optimal charging of the electric vehicles to support network operation, reduce peak and help the utilization of renewable energy. The methodology is implemented in a multi-period DC OPF where the network and EV constraints are modelled as a part of problem formulation. Presented model considers the real life driving statistics of the light/medium size vehicles, based on the UK driving patterns, which are also discussed in great details in this chapter. The methodology is tested on a meshed distribution network.

Chapter 6 brings the conclusions and discussions based on this work. This chapter also discusses possible future work as a continuation of this research.

CHAPTER 2. Smart Appliances and shifting algorithm

2.1 Introduction

This chapter focuses on the appliances that operate in limited-duration cycles, such as washing machines, dish washers and tumble dryers. Their starting time can be anticipated or postponed within a certain time interval allowed by the consumer. Such appliances, when postponed, make a virtual reduction of a block of demand that is fully recovered later, once the cycle of the appliance takes place.

Household appliances form a significant part of energy consumption, representing around 10% of the total annual energy consumption in the UK (value estimated based on [66]). The contribution of an appliance to system flexibility depends on its placement within the daily demand profile. The contribution is higher when their operation pattern coincides with more critical operation periods such as peak demand.

An estimate of the diversified daily demand of different appliances in the UK is illustrated in Figure 2-1 [66]. It is possible to observe that some appliances, e.g. refrigerators and freezers, have a nearly constant demand while others, such as dishwashers (DWs), have a higher demand in the evening. Obtaining the diversified load curves for each type of appliance requires monitoring a large number of consumers for a long period of time [63], [64]. It is out of scope of this work. The aggregated system demand from domestic appliances is significant reaching a peak of 14 GW in the UK system[4]. Consequently there is a potential to use this type of loads to provide demand flexibility.

On the other side, a survey [65] reveals that the acceptance of the smart operation mode highly depends on the appliance type. More specifically, the customers are generally reluctant to the interruption of the operation cycle of the appliances: for most appliances the maximal allowed interruption time does not exceed 15 minutes, therefore this option was not considered in the work presented. This research focuses on a batch of shiftable appliances composed of washing machines (WM), Dish Washers (DW), and Washing Machines equipped with a Tumble-Dryer[5] (WM+TD). These are selected based on data availability, and flexibility potential offered by customer acceptance. The methodology proposed is sufficiently general to be applied to other appliances.

[4] Estimate obtained using appliance energy demand and penetration data obtained from [66] and considering a total number of 25 million households in the UK.

[5] It is assumed that the Tumble Dryer is used immediately after washing is finished.

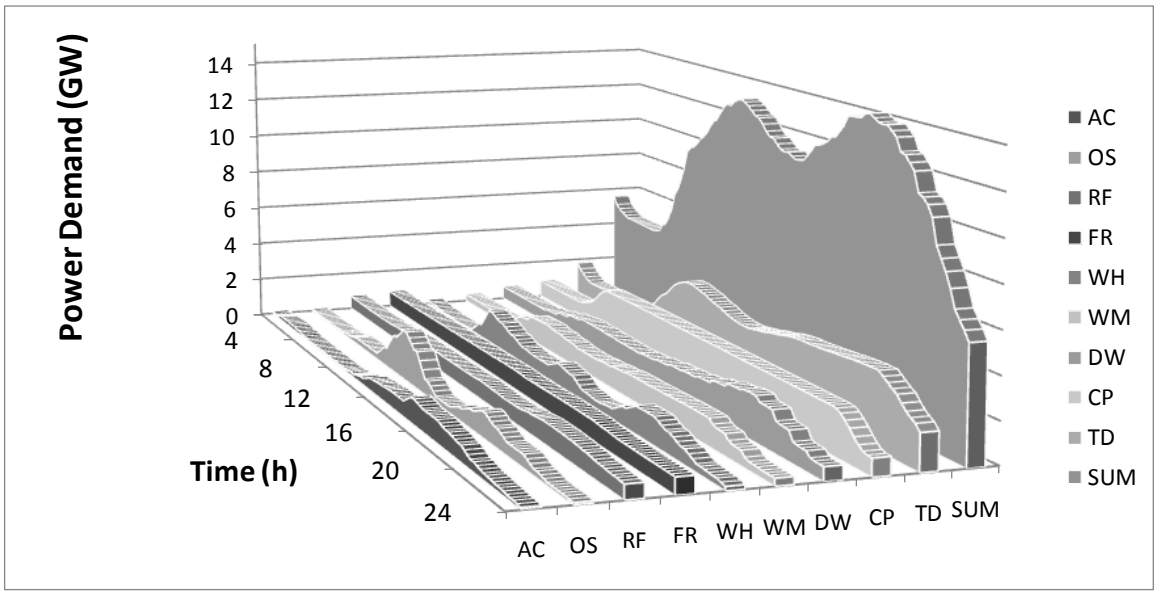


Figure 2-1: Domestic appliances' demand in the UK

WM-Washing Machine	DW - Dishwasher	TD-Tumble dryer	RF – Refrigerator	FR -Freezer
CP-Circulation Pump	AC-Air-Conditioning	WH-Water-Heater	OS –Oven and Stove	

For the selected batch of wet appliances, several smart control options are available. For example, in case of a WM, these options are as follows [66]:

1. postpone the start time of the washing cycle,
2. interrupt the water heating phase for a certain period of time,
3. reduce power demand by automatically choosing a lower temperature for the program,
4. postpone the final rinsing phase, and
5. use an alternative hot water supply instead of water heating in the WM

Options 2 to 4 deteriorate the efficiency of the appliance per cycle and will not be considered in this work. Namely, washing machine heats the water during its operation cycle. If the operation cycle is interrupted, or the heating power reduced, temperature of the water lowers. When the operation cycle continues, more energy would be needed to recover water temperature than if there was no cycle interruption. From these reasons the energy efficiency of the appliance would be worsen, and so the delay start is preferred over operating cycle interruption. Also, option 5 will be disregarded since it requires a viable alternative for water heating. Thus, option 1 is selected and will be used for this research. Similar considerations apply to Dish Washer and Tumble dryer.

Section 2.2 offers important information on the customers' attitude about the possibility of using their appliances as a tool for DSR, Section 2.3 gives detailed data on the appliances that will be used

in this work, Section 2.4 explains the shifting algorithm, and Section 2.5 describe a smart appliance model used.

2.2 Consumer Acceptance

When conducting a study about demand side flexibility, the role of the consumer cannot be neglected. Even if the smart appliance technology is available, economically viable and able to bring environmental benefits, its deployment cannot be done without engaging the appliance user. A smart appliances consumer acceptance study has been carried out in the SMART-A project [65].

This study is based on quantitative and qualitative consumer research using interviews, questionnaires and focus groups and is conducted in the UK, amongst other countries. It aims to reveal to which extent consumers will allow load-shifting, including delaying the start of washing cycles or intermediate interruptions of the operation of appliances. The research questions were focused on the readiness and flexibility of consumers to change their behaviour and the benefits they expect.

The study shows that in spite of having in general a positive attitude towards smart grid concept, consumers have many objections and preconditions regarding the use of smart appliances. The acceptance of the smart operation mode is highly appliance-specific, and cannot be generalized. These conclusions are reinforced by a set of interviews with appliance industry representatives involved in previous smart appliance consumer research initiatives.

Some of the relevant quantitative results for washing machine, dish washer and tumble dryer are given in Table 2-1[6].

Table 2-1: Smart appliances acceptance survey

Device type	Shifting Operation	
	acceptance	Delay
Washing machine (WM)	77%	Up to 3h
Tumble dryer (TD)	77%	Up to 3h
Dish washer (DW)	77%	More than 3h

In all cases more than three quarters of the consumers would accept postponing operation cycles. The majority of the consumers would expect an economic compensation for shifting their appliances in the form of reduction of electricity prices or a discount on the electricity bill. A minority would

[6] These results are drawn from a population of 11000 consumer surveys, 10 phone interviews and 3 focus groups all in the UK.

accept time shifting of their appliances if it guaranteed an increased utilisation of renewable energy. The level of flexibility, however, depends on the appliance. Washing clothes is a very sensitive area because consumers are reluctant to leave the device operating unattended and the clothes wet inside the machine, so only short delays are allowed. For DW the flexibility is comparatively higher (more than 3h) because consumers do not put the same importance on the time when the device operates.

The quantitative information about consumer flexibility, for different appliances is included in the modelling process. This enables an understanding of how consumer attitudes may impact the overall potential of the technology.

2.3 Shifting Devices Data

A summary of the smart appliances that will be used in this work is presented in Table 2-2:

Table 2-2: Summary of device types

Device type	Acronym	Max. Delay	Operation cycle duration	Penetration factor	Energy consumption per cycle
		[h]	[h]	[%]	[Wh]
Washing machine 1h	WM1	1	2	20	887.5
Washing machine 2h	WM2	2	2	20	887.5
Washing machine 3h	WM3	3	2	20	887.5
Dish Washer	DW	6	2	80	1192.5
Washing machine + Tumble Dryer	WM+TD	3	4	20	3347.5

The only difference between WM1, WM2 and WM3 is the maximal delay time for their shifting. All other characteristics are identical. Maximum Delay defines the control capabilities for each type of devices. For example, the operation cycle for a Washing machine WM3 may be delayed up to 3 hours. Penetration factor defines the percentage of households having a specific type of device. The values for these two quantities are chosen based on the survey performed for Europe Union research project [65].

Diversified profiles per household for washing machine, dish washer and tumble dryer in 1h resolution are shown in Figure 2-2 a, b and c (left hand side), respectively. They are given in [66] as

15 minute data, and here averaged to 1h. System-wide consumption for each type of device is then simply obtained by multiplying these diversified profiles by the number of households and by penetration factor.

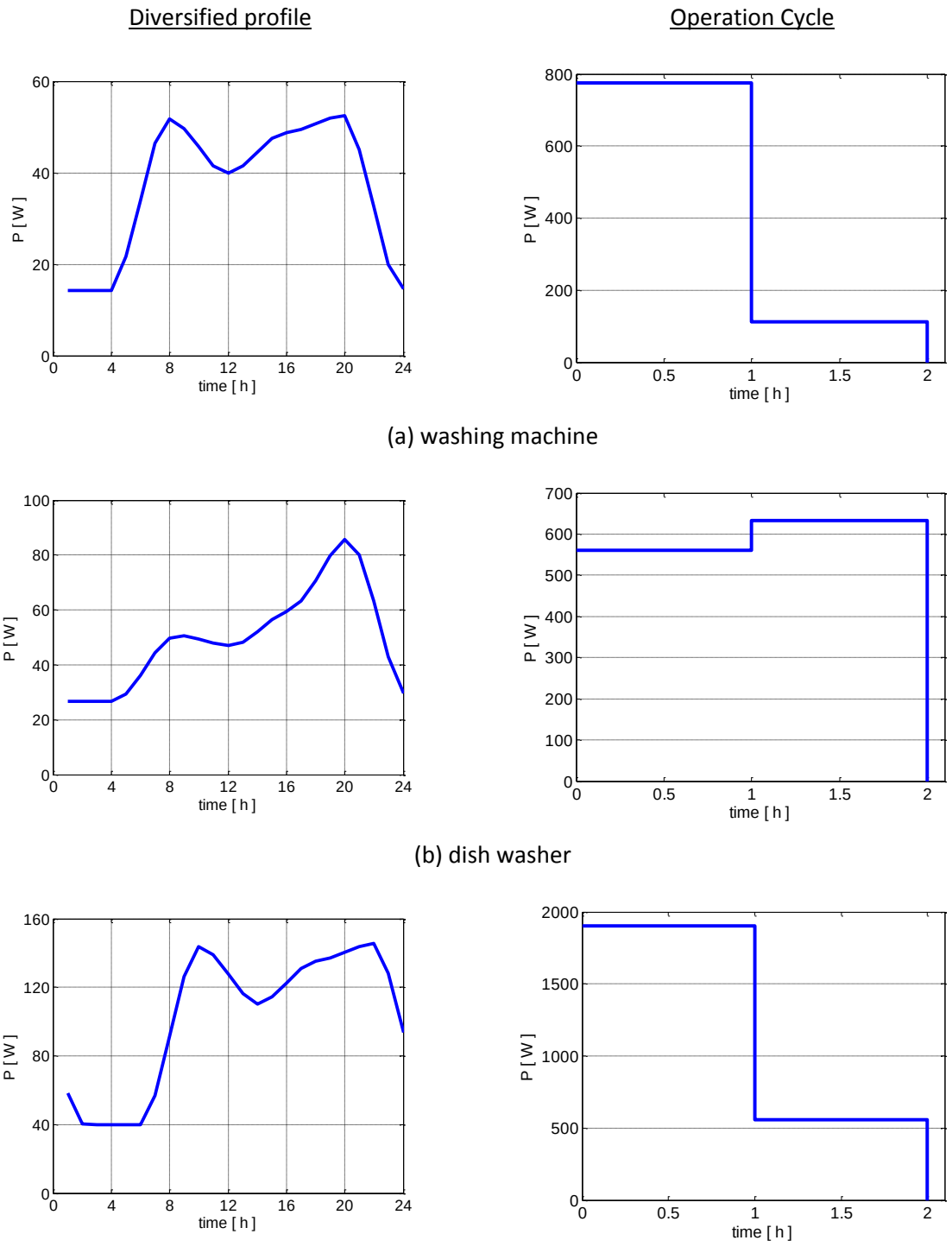


Figure 2-2: Diversified profiles and operation cycles for washing machine, dish washer and tumble dryer

Diversified profiles give information on the time of day a specific device is most used. For example, for washing machine (Figure 2-2a), three characteristic periods can be distinguished: there are two peaks, one in the morning and another one in the evening, and there is also relatively low demand during the night.

Operation cycle patterns for washing machine, dish washer and tumble dryer, in 1h resolution are also given in Figure 2-2, right hand side [66].

Operation cycle for a washing machine with a tumble dryer (WM+TD) is obtained as follows: assuming that a tumble dryer is used immediately after washing cycle has completed, its operation cycle is merged with a washing machine's operation cycle. The unified pattern is then presented in Figure 2-3.

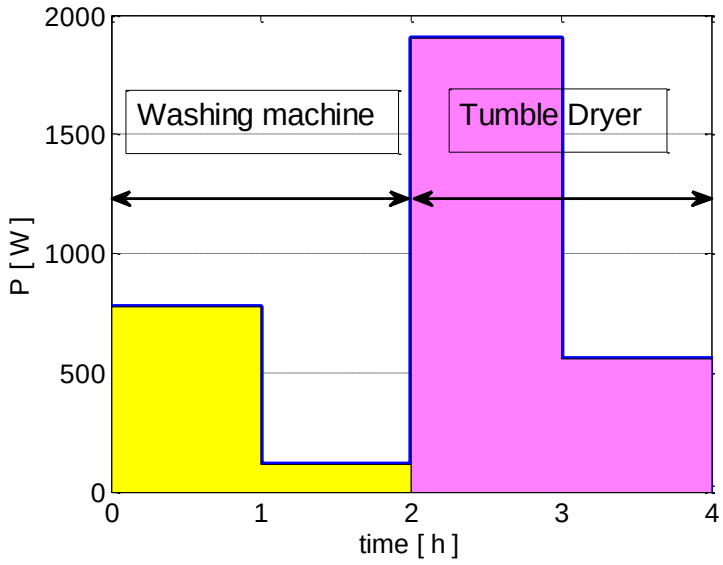


Figure 2-3: Operation cycle for a washing machine with tumble dryer

This device can be shifted up to 3 hours [65]. Energy consumption for a WM+TD is obtained as a sum of energies of a washing machine (887.5Wh) and of a tumble dryer (2460Wh), and in total it is 3347.5Wh.

2.4 Shifting Algorithm

Shifting algorithm, presented in [62], originally was designated for the cost optimization and for managing the loads in order to obtain a desired (pre-defined) load profile at system level. It was applied to a single-bus system and was formulated as a linear-constrained quadratic minimization problem. In the following sections it will be shown how this model can be altered and implemented to support networks operation. The schematic diagram of the algorithm is given in Figure 2-4:

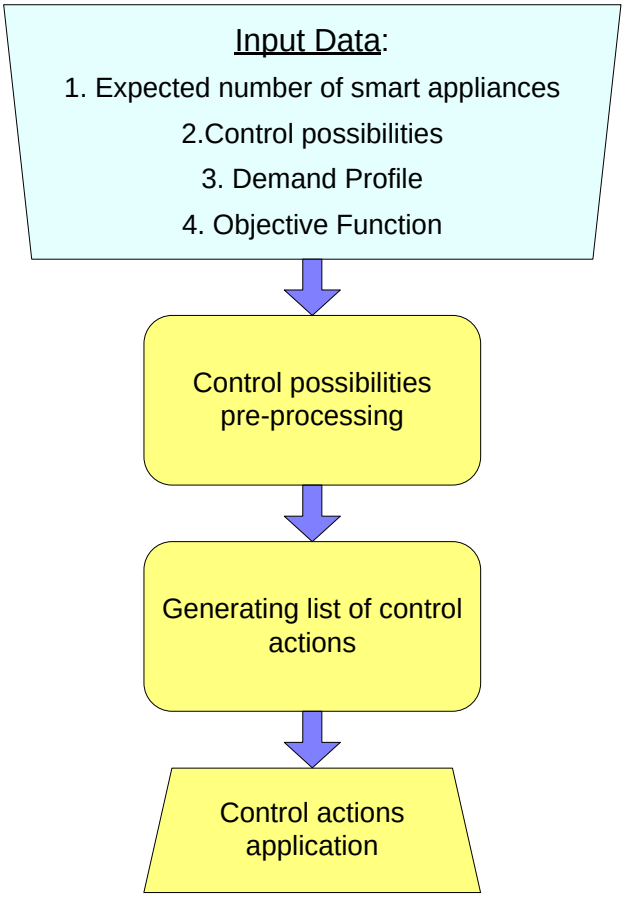


Figure 2-4: Schematic diagram of the shifting algorithm

The explanation of each component of the algorithm is given below.

2.4.1 Input data to the algorithm

The input data to the algorithm is as follows:

Expected number of smart appliances to be connected to the network, for each device type and for each time step: this represents natural diversity of the appliances when no DSR activity is taken and reflects behavioural habits of the customers. It determines the number of available devices (in each bus) that can be shifted from a specific time step. Expected number of available smart appliances can be estimated using diversified curve disaggregating [62]:

$$C_t = \sum_{w=1}^{d} D_{t-(w-1)} \cdot p_w, \quad t = 1,2,\dots,n \tag{1}$$

In (1), the unknown to be found is D_t - the number of devices starting their operation at time t. C_t is power at time t read from the diversified consumption curve, n represents the optimization horizon, d is duration of the device operation cycle and p_w, $(w = 1, 2, \dots, d)$ - the device consumption at each time step of the operation cycle. Number D_t of devices starting their operation at time t is

rounded to the nearest integer number. This kind of disaggregating procedure must be performed for each type of device. Power C_t at time step t will be composed of the demand of the devices starting their operation at t and of the demand of the devices that have started their operation at the previous time steps. Typical appliance usage patterns for the UK are shown in Figure 2-5. Further details on diversified curve disaggregating are shown in APPENDIX 2.

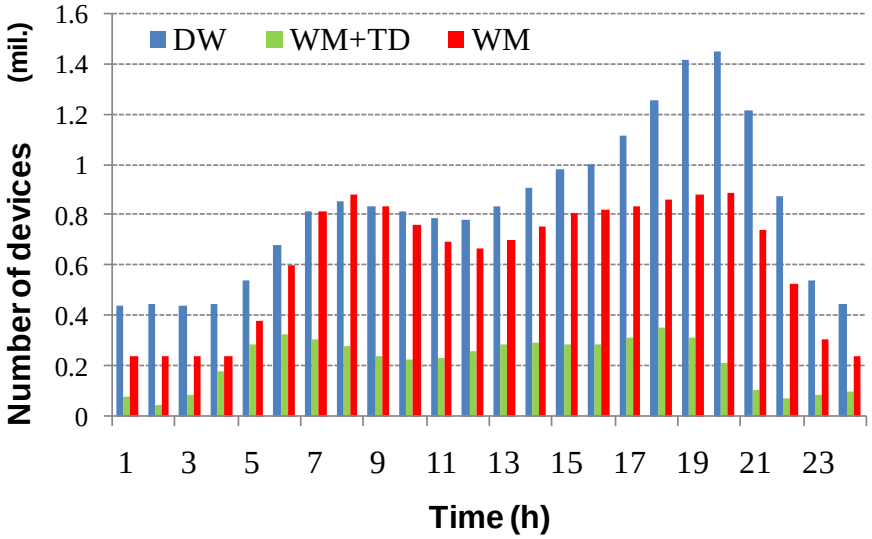


Figure 2-5: Estimated number of appliances vs. starting time

Control possibilities for each type of appliance: This specifies whether the operation cycle shifting is allowed or not; if yes, for how many time steps it may be delayed. Control possibilities may also contain *not before* and *not after* times to start the appliance, etc.

Demand profile: This is actually a forecasted load profile for the considered time horizon. In the case of a network, a demand profile must be provided for each bus.

Objective function: The objective function depends on the desired goal. For example, it could be:

- system peak reduction,
- generation cost reduction,
- power losses minimization,
- minimization of the difference in load profile from a pre-defined shape (as done in [62]), or
- minimisation of operating costs by managing network congestion problems (formulation of the algorithm will be described in details in Section 3.2)

2.4.2 Control possibilities pre-processing

In the control possibilities pre-processing stage of the algorithm the following quantities are calculated (based on the shifting availability and flexibility of each type of device):

- First possible time step $s_k(t)$ where the appliance of type k, which is expected to start operation cycle at step t, can be shifted to. Attention must be paid so that the operation cycle does not end beyond the time horizon. If not specified explicitly as an input data, for each type of devices that start the operation cycle at time step t, the first possible time step is considered to be $s_k(t) = t + 1$.

- Number $w_k(t)$ of successive time steps (starting from $s_k(t)$ determined previously) which are also possible connection times. If shifting for a specific device is not allowed or not possible, then $w_k(t)$ is zero, meaning there is no shift in time allowed for that device.

  If shifting is allowed, the number of successive possible connection time steps must not be greater than the maximum allowed delay. At the same time, the operation cycle must not end beyond the time horizon. Both conditions may be expressed as:

$$w_k(t) = \min\left(DELAY_k^{MAX} - 1, T_h - s_k(t) - d_k + 1\right) \quad (2)$$

  In previous equation, index k denotes type of appliance, t is the time step when the appliance is expected to start, T_h is time horizon length, $s_k(t)$ is the first time step where the appliance can be shifted to, $w_k(t)$ is the number of successive time steps where the appliance can also be moved to, d_k is the duration of operation cycle, and $DELAY_k^{MAX}$ is maximum allowed time for shifting. Constraints $T_h - s_k(t) - d_k + 1$ also ensure that the shifted devices will complete their operation cycles within the optimisation horizon.

Note that $s_k(t)$ and $w_k(t)$ must be determined for each device type and for each time step before the algorithm is launched.

2.4.3 Generating a list of control actions

The shifting algorithm is run in advance, before the start of the control period (for example, it may be run one day ahead). At that stage the optimal control actions are calculated. These are the actual number of devices to be moved from their expected start time to the subsequent time steps in accordance to the objective function, for each device type and time step in each bus of the network.

From the list of control actions, it is possible to estimate:

- total power of all disconnected and connected devices in the system at each time step,
- power of disconnected and connected devices in each bus of the network at each time step,

- power of disconnected and connected devices for each type of device at each time step,
- total disconnected/connected energy for the given interval of time, etc.

These information will be used to analyse which type of device is most shifted, when, and where (which bus of the network). Knowing this, it is possible to assess the contribution of each type of device to the problem goal and consequently to obtain the value per appliance for each type of device.

2.4.4 Control actions applications

When the algorithm finishes, a solution is found and a list containing the optimal value of the variables (the shifting actions) is obtained. The actions should be executed in real time during the control period using the two way communication capabilities of the system. The algorithm has an estimate of the number of devices connected but does not know which particular WM, DW or WM+TD will be connecting at that time. Each time that a device is connected, it sends a signal to the system operator letting him know that the device is ready for operation. System operator then checks the list of possible control actions and depending on the system condition sends either the immediate connection permission signal or a connection delay signal back to the device.

In real-time application of the shifting algorithm, two potentially conflicting situations may arise [62]:

- The most burdensome case is when the number of connection requests is less than expected. In other words, the shifting algorithm has got a schedule to shift a certain number of appliances, but some of them are not connected at their expected time. A possible solution would be to reschedule the non-executed control actions to the next time step.
- The number of controllable devices requesting connection is greater than expected. In this case, control actions from previous time step are executed first (if any). If there are still more connection requests, the controller sends the immediate connection permission signal.

2.5 Modelling of Smart Appliances

Let $Pd_b^p(t)$ and $Pd_b^c(t)$ represent the amount of load that is connected and disconnected, respectively, at bus b, due to control actions at time step t. These changes of demand are then added to the original demand $Pd_b(t)$. New demand is now:

$$Pd_b^{DSR}(t) = Pd_b(t) - Pd_b^c(t) + Pd_b^p(t), \qquad \forall t \in \mathbf{T}, \forall b \in \mathbf{L_{BUS}} \tag{3}$$

Equation (3) states the new load profile Pd_b^{DSR} at bus b during time step t is originally forecasted load Pd_b, less disconnected power Pd_b^c, plus payback power Pd_b^p.

The power $Pd_b^p(t)$ of connected devices at bus b at time step t consists of two parts:

- Power due to new device connections scheduled for time step t.
- Power due to device connections scheduled for the time steps that precede step t.

Mathematically, it can be written as follows:

$$Pd_b^p(t) = \sum_{k \in \mathbf{L_{type}}} \sum_{i \in \mathbf{T}} X_{itkb} \cdot p_{1k} + \sum_{k \in \mathbf{L_{type}}} \sum_{i \in \mathbf{T}} \sum_{l=1}^{d_k - 1} X_{i(t-l)kb} \cdot p_{(l+1)k}, \quad \forall t \in \mathbf{T}, \forall b \in \mathbf{L_{BUS}} \tag{4}$$

where X_{itkb} is a number of shifted devices of type k at bus b, from time step i to time step t, and p_{lk} is a power consumption during l^{th} time step of the operation cycle of a device of type k (see Figure 2-2 – operation cycles).

The power $Pd_b^c(t)$ of disconnected devices at bus b can also be separated into two parts:

- Power due to disconnection of devices that were originally expected to start their consumption at time step t.
- Power due to the disconnection of devices that were originally supposed to start their consumption at the time steps before t.

Mathematical formulation can be done in a similar manner as above:

$$Pd_b^c(t) = \sum_{k \in \mathbf{L_{type}}} \sum_{j \in \mathbf{T}} X_{tjkb} \cdot p_{1k} + \sum_{k \in \mathbf{L_{type}}} \sum_{j \in \mathbf{T}} \sum_{\substack{l=1 \\ 0<t-l}}^{d_k - 1} X_{(t-l)jkb} \cdot p_{(l+1)k}, \tag{5}$$

$\forall t \in \mathbf{T}, \forall b \in \mathbf{L_{BUS}}$

Constraint $(0 < t - l)$ in the second term keeps the time indices within time horizon set, which contains only positive numbers.

Constraints related to the shifting algorithm are as follows:

- The number of shifted devices cannot be negative:

$$X_{ijkb} \geq 0, \qquad \forall i, j \in \mathbf{T}, \qquad \forall k \in \mathbf{L_{type}} \qquad \forall b \in \mathbf{L_{BUS}} \tag{6}$$

- X_{ijkb}- is an integer number
- devices cannot be shifted back in the past and also their controllability constraints must be satisfied:

$$X_{ijkb} = 0 \text{ if } \begin{cases} j < i, \\ j < s_{ik} \\ j > s_{ik} + w_{ik} \end{cases} \quad (7)$$

$\forall i, j \in \mathbf{T}, \quad \forall k \in \mathbf{L_{type}} \quad \forall b \in \mathbf{L_{BUS}}$

The first constraint $(j < i)$ allows shifting only forward in time. Second constraint $(j < s_{ik})$ considers control possibilities of the algorithm: s_{ik} is the first possible time step where the devices can be shifted to, so this constraint says the devices cannot be shifted before time step s_{ik}. Third constraint $(j > s_{ik} + w_{ik})$ says that operation cycle of devices must finish within allowed time w_{ik} (compare also with Equation (2)).

- At each bus *b* and at each time step i, the total number of devices of type k that are moved to all other time steps cannot be greater than the number of devices originally scheduled at time step i:

$$D_{ikb} \geq \sum_{j \in \mathbf{T}} X_{ijkb}\,, \qquad \forall i \in \mathbf{T}, \qquad \forall k \in \mathbf{L_{type}} \qquad \forall b \in \mathbf{L_{BUS}} \quad (8)$$

The expected number of the devices D_{ikb}, starting the operation at time step i, is determined in Section 2.4.1, Equation (1).

All decision variables related to the control of smart appliances are associated to each bus of the network. In other words, demand side response is now performed for each bus of the network.

2.6 Summary

A significant potential of household appliances to provide demand flexibility has been recognized, since they make a large part of demand, reaching 10% of the total annual energy consumption in the UK and the peak of almost 14GW.

A batch of shiftable appliances used for this research consists of devices with limited duration of operating cycles: washing machines, dish washers and washing machines equipped with a tumble-dryer. These are selected based on flexibility offered by customer acceptance. The acceptance of the smart operation mode and the level of flexibility are highly appliance-specific. The quantitative information about consumer flexibility for different types of appliances is included in the modelling process.

Interruption or modification of the operation cycle of these devices may increase their energy consumption, and so the energy efficiency of the appliance would be lowered. From this reason, the operation cycle postponing, rather than the cycle interruption, is modelled in this work.

For each time step of the optimisation horizon, the expected number of available smart appliances that start their cycles is estimated on the basis of the appliances' diversified profiles and operation cycle patterns.

The shifting algorithm is run in advance, before the control period begins. At that stage the optimal control actions are calculated. These are the actual number of devices to be moved from their expected start time to the subsequent time steps, for each device type, time step and in each bus of the network. Control actions are constrained by control possibilities determined in the pre-processing stage of the algorithm: the first possible time step where an appliance can be shifted to and also the number of successive time steps which are also possible connection times.

Based on the number of shifted devices in each time step and in each bus of the network, which are the results of the optimisation, the power of connected and disconnected devices in a bus is calculated.

CHAPTER 3. Value of Storage and Smart Appliances for Network Congestion management in Transmission Networks

3.1 Introduction

In this Chapter, a methodology to quantify reductions in operation costs is developed and tested. The methodology integrates the shifting algorithm described in the previous chapter and storage technologies into transmission network operation. The methodology is implemented in a multi-period Optimal Power Flow (OPF) algorithm able to schedule both generation and demand side to reduce congestion costs. The algorithm dispatches the generators in the merit order, engaging the least expensive ones first (usually wind generators). However, due to network constraints, a situation may arise when out of merit generators are used instead. This increases the network operation costs. Proposed methodology generates the optimal control actions for demand side or energy storage throughout different network buses to reduce out of merit generation cost.

A multi-period simulation is required to model the inter-temporal link between different optimization time steps, as the fully controlled demand pattern allocates the demand reductions and recoveries over the whole optimization period.

Another goal of this Chapter is to explore possible usage of energy storage in transmission networks. The storage plant modelled in this work is a generic storage device with losses included. This approach has been used in order to capture the benefits of storage operation modes regardless of any particular technology. Especially, the power capacity and storage efficiency and their impact on power system operation are investigated.

The benefits of Smart Appliances (SA) and Energy Storage (ES) are evaluated using cost avoidance criteria: the benefit is defined as the difference between the annual results obtained without and with SA and ES. The used metrics are the reductions in operation costs and wind energy curtailed. The value per appliance is estimated as the reductions in operation costs divided by the number of devices. The value of storage is obtained as the reduction in operation costs divided by the storage capacity.

This chapter is organized as follows: Section 3.2 gives the formulation of the DC OPF algorithm where DSR and Storage models are included as a part of the constraints. Section 3.3 defines the metrics used to evaluate the value of storage and DSR. Section 3.4 describes the GB transmission system that will be used for algorithm testing and also presents the results obtained, whilst Section 3.5 presents the conclusions.

3.2 Proposed Linear Multi-period Optimal Power Flow

A multi-period OPF whose objective is to minimize the total network operation costs is at the core of the algorithm. Since the methodology is based on a DC OPF, the optimization problem is linear. Mathematical formulation is as follows:

Minimize

$$F = \sum_{t\in\mathbf{T}}\sum_{g\in\mathbf{G}} c_g P_g(t) + \sum_{t\in\mathbf{T}}\sum_{b\in\mathbf{L_{BUS}}} c_{LS}\cdot load_shed_b(t) + \sum_{t\in\mathbf{T}}\sum_{b\in\mathbf{G_{BUS}}} c_{OS}\cdot over_slack_b(t) \quad (9)$$

The first term on the right-hand side (RHS) represents the total generation cost. The second term is the involuntary loss of load. Due to high values of the load shed costs c_{LS}, the shed power differs from zero only in the cases when there is a lack of generation or network capacity to supply the load. The third term is introduced to avoid any potential infeasibility in the solution. Decision variable $over_slack_b(t)$ represents artificial load which differs from zero only in case of low load, when the output power of the generators cannot be further lowered. Normally, c_{OS} has a very high value, so $over_slack$ variables will be used only to prevent infeasibility.

3.2.1 Power Balance Constraints

Nodal power balance constraints must be written for each bus in the network. The total power injection into each bus must be equal to the total power supplied from the bus, including power exchange with other buses. This is described by (10):

$$S_b^d(t) - S_b^c(t) + \sum_{g\in\mathbf{NG_b}} P_g(t) + load_shed_b(t) = \\ = Pd_b^{DSR}(t) + P_b^{EX}(t) + over_slack_b(t), \quad (10)$$

$\forall t \in \mathbf{T}, \forall b \in \mathbf{N_{BUS}}$

In (10), first two terms depict the storage activities: $S_b^d(t)$ is storage discharge, i.e. injecting the power into the bus b at time t, while $S_b^c(t)$ is storage charging, which is equivalent to additional demand in the bus. The third term represents generation in bus b. The last term is load shed at bus b. Load shed is applicable to load buses only and is equivalent to additional generation in the bus and so has the same sign as generation.

The first term on the right hand side (RHS) of (10) is demand, modified by demand side response. This term links the network model (OPF) with a demand control model. Demand control model may be shifting algorithm (described in CHAPTER 2, Section 2.5), EV model (it will be described in

CHAPTER 5) or any other model (such as water heaters, space heating, air conditioning etc.) suitable for load control in electricity networks, making this formulation versatile.

The second term on the RHS in (10) is the power exchange from bus b to all buses p, if bus b and bus p are connected with at least one branch of the network [71]:

$$P_b^{EX}(t) = \sum_{p \in \mathbf{N_{BUS}}} B_{bp}\delta_p(t), \qquad \forall b \in \mathbf{N_{BUS}}, \forall t \in \mathbf{T} \tag{11}$$

where δ_p is the bus p voltage angle, and B_{bp} is an element of the system susceptance matrix $\mathbf{B}$, at row b and column p [72].

It is assumed that power flows **from** bus b **to** bus p, so the positive sign for this power is **from** bus b. In this way, the (positive) exchange power is added to the total demand in bus b. The value of voltage angle in the reference bus is 0 rad (although it can be set to any other value as well).

The last term in (10) is introduced to avoid infeasibilities.

3.2.2 Network constraints

The power flowing through a branch must not exceed the thermal capacity limit of the branch. Therefore, the network capacity constraints are:

$$-C_{bp}^{branch} \le P_{bp}^{branch}(t) = B_{bp}^{branch}\left(\delta_b(t) - \delta_p(t)\right) \le C_{bp}^{branch}, \quad \forall t \in \mathbf{T}, \forall b, p \in \mathbf{N_{BUS}} \tag{12}$$

where C_{bp}^{branch} is the power limit in the branch connecting buses b and p, whilst P_{bp}^{branch} is the power flow through the branch. B_{bp}^{branch} is the reciprocal reactance of the branch connecting busses b and p whilst δ_b and δ_p are voltage phase angles in busses b and p, respectively. If there are more than one line connecting busses b and p, then this constraint is imposed to each of them.

3.2.3 Generator constraints

The output power of the generators must remain within the given limits, which are the minimum stable generation and maximum power, so the constraints imposed to each generator are:

$$P_{g,min} \le P_g(t) \le P_{g,max}, \quad \forall t \in \mathbf{T}, \forall g \in \mathbf{G} \tag{13}$$

Another set of constraints imposed to the generators is ramp-up and ramp–down constraints:

$$P_g(t) - P_g(t-1) \le Ramp_g^{up} \cdot \Delta t, \;\; P_g(t-1) - P_g(t) \le Ramp_g^{down} \cdot \Delta t$$
$$\forall t \in \mathbf{T}\backslash\{1\}, \forall g \in \mathbf{G} \tag{14}$$

These constraints prevent the generators from changing their outputs in two consecutive time steps for more than the rate defined by ramping parameters $Ramp_g^{up}$ and $Ramp_g^{down}$.

3.2.4 Storage Model – Optimal Storage Capacity Allocation

The model for optimal distribution of energy storage capacities throughout the network is developed and presented in this section.

The first group of constraints are related to storage power limits:

$$0 \le S_b^c(t), S_b^d(t) \le S_b^{\max} \qquad \forall t \in \mathbf{T}, \forall b \in \mathbf{S_{BUS}} \tag{15}$$

$\mathbf{S_{BUS}}$ is subset of $\mathbf{N_{BUS}}$ where storages are connected. Constraints (15) limit the charge power $S_b^c(t)$ and discharge power $S_b^d(t)$ so that it cannot exceed the storage rated power at any time. Storage rated power $S_b^{\max}$ is a decision variable which identifies the areas (buses) of the network where storage will bring the most benefits to the system.

Total installed storage capacity in the system is an input parameter:

$$\sum_{b \in \mathbf{S_{BUS}}} S_b^{\max} \le S_{cap}^{max} \tag{16}$$

It will be examined how this parameter impacts the benefits brought by storage.

Energy contained in storage at the end of current time step is calculated as the energy content at the end of previous time step plus energy charged during the current time step minus energy discharged during the current time step. Energy being stored is multiplied by an efficiency coefficient, which takes into account the storage energy losses. Therefore, the storage energy balance constraints are:

$$ES_b(t) = ES_b(t-1) + \left(\eta_b \cdot S_b^c(t) - S_b^d(t)\right) \times \Delta t, \qquad \forall t \in \mathbf{T}\backslash\{1\}, \forall b \in \mathbf{S_{BUS}} \tag{17}$$

where $ES_b(t)$ is the energy content in the storage at bus b at the end of the current time step, $ES_b(t-1)$ is the energy content in the same storage at the end of previous time step, η_b is storage efficiency, and Δt is time interval (1 hour).

Note that equation (17) is not defined for the first time step of the optimization horizon ($t = 1$). At the beginning, the initial energy in storage is defined as:

$$ES_b(t=1) = ES_b^{INI}, \quad \forall b \in \mathbf{S_{BUS}} \tag{18}$$

The initial value ES_b^{INI} is given as the input data.

3.3 Metrics for DSR and Storage Value Evaluation

One of goals of this research is to quantify the benefits that DSR and storage bring to the reduction in congestion costs and improvement in the utilisation of existing network capacity. The benefits are quantified using the following metrics:

3.3.1 Reduction in the cost of operation

Total operation cost for a given optimization horizon $\mathbf{T}$ is given by F in (9). In order to quantify the value of DSR and/or storage, first a base case (with neither DSR nor storage) is performed for the whole year, and the obtained value of F is recorded. Let it be F^B. Then the procedure is repeated, but this time with DSR and/or storage. The obtained value for this case is designated as F^N. The reduction in the operation cost is then defined as:

$$R_{oc} = F^B - F^N \tag{19}$$

Note that $F^B \geq F^N$, and so R_{oc} is always a non-negative number. As R_{oc} increase so does the value of DSR and/or storage.

3.3.2 Reduction in the wind curtailed in the system

One of the objectives of this work is to maximize renewable energy utilization whilst minimizing operation costs. Without loss of generality, this work will focus on wind energy. However, due to network limits, some (or all) of the wind generators must be curtailed. In order to estimate the impact of DSR and storage on the reduction in wind curtailment, the wind spillage is calculated for the base case, with no DSR/storage facility in the system; let the calculated wind curtailment for this base case is W_c^B. This quantity is calculated as the difference between total yearly available wind energy and total yearly energy actually produced from the wind generators. A similar calculation is performed for the case when DSR and/or storage is included into the system; let the obtained wind curtailment for this case is W_c^N. Then, the reduction in wind curtailment due to activity of DSR and/or storage is given as:

$$R_{wc} = W_c^B - W_c^N \tag{20}$$

3.3.3 Line utilization and Line Loading Duration Curve

The utilization of the lines in the network is characterized by the annual load factor. This metric will permit the evaluation of the benefits of DSR and/or storage as an indication of the efficient use of the existing line capacity. The load factor for branch i is defined as a ratio of the total yearly energy flow (in both directions) through a line, and maximum possible energy that could be transferred by that line (yearly transferred energy through the line at rated power):

$$LF_{branch} = \frac{\Delta t}{C_{bp}^{branch} \cdot \mathbf{T}} \sum_{t \in \mathbf{T}} \left| P_{bp}^{branch}(t) \right| \qquad \forall branch \in \mathbf{N_{BR}} \tag{21}$$

The line utilization factor is between $0 \leq LF_i \leq 1$ and the closer the factor to 1, the better the line utilization, but also it may indicate highly congested branches. This metric can be used to investigate how DSR and/or storage influence the utilization of the lines by comparing its value with the base case (without DSR and storage).

Line Loading Duration Curve is a sorted (usually in descending order) power flow through a line during the year. It can give some visual impression of impact of DSR and/or storage technologies to the utilization of the network lines.

3.3.4 Value of Smart Appliances and Storage

Value per appliance is obtained simply by dividing the reduction in operation cost (R_{oc}) by the total number of devices available for shifting in the system:

$$V_{avg} = \frac{R_{oc}}{\sum N_i} \tag{22}$$

where N_i is the number of type i devices. The average value per appliance is the annual saving attained by one shifting device.

If the value per appliance of specific type is of interest, it may be determined through DSR activity. DSR activity is defined as amount of shifted energy multiplied by the shifting time. Now, the value per appliance of specific type becomes:

$$V_i = \frac{DSR_{i,activity}}{\sum DSR_{i,activity}} \cdot \frac{R_{oc}}{N_i} \tag{23}$$

Note the total number $\sum N_i$ of shifting devices (for all types) is used in denominator in Equation (22), in contrast to (23), where only the number N_i of devices of the specific type is used.

The values obtained in (22) and (23) are then capitalized by multiplying them by present worth inflation series factor, which is defined as [67]:

$$PWV = \frac{1 - \left(\frac{1+a}{1+i_r}\right)^n}{i_r - a} \tag{24}$$

where i_r is the interest (discount) rate, a is the inflation rate and n is a time span of interest given in years.

The value of one installed kW of storage capacity is obtained by dividing the reduction in operation cost by the total installed storage capacity in the system:

$$V_{sto} = \frac{R_{oc}}{\sum_{b \in \mathbf{S_{BUS}}} S_b^{\max}} \quad (25)$$

where $S_b^{\max}$ is the capacity of storage allocated to bus b. The value of storage represents savings attained by one installed kW of storage. Capitalized value of storage is obtained by multiplying V_{sto} by PWV.

3.4 Case Study

The problem of lack of network capacity is emphasized with the intention to produce more energy from intermittent sources, especially wind generators from remote areas, far from demand centres. In this condition, especially regarding UK transmission system, with limited capacity between the northern part of the network where most wind generation capacity is planned to be built and the southern part of the network where the large demand centres are placed, a problem of energy shipping from one part of the network to another one, arises. This is why the first set of studies is focused on increasing wind penetration levels at which the value of DSR and storage is explored.

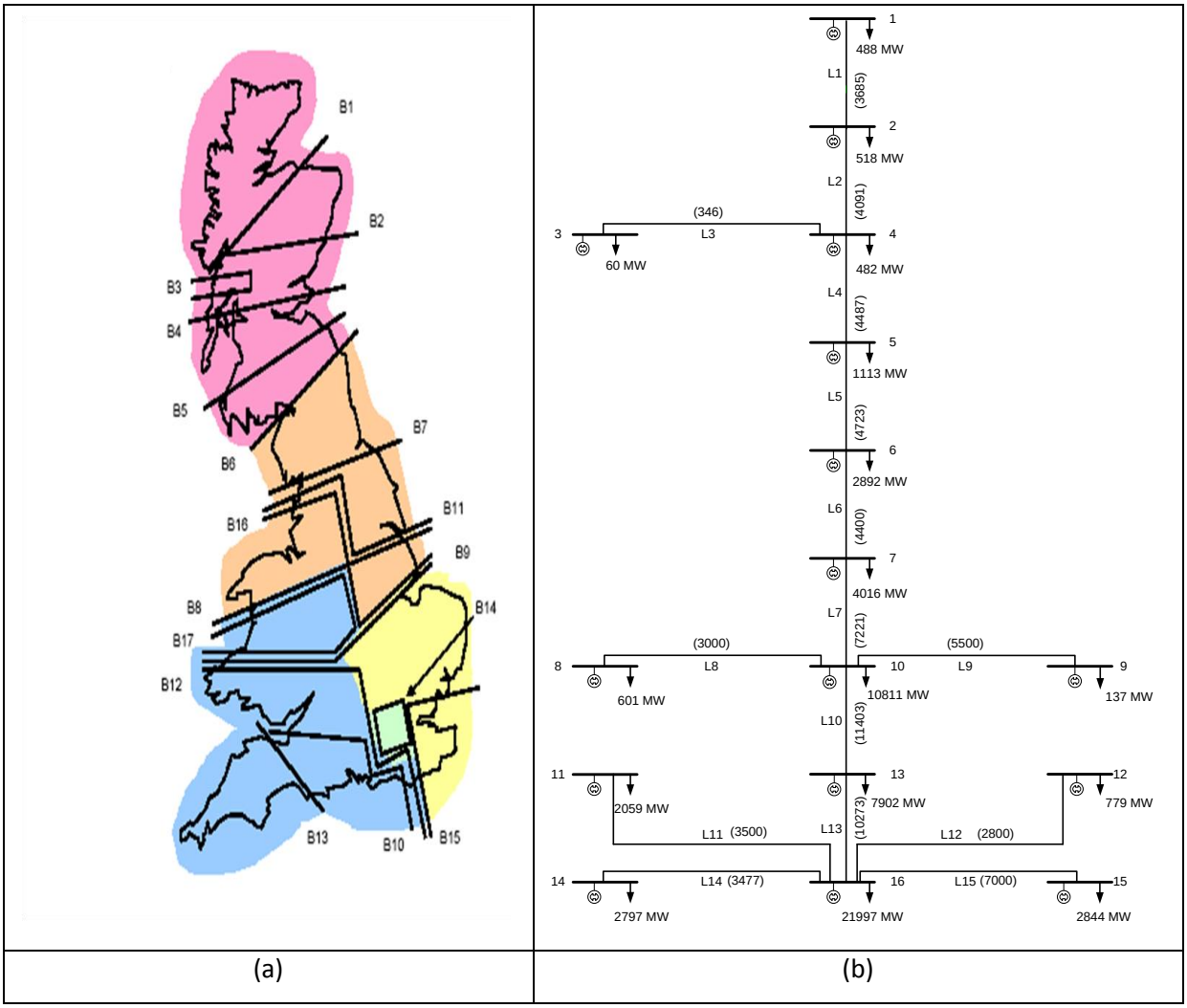
The problem of network congestion also rises with load growth: larger amounts of energy must be generated and transmitted to the load, which means that network capacity might become even more critical. A set of simulations is made to determine a value of DSR and storage under these conditions.

Finally, a sensitivity analysis regarding generation flexibility is performed. Generation inflexibility itself does not cause network congestion, but in case of high wind penetrations may lead to a huge amount of wind curtailment. In that case, DSR and storage bring additional flexibility to the system, which is otherwise provided only by generators, and thereby ensure smooth system operation. This will also add a value to DSR and Storage facilities.

The studies are intended to provide both qualitative and quantitative analyses of the value that DSR and storage bring to the system operation as well as the impact of the parameters outlined above on their value. Results obtained can be used to assess a techno-economic viability of DSR and Storage and their integration in congested networks.

3.4.1 Test System

The proposed DC algorithm has been tested on the network representing the GB transmission system. The GB system could be conveniently divided in 16 areas, symbolizing 16 Great Britain zones. The zones are connected with 15 branches representing the main transmission boundaries, as shown in Figure 3-1a [73].



(a) (b)

Figure 3-1: GB transmission system boundaries (a) and the sixteen bus-bar diagram (b)

If each zone is symbolized by a single bus, then a 16 bus-bar system is obtained, the electrical diagram of which is shown in Figure 3-1b. Line capacities (in MW) are shown in the parentheses next to each line. Peak demand for each bus is also shown in the same figure, next to the corresponding bus, indicated by an arrow. Total peak demand for the whole system is 59.5GW and total yearly energy consumption is 344TWh. Wind power and demand are given as yearly time series in hourly resolution.

There are ten different types of generation (i.e. ten different generator technologies): wind, nuclear, marine, gas, coal, other renewable, water, marginal gas, marginal coal and peakers. All generators of the same type attached to the same bus of the network are aggregated together and represented as one single entity. As a result, a total of 68 units in the system are obtained. Total installed conventional generation capacity is about 70GW. Table A. 3-1 in APPENDIX 3 details the distribution of generation capacities amongst technologies and network buses, and also lists the production cost and CO_2 emissions per MWh produced for each technology. In this case study, the chosen network

and generation capacity, including the wind installed capacity, describe GB system in period 2016-2020, according to DTIM User report [74].

Figure 3-2a shows wind and total generation capacity distribution on network buses for the case of 20% wind penetration[7]. Distribution of load (peak values) among buses is represented in Figure 3-2b.

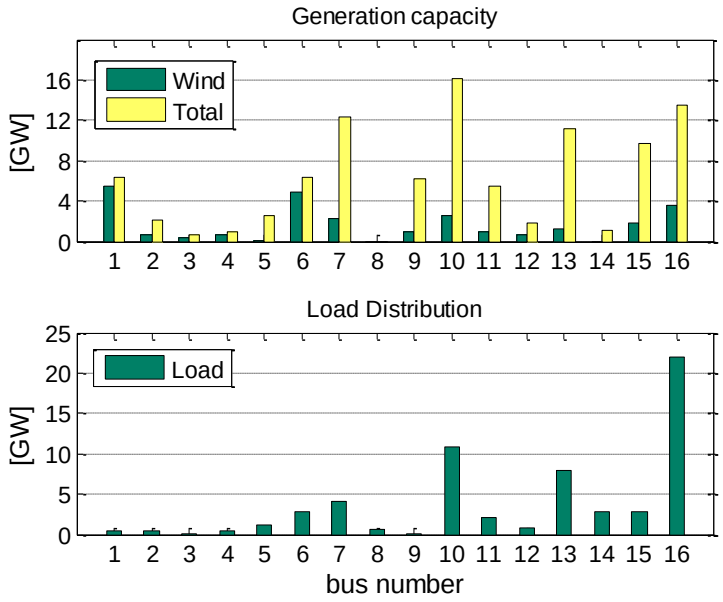


Figure 3-2: Distribution of wind and total generation capacity (a) and distribution of load (b) on network buses

In the northern part of the UK (buses 1 to 7) there are less generation and less demand, but there is relatively high wind penetration – more than a half of total wind capacity is installed in this part of the network. In the southern part of the UK (especially in buses from 10 to 16) there is much more conventional generation and also large demand centres. Under such conditions, congestion problems arise during high wind periods when the energy produced by wind generation in the north is to be shipped to the south.

3.4.2 Reference case results

This section diagnoses the status of the system in terms of network capacity and its ability to integrate wind. For that reason, various wind penetration levels are considered: 0%, 10%, 20%, 30% and 50% of the yearly energy consumption (344TWh).

As wind penetration increases, wind curtailment also increases, which is shown in Table 3-1. At lower wind penetrations (around 10%) there are no congestions in the network and all available

[7] Wind penetration is defined as yearly available wind energy compared to the yearly energy demand.

wind energy is absorbed by the system. At higher wind penetrations (30% and more) wind is curtailed not only because of network congestion, but also due to lack of demand (in some periods demand is lower than available wind power) and due to nuclear generators inflexibility.

Table 3-1: Reference case results vs. wind penetration

Wind penetration [% of yearly energy demand]	0	10	20	30	50
Wind penetration [TWh]	0	34	68	103	172
Wind Curtailment [% of available wind energy]	0	0	4	12	24
Operation Costs [x 10^3 M£/year]	11.64	9.69	8.39	7.48	6.12
CO_2 emissions [x 10^6 ton / year]	142	123	107	94	74

Apart from wind curtailment, two other variables will be particularly analyzed. These are yearly operation costs and CO_2 emissions. Table 3-1 shows both yearly operation costs and CO_2 emissions decrease with wind penetration. This is not surprising result, as it is assumed no cost and zero carbon emissions are assigned to wind energy.

Just as an example of the congestion in the network, Figure A. 3-26 in APPENDIX 3 shows a snapshot taken during maximum wind (hour 6124) in the system with 20% of wind penetration. In this particular system condition, total available wind power has a maximum of 26098MW, while demand is 38837MW. Line 7 (connecting Bus 7 and Bus 10) is highly congested being a bottleneck in the system. Because of this congestion, a part of wind energy in the northern buses (Bus 1 – Bus 3) cannot be used and must be curtailed. All other wind generators are at maximum output, giving total of 20350MW to the system.

3.4.3 DSR Results

In the UK power system, there are about 25 million households. For this analysis, the shifting algorithm and smart appliances explained in CHAPTER 2 are simulated. Main characteristics of the devices are as given in Table 2-2.

In order to explore the role of the smart appliances thoroughly and to find all the sources of the benefits they bring to the system, a sensitivity analyses regarding changes in various system and DSR parameters is performed. The following variations in the input parameters have been explored in particular:

- increase of wind penetration
- increase of load

- increase of generator flexibility
- increase of DSR penetration and flexibility

However, to get a more global picture of the role of DSR and to analyze which of the parameters are more influential, it was necessary to observe the variations in several parameters altogether, making a systematic sensitivity analysis.

Increase of wind penetration

This section explores the effects of smart appliances when wind penetration takes 0, 10%, 20%, 30% and 50% of the yearly energy consumption.

Together with wind changes, various levels of smart appliances penetration are taken, i.e. 10%, 50% and 100% of the value given in Table 2-2. These penetrations are designated as “Low”, “Medium” and “High” in Table 3-2, respectively. Another parameter that is also influential to the benefits of smart appliances is their flexibility in terms of shifting capabilities. “Normal” DSR flexibility is defined in column ‘Max. Delay’ in Table 2-2. Besides that, two other extreme shifting capabilities have been analyzed: low flexibility (all smart appliances cannot be shifted for more than 1h), and high DSR flexibility (all smart appliances can be shifted up to 12 hours). For clarification, this information is tabulated in Table 3-2.

Table 3-2: Smart appliances parameters variations

Device Type	Flexibility [h]			Penetration factor [%]			No. of devices for 100% penetration [million]
	Low	Normal	High	Low	Medium	High	
WM1	1	1	12	2	10	20	5
WM2	1	2	12	2	10	20	5
WM3	1	3	12	2	10	20	5
DW	1	6	12	8	40	80	20
WM+TD	1	3	12	2	10	20	5

The effect of DSR on reduction in wind curtailment is given in Figure 3-3.

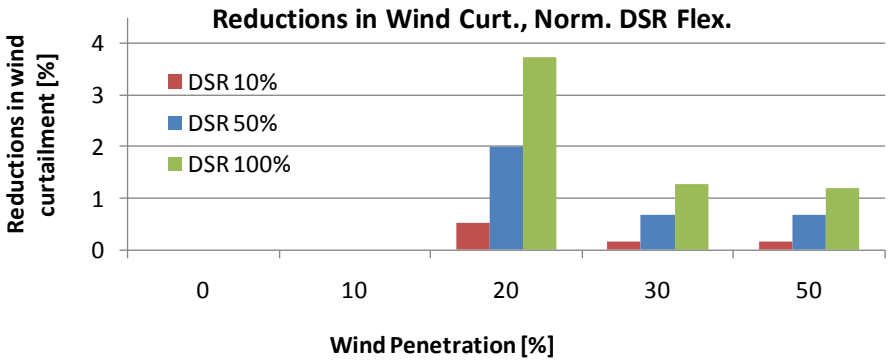


Figure 3-3: Effect of DSR on reduction in wind curtailment

For a wind penetration of 10% the system is capable of absorbing all the available wind energy. With further wind penetration, DSR helps the system to absorb more wind. However, since DSR capabilities are limited, higher wind penetrations lead to more and more wind energy being curtailed in spite of DSR presence. That is why the wind curtailment reduction, relative to wind curtailed energy starts decreasing. Figure 3-3 also shows that reduction in wind curtailment increases with penetration of smart appliances. The analysis also suggests the higher the DSR flexibility, the higher the reduction in wind curtailment (see Figure A. 3-1 in APPENDIX 3). In general, wind generation capacities are located in the areas far from demand centres, and due to a congested line between them DSR has a low impact on reduction in wind curtailment.

Figure 3-4 shows the impact of DSR on reduction in generation costs. The results are given relative to the base case, which is equivalent to 0% DSR penetration.

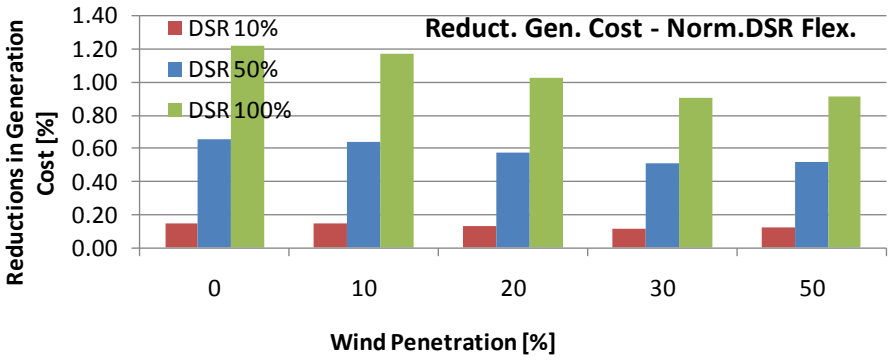


Figure 3-4: Effect of DSR on reduction in generation costs

Reduction in generation costs is defined as the difference between generation costs without DSR and the costs with DSR (see also Section 3.3.1, Eq. (19)). It can be noticed that the higher reduction in generation costs is obtained for low wind penetrations. When there is no wind, the most expensive generators are dispatched during peak periods. DSR reduces the need to use these most expensive generators and instead it displaces them with several times less expensive ones. However,

when there is wind energy available in the system, the most expensive generators are displaced in favour of wind generation (see also operation costs row in Table 3-1). Thus the number of hours when the most expensive generators are used is reduced, and the reduction in generation cost is now obtained by replacing the less expensive generators with cheaper ones which brings smaller benefit to the system. At the same time, total generation costs also decrease with wind penetration (Table 3-1). The relative reduction in generation costs for this system lies within a narrow range 0.2-1.2%. Reduction in generation costs also increases with both penetration of smart appliances (Figure 3-4) and DSR flexibility (see Figure A. 3-2 in APPENDIX 3).

Adjustment in generation for each generator technology, due to DSR action, is given in Figure 3-5 for different levels of wind penetration.

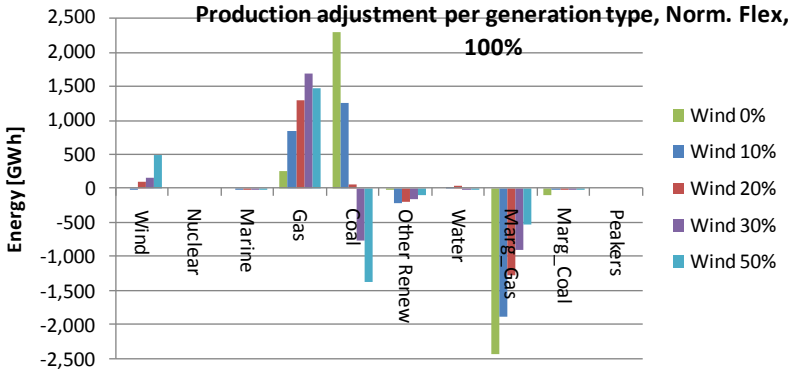


Figure 3-5: Effects of DSR on generation adjustment (per technology)

The intensity of generation adjustments depends largely on DSR flexibility (see Figure A. 3-3 in APPENDIX 3). However, the pattern of adjustments depends on generation technology and on wind penetration.

When a detailed time evolution for each generation type is examined, it can be noticed that in the case of normal DSR flexibility and zero wind, in winter time when the load is generally high, there is a shift from marginal gas to coal generation. The same happens in spring and summer during peak times. When there is wind installed, marginal gas generators are partly displaced by wind. In winter time, during peak hours, there is shift from marginal gas to coal, and in off-peak there is shift from marginal gas and coal to gas. In spring and autumn, since marginal gas is already displaced by wind, there is a shift from coal to gas (which does not bring that much benefit due to relatively small difference in generation cost of these two technologies). Also note that as wind penetration increases, the wind generation adjustment also increases, since there are more periods when the wind has to be shed, but now DSR moves demand to the periods of high wind thus reducing wind curtailment.

Figure 3-6 shows reduction in cost per generation type. The results are given relative to the base case, which is equivalent to 0% DSR penetration. It can be seen that one of the most expensive generators – marginal coal generators reduce their cost (which means reduce their production) for about 80% due to DSR activity. Other expensive generators, such as Marginal Gas and Other Renewable reduced their cost (production) up to 20%. Cheaper generation technologies increased their production and so their cost reduction is negative. However, since these technologies produce most of the demanded energy, their relative cost increase is insignificant. Wind generation also increase production, but as it is assumed that wind energy has zero cost (in order to prioritize wind energy utilization), there is no cost increase for this generation.

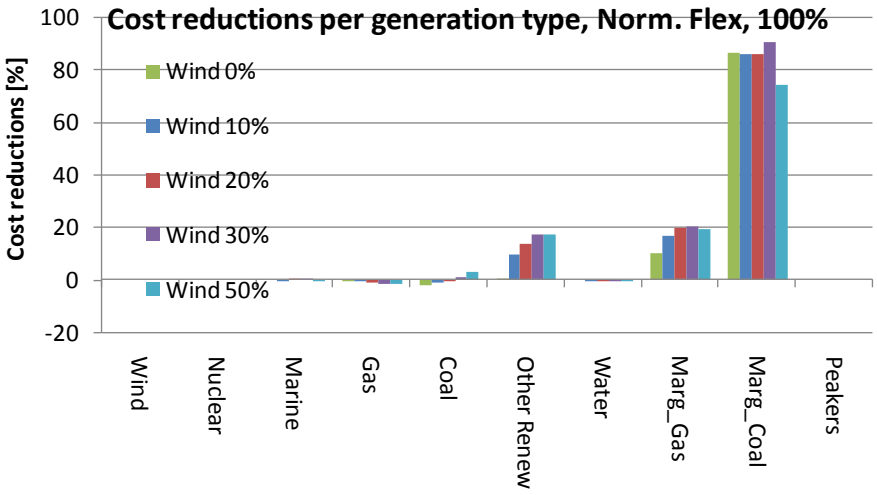


Figure 3-6: Reduction in production cost per technology

Another important quantity that has been analyzed, especially in the context of electric power system impact on environment, is CO_2 emissions. Values of emissions [kg CO_2 /MWh] for each technology type are given in Table A. 3-1 in APPENDIX 3. Based on these values and the generation adjustment per technology (Figure 3-5), the reductions in CO_2 emissions are obtained.

In the case of low wind penetrations, there is generally a shift from marginal gas to coal generation, as explained previously (Figure 3-5). As the coal generators have higher CO_2 footprint than marginal gas generators, there is a negative impact of DSR on CO_2 emissions. This is illustrated in Figure 3-7.

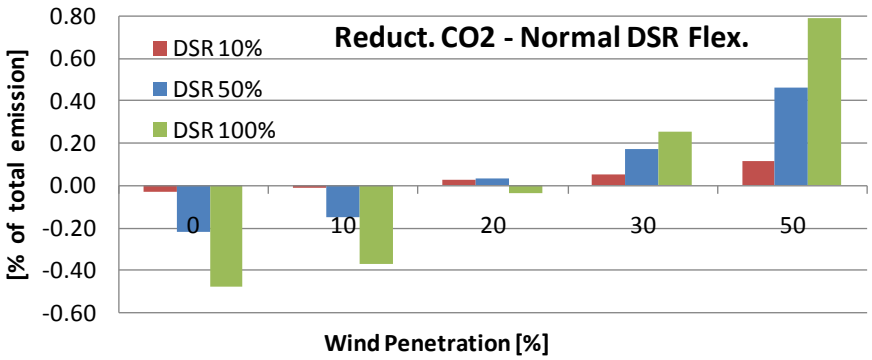


Figure 3-7: DSR effect on reduction in CO_2 emissions

It can be noticed that reductions in CO_2 emissions increase with wind penetration. In systems with higher wind penetrations (30% and more), marginal gas generators are partly displaced by wind generation and so there is mostly a shift from coal to gas generation. Since coal has almost double CO_2 emissions than gas, there is a positive impact of DSR on reduction in CO_2 emissions. Coal generators will be less dispatched as wind penetration further increases so this shift from coal to gas generation will be reduced. In that case the additional reduction in CO_2 emissions comes from wind curtailment lessening as wind generation is assumed to be carbon free. Reductions in CO_2 emissions increase as both DSR penetration and DSR flexibility increase (see Figure A. 3-4 in APPENDIX 3).

Obtained changes in CO_2 emissions are relatively small, order of magnitude of 1% for 100% DSR penetration. However, it should be noted that CO_2 emissions were not included in the model, as it was not the main focus of the research. However, CO_2 emissions can easily be included by introducing a new term in the objective function (9), whereby production for each generation type could be weighted with a CO_2 emissions factor from Table A. 3-1 in APPENDIX 3.

Figure 3-8 shows capitalized value per appliance, for normal DSR flexibility and for different wind and smart appliance penetration levels. For this work, the capital interest rate of 10%, inflation rate of 0% and life span of 10 years is used, giving the present worth value factor $PWV = 6.145$ (see Section 3.3.4, Equation (24)).

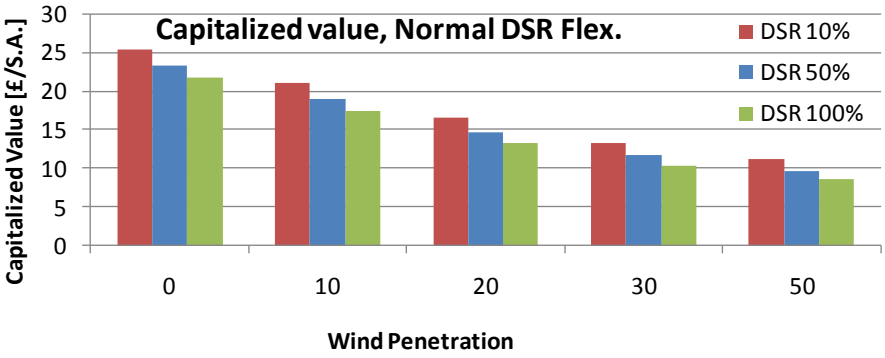


Figure 3-8: Average capitalized value of DSR per appliance

The value comes only from reduction in generation cost. From definition (22) it is notable that capitalized value is proportional to reduction in generation cost, and inversely proportional to the number of shifting devices. Reduction in generation cost increases with increased number of shifting devices but at lower rate than the number of devices. That is why the value per appliance decreases with increasing penetration of DSR even though the reduction in generation cost increases. It has a significant consequence that the first installed device (or the first installed MW) of DSR has the highest value. As the reductions in operation costs decrease with wind penetration, so does the capitalised value of smart appliance. Figure 3-8 illustrates that capitalized value of DSR for this specific system is relatively low, being in range from £10 to £25 per appliance. Capitalized value also increases with DSR flexibility, as shown in Figure A. 3-5 in APPENDIX 3.

Capitalized value per appliance type is obtained as explained in Section 3.3.4 and shown in Figure 3-9 for case of normal DSR flexibility and 100% DSR penetration.

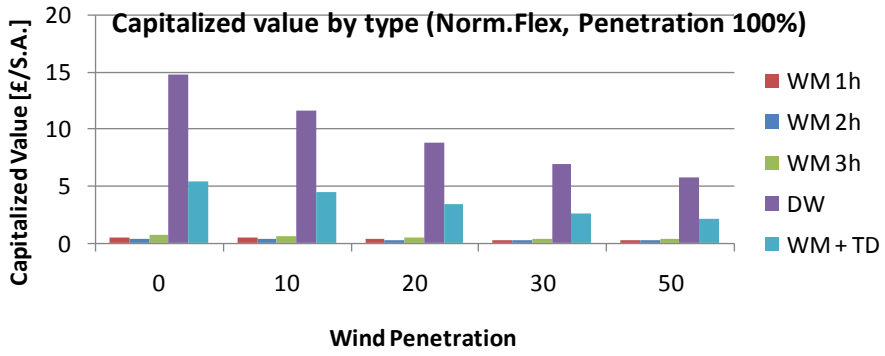


Figure 3-9: Capitalized value per type of device

It can be seen that dishwasher (DW) brings the highest value to DSR. The reason for this is because DW has the highest penetration and highest flexibility compared to the other types of devices. Due to high flexibility of DW, they will always be shifted into the periods of high wind, thus reducing wind curtailment and the operation costs. Consequently, their value will be higher comparing to the less

flexible types of appliances. Also even though WM+TD have the same penetration as WM1h, WM2h or WM3h, which is much less than DW, the value of this type of device is relatively high. The reason for this is that the activity of this device is also relatively high (compared to its penetration), since the energy shifted by one single WM+TD device is 3.3475kWh, which is almost double than DW and almost four times more than washing machines. So, even though the number of WM+TD devices is relatively small, the energy shifted by them is still significant.

Increase of load

This section considers increase in load and its influence on the benefits of flexible demand. Each year load increases due to connection of new customers, industry expansion, increasing life standard of the existing customers, or electrification of non-electric sectors such as space or water heating and transport. International Atomic Energy Agency (IAEA) predicts the average annual growth in electricity generation in period 2000-2030 to be around 2.4% [75]. Growth in electricity generation in year 2010, comparing to year 2009 in the UK was 1.2% [76]. An average annual UK supply growth from 1970 to 2009 had a rate of 1.5% [77].

The starting point for the analysis is the system described in reference case, Section 3.4.2, with wind penetration fixed to 30% of yearly energy demand. Considered scenarios are load increase for 10% and 15% comparing to reference case. The other network parameters remain the same.

The first point to note is that as the load increases there is a reduction in wind curtailed, as shown in Table 3-3 (values are obtained without using DSR).

Table 3-3: Wind curtailment for different levels of load

Load increase [%]	0	10	15
Wind Curtailment [TWh/year]	12.5	11.1	10.6
Wind Curtailment [% of available wind energy]	12.2	10.9	10.3

As the load grows, during high wind periods, the part of the wind that would otherwise be curtailed now is used to supply increased load. In other words, increase of load naturally reduces wind curtailment. However, as load grows from 10% to 15% there is a relatively small difference in wind curtailed reduction, only 0.6%. Because of highly congested line L7 (Bus 7 – Bus 10) wind generators in the north are not able to supply demand in the south during high wind periods. Specifically, of all wind energy curtailed, about 99% is in buses 1 – 4, as shown in Figure 3-10.

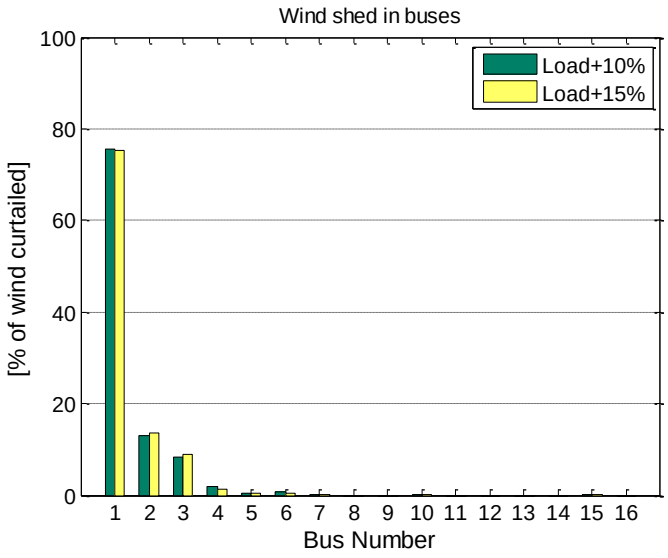


Figure 3-10: Distribution of wind curtailment on network buses

DSR has a positive impact on wind curtailment, as shown in Figure 3-11.

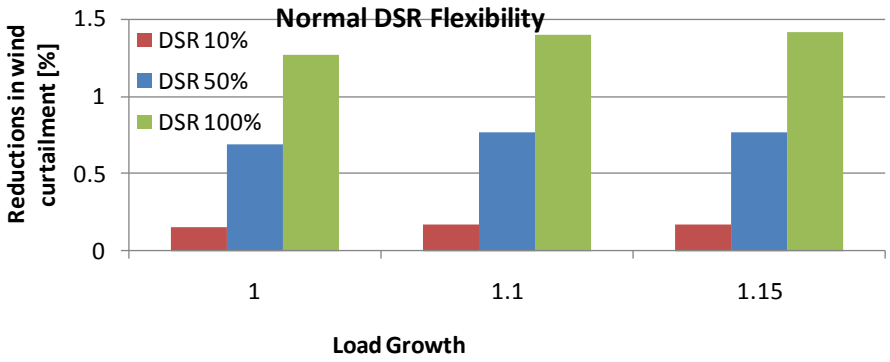


Figure 3-11: Effect of DSR on reduction in wind curtailment as load increases

As load grows, the periods of excess of wind are reduced and so DSR has less opportunity to reduce wind curtailment any further. This is emphasized by the fact that demand centres, where DSR is available, are remote from wind generators. Hence the reduction in wind energy curtailed decreases (in absolute values) slowly as load increases. Also, increased load naturally reduces wind curtailment, so the relative reduction in wind curtailment grows with load. Reductions in wind curtailment increase with both penetration of smart appliances (Figure 3-11) and their flexibility (Figure A. 3-7 in APPENDIX 3).

Figure 3-12 shows the reduction in generation cost.

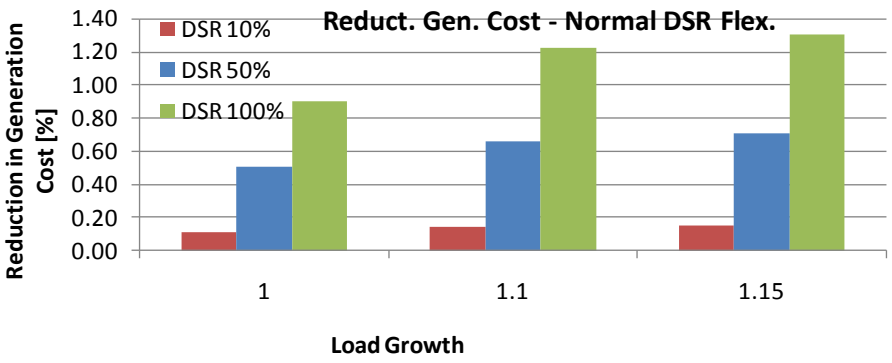


Figure 3-12: DSR impact on Reduction in operation cost as load increases

As load increases generation cost also increases. To cover high load and low wind periods the most expensive generators (marginal and peakers) must be dispatched. Any avoidance of using these expensive generators will bring significant reduction in system operation costs. As these generators are near demand centres, DSR has an opportunity to act and reduce generation costs. As load grows, this effect is more expressed. Figure 3-12 shows the reduction in operation cost increases with penetration of smart appliances. Figure A. 3-8 in APPENDIX 3 shows the reduction in operation cost increases with DSR flexibility.

Impact of DSR on reduction in CO_2 emissions is given in Figure 3-13. It can be noticed that changes in CO_2 emissions intensify with DSR penetration (and DSR flexibility, as shown in Figure A. 3-9 in APPENDIX 3).

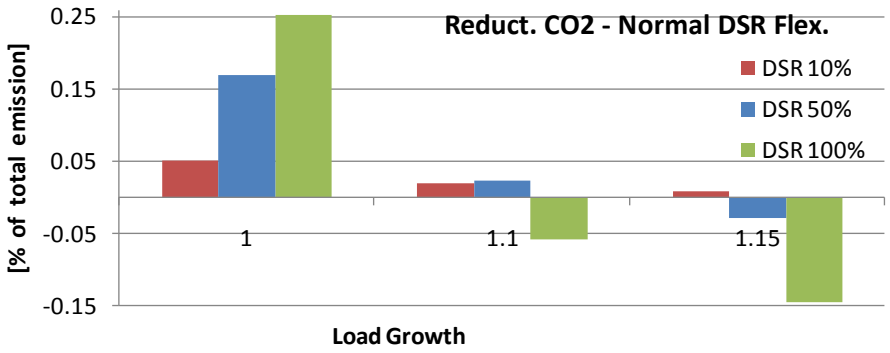


Figure 3-13: DSR impact on reductions in CO_2 emissions vs. load growth

Load growth has a negative impact on CO_2 emissions. It can be explained by observing Figure 3-14.

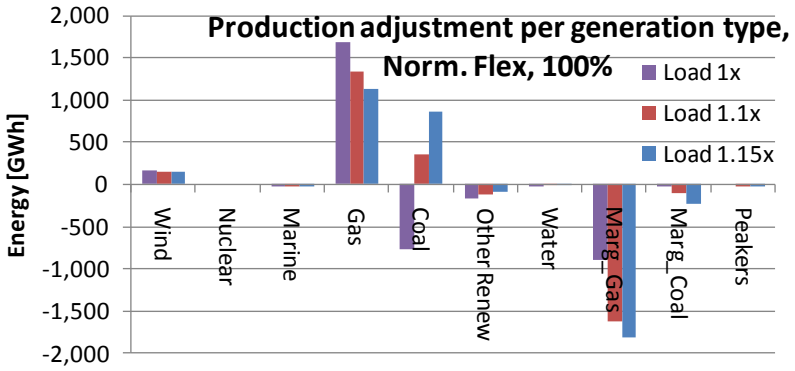


Figure 3-14: Production adjustment per generation type, for normal DSR flexibility, 100% DSR penetration

For the case when load is not increased (case "Load 1x"), DSR helps to shift generation mostly from coal and marginal gas generators to gas and wind generators. Due to the high differences in CO_2 emissions between coal (700 $kgCO_2$/MWh) and gas (390 $kgCO_2$/MWh) generators, there is relatively high reduction in CO_2 emissions in this case. As load grows, DSR increases the shift from expensive marginal gas generators to gas generators, which does not impact CO_2 emissions, and also from marginal gas generators to coal generators which actually increases CO_2 emissions.

DSR activity for different DSR penetration and for different load levels is given in Figure 3-15. DSR activity increases with both DSR penetration and flexibility (see also Figure A. 3-10 in APPENDIX 3). Load growth also has a positive impact on DSR activity. As load grows, the number of hours when the most expensive generators (marginal and peakers) are used also increases, which gives more incentives and opportunities for DSR to act.

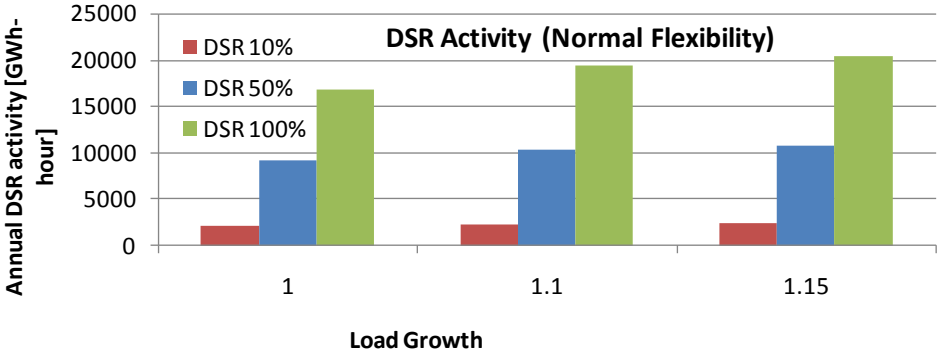


Figure 3-15: DSR activity for load growth

Capitalized value of DSR is given in Figure 3-16. From this figure, it can be seen that the capitalized value grows with load, whilst it decreases as DSR penetration rises (this last phenomenon has already been explained in Figure 3-8). As load grows expensive generators are used, so the cost reduction is also higher whenever these generators are avoided.

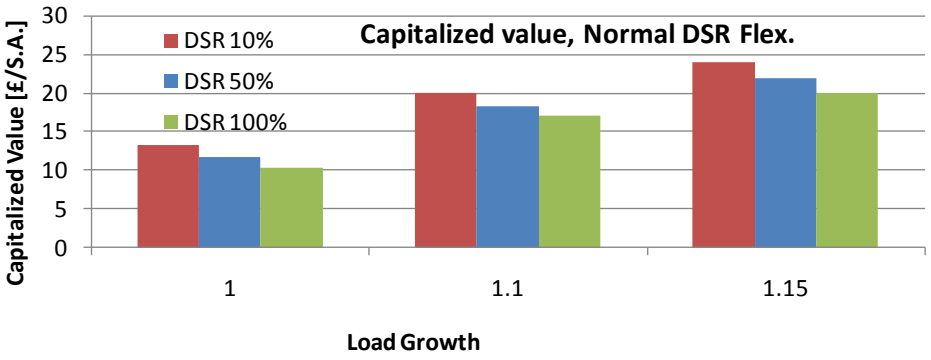


Figure 3-16: Capitalized value of DSR vs. load growth

Impact of generation flexibility

In this section the impact of generator flexibility on the value of DSR is analysed. Generator's flexibility is defined as its capability to increase or reduce its output within a specified time span and is determined by ramping up and ramping down constraints (through parameters $Ramp_g^{up}$ and $Ramp_g^{down}$ in Equation (14), Section 3.2.3). More flexible generation is more capable of responding to sudden and abrupt changes in load or wind penetration.

Even though these parameters may differ from individual generator to individual generator, it is more common to classify the generation technologies according to their flexibility. For example, nuclear generators are usually denoted as inflexible ($Ramp_g^{up} = Ramp_g^{down} = 0$). Coal generators are usually classified with low values of flexibility and gas turbines and hydro generators are often classified with high values of flexibility.

For the purposes of this research generator flexibility is grouped into three categories as shown in Table 3-4. Here, ramping up and down parameters are given in per cent of maximum generator output.

Table 3-4: Considered generation flexibility levels

Flexibility	$Ramp_g^{up}$	$Ramp_g^{down}$
	[% of generator max. power]	
Low	10	10
Medium	15	15
High	30	30

Values in Table 3-4 assume the same flexibility (low, medium or high) for all generator technologies. The exceptions are nuclear generators that are treated as inflexible (they cannot change their

output) and wind generators that are driven by wind available (no ramping constraints on wind generation). Corresponding reference case is 30% of wind penetration.

Figure 3-17 shows wind curtailment versus generation flexibility. As expected, with low generation flexibility, the system is less able to capture available wind. As conventional generation flexibility increases, curtailed wind energy decreases, because now generators can follow the wind, i.e. they can reduce their production when wind hastily increase. Even with higher generation flexibility, there are still some wind energy curtailed caused by network congestion and lack of demand.

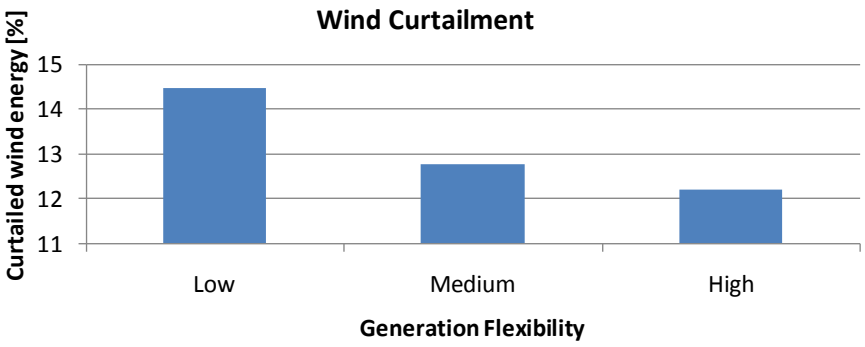


Figure 3-17: Wind curtailment vs. generation flexibility

As shown above, increased generation flexibility reduces wind curtailment. It means the number of time periods when conventional generators cannot reduce their production as fast as wind increases, is reduced as flexibility increases. So DSR has fewer opportunities to lessen already decreased wind curtailment, as shown in Figure 3-18.

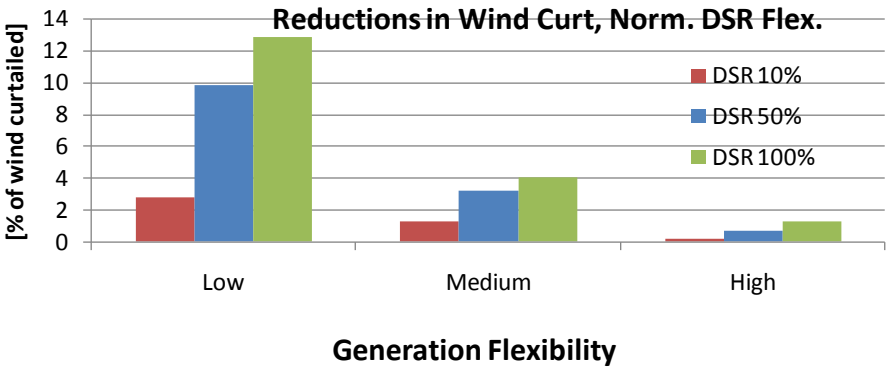


Figure 3-18: Effect of DSR on reduction in wind curtailment vs. generation flexibility

Figure 3-19 shows the impact of DSR on reduction in generation costs.

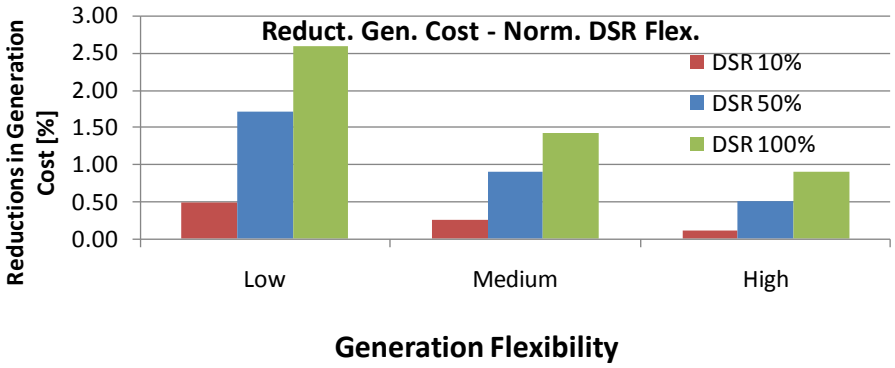


Figure 3-19: Reduction in generation cost vs. generation flexibility

It can be seen that the highest reduction in generation costs is obtained for low generation flexibility. In low flexible systems as load rises, even the amount of load is not high, but the slope of load increase is steep, more expensive generators are dispatched in order to follow this increase in load. Similarly, in order to track the rate of load lowering, expensive marginal generators have been dispatched even though there is enough capacity in gas and coal generators. With DSR, the need to dispatch expensive marginal generators is reduced thereby reducing the costs. The benefits of DSR thus come from lowering the slope of load (both when it rises and falls). This effect is reduced with higher generation flexibility, when conventional generators can match production with load changes and so the system will not use expensive generators. The significance of the lower slope of demand curve when DSR is applied lays in the fact that the requirements for fast acting generators are reduced. As the fast acting generators have high production costs, their avoidance will lead to the significant cost reductions. This is a very important finding of the research, which has not been found in the open literature.

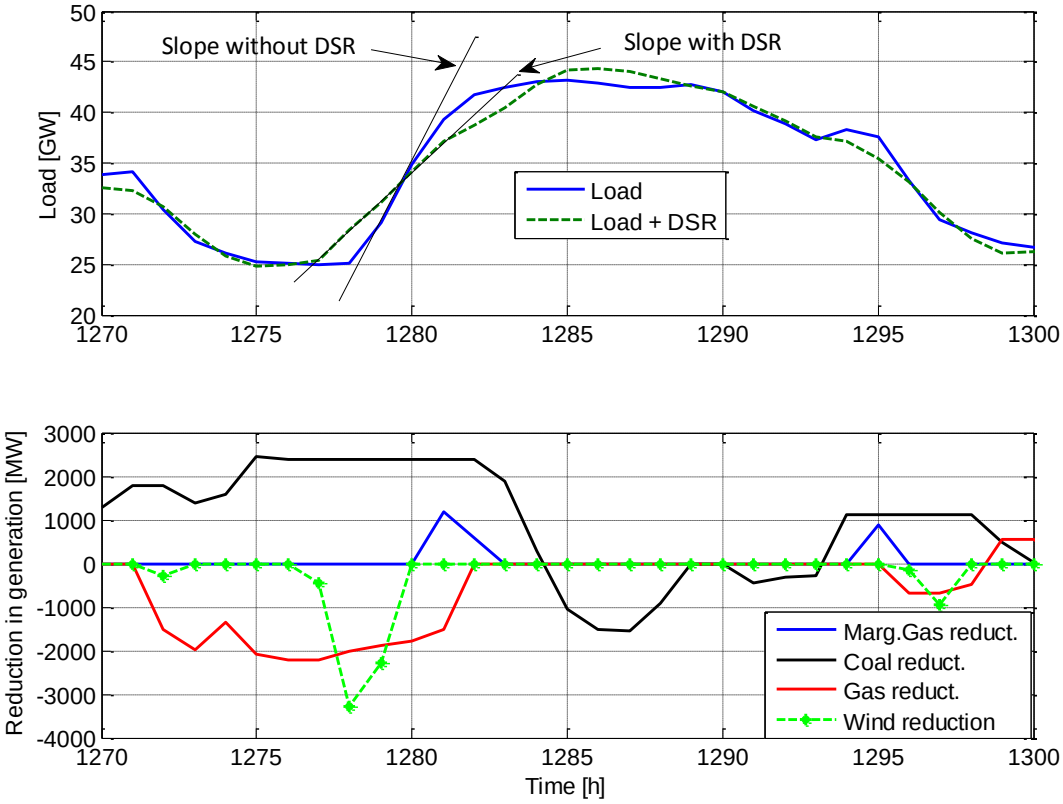


Figure 3-20: DSR impact on reduction in the slope of load changes

Figure 3-20 (upper chart) shows that DSR reduces the slope of load changes in the low flexible system. Without DSR the load increase is steeper, and so the system had to curtail wind and dispatch more coal generators between the hours of 1276 and 1280. If it used wind instead, then when the slope is the steepest (hour 1279-1280), system could not increase generators production enough to cover the rise in load. Even when the coal generators have been committed the system has to dispatch marginal gas generators. Figure 3-20 (lower chart) shows the reduction in generation when DSR is applied. It can be seen that in between the hours of 1276 and 1280 there is negative reduction in wind, meaning wind generators increase the output. Wind and gas generators are more used instead of coal. Reduction in marginal gas generators at time of the steepest increase and decrease of load is also notable.

Impact of DSR on system-level reduction in CO_2 emissions for different generation flexibility levels is given in Figure 3-21.

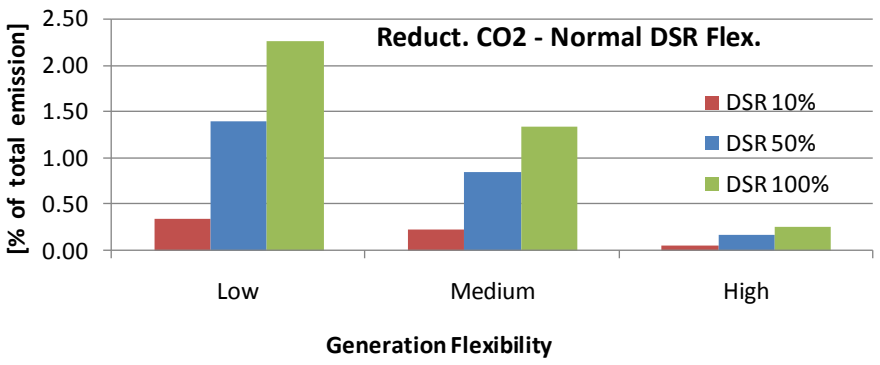


Figure 3-21: Impact of DSR on reduction in CO_2 emissions vs. generation flexibility

It can be seen that reduction in CO_2 emissions decreases as generation flexibility rises. As generation flexibility increases more wind is integrated in the system and so there is less opportunity for DSR to make a shift from coal and gas generators to wind. When DSR is applied in more flexible systems, there is a shift from coal to gas generators thus decreasing the reduction in CO_2 comparing to less flexible systems.

DSR activity for different DSR penetration and for different generation flexibility is given in Figure 3-22. Whilst DSR activity increases with DSR penetration, it decreases with generation flexibility. As generation flexibility increases, the number of hours when the most expensive generators (marginal and peakers) are used decreases, which gives fewer opportunities for DSR to be used.

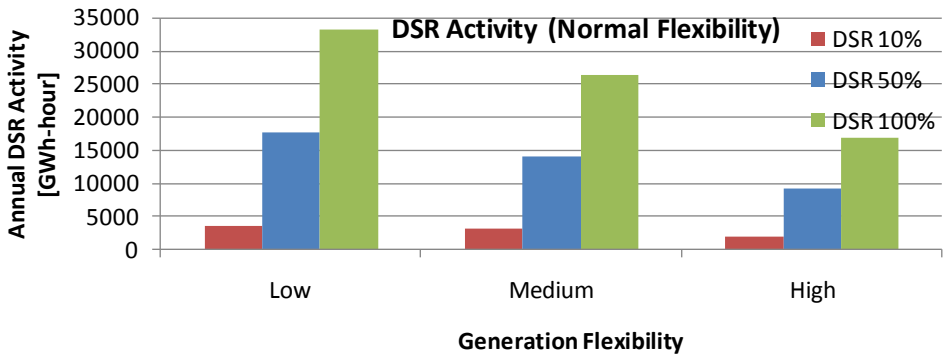


Figure 3-22: DSR activity vs. generation flexibility

Capitalized value of DSR is given in Figure 3-23. From this figure, it can be seen that the capitalized value decreases with both DSR penetration and generation flexibility. The reason for this is as generation flexibility grows there is less need for high expensive generators, so the cost reduction also shrinks.

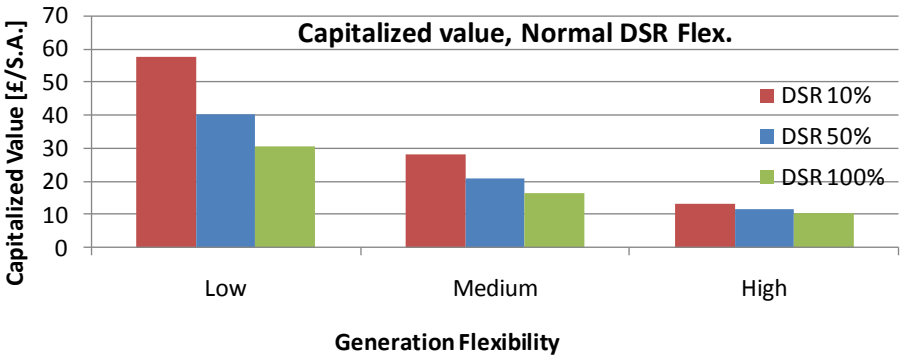


Figure 3-23: Capitalized value of DSR vs. generation flexibility

3.4.4 Storage Testing on a DC Model

In this section, the role of storage in the UK transmission system is examined. Similar to DSR, the following scenarios will be considered regarding changes in:

- Wind penetration
- Load growth
- Generation flexibility

As explained in Section 3.2.4, given the total storage capacity, the optimization model will allocate this capacity among buses, minimizing the total operation costs. From this it may be concluded which buses are the optimal location(s) for the storage. System parameters are the same as before.

Sensitivity analysis is made in terms of total storage capacity and storage efficiency, for all combinations of values shown in Table 3-5. The assumed storage energy capacity is 120h discharging at rated power.

Table 3-5: Considered values of total storage capacity and storage efficiency

Parameter	Value		
Total Storage Capacity [GW]	2.5	5	7.5
Storage efficiency [%]	80	90	100

Changes in wind penetration

This section is intended to explore the effects of storage when wind penetration takes 0, 10%, 20%, 30% and 50% of the yearly energy consumption (see Table 3-1).

The effect of Storage on reduction in wind curtailment is given in Figure 3-24.

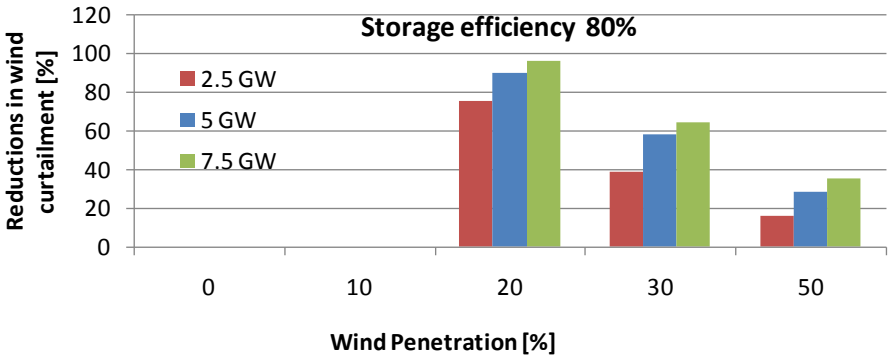


Figure 3-24: Effect of Storage on reduction in wind curtailment

For wind penetration of 20%, a total storage capacity of 2.5GW brings significant reductions around 80% in the wind curtailed. The portion of saved wind energy increases with storage capacity. As the wind penetration increases, wind curtailed also increases so the relative wind savings are less. Reductions in wind curtailment decrease with storage efficiency (see Figure A. 3-15 in APPENDIX 3). With lower storage efficiency, a part of wind energy, that would otherwise be curtailed, is used to cover energy losses in storage. The results suggest that storage has much more influence on managing network congestion than DSR. There are two fundamental reasons for this:

- Flexibility: Storage is much more flexible than DSR
- Location: Storage can be placed on the transmission networks where it is really needed, in contrast to DSR which is available only in large demand centres, and does not have a strong impact in other parts of the network.

Figure 3-4 shows the impact of Storage on reduction in generation costs.

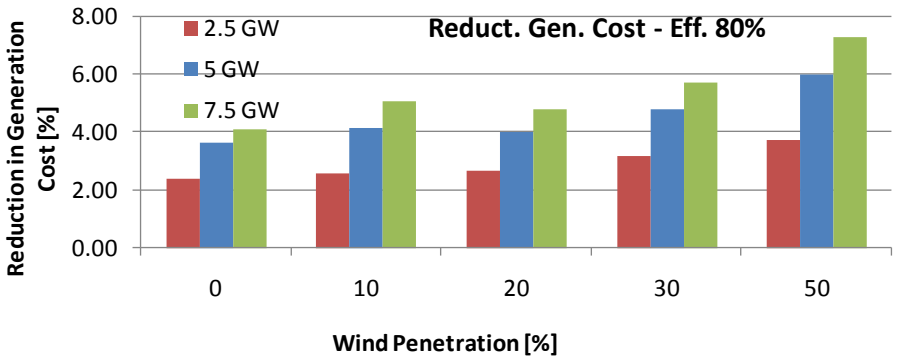


Figure 3-25: Effect of Storage on reduction in generation costs

In case of low wind penetrations (up to 10%), the most expensive generators are dispatched. Storage reduces the need to use these most expensive generators and thus displacing them with several times less expensive ones: it is charged during off peak periods from less expensive generators and

discharged during peak hours. As the generation costs naturally decrease with wind penetration (Table 3-1), the relative reduction in generation costs slightly increase. With further increases of wind penetration (20%) the most expensive generators are displaced by wind generation. Storage helps reduction in generation costs by displacing marginal gas generators with less expensive generators and with the wind energy that would otherwise be curtailed. However, when wind penetration further increases, significant wind curtailment occurs. Storage is then used to reduce this wind curtailment, displacing energy from both marginal and coal and gas generators with wind energy, thus reducing generation cost further. This is illustrated in Figure 3-26 where adjustments for each generator technology are given for different levels of wind penetration and storage 5GW, efficiency 80%. Reductions in generation costs also increase with available storage capacity and efficiency (see Figure A. 3-16 in APPENDIX 3).

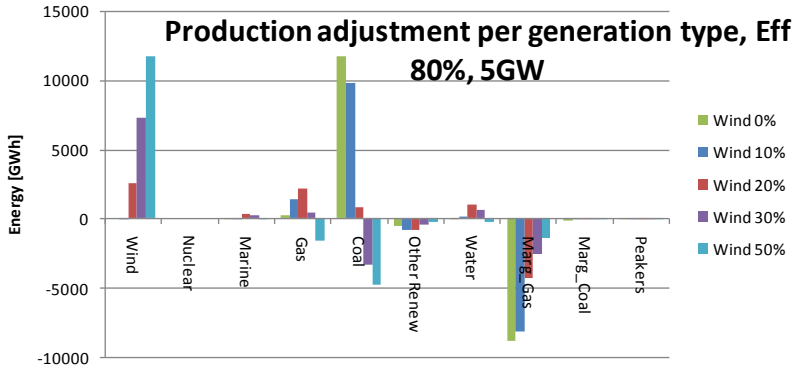


Figure 3-26: Impact of storage on generation adjustment per technology type

Figure 3-27 shows the system level reduction in CO_2 emissions for storage efficiency 80% and different total installed storage capacities and wind penetrations. In case of low wind, there is, in total, a shift of generation from marginal gas to coal (see Figure 3-26). Since coal has much higher CO_2 emissions (700 kg/MWh) than marginal gas (390 kg/MWh), and also due to storage efficiency coal generators now have to produce more energy to cover the losses in storage, there is a negative impact of storage on reduction in CO_2 emissions.

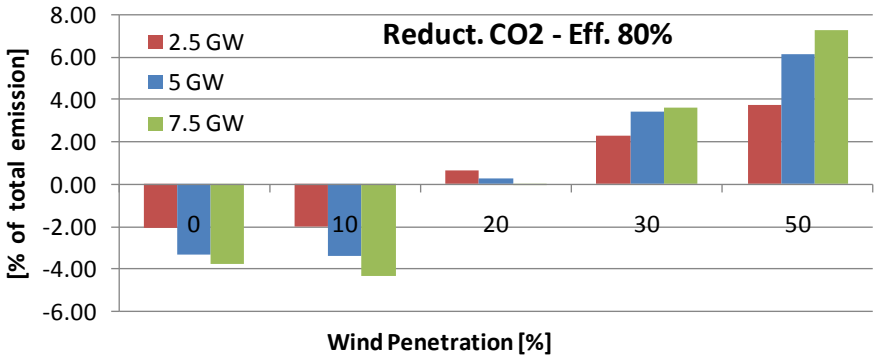


Figure 3-27: Storage effect on reduction in CO_2 emissions

In case of 20% wind penetrations, there is mostly a shift from marginal gas to gas and wind generators, which in total has a small impact on CO_2 emissions. In case of higher wind penetrations, reductions in CO_2 emissions come mostly from less wind curtailment. Storage efficiency intensifies this impact (see Figure A. 3-17 in APPENDIX 3). Storage capacity has a negative impact on CO_2 emissions in systems with small wind penetrations, and a positive impact in systems with significant wind curtailments.

Figure 3-28 shows the storage capacity allocation throughout the network busses for different wind penetrations. As explained in Section 3.2.4, the optimization distributes the given total available storage capacity to minimize the operational costs. Storage efficiency does not have an impact on this distribution and so only the case of 80% efficiency is shown.

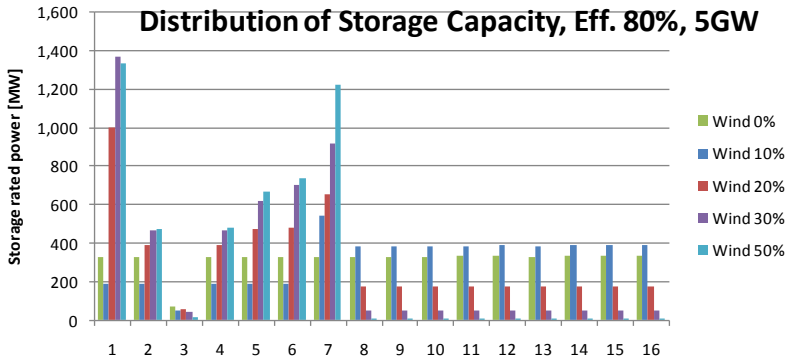


Figure 3-28: Distribution of storage capacities through network nodes

From the obtained results, it can be seen that the storage capacity allocation strongly depends on wind penetration. In the case of no wind, there are no network congestions and storage is evenly distributed amongst the buses as no bus is prioritized for storage allocation. The only exception is Bus 3, which is connected with a weak line to the network (346MW). Also, there is relatively small wind installed capacity in Bus 3 (1.4% of total wind capacity) and so there is no need for large

storage in this bus. With smaller wind penetration (10%) there is no wind curtailment, but network is almost congested. Especially, line Bus 6 – Bus 7 is at almost full capacity at hour 6675, preventing to use low production cost water and marine generators. Allocated storage capacity in buses 1-6 lead to fully utilization of these inexpensive generators. Storage capacity allocated in the southern part of the network is utilized to displace marginal gas generators with lower cost generation technologies. With higher wind penetration the most challenging goal is to transfer wind energy from north (buses 1-7) to the southern part of the network. There is network congestion leading to significant wind curtailment in the northern part of the system. That is why more storage capacity is allocated to the north and less to the south. Storage capacity is allocated close to the congested lines (line Bus 1 – Bus 2, line Bus 6 – Bus 7 and line Bus 7 – Bus 10).

Figure 3-29 shows line load factor for case of 30% wind penetration without storage and with storage 5GW installed capacity, 80% efficiency.

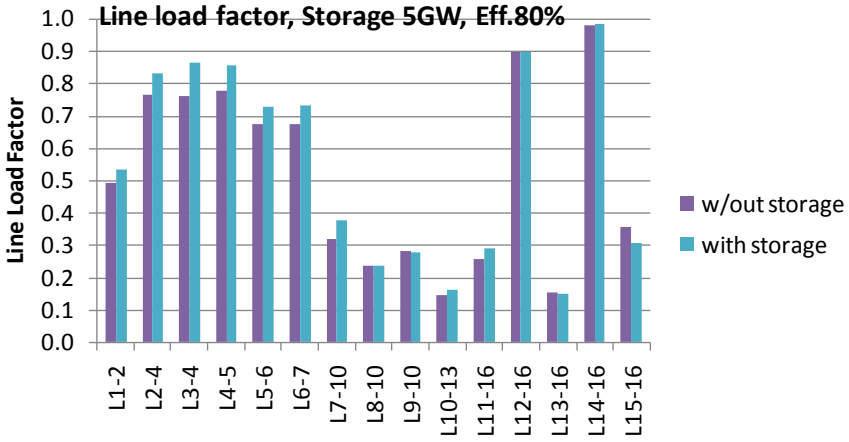


Figure 3-29: Impact of Storage on Line loading factors
(total storage capacity 5GW, efficiency 80% and wind penetration 30%)

It can be noticed that storage increases line loading factors for the weaker northern lines (buses 1-10). Storage does not have a strong impact on line loading for the southern lines, as these lines are not congested.

Capitalized value of storage is given in Figure 3-30 for different wind penetration levels and different storage size. The values are capitalized applying equation (24), where capital interest rate of 10% and life span of 10 years are used.

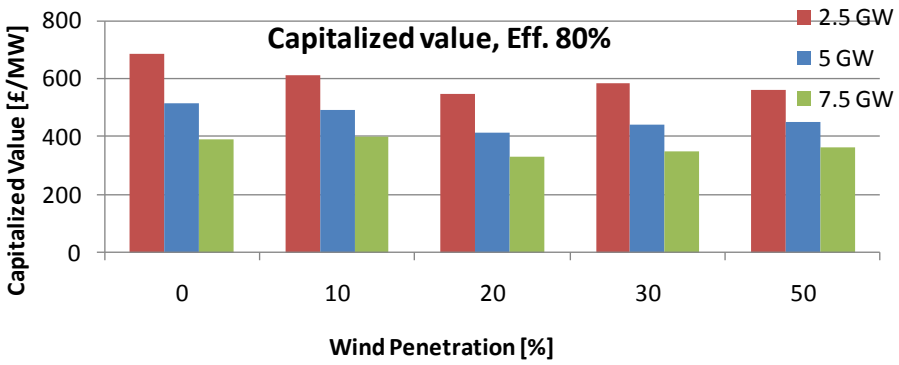


Figure 3-30: Capitalized value of storage

From definition (25), the capitalized value is proportional to the reduction in operation cost and inversely proportional to the total storage size. Reductions in operation costs increase with installed storage capacity, but at lower rate. Similar to DSR, it means that the first installed MW of Storage has the highest value. The capitalized value of Storage is in the range from £400/MW to £700/MW in the case of no wind installed and in range £350/MW to £600/MW otherwise. Lower range limits correspond to high installed capacity (7.5GW) whilst upper range limits correspond to low installed capacity (2.5GW).

The role of storage at high wind penetration can be seen if power flows are observed and compared with the reference case, for example with case of wind penetration 20% which situation is shown in Figure A. 3-26. The snapshot with storage 5GW, efficiency 80%, is given in Figure A. 3-27 in APPENDIX 3. Situation in the system with storage is now significantly changed compared to the reference case. Lines L6 (Bus 6 - Bus 7) and L7 (Bus 7 – Bus 10) are at full load. All storage in the north, where wind curtailment occurs, is being charged at full power. Storage in the south is charged to increase generation from cheap gas and coal generators and will be discharged later to reduce generation from expensive marginal generators. The charging power is driven by the capacity available in lower cost generation technologies.

During peak demand and lower wind blowing (snapshot of which is given in Figure A. 3-28 in APPENDIX 3), all available wind energy is used. Line 6 and Line 7 are again at full capacity, storage in the north is being charged, whilst storage in the south is being discharged. In this mode of storage operation, the flows through the congested lines (L6 and L7) are reduced and kept within operational limits.

Figure 3-31 shows storage impact on total demand in the case of 20% wind penetration and storage 5GW, 80% efficiency. It can be seen that during periods of high wind, storage is charged, making

total load even higher. In some circumstances, for example if the periods of high wind coincide with system peak, it can cause a conflict situation, especially in lower voltage networks.

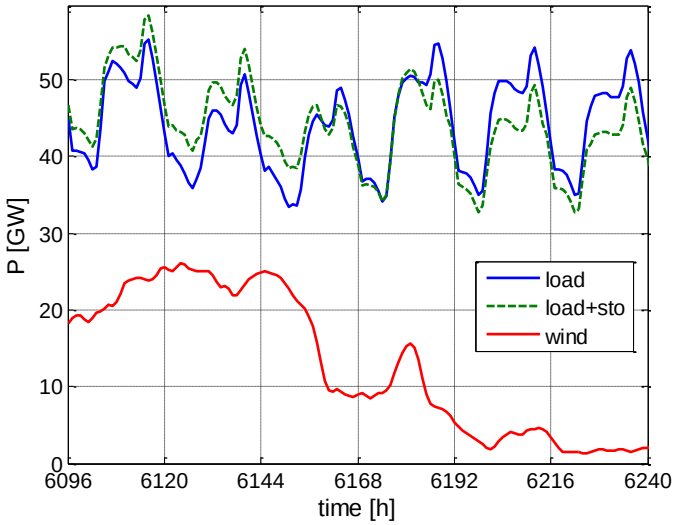


Figure 3-31: Time evaluation of load with and without storage and available wind at the system level
(20% wind penetration, storage 5GW, 80% efficiency)

Figure 3-32 shows Bus 1 available wind power, actual wind generation, load profile and storage charging and discharging, for case of 20% wind penetration, storage 5GW, 80% efficiency. It can be seen that storage charging and discharging patterns in this node are driven only by wind profile: when wind is high, there is storage charging, when wind is low storage is discharged. Storage activity does not depend on load profile. This is because there is relatively low load in this bus (less than 500MW), whilst there is 5.5GW of installed wind capacity.

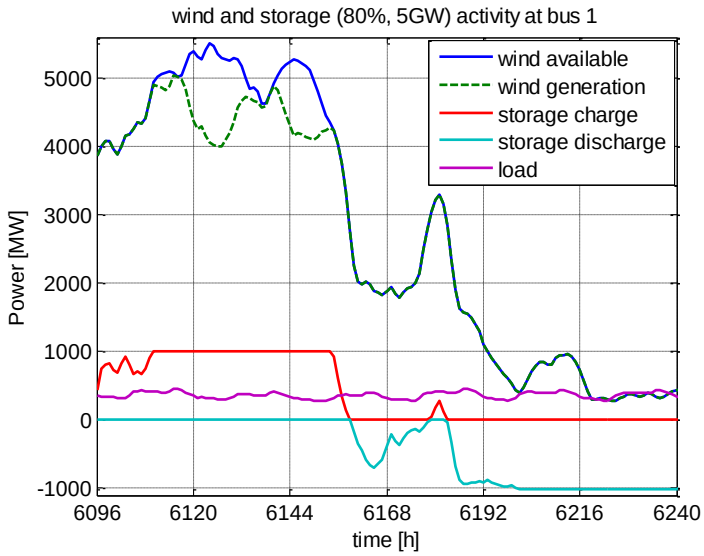


Figure 3-32: Storage activity at Bus 1 (20% wind penetration, storage 5GW, 80% efficiency): storage activity follows wind

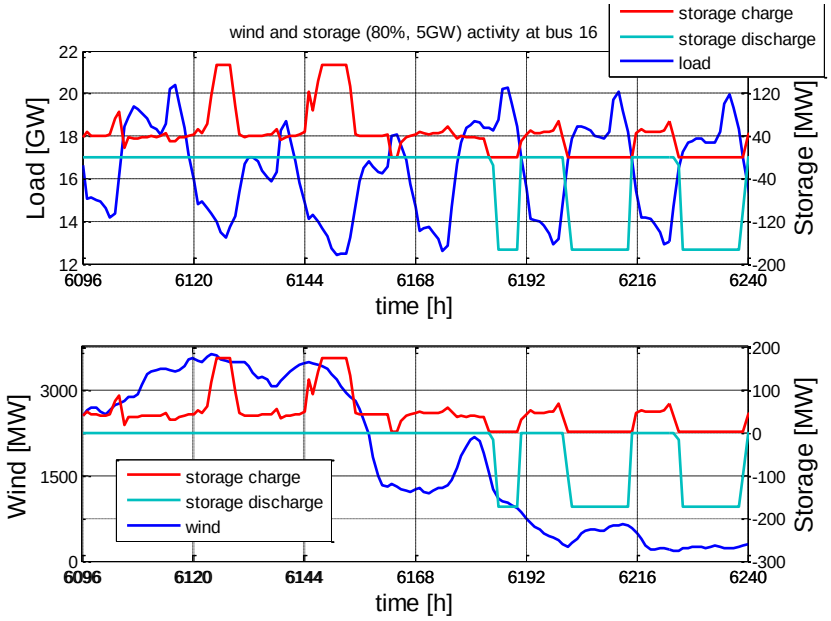


Figure 3-33: Storage activity at Bus 16

Upper chart in Figure 3-33 shows load profile and storage activity at Bus 16, whilst lower chart shows wind profile and storage activity in the same bus. Storage at Bus 16 charges when there is high wind (hours 6096-6186) regardless of the value of load. During lower wind periods, however, Storage at Bus 16 follows load: discharges during high demand and charges when demand is low.

Increase of load

The same increase of load (10% and 15% comparing to reference case) is applied as with DSR.

Similar to DSR, increase of load naturally increase the utilization of wind energy, thus leaving less opportunity for Storage to act for wind energy saving purposes. That is why the reduction in wind curtailment obtained by storage decreases with wind, Figure 3-34.

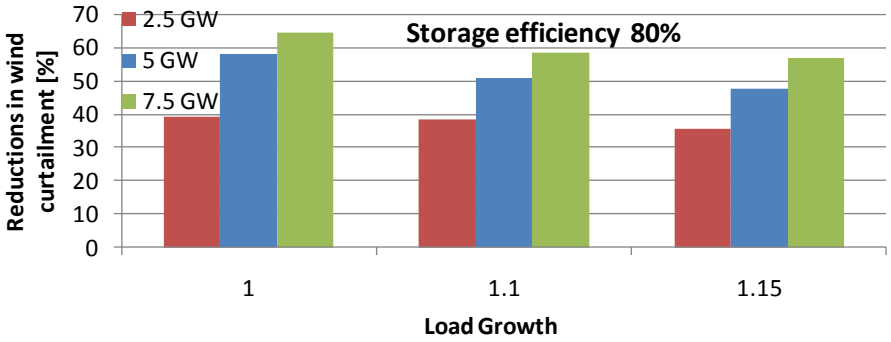


Figure 3-34: Effect of Storage on reductions in wind curtailment as load increases, wind penetration 30%

Figure 3-34 shows that the reduction in wind curtailment depends on load growth and storage size. Storage efficiency has a slightly detrimental impact on wind curtailment reduction (Figure A. 3-19 in APPENDIX 3). Comparing to DSR (Figure 3-11), it can be seen that reduction in wind curtailment is now much higher: in case of DSR, it is circa 1%, but with storage it is 40-60%. There are two basic reasons for this:

- storage flexibility: storage is capable of storing the energy for relatively long time periods (days), whilst DSR has flexibility in order of hours
- storage location: storage is located near wind generators and congested branches, whilst DSR is located in demand centres, where there is no congestion in transmission system

Figure 3-35 show the reduction in generation cost. The shape of graphs is similar to DSR results, and all explanations given above still apply. However, the values of reduction in generation costs are much higher in the case of storage – for example, in the case of load growth of 15% it is up to 8% for storage comparing to approximately 1.2% for DSR. This is a consequence of storage flexibility.

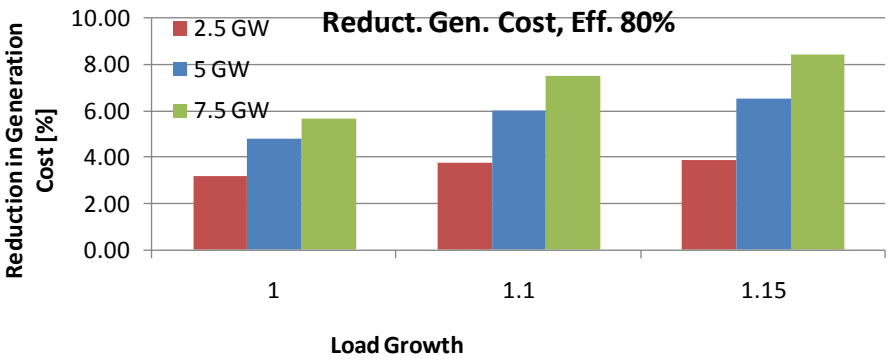


Figure 3-35: Storage impact on reduction in generation cost as load increases, wind penetration 30%

It can be noticed from Figure 3-35 that reduction in generation costs increase dominantly by storage size and load growth. Storage efficiency has also a positive impact on reduction in operation costs (Figure A. 3-20 in APPENDIX 3).

The impact of Storage and load growth on reduction in CO_2 emissions in the case of 80% storage efficiency and 30% wind penetration is given in Figure 3-36.

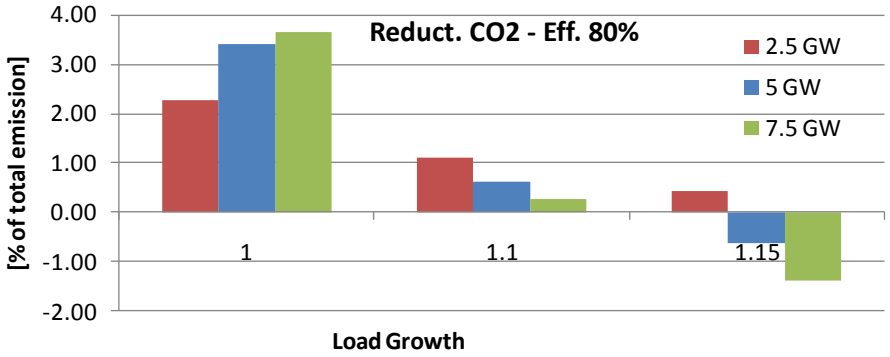


Figure 3-36: Storage impact on reduction in CO_2 emissions as load grows

Load growth has negative impact on CO_2 emissions, which can be explained by observing Figure 3-37, which shows generators' output adjustment for different generation technology.

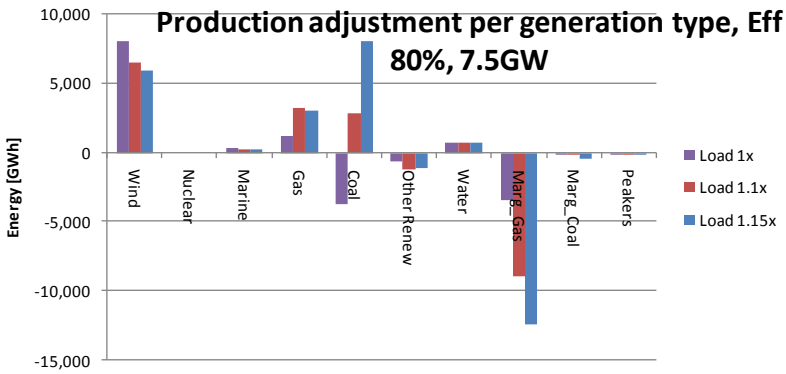


Figure 3-37: Impact of storage on generation adjustment per technology type as load grows

For base load (increase 0%), storage mostly helps shifting production from coal and marginal gas generators to wind generation and in a smaller amount to gas generators. This will bring relatively high reduction in CO_2 emissions, and also this effect increases with storage size.

As load grows there is more energy shift from expensive marginal gas to coal and gas generators. At the same time, storage will have less impact on reduction in wind curtailed energy as wind energy is naturally more utilized by the load, which decreases CO_2 emissions reduction. The effect of this also increases with storage size. When load reaches 15% of increase for storage size 5GW and more, the energy shifted from marginal gas to coal due to storage is so high that CO_2 emissions increase. As stated above, it is assumed that each storage facility can discharge 120h at rated power. It means, the higher storage power, the higher storage energy capacity, which enables to store more cheaper energy, in this case from coal generators, which are high CO_2 emitters.

Storage efficiency has a positive impact on reduction in CO_2 emissions: the higher the storage efficiency, the less energy is lost in storage and so the generators have to produce less energy and consequently emit less CO_2, as demonstrated in Figure A. 3-21 in APPENDIX 3.

The capitalized values of Storage are given in Figure 3-38, where it can be seen they grow with load. The reason for this is the same as before - as load grows, more high expensive generators are used, and the cost reduction is also higher whenever these generators are avoided. Value of storage slightly increases with its efficiency, as shown in Figure A. 3-22, APPENDIX 3. Higher efficiency means less energy is lost in storage thus leading to higher storage value.

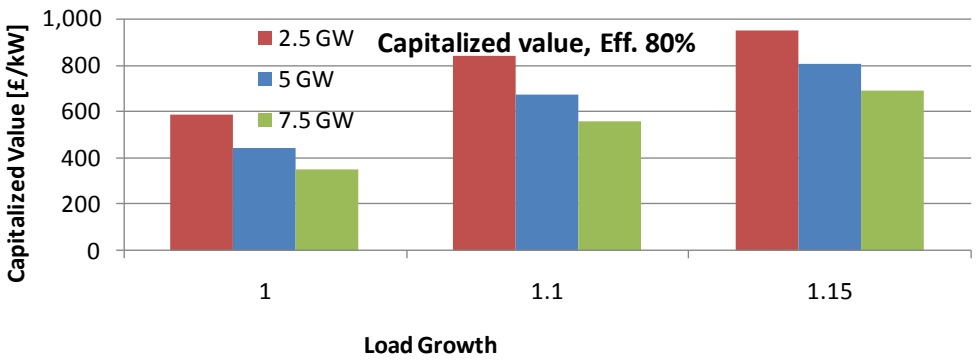


Figure 3-38: Capitalized value of Storage vs. load growth

Impact of generation flexibility

Three levels of generator flexibility: low, medium and high (see Table 3-4) are examined and system operation is compared with and without storage, for wind penetration of 30%. The obtained results are similar to those with DSR and so the similar conclusions apply. Only the basic results will be presented here and some parallels with DSR will be drawn.

As generation flexibility increases, the number of periods when the conventional generators cannot reduce their production fast enough to follow wind increase is reduced. From this reason the impact of Storage on reductions in wind curtailment decreases with generation flexibility as shown in Figure 3-39. The same figure shows that storage size has a positive impact on wind curtailment (storage efficiency does not have an important role on reduction in wind curtailment – regardless the storage efficiency, all available wind excess will be exploited, so only the case of storage efficiency 80% is shown). Compared to the reductions in wind curtailment obtained with DSR (Figure 3-18) it can be seen that Storage performs several times better results.

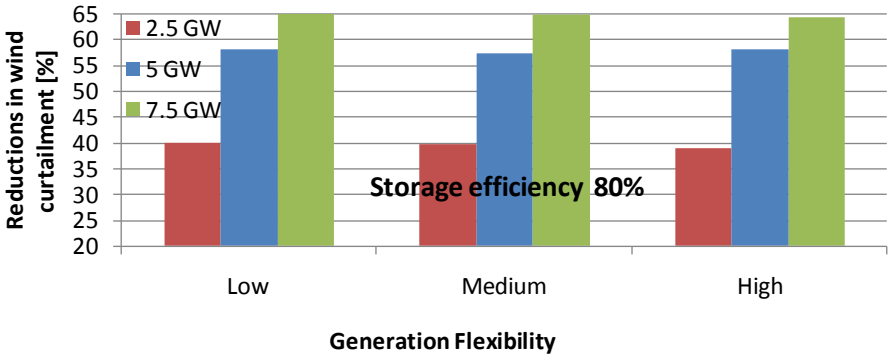


Figure 3-39: Effect of Storage on reduction in wind curtailment vs. generation flexibility

Figure 3-40 shows the impact of Storage on reductions in generation costs. The reductions in generation costs decrease with generation flexibility and increases with storage installed capacity and in smaller measure with storage efficiency (again only case of 80% efficiency is shown).

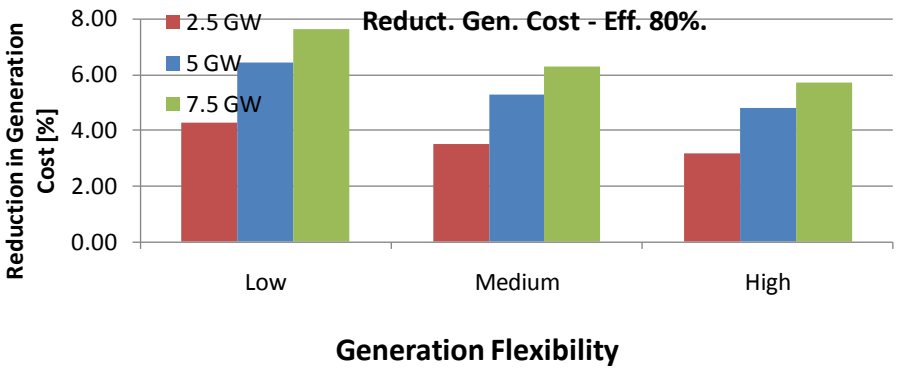


Figure 3-40: Reduction in generation cost vs. generation flexibility

It can be noticed that the highest reductions in operation costs are obtained for low generation flexibility. Similar to DSR, reducing the gradient of load, Storage brings the benefits to the system by replacing expensive generators with cheaper ones. As explained above, this effect is less obvious as generation flexibility increases.

Impact of Storage on system-level reduction in CO_2 emissions is given in Figure 3-41.

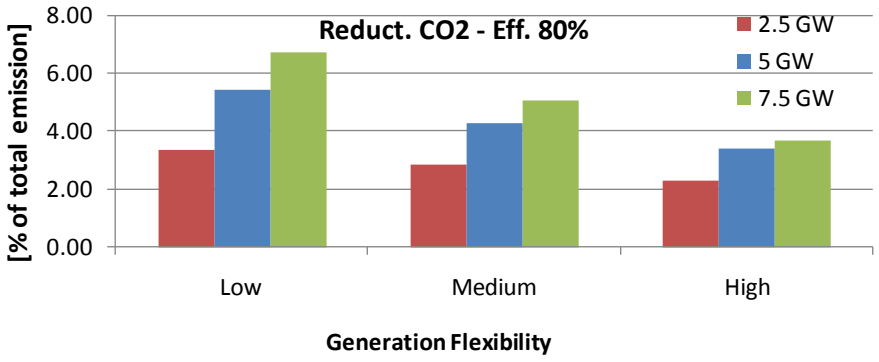


Figure 3-41: Impact of Storage on reduction in CO_2 emissions vs. generation flexibility

The reductions in CO_2 emissions increase with Storage size whilst decrease with generators' flexibility. The explanation is the same as with DSR. Storage efficiency has a positive impact on reductions in CO_2 emissions as shown in Figure A. 3-23, APPENDIX 3.

The capitalized values of Storage are given in Figure 3-42 and it can be seen that this decreases with both Storage installed capacity and generator flexibility. The reason for this is as generation flexibility grows there is less need for high cost generators and so costs reduce. Value of storage grows with Storage efficiency, as shown in Figure A. 3-24, APPENDIX 3.

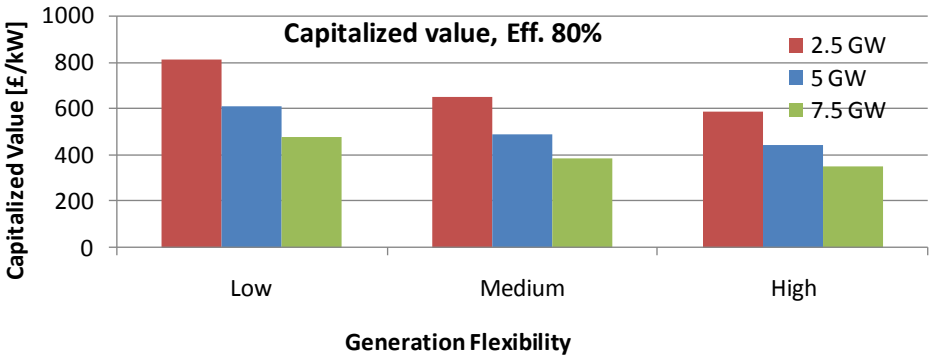


Figure 3-42: Capitalized value of Storage vs. generation flexibility

3.5 Conclusions

In this chapter, a methodology to support transmission network operation using demand side response and storage technologies is developed. The methodology is applied to and tested on the GB transmission network model. The results obtained demonstrate that DSR and storage contribute to reducing network congestion and facilitate the utilization of wind energy in the existing network.

The key drivers for the value of DSR are shown to be:

- the amount of wind penetration to the network
- the network congestion levels
- penetration of controllable appliances
- controllable appliances' characteristics especially flexibility regarding shifting in time and energy consumption per cycle

The specific key drivers for the value of Storage are:

- storage size
- storage efficiency

The obtained results suggest that the potential use of DSR and storage is a system-specific and depends on the location of load, which restricts its capability to reduce the wind curtailment.

Summary on DSR results

The reductions in the wind curtailment (relative to the total wind curtailed) brought by DSR, decrease with wind penetration. For this specific system, the wind curtailment occurs at wind penetrations of 20% and more. For 20% of wind penetration, the highest reductions in wind curtailment are observed in the case of 100% DSR penetration: for normal DSR flexibility the reductions are about 4% of total curtailed wind energy and for high DSR flexibility the reductions are around 8%.

Reductions in generation costs also decrease with wind penetration, being in the range from 0.9% to 1.2% for normal DSR flexibility and 100% DSR penetration. The reductions are higher for low wind penetrations as DSR is used to displace expensive marginal generators. Reductions in generation costs increase with DSR flexibility.

Regarding the reductions in CO_2 emissions, the results demonstrate that the utilization of DSR may even increase the emissions. It happens in the cases of no wind or low wind penetrations when expensive marginal gas generators are displaced with less expensive coal generators, which are more CO_2 intensive. Maximum reductions in CO_2 emissions in the case of 100% DSR penetration, normal DSR flexibility and 50% wind penetration are around 0.8%.

The capitalized value per appliance decreases with wind penetration and lies in the range from £10/SA to £25/SA in the case of 100% DSR penetration and normal DSR flexibility. The value of a particular type of the device increases with flexibility. In this case Dish Washer exhibits the highest flexibility and has the highest capitalized value from £6/DW to £15/DW. In general, the value increases with DSR flexibility. Another parameter that brings a value to a particular type of shifting devices is the energy per operation cycle. It was shown that WM+TD has much higher capitalized value (from £2.5/WM+TD to £5/WM+TD in the case of 100% DSR penetration and normal DSR flexibility) than a WM with the same flexibility, whose value is below £1/WM.

The impact of DSR on reductions in generation costs and consequently on the capitalized value is more beneficial in the case of increased load, as the more expansive generators are displaced with less expensive ones, but on the other hand, it will lead to increase in CO_2 emissions.

It was also demonstrated that DSR has higher value in the systems with low flexible generation since DSR reduces the gradient of demand variations.

The increased flexibility brought by DSR improves system efficiency, reduces operating costs, carbon emissions and increases utilisation of renewable sources.

Summary on Storage results

Similar to DSR, reductions in wind curtailment brought by Storage also decrease with wind penetration. However, the reductions in wind curtailment are now much higher, more than 90% of total curtailed wind energy in the case of 7.5GW storage and 20% of wind penetration.

Reductions in generation costs are in the range from 4% to 8% for storage 7.5GW and 80% efficiency. The reductions increase with wind penetration since storage utilizes wind energy that would otherwise be curtailed. Reductions in generation costs slightly increase with storage efficiency.

In the cases of no wind or low wind penetrations, reductions in CO_2 may become negative, for the same reason as in the case of DSR. Maximum reductions in CO_2 emissions in the case of storage 7.5GW, 80% efficiency and 50% wind penetration are around 7%, which is an order of magnitude higher than with DSR.

The capitalized value of storage decreases with wind penetration and lies in the range from £350/MW to £700/MW, depending on the storage installed capacity. The value slightly increases with efficiency.

The impact of load growth and generation flexibility is similar as in the case of DSR.

Both DSR and Storage change demand profile in such a way to follow the wind which may lead to a potentially conflicting situation to shift load to or charge storage at peak demand time. In the buses with large installed wind capacity and relatively small load (such as in the north of the UK), storage activity is mostly driven by wind. In buses characterized with high demand (southern part of the UK), storage activity is driven by both load and wind. The role of storage in nodes with high demand and diverse generation mix is to facilitate price arbitrage: it reduces generation of expensive marginal generators and increases production from less expensive generators. In congested areas (northern and central part of GB network) the role of storage is focused on increased utilization of wind energy.

In general, storage exhibits better performances than DSR in all parameters considered. There are two fundamental reasons for that:

- storage flexibility (much higher than demand response)
- storage location (possibility to build storage where there is a need for it)

Direct comparison between smart appliances and storage is not presented as DSR penetration is defined by the number of shifting appliances, whilst storage is defined by MW of installed capacity.

CHAPTER 4. Value of Storage and Smart Appliances for Network Congestion management in Distribution Networks

4.1 Introduction

The linear model, described in CHAPTER 3 is good enough for applications in transmission or sub-transmission networks, where the branch resistances can be ignored. In such the networks all the voltage magnitudes are at their nominal values, and the only voltage change is their angular displacement caused by real power flow over the branch reactance. However, in distribution networks, branch resistances and reactive power flows cannot be ignored. Under these conditions, both voltage magnitude variation and power losses in the network branches will occur.

The power flows equations are now described with trigonometric functions that cannot be approximated by a linear form, thus making the problem non-linear.

Non liner optimization problems are difficult to solve numerically, especially the problems of large dimensions such as those found in optimal power flows. The main difficulty is to assure a stable numerical solution is obtained. In order to keep focused on the subject and not to scatter on numerical methods for non-linear optimization problems solving, commercial optimization software is used.

The optimization involves examination of the system operation over a time horizon of a day and considers:

- Constraints, such as:
  - power balance constraints,
  - network thermal constraints,
  - voltage limits,
  - storage and DSR constraints
  - generators constraints
- Coordinated actions across multiple time periods that are required to optimize operation of storage and DSR

In this way, a full non-linear model accomplishes the main objective of the work – to explore all possible sources of values for DSR and Storage in distribution networks, such as:

- Congestion Management,
- Voltage Control,

- Network losses reduction,
- Benefits of deferring network reinforcement, enhancing security of supply and improving power quality.

Another objective of this work is to develop a methodological framework that could be applied to optimal control of active distribution networks in real time.

Section 4.2 gives the formulation of the AC OPF algorithm where DSR and Storage models are included as a part of the constraints. Section 4.3 introduces the optimal storage sizing and location model, whilst section 4.4 gives a brief discussion on the solution methodology applied. The proposed algorithm is tested on two case studies, described in sections 4.5 and 4.6. Section 4.7 brings the conclusions.

4.2 Non-Linear Multi-period Optimal Power Flow considering Storage and DSR

In the linear model, all voltage magnitudes are assumed to be fixed at their nominal value (1p.u.), and voltages are determined only by their angles. In non-linear (AC) model, however, not only the angle but also the magnitude of a voltage is subjected to changes – they all are the decision variables of the problem. Thus the voltages are now defined with both magnitude and angle [78]:

$$\underline{V}_b(t) = V_b(t) \cdot e^{j\delta_b(t)} \qquad \forall b \in \mathbf{N_{BUS}} \;\; \forall t \in \mathbf{T} \tag{26}$$

where $\underline{V}_b(t)$ is complex voltage at bus b and time step t, $V_b(t)$ is voltage magnitude, $\delta_b(t)$ is voltage angle and j is the imaginary unit ($j^2 = -1$).

Beside voltage magnitudes, another characteristic of AC models is reactive power, which can be characterized through power factor, $\cos\varphi$ [78]:

$$\cos\varphi = \frac{P}{S} = \frac{P}{\sqrt{P^2 + Q^2}} \tag{27}$$

In (27), φ is the angle between voltage and current phasors [78], P is active power, S is apparent power, whilst Q is reactive power. Knowing $\cos\varphi$, it is relatively straightforward to calculate $\Psi = \tan\varphi$, which represents the ratio between reactive and real power. Starting from (27), one gets:

$$\Psi = \tan\varphi = \frac{\sqrt{1 - \cos^2\varphi}}{\cos\varphi} = \frac{Q}{P} \tag{28}$$

Equation (28) allows to compute reactive power Q, providing that active power P and power factor are known. In this way, reactive power can be calculated for each bus of the network. For the sake of

simplicity, it is assumed that power factor $\cos\varphi$ is time independent and takes the unique value for the whole network. Reactive demand Qd_b is thus proportional to the real demand:

$$Qd_b(t) = \Psi \cdot Pd_b(t) \qquad \forall t \in \mathbf{T},\ \ \forall b \in \mathbf{L_{BUS}} \tag{29}$$

The objective function is to minimize the total network operation costs, which mathematically can be formulated as follows:

Minimize

$$\begin{aligned} F = \sum_{t\in\mathbf{T}}\sum_{g\in\mathbf{G}} c_g P_g(t) \ + \sum_{t\in\mathbf{T}}\sum_{b\in\mathbf{L_{BUS}}} c_{LS}\cdot\left(load_shed_b(t) + \Psi\cdot Qshed_b(t)\right) \\ + \sum_{t\in\mathbf{T}}\sum_{b\in\mathbf{G_{BUS}}} c_{OS}\cdot\left(over_{slack_b(t)} + Qover_slack_b(t)\right) \end{aligned} \tag{30}$$

where $load_shed_b(t)$ is the involuntary loss of active power at bus b at time step t, while $Qshed_b(t)$ is the corresponding loss of reactive power. This term is introduced to prevent optimizer to shed reactive power only, when maintaining network (voltage and line) constraints. $over_slack_b(t)$ and $Qover_slack_b(t)$ are decision variables representing an artificial load. These variables will only take positive values in case when the generators reach their lower production limits being still higher than load. Cost of using over-slack load c_{OS} has a very high value, so $over_slack_b(t)$ and $Qover_slack_b(t)$ normally take zero values.

4.2.1 Power Balance Constraints

Nodal power balance constraints must be imposed to each bus in the network. The total active power injection in each bus must be equal to the total power demand in that bus, including the power exchange with other buses, at all time instances:

$$\begin{aligned} S_b^d(t) - S_b^c(t) + \sum_{g\in\mathbf{NG_b}} P_g(t) + load_shed_b(t) = \\ = Pd_b^{DSR}(t) + P_b^{EX}(t) + over_slack_b(t), \end{aligned} \tag{31}$$

$\forall t \in \mathbf{T}, \forall b \in \mathbf{N_{BUS}}$

The meaning of all the terms in Eq. (31) is the same as for Linear Model (see CHAPTER 3 - Section 3.2.1). On the Left Hand Side (LHS) of (31): $S_b^d(t)$ is storage discharge, i.e. injecting the active power into the bus b at time t, while $S_b^c(t)$ is storage charging, which is equivalent to additional demand in the bus; sum represents generation in bus b; the last term on the LHS of (31) is load shed at bus b. On the RHS of (10) Pd_b^{DSR} is active demand power, modified by demand side response; P_b^{EX} is the

active power exchange between considered bus b and other buses; $over_slack_b(t)$ is introduced to avoid infeasibilities.

Similar constraints must be imposed for reactive power as well:

$$\sum_{g \in \mathbf{NG_b}} Q_g(t) + Q_shed_b(t) = \\ = Qd_b^{DSR}(t) + Q_b^{EX}(t) + Qover_slack_b(t), \quad \forall t \in \mathbf{T}, \forall b \in \mathbf{N_{BUS}} \tag{32}$$

The meaning of the terms in (32) is similar as those in (31): Q_g is reactive power output of generators, $Q_shed_b(t)$ is involuntary loss of reactive power; Qd_b^{DSR} is reactive power demand with DSR, Q_b^{EX} is reactive power exchange from bus b, and $Qover_slack_b$ is introduced to avoid infeasibility of the solution. Note that storage in this formulation is not used to control reactive power (no storage terms in (32)). However, it is relatively easy to incorporate reactive power produced by storage in (32) as it was done for the active power in (31).

Power exchange between considered bus b and other buses p in the network (providing they are connected with at least one branch of the network) must be now taken into account for both real and reactive power. It is assumed that active and reactive powers flow from considered bus b to bus p, so the positive sign for power is from bus b. In this way, the (positive) exchange power is added to the total demand in bus b (terms $P_b^{EX}(t)$ and $Q_b^{EX}(t)$ in (31) and (32)).

Real power exchange between bus b and other buses is given by:

$$P_b^{EX}(t) = \sum_{p \in \mathbf{N_{BUS}}} V_b(t)V_p(t)\big(G_{bp}\cos\delta_{bp}(t) + B_{bp}\sin\delta_{bp}(t)\big) \\ \forall b \in \mathbf{N_{BUS}} \ \forall t \in \mathbf{T} \tag{33}$$

δ_{bp} is defined as a difference between voltage angles in buses b and p:

$$\delta_{bp}(t) = \delta_b(t) - \delta_p(t) \qquad \forall b, p \in \mathbf{N_{BUS}} \ \forall t \in \mathbf{T} \tag{34}$$

G_{bp} and B_{bp} are real and imaginary parts of an element of bus admittance matrix **Y**.

Similarly, reactive power exchange between bus b and all other buses is given by:

$$Q_b^{EX}(t) = \sum_{p \in \mathbf{N_{BUS}}} V_b(t)V_p(t)\big(G_{bp}\sin\delta_{bp}(t) - B_{bp}\cos\delta_{bp}(t)\big) \\ \forall b \in \mathbf{N_{BUS}} \ \forall t \in \mathbf{T} \tag{35}$$

Derivation of equations (33) and (35) is given in APPENDIX 1.

4.2.2 Demand Side Response Constrains

DSR constraints described in CHAPTER 2, Section 2.5, are still valid. They define the real power Pd_b^p of connected and Pd_b^c of disconnected devices that will be added to the original load profile – Equation (3). The reactive power of connected and disconnected devices is not directly managed but is indirectly estimated using (36) and (37):

$$Qd_b^c(t) = \Psi \cdot Pd_b^c(t) \tag{36}$$

$$Qd_b^p(t) = \Psi \cdot Pd_b^p(t) \tag{37}$$

Now, by analogy to Equation (3), the reactive demand modified by demand side response becomes:

$$Qd_b^{DSR}(t) = Qd_b(t) - Qd_b^c(t) + Qd_b^p(t), \qquad \forall t \in \mathbf{T}, \forall b \in \mathbf{L_{BUS}} \tag{38}$$

4.2.3 Network constraints

The AC model is usually applied to distribution networks, where voltage magnitude constraints are often violated. The reason for this is that distribution lines, such as cables, have relatively high impedance, causing relatively high voltage drop across the line. Therefore, the constraints to keep voltage magnitudes in a specific range are required:

$$V_{min} \leq V_b(t) \leq V_{max} \qquad \forall b \in \mathbf{N_{BUS}} \ \forall t \in \mathbf{T} \tag{39}$$

where V_{min} and V_{max} are minimal and maximal value that voltage magnitude can take.

A bus where both voltage magnitude and angle are pre-defined is named slack bus. Usually, the slack bus coincides with the bus where the biggest plant (supply point) is placed, and its angle is set to be 0 rad. In this model it is assumed that there is only one slack bus in the system.

Also, in AC model there is another class of buses where the voltage magnitude can be controlled. These buses are called generator buses or PV buses. Voltage magnitudes in these buses are usually set in advance [78] and held constant:

$$V_b(t) = V_b, \qquad \forall b \in \mathbf{N_{PV}} \ \forall t \in \mathbf{T} \tag{40}$$

where N_{PV} ($N_{PV} \subset N_{BUS}$) is the set of PV bus indices.

Similar to the linear model, the power flowing in the branches must be maintained within the specified limits. The main difference is that in the non-linear model there are real and reactive powers flowing through the network branches, both causing line congestion. This is why the apparent power for line limits, rather than merely real power is used in non-linear model.

Next two equations define real and reactive power flowing through branch i connecting buses i_S and i_R [79]. Equations are derived for the power leaving bus i_S:

$$P_i^S(t) = a_i^2(t)V_{i_S}^2(t)G_i - a_i(t) \cdot V_{i_S}(t)V_{i_R}(t)\left(G_i \cos\delta_{i_{SR}}(t) + B_i \sin\delta_{i_{SR}}(t)\right) \quad (41)$$

$$Q_i^S(t) = -a_i^2(t)V_{i_S}^2(t)B_i - a_i(t) \cdot V_{i_S}(t)V_{i_R}(t)\left(G_i \sin\delta_{i_{SR}}(t) - B_i \cos\delta_{i_{SR}}(t)\right) \quad (42)$$

$(\forall i \in \mathbf{N_{BR}}, \forall t \in \mathbf{T})$

In (41) and (42) introduced are:

i - branch index

i_S, i_R - buses of the network connected by branch i. For easier referencing, bus i_S is called *sending bus*, while bus i_R is called *receiving bus*.

P_i^S - real power through branch i leaving the sending bus i_S,

Q_i^S - reactive power through branch i leaving the sending bus i_S,

V_{i_S} - voltage magnitude at sending bus i_S,

V_{i_R} - voltage magnitude at receiving bus i_R,

$a_i(t)$ - off-nominal transformer ratio for branch i at time step t,

G_i - conductance of branch i,

B_i - susceptance of branch i,

$\delta_{i_{SR}}$ is the difference of bus voltage angles in buses i_S and i_R:

$$\delta_{i_{SR}}(t) = \delta_{i_S}(t) - \delta_{i_R}(t) \quad (43)$$

Then, apparent power S_i^S through the branch i leaving bus i_S is:

$$S_i^S(t) = \sqrt{\left(P_i^S(t)\right)^2 + \left(Q_i^S(t)\right)^2} \qquad (\forall i \in \mathbf{N_{BR}}, \forall t \in \mathbf{T}) \quad (44)$$

In an AC model, power losses in each branch of the network are taken into account. Due to power losses, real and reactive power leaving bus i_S will not be equal (by absolute value) to the corresponding power coming to bus i_R. Real and reactive powers coming to the bus i_R are [79]:

$$P_i^R(t) = V_{i_R}^2(t)G_i - a_i(t) \cdot V_{i_S}(t)V_{i_R}(t)\left(G_i \cos\delta_{i_{SR}}(t) - B_i \sin\delta_{i_{SR}}(t)\right) \quad (45)$$

$$Q_i^R(t) = -V_{i_R}^2(t)B_i + a_i(t) \cdot V_{i_S}(t)V_{i_R}(t)\left(G_i \sin \delta_{i_{SR}}(t) + B_i \cos \delta_{i_{SR}}(t)\right)$$
$$(\forall i \in \mathbf{N_{BR}}, \forall t \in \mathbf{T}) \tag{46}$$

Apparent power S_i^R through the branch i, coming to bus i_R is:

$$S_i^R(t) = \sqrt{\left(P_i^R(t)\right)^2 + \left(Q_i^R(t)\right)^2} \qquad (\forall i \in \mathbf{N_{BR}}, \forall t \in \mathbf{T}) \tag{47}$$

Thermal capacity constraints require that the apparent power through each branch of the network, in either direction, must be less than a maximal allowed value S_i^{lim} [MVA] for that branch:

$$\max(S_i^S(t), S_i^R(t)) \leq S_i^{lim} \qquad (\forall i \in \mathbf{N_{BR}}, \forall t \in \mathbf{T}) \tag{48}$$

Another set of constraints limit the difference of voltage angles of two nodes connected by a branch:

$$\left|\delta_{i_S}(t) - \delta_{i_R}(t)\right| \leq \delta_i^{\lim} \qquad (\forall i \in \mathbf{N_{BR}}, \forall t \in \mathbf{T}) \tag{49}$$

4.2.4 Generator constraints

The generator constraints for real power are the same as in the linear model (see CHAPTER 3, Section 3.2.3):

$$P_{g,\min} \leq P_g(t) \leq P_{g,\max}, \quad \forall t \in \mathbf{T}, \forall g \in \mathbf{G} \tag{50}$$

However, in the AC model, an additional set of constraints must be introduced for reactive power:

$$Q_{g,\min} \leq Q_g(t) \leq Q_{g,\max}, \quad \forall t \in \mathbf{T}, \forall g \in \mathbf{G} \tag{51}$$

$Q_{g,min}$ and $Q_{g,max}$ are lower and upper generator limit for reactive power. Constraints (51) say that reactive power of all generators must be within given range at each time step.

Another set of constraints imposed to the generators is ramp-up and ramp–down constraints:

$$P_g(t) - P_g(t-1) \leq Ramp_g^{up} \cdot \Delta t, \;\; P_g(t-1) - P_g(t) \leq Ramp_g^{down} \cdot \Delta t$$
$$\forall t \in \mathbf{T}\backslash\{1\}, \forall g \in \mathbf{G} \tag{52}$$

These constraints state the generators cannot change their active power output in two consecutive time steps for more than the rate defined by ramping parameters $Ramp_g^{up}$ and $Ramp_g^{down}$. Ramp constraints for reactive power are not considered here, since excitation control of generators can change reactive power output within a minute. However, reactive power ramping constraints may be readily added to the model.

4.3 Storage Model

Storage model described in CHAPTER 3, Section 3.2.4 distributes the total available storage capacity amongst selected buses according to the optimal operation conditions.

In this section another storage model will be presented where both storage size and storage location are optimized. In this model, the optimization is given several possible locations (buses) eligible to place storage and the optimization then chooses between the locations. For example, in the network with N buses, there are k buses where storage could fit, and there are m $(m \leq k)$ storage devices available. The optimization chooses up to m (out of k) buses in which the storage will be located, giving the optimal operation costs. Note that this is mixed-integer non-linear programming problem, which is very demanding from the computation point of view.

The formulation is as follows:

First group of constraints are related to storage power limits:

$$0 \leq S_b^c(t), S_b^d(t) \leq S_b^{\max} \qquad \forall t \in \mathbf{T}, \forall b \in \mathbf{S_{BUS}} \tag{53}$$

$\mathbf{S_{BUS}}$ is a subset of network buses eligible for storage connection. Storage rated power S_b^{max} is a decision variable. In this work S_b^{max} is assumed to be a continuous variable, although it is possible to be given as a set of pre-defined values so the optimization could choose from the set.

The sum of storage rated power in all buses adds to the total available storage power capacity:

$$\sum_{b \in \mathbf{S_{BUS}}} S_b^{\max} \leq S_{cap}^{max} \tag{54}$$

Total installed storage capacity in the system S_{cap}^{max} is an input parameter. Usually, S_{cap}^{max} is a large number to ensure that necessary amount of storage capacity is allocated. On the other hand, in order to prevent storage rated power over sizing, S_b^{max} is included to the objective function (61).

Another set of constraints relates network topology and storage:

$$0 \leq S_b^c(t), S_b^d(t) \leq storage_location(b) \cdot S_{cap}^{max} \qquad \forall t \in \mathbf{T}, \forall b \in \mathbf{S_{BUS}} \tag{55}$$

$storage_location(b)$ is a binary decision variable which takes value 1 if storage is allocated to bus b and 0 otherwise. If storage is not allocated to bus b, then $storage_location(b)$ takes value 0, forcing charging power $S_b^c(t)$ and discharging power $S_b^d(t)$ to be zero as well. Strictly mathematically speaking, constraint (55) is not necessary if binary variable $storage_location(b)$ is incorporated in (53) to get:

$$0 \le S_b^c(t), S_b^d(t) \le storage_location(b) \cdot S_b^{\max} \qquad \forall t \in \mathbf{T}, \forall b \in \mathbf{S_{BUS}} \tag{56}$$

However, in this case there is a product of two decision variables, one of which is a binary, and this significantly slows the optimization time (FICO Xpress Optimization Solver). Thus from practical reasons a set of constraints (53)- (55) is used instead of only (54) and (56).

Number m of storage devices available to be allocated in k buses is also an input parameter:

$$\sum_{b \in \mathbf{S_{BUS}}} storage_location(b) \le m \tag{57}$$

Energy contained in the storage at the end of current time step is calculated as the energy content at the previous time step, plus energy charged during the current time step, minus energy discharged during the current time step:

$$ES_b(t) = ES_b(t-1) + \left(\eta_b \cdot S_b^c(t) - S_b^d(t)\right) \times \Delta t, \qquad \forall t \in \mathbf{T}\backslash\{1\}, \forall b \in \mathbf{S_{BUS}} \tag{58}$$

where $ES_b(t)$ is the energy content in the storage in bus b at the end of the current time step, $ES_b(t-1)$ is the energy content in the same storage at the end of previous time step, η_b is storage efficiency, and Δt is time interval.

At the first time step ($t = 1$) the energy is:

$$ES_b(t=1) = ES_b^{INI} + \left(\eta_b \cdot S_b^c(1) - S_b^d(1)\right) \times \Delta t, \quad , \qquad \forall b \in \mathbf{S_{BUS}} \tag{59}$$

The initial energy ES_b^{INI} is given as the input data.

Maximum energy content in storage devices is also constrained:

$$ES_b(t) \le ES_b^{max}, \quad \forall b \in \mathbf{S_{BUS}} \tag{60}$$

where ES_b^{max} is a decision variable. For the same reason as with S_b^{max}, to prevent storage energy capacity oversizing ES_b^{max} is also added to the objective function, which now becomes:

$$\begin{aligned} F = \sum_{t \in \mathbf{T}} \sum_{g \in \mathbf{G}} c_g P_g(t) \; + \sum_{t \in \mathbf{T}} \sum_{b \in \mathbf{L_{BUS}}} c_{LS} \cdot \left(load_shed_b(t) + \Psi \cdot Qshed_b(t)\right) \\ + \sum_{t \in \mathbf{T}} \sum_{b \in \mathbf{G_{BUS}}} c_{OS} \cdot \left(over_{slack_b(t)} + Qover_{slack_b(t)}\right) \\ + \sum_{b \in \mathbf{S_{BUS}}} \left(c_{sto}^{energy} ES_b^{max} + c_{sto}^{power} S_b^{\max}\right) \end{aligned} \tag{61}$$

where c_{sto}^{energy} [£/MWh] and c_{sto}^{power} [£/MW] are tuning coefficients and represent the cost of installing one unit of storage energy capacity and storage power capacity, respectively.

In this work, storage device is not related to any specific technology; in fact, it can be made of any existing storage technology such as battery, chemical, compressed air etc. The main concern of storage is to support active power requirements. Of course, it is possible to expand the storage model to enclose reactive power as well and it will be shown in the second case study, but VAR control from energy storage is not economically justified [80]. Namely, bus voltages and reactive power flows in distribution networks could be effectively controlled with much cheaper devices such as capacitor banks, under-load tap changing transformers (ULTC) or static VAR compensators (SVC) [81],[82].

4.4 Solution method

The optimization problem described in Sections 4.2 and 4.3 is a mixed-integer non-linear problem whose dimension depends on network size. In order to solve such problems, commercial optimization software FICO Xpress [83] has been used. Non-linear problems are loaded and solved by invoking SLP module, which states for Successive Linear Programming [84]. In summary, the numerical method that has been employed in SLP module makes a linear approximation to the original nonlinear problem. Linearization is made in vicinity of initial point. It is a common practice in AC power flows to choose the initial point by setting bus voltage magnitudes to 1.0 p.u. and voltage angles to 0rad [78]. If the linear optimal solution is enough close to the initial point, then the SLP is considered successfully converged and the procedure stops. If not, the next iteration starts: a new initial point is calculated from the results of previous iteration and a new linear approximation is created. This iterative procedure is repeated until the solution converges [84]. However, the actual algorithm that is in the core of the optimization engine is not disclosed.

FICO Xpress-SLP has a number of tuning parameters which help to create good approximations to the original problem and therefore help speed up the convergence. Figure 4-1 refers to an example where the non-linear problem has more than 5,000 variables and converges in about 40s time.

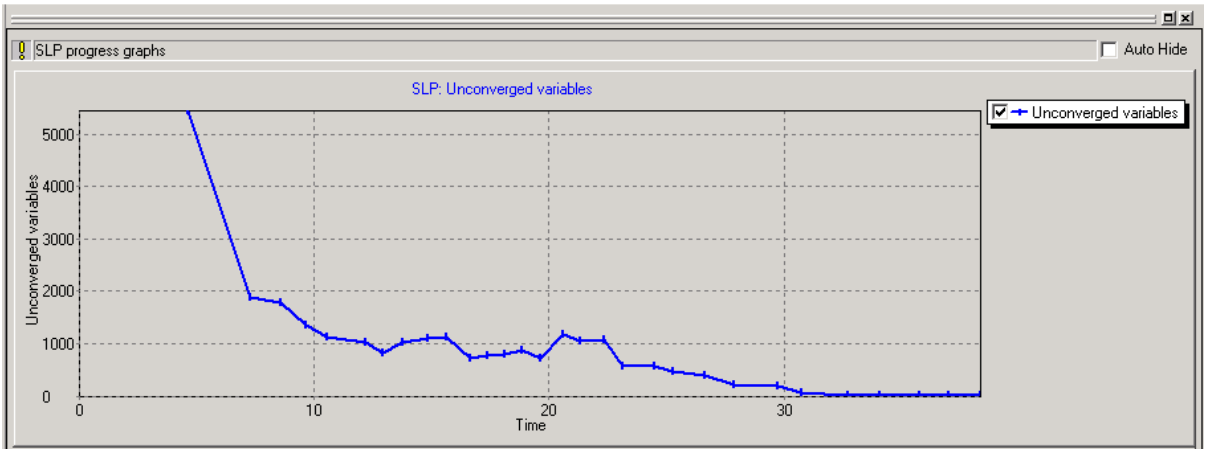


Figure 4-1: SLP speed of convergence: number of unconverged variables vs. time

4.5 Case Study 1

4.5.1 Test system description – 38 bus radial distribution network

The proposed methodology is applied to a radial 11kV distribution network with 38 buses and 37 branches, presented in Figure 4-2. The system shown in Figure 4-2 refers to EdF's (now UK Power Networks) East Dereham – Middlemarch Feeder, as a part of an IFI project [85].

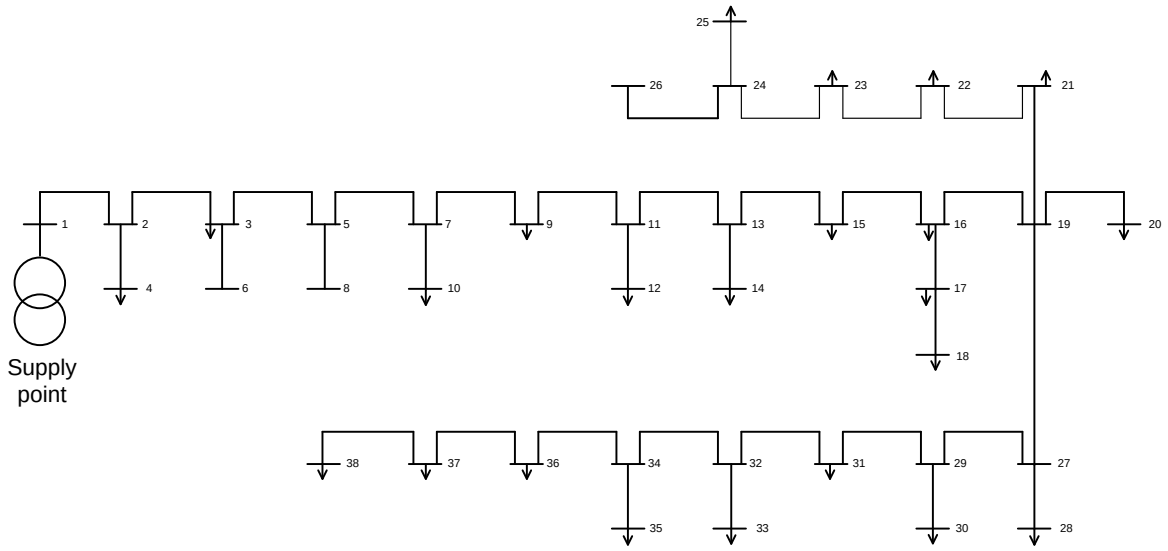


Figure 4-2: Distribution network 38 bus test system

The main system characteristics of the network from Figure 4-2 are summarized in Table 4-1, while details on load and branches are given in APPENDIX 4.

Table 4-1: Main Network Data

Voltage Level	No. of Buses	No. of Branches	No. of Loads	Peak Load	Consumed energy / Day
11 kV	38	37	23	2.96 MW	56.9 MWh

Load exists in 23 of 38 buses (load is indicated by an arrow next to the corresponding bus) and has a total peak demand of 2.96 MW. The assumed power factor for this network is $\cos\varphi = 0.98$. Voltage limits in all buses are assumed to be in range $\pm$6% of the nominal voltage. Transformer in supply point has voltage regulation capability in range $\pm$10% [86]. The network considered is a semi-urban area, thus the problems related to the lack of network capacity and under-voltages in distant buses are examined. Network lines are underground cables, dug in conduits, which makes their replacement or reinforcement costly. Demand is given as hourly time series data. By this, a typical winter day is selected for analyses as a more critical case since demand in the UK is generally higher during winter and gives more stress to the network [87].

Snapshot of the performed power flows during peak demand is given in Table A. 4-2 and Table A. 4-3, APPENDIX 4, from which one concludes that during peak time neither overloaded branches nor under-voltages in buses are detected in the system.

The capacity of the Supply Point is assumed to be large enough, thus the only constraints are the branch thermal limits and bus voltage magnitudes.

The cost of energy not served is assumed to be £3000/MWh.

4.5.2 Reference Case Results

In this section, the analysis will be focused on the permanent long-term load growth and its effects on network conditions. The increase of load causes bus voltage magnitudes to fall below the acceptable values specified in standards. This is a well known problem which is discussed in great details in distribution network planning literature, for example in [88]. Under-voltages may cause severe problems to the customers, such as: overheating or stalling of the induction-motors as their torque drops, dimming the incandescent lights, noisy motors and transformers, prolonged utilization of thermal loads etc. [63]. Also, load growth will lead to over-loading of network branches, and eventually some (or all) of them will have to be reinforced. Both under-voltages and line over-loading may be resolved by reinforcing the lines, replacing them with the lines of greater cross-section, which means lower impedance. However, this replacement is related with relatively high costs, especially in urban areas, where the cables are usually dug into the trenches under the streets.

In some cases reinforcement is even not possible, for example if there is not enough room to replace the overloaded transformer with a larger one. This section will give a techno-economical analysis of the underground cables replacement due to load growth, and justify or rule out the installation of non-network facilities such as Storage and DSR.

The analysis is performed by increasing demand from 0% to 30% in steps of 1%. Under the assumption that annual demand growth rate has a steady value of 1.3% [87], the load growth in year t can be expressed by using the following exponential expression [63]:

$$p(t) = (1 + 0.013)^t p_0 = 1.013^t p_0 \tag{62}$$

where p_0 is the load at current year (year 0), t is time expressed in years, and $p(t)$ is demand in year t. Equation (62) allows calculating time (year) when load reaches a certain level. For example, load grows 30% after

$$t = \frac{log 1.3}{log 1.013} = 20.3\ years \approx 20\ years \tag{63}$$

The result is rounded to the nearest integer. This means that analysed load growth of 30% covers observation period of 20 years. Then the costs incurred in that year may be referred to the present year and compared using present worth analysis [88].

As mentioned above, in case of base load (current year, 0% load increase), no under-voltage nor line overload occur. The simulation is then performed for each step of load growth.

It was found that the network is capable to sustain load growth in first three years. However, when load increases 5% which happens in Year 4, the under-voltages and line overloading appear. The obtained results on under-voltages for the whole network are summarized in Figure 4-3.

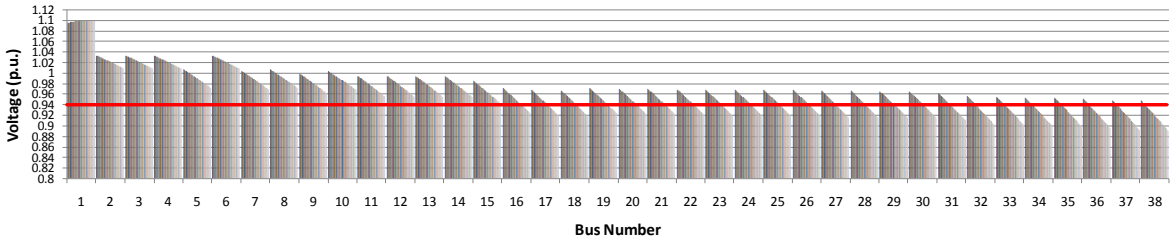


Figure 4-3: Minimal voltage throughout network vs. load growth

Figure 4-3 shows distribution of minimal voltages throughout the network as load increases. A trapezoidal bar over each bus number is actually consisted of 31 tiny bars, representing load growth from 0% to 30%, in steps of 1%. Horizontal line stands for lower voltage limit, which in this case is 0.94p.u. It can be noticed that voltage in all buses decrease (except in Bus 1 – supply point) as load grows. Buses 2-15, which are electrically close to the supply point (in Bus 1) do not experience

under-voltage within considered range of load growth. On the contrary, voltage in buses that are most distant from supply point, i.e. buses 37 and 38, falls below the limit of 0.94p.u. when load grows 5%, which happens in Year 4. As load continues growing, more and more buses experience under-voltage conditions. These under-voltages propagate from the most distant bus toward the supply point, as illustrated with shaded area in

Figure 4-4.

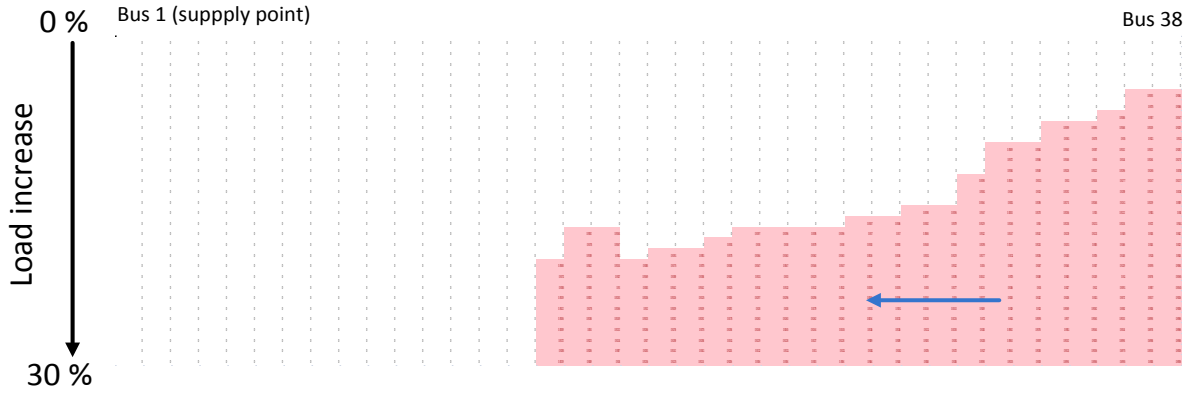


Figure 4-4: As load increases, under-voltages propagate towards supply point

Table 4-2 tabulates network lines for which the thermal capacity constraint is violated as load increases.

Table 4-2: Line thermal capacity constraints violation vs. load growth

Load Growth [%]	Year	Overload line From Bus – To Bus	Length [m]	Replace Cost (PV) [£]
5	4	1 - 2	275	18960
14	10	13 - 15	50	2527
21	15	2 - 3	1900	76664
21	15	15 - 16	200	8070
25	17	5 – 7	211	7530
27	19	3 - 5	326	10956
27	19	7 - 9	7800	262142
TOTAL:		7 lines	10762	386849

First column in Table 4-2 shows the level of demand growth at which the overloading occurs, and the second column gives the year when it happens. The year is calculated using Equation (63). Third column identifies the line itself, and 4th specifies the line length. Finally, 5th column shows the present value of replacement cost. In the bottom row in Table 4-2 , total number of replaced lines, their total length and total present value of replacement costs are listed.

Replacement cost is calculated when the line length is multiplied by the unit cost for asset replacement. The unit cost for replacement of 11kV underground cable is £82,900 [£/km] [90]. In

order to compare replacement costs arising in different years and to calculate the total cost, the Present Value (PV) method is used [88], referring all the costs to the current year:

$$C(t) = C(1+i)^{-t} = l \cdot c_{ugr} \cdot (1+i)^{-t} \tag{64}$$

In (64), $C(t)$ is the present value of the cost C (given in monetary units) t years in the future; l [km] is the length of the line that is replaced, $c_{ugr} = 82{,}900\ [\frac{£}{km}]$ is the cost for replacement 1km of 11kV underground cable, and i is the interest rate which for this work is assumed to be 5%[8].

The results of above preliminary analysis may be summarized as follows: time span of observing the network is 20 years, during which load grows 30%. In first 18 years there are totally 7 lines to be replaced, total length of which is over 10km and the present value of the replacement cost is £387k. This is illustrated in Figure 4-5. In the last two years (year 19 and year 20) when load grows 28-30%, there are no new overloaded lines.

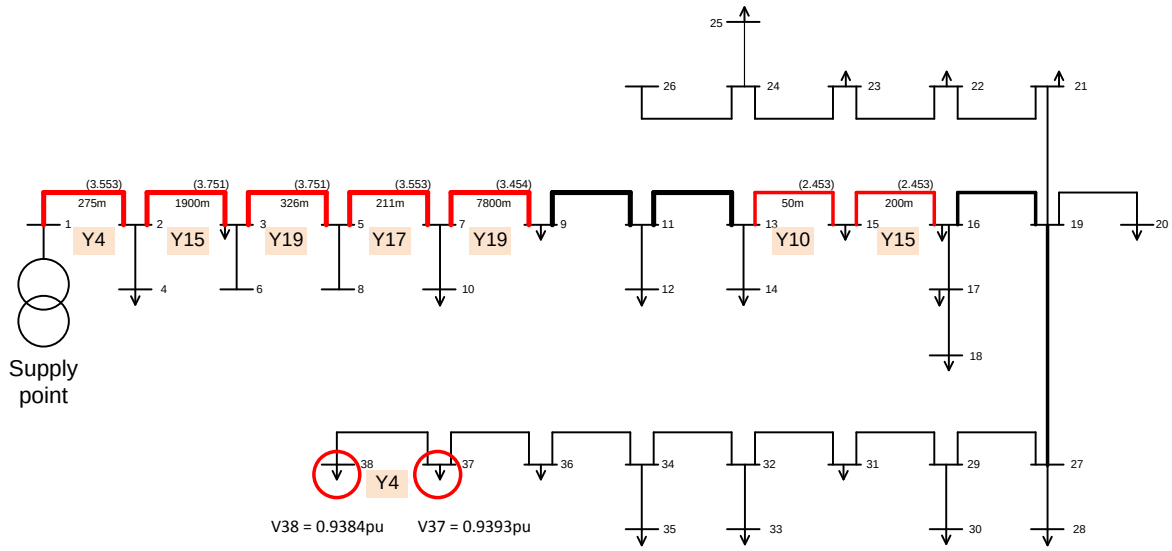


Figure 4-5: Congested lines caused by load growth

In Figure 4-5, congested (overloaded) lines are designated with a label beneath the lines specifying the year when the overloading occurs. Numbers in the brackets above the congested lines indicate thermal capacity in MVA. The length of each overloaded line is also specified in the figure. For example, in Year 4 when load increases 5%, line Bus 1 – Bus 2 becomes overloaded, which requires replacement 275m of the underground cable.

As for voltages, in the first 15 years, when load grows up to 21%, there are totally 23 buses in which low voltage limit is violated. These buses are Bus 16 to Bus 38, inclusively. The other buses do not go

[8] Forecasted long-term average interest rate for the UK in period 2017-2021 is 4.7%. Source: http://www.pwc.co.uk/the-economy/issues/long-term-interest-rates-forecasts.jhtml

under-voltage in spite of further load increase. The first two buses experiencing under-voltage are Bus 37 and Bus 38 when load increases 5%. This happens in Year 4 which is also illustrated in Figure 4-5.

4.5.3 DSR Results

In order to explore the benefits that DSR could potentially bring to managing congestions in distribution networks, the same batch of smart appliances is used as it was in CHAPTER 3. These appliances are:

- Washing machine
- Dish washer
- Washing machine with tumble dryer

The input data requirements considering smart appliances are the same as detailed in CHAPTER 2, and here will be summarized shortly:

- the forecasted load profile in each bus in the system
- operation cycle for each type of device
- control possibilities for each device
- expected number of controllable devices available at each time step

Smart Appliance characteristics, i.e. maximum time allowed for shifting and consumption pattern per operation cycle are the same as described in Table 2-2. Since this network represents a semi-urban area, penetration factor for washing machine is assumed to be greater than the national average 80% and is assumed to be 100%. Penetration of dish washer is assumed to remain on the same level as before, 80%, as indicated in Table 4-3.

Table 4-3: Summary of device types

Device type	Acronym	Shifting Capabilities	Consumption pattern duration [h]	Penetration factor [%]	Number of devices
Washing machine 1h	WM1	1h	2	25	750
Washing machine 2h	WM2	Up to 2h	2	25	750
Washing machine 3h	WM3	Up to 3h	2	25	750
Dish Washer	DW	Up to 6h	2	80	2400
Washing machine + Tumble Dryer	WM+TD	Up to 3h	4	25	750

Diversified consumption pattern, operation cycle and energy consumption per cycle for each type of Smart Appliance are detailed in Section 2.3, CHAPTER 2.

The number of customers in the network is estimated based on the total network peak. Since the network peak is around 3MW, and assuming that diversified load peak for household is about 1kW [92], it comes out that the number of households is around 3,000.

Expected number of smart appliances to start consumption throughout the day and for each type of device, is calculated using diversified curve disaggregation technique, as described in CHAPTER 2, Section 2.4.1.

Similar analysis is performed as in Section 4.5.2, this time with a batch of Smart Appliances applied to the test system. Again, the load was increased up to 30%, in steps of 1%. Assuming that annual load growth is 1.3%, this increase of load covers time period of 20 years. Network parameters and load are the same as depicted in Section 4.5.1.

The results of the analyses show that DSR helps network to endure load growth up to 18%, which happens in Year 13. When load increases 18%, Bus 37 and Bus 38 go under-voltage, and line between Bus 1 – Bus 2 becomes overloaded. With further increase of load, more and more buses experience under-voltage conditions, as shown in Figure 4-6. However, in contrast to the case without DSR where voltage limits were violated in 23 buses, in the case with DSR under-voltage is detected in 12 buses, namely buses 27-38, inclusively. It clearly shows that DSR could be effectively applied to mitigate voltage problems in distribution networks.



Figure 4-6: Under-voltages propagation towards supply point when DSR is applied

Table 4-4 shows overloaded network lines.

Table 4-4: Line thermal capacity constraints violation vs. load growth

Load Growth [%]	Year	Overload line From Bus – To Bus	Length [m]	Replace Cost (PV) [£]
18	13	1 - 2	275	12200
27	19	13 - 15	50	1680
TOTAL:		2 lines	325	13880

There are totally 2 lines to be replaced (7 lines in base case - compare with Table 4-2), first one in Year 13 and second one in Year 19, as shown in Figure 4-7. Total length of these two lines is 325m (over 10km in base case) and the present value of the replacement cost is £14k (compared to £387k in base case). From the results presented, it can be concluded that for this network the application of DSR allows to defer the investments in network reinforcement for about 9 years: instead of reinforcing line Bus 1 – Bus 2 in Year 4, as it was required before (see Table 4-2), now this line has to be reinforced in Year 13. Cost savings brought by DSR are £373k, which is the difference of total costs without DSR and the costs when this facility is used.

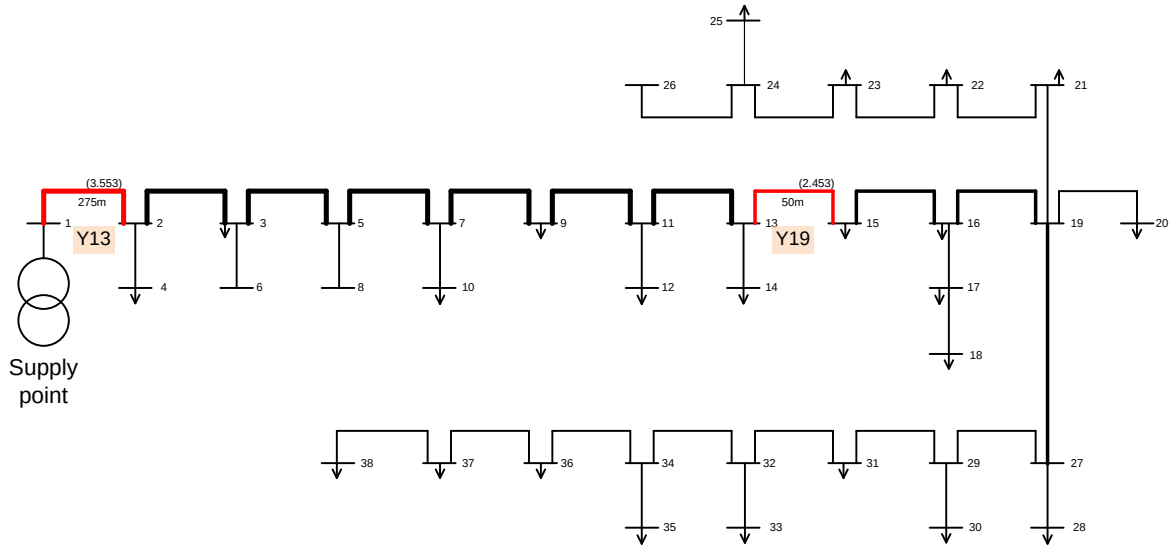


Figure 4-7: Congested lines caused by load growth in case when DSR is applied

As explained above, when load increases 18% in Year 13, overloading in line Bus 1 – Bus 2 and under-voltage in Bus 37 and Bus 38 occur. It is interesting to compare power flow through this most congested line and voltage in the most distant bus (Bus 38) in the situation that just precedes the constraints violation, i.e. when load increases 17%. This is shown in Figure 4-8.

Figure 4-8a shows time evolution of voltage in Bus 38 when load increases 17%. It can be noticed that voltage goes as low as 0.92p.u. if DSR is not exercised (solid line). This is below the limit of 0.94p.u. represented by solid straight line in Figure 4-8a, during peak hours (hours 16-20). On the

contrary, when DSR is applied, voltage does not fall below the limit (dashed line). DSR shifts load from peak hours to off-peak hours. This is why the voltage in after-peak hours (from 8pm to 12pm), when DSR is applied, is lower than the voltage without DSR in the same period. In general, even without voltage and line capacity constraints, DSR has a tendency to flatten voltages, which is related with network losses, and more details on this may be found in Section 4.5.6 of this chapter. An example where this happens is during period of low demand (1-5am). At the beginning (hours 1-3am), DSR reduces load (see dashed line in Figure 4-8c that represent net DSR activity) which leads to voltage increase, and from 4-6am it increases the load, lowering the voltage.

Figure 4-8b shows apparent power flow through line Bus 1 – Bus 2, observed from Bus 1 side. Note that this power at the same time presents total demand plus network losses. When DSR is not applied (solid curve), apparent power in branch Bus 1 – Bus 2 during peak hours (hours 16-20) goes above thermal capacity limit of 3.553MVA, represented by solid straight line. When DSR is applied, apparent power does not excess the limit (dashed line).

Figure 4-8c shows DSR reduction and payback at system level. Load reduction is conventionally assumed to have negative sign, as it is deducted from the load, whilst load payback is assumed to have positive sign, as it is added to the load. Dashed line in Figure 4-8c presents net DSR, obtained as a sum of load reduction and load payback. As expected, net DSR takes lowest negative values at peak hour (5pm). Then as peak ceases so the net DSR does (goes toward zero). After 8pm payback becomes greater than load reduction (in absolute values). It is important to note that the total payback energy during a day is equal to the total reduced energy, i.e. all energy is recovered.

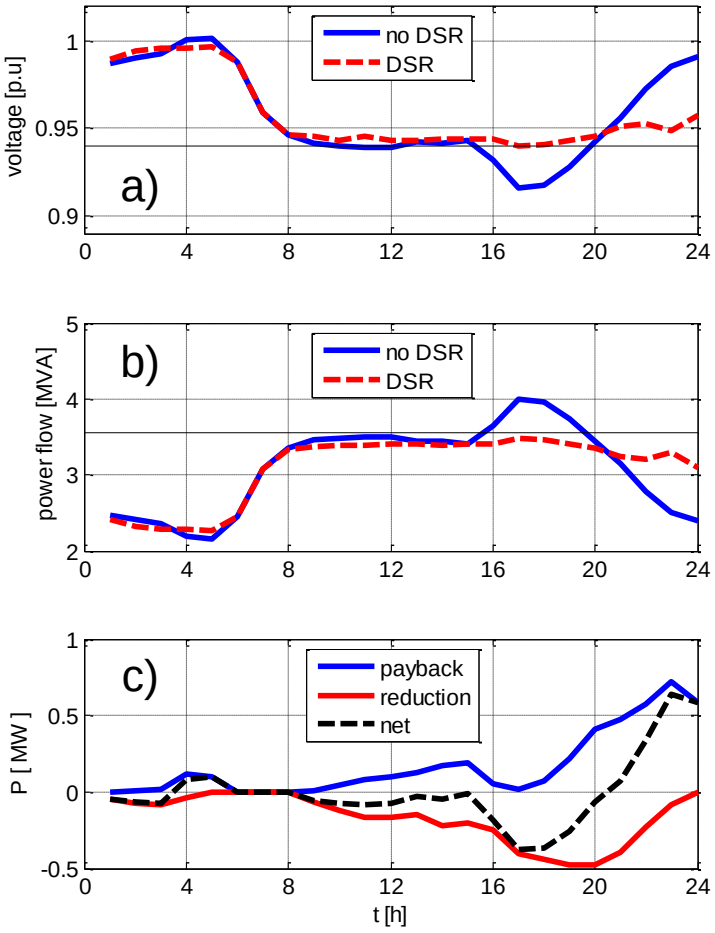


Figure 4-8: a) voltage in Bus 38; b) apparent power flow through line Bus 1 – Bus 2; c) DSR reduction and payback at system level

The information on shifted devices is important to make a judgement on the contribution that each type of smart appliance adds to the total system benefit. This information contains, for each device type, the number of shifted devices, time step from which they are shifted, time step where they are shifted to, and bus number. Only few excerpts of this information are tabulated in Table 4-5.

Table 4-5: Details of shifted devices

From time	To time	Device type	Bus	No. of devices
...				
9	10	WM 1h	15	1
9	10	WM 1h	16	2
...				
10	14	DW	9	5
...				
15	18	WM+TD	37	4
...				

Information on shifted devices is used to calculate DSR activity. DSR activity is defined as amount of shifted energy multiplied by the time difference between destination time (time step the device is shifted to) and origin time (time step the device is moved from – this is originally scheduled time for device operation):

$$DSR_k = E_k \sum_i N_k(i) \cdot (T_{to}(i) - T_{from}(i)) \tag{65}$$

where DSR_k is DSR activity for device type k and E_k is energy consumption per operation cycle for device type k (energy consumption per cycle is given in Table 2-2). Summation in (65) is done for all rows in Table 4-5 that contain device type k. N_k, T_{to} and T_{from} are data from fifth, second and first column in Table 4-5, respectively.

Results on DSR activity are shown in Figure 4-9a for the case of 17% load increase. As expected, it can be noticed that more flexible devices, in terms of shifting in time, exhibit higher DSR activity. For devices of the same kind, such as WM1h, WM2h and WM3h, that differ only in shifting flexibility and that have all other parameters the same, dependence DSR activity on shifting flexibility is almost linear. Since DSR activity depends also on energy consumption per cycle (factor E_k in (65)), devices that have the same shifting capabilities but different energy consumption per cycle will manifest different DSR activities. For example, WM3h and WM+TD both may be shifted up to 3h. However, since WM+TD has much higher energy consumption per operation cycle (3.3475kWh for WM+TD comparing to 0.887kWh for WM3h), WM+TD shows higher DSR activity. Dish Washer (DW) demonstrates highest DSR activity mainly as it is the most flexible device (may be shifted up to 6h) but also because it has higher energy consumption per cycle than a washing machine.

Number of shifted devices for each type of appliance is shown in Figure 4-9b. Comparing Figure 4-9a with Figure 4-9b, one can more clearly see the impact of energy consumption per operation cycle on DSR activity. For example, number of shifted washing machines with tumble dryer (WM+TD) is approximately the same as for the other washing machines, but DSR activity of WM+TD is much higher than the activity of all other washing machines together. This is due to TD, which has relatively high energy consumption per operation cycle. This is designated in Figure 4-9a with red numbers over the bars, representing percentage of total DSR activity. One can see that almost 22% of DSR activity is due to WM+TD, while the other three types of washing machines participate together less than 14%.

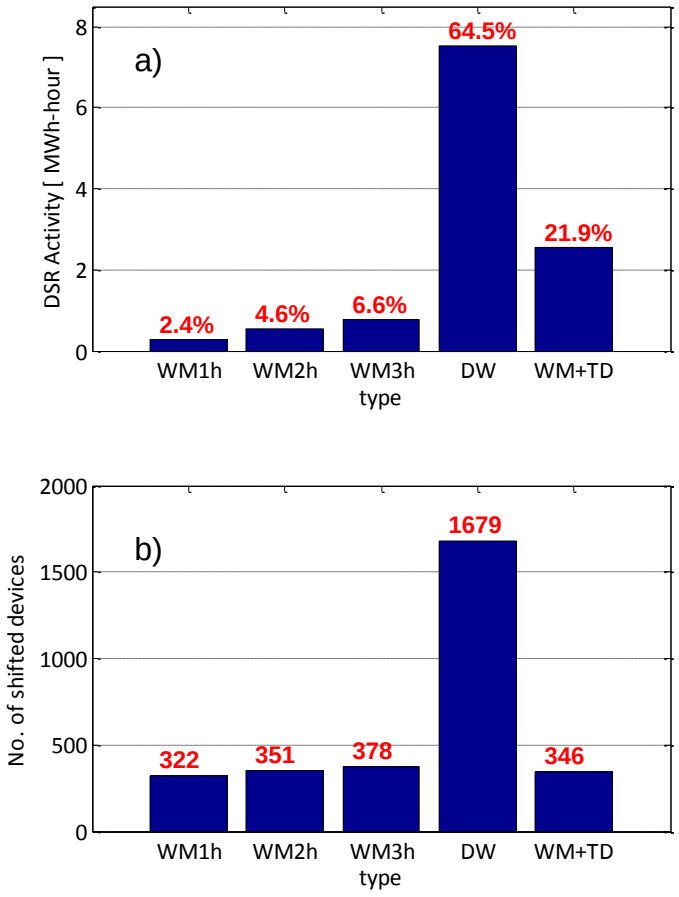


Figure 4-9: a) DSR activity; b) number of shifted devices

In this case study it is assumed that all households have a washing machine (see Table 4-3), so the number of washing machines on the network is equal to the number of households: 3,000. However, total number of actually shifted washing machines (for all types) is 1397, which is less than half of

the full amount. The others that have not been shifted mostly start their operation during off-peak time, and their shifting would not contribute reduction in operation costs.

It is also assumed that 80% of households have a dish washer (DW) – see Table 4-3, thus the estimated number of DW on the network is 2,400. As Figure 4-9b shows, 1679 of them (70%) participate in energy shifting, which is much higher percentage than WMs. The reason for this is relatively high flexibility of DW (may be shifted up to 6h) comparing to all other types of devices. So, the higher flexibility of a device, the higher probability it will be used for managing network congestions.

Figure 4-10 shows the total number of shifted WM1h (Figure 4-10a) and DW (Figure 4-10b) for the whole network, together with their originally scheduled time ('from hour') and the time scheduled after the optimization ('to hour'). This figure is obtained based on Table 4-5, when the rows with WM1h (DW) are extracted and summed up for all network buses. Similar graphs may be made for other types of smart appliances as well.

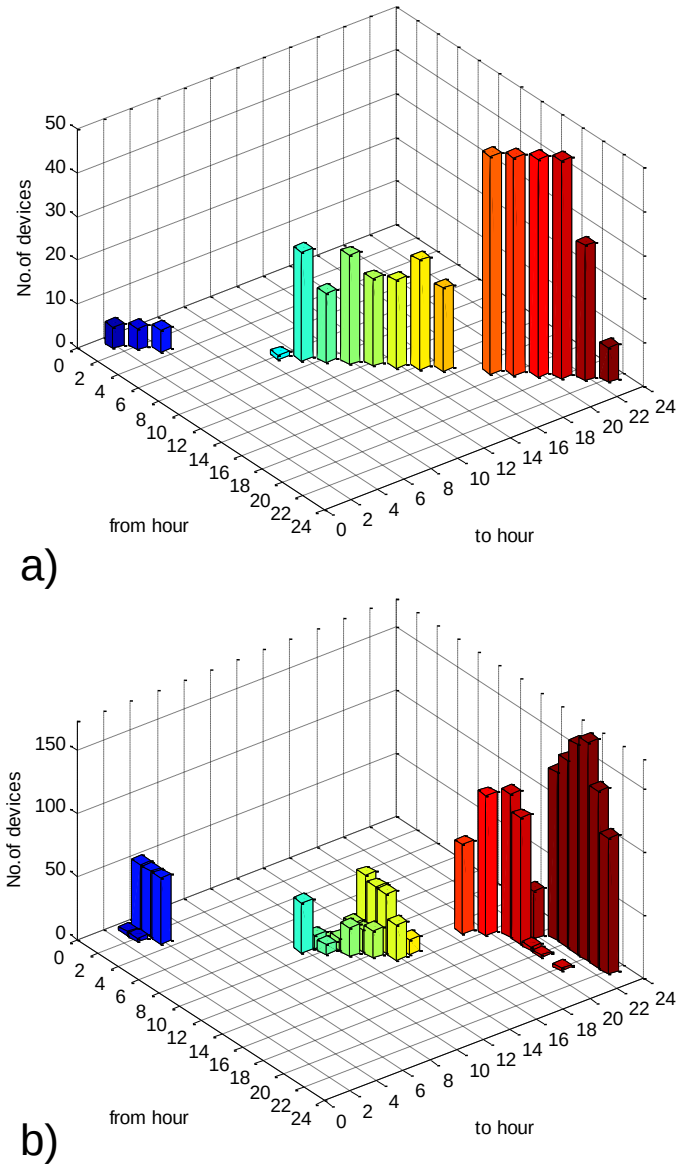


Figure 4-10: DSR scheduling of WM1h (a) and DW (b) for the whole network

Figure 4-10a shows that in case of WM1h, due to its small flexibility, most devices are shifted around system peak – both 'from hour' and 'to hour' are within peak period (17-20h). On the contrary, DW has more flexibility (up to 6h) and therefore these devices are relocated away from peak period: for most devices 'from hour' is peak period (17-20h), but the time where they are moved to is the period of lower demand (21-23h).

The value of the smart appliances and the economic impact they bring to the system will be given in Section 4.5.5, where a comparative economical analysis between DSR and storage will be made.

4.5.4 Storage Results

Specified storage attached at the most distant bus

In previous sections it was shown that under-voltage problems start from electrically distant buses in the network and propagate towards supply point as load increases (see

Figure 4-4 and Figure 4-6). From this reason, installing of energy storage in the most distant bus (Bus 38 in Figure 4-2) is explored. The storage has the following characteristics:

Table 4-6: Storage characteristics

Parameter	Value
Rated Power	200 kW
Energy Capacity	1.2 MWh
Efficiency	83%
Type	battery

This situation is similar to the case described in CHAPTER 3, where storage capacity was allocated among selected buses. In this case, the number of selected buses is reduced to – one. With specified storage attached to Bus 38, performed is the same analysis as before: load was increased up to 30% in steps of 1%, which covers time period of 20 years (assuming annual load growth of 1.3%). All other network and load parameters are the same as before.

The results of the analyses show that specified storage installed at Bus 38 helps network to support load growth up to 12%, which happens in Year 9. When load increases 12%, line between Bus 1 – Bus 2 becomes overloaded. In Year 11, when load increases 15%, Bus 37 and Bus 38 go under-voltage. With further increase of load, under-voltage conditions propagate towards Supply Point, as shown in

Figure 4-11. There are total 23 buses going under-voltage during the observation period, which is the same with base case (with no storage). The only difference is that under-voltage in Bus 37 and Bus 38 occur in Year 11 with storage, comparing to Year 4 in Base Case without storage.

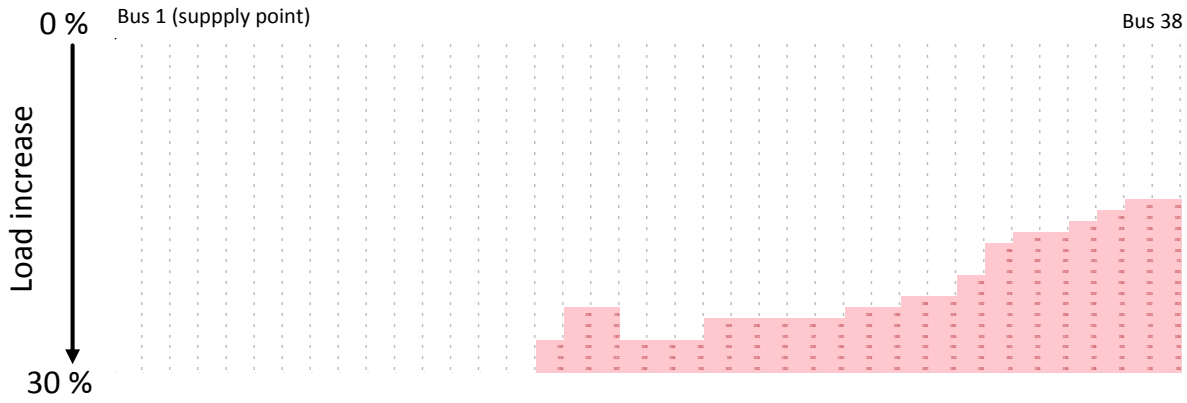


Figure 4-11: Under-voltages propagation towards supply point in case when Storage 200kW, 1.2MWh is installed in Bus 38

Table 4-7 shows overloaded network lines, load level and year when overloading occurs, as well as line length and present value of replacement costs.

Table 4-7: Line thermal capacity constraints violation vs. load growth

Load Growth [%]	Year	Overload line From Bus – To Bus	Length [m]	Replace Cost (PV) [£]
12	9	1 - 2	275	14858
24	17	13 - 15	50	1839
28	19	2 - 3	1900	61991
TOTAL:		3 lines	2225	78688

There are totally 3 lines to be replaced, total length of which is 2.2km, and the present value of the replacement cost is £79k (compare to Base Case: cost to reinforce 7 lines with over 10km was £387k, see Table 4-2). Figure 4-12 highlights the lines in the network to be reinforced and indicate the years when the reinforcement should take place. From the results presented, it can be concluded that for this network with Energy Storage installed at the most distant bus, network reinforcement may defer for about 5 years: instead of reinforcing line Bus 1 – Bus 2 in Year 4 in Base Case, with storage it has to be reinforced in Year 9. Total costs saving due to this particular storage installed in the most distant bus is almost £308k, compared to Base Case.

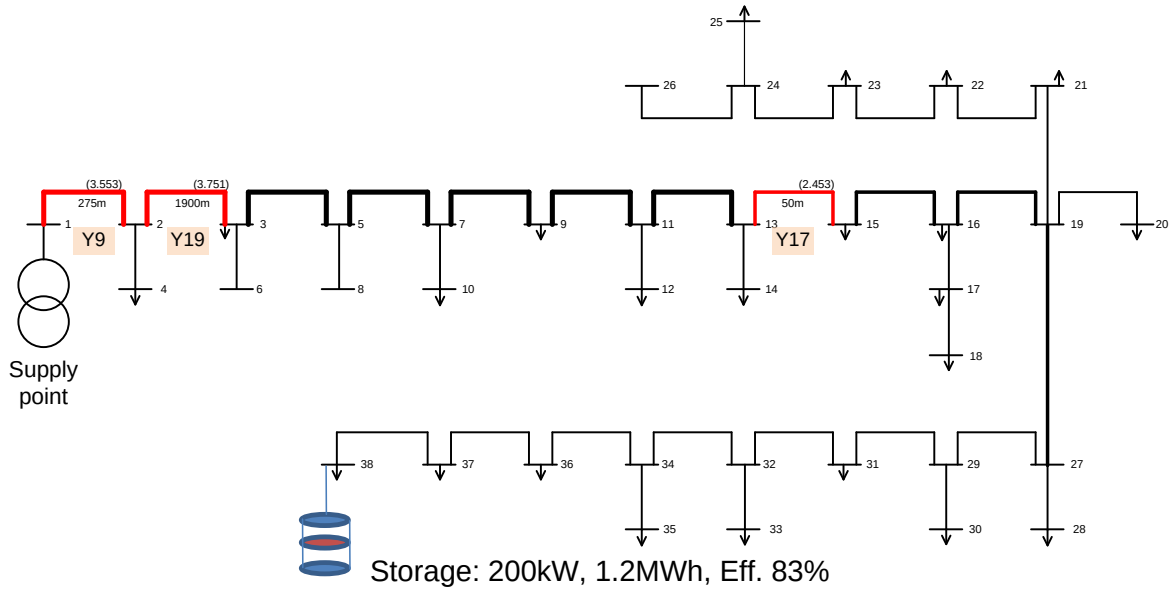


Figure 4-12: Congested lines and reinforcement schedule caused by load growth in case when given storage is installed in the most distant bus

Figure 4-13 shows voltage in the most distant bus (Bus 38), power flow through line Bus 1 – Bus 2 and storage activity just before and after the overload occurs, i.e. when load increases 11% and 12%.

By analyzing Figure 4-13 c) that shows storage activity, it can be concluded that it is the storage power rather than storage energy capacity that limits the utilization of this specific storage in the network: storage has energy capacity of 1.2MWh, thus it is capable to discharge rated power of 200kW in duration of 6h. Peak duration itself is 3 hours, from 4pm to 7pm. However, when load increases 12%, there is line overloading in spite of storage being discharged at full power at 5pm and 6pm. This overloading occurs since storage rated power is not enough to support increasing load. It is worth noting that storage prevents voltage magnitude in Bus 38 falling below the lower limit of 0.94p.u, as shown in Figure 4-13a. The same chart shows that voltage drops to 0.93p.u. when load increases 11% if storage is not applied.

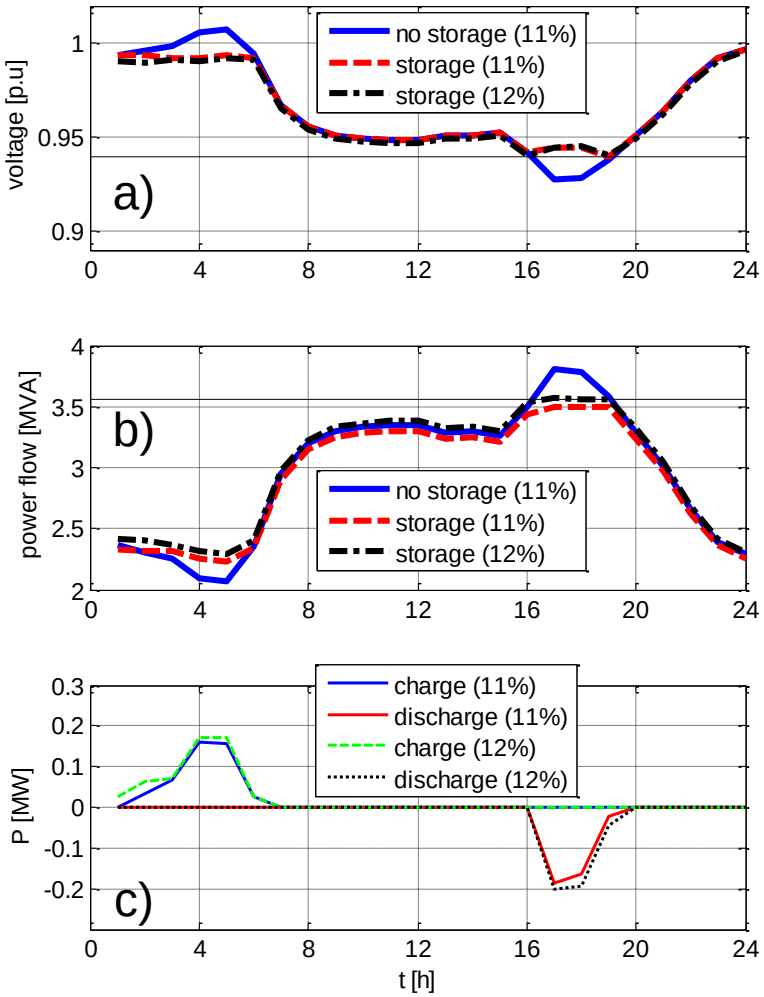


Figure 4-13: voltage in the most distant bus (Bus 38) (a); apparent power flow through the most congested line (Bus 1 – Bus 2) (b); Storage activity (c)

Also note in period 1-6am voltage in the most distant bus in case of storage is lower than in base case (Figure 4-13a). It is due to storage charging in this period. Storage charging is even higher at 4-6am, when system demand is lower and voltage in the network is higher (compare to solid line in Figure 4-13a representing the voltage in base case). This voltage self-regulation by storage (to charge during light demand and discharge during heavy demand) is not specifically modelled. However, it is the consequence of reducing network losses, as it will be explained in Section 4.5.6. Note that energy discharged from the storage is always less than the energy stored (Figure 4-13c), due to energy conversion losses in storage. The role of storage efficiency will be discussed when the losses in the network are analyzed.

Optimal Storage size and location

In previous section it was demonstrated that specified storage (200kW, 1.2MWh) installed in the most distant bus is insufficient to successfully resolve network congestion problems when load increases over 11%. Related to this, several questions arise:

- What is the maximal load growth that can be resolved by storage utilization?
- What are storage optimal rated power and optimal energy capacity to support that maximal load growth?
- Where (which bus) should the storage with parameters found above be placed?

In order to answer these questions, storage model described in Section 4.3 is applied. A set of twelve buses eligible for storage installation is: 2, 6, 11, 18, 23, 26, 27, 28, 29, 34, 36, and 38, as indicated with circles around buses in Figure 4-14. The selection of eligible buses for storage placement depends on the space available for storage and auxiliary equipment installation, bus infrastructure, etc. Usually a DNO would install a single storage in the feeder, so the optimization has to choose only one amongst these 12 buses to place the storage at. If there were two storage devices, then the optimization would chose two buses, etc. The estimated total storage cost is £1,000 per installed kW [93].

As before, load was increased up to 30% in steps of 1%. All other network and load parameters remain intact.

The results of the analyses show that the optimal storage location is Bus 29, as shown in Figure 4-14. Optimal storage size is found to be 750kW and 3.7MWh. This storage helps network to endure load growth up to 25%. In Year 18 when load increases 26%, lines Bus 1 – Bus 2 and Bus 13 – Bus 15 become overloaded and at the same time Bus 37 and Bus 38 go under-voltage. When load further increase to 30%, there are total five buses going under-voltage (Bus 34 to Bus 38, inclusively), comparing to 23 buses in Base Case.

Figure 4-14 highlights the lines in the network to be reinforced and indicates the years when the reinforcement should take place.

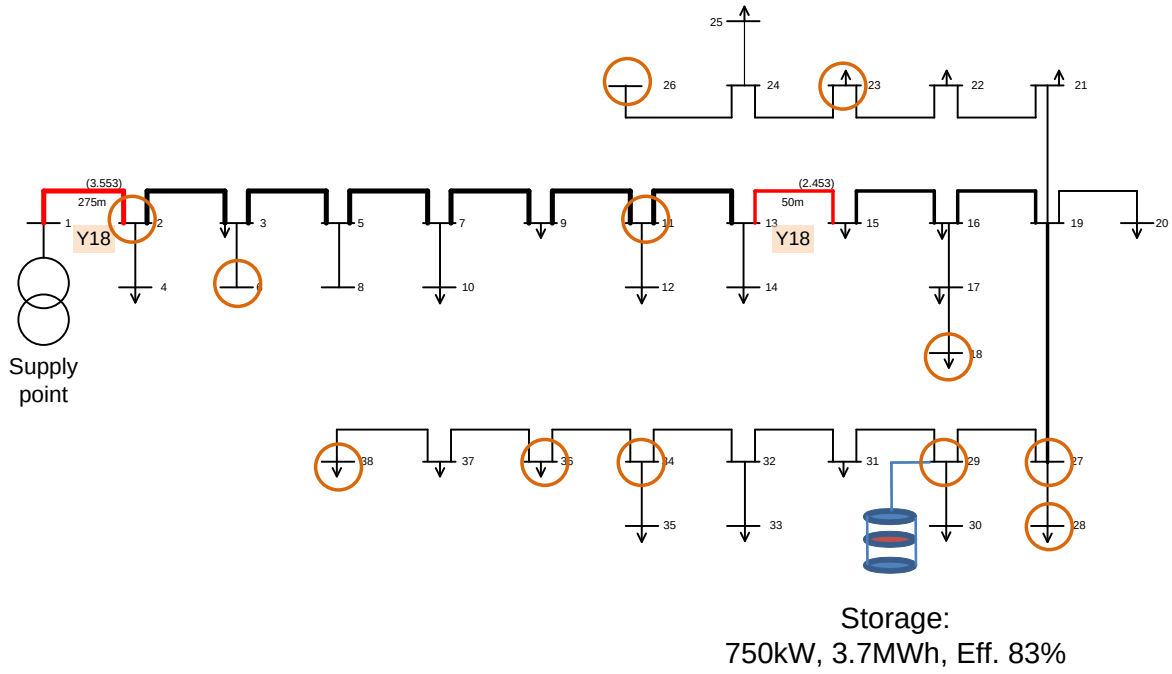


Figure 4-14: Congested lines and reinforcement schedule in case of optimal storage location and size

Table 4-8 lists the overloaded network lines. It also shows load level and year when overloading occurs as well as line length and present value of replacement costs.

Table 4-8: Line thermal capacity constraints violation vs. load growth

(optimal storage location and size)

Load Growth [%]	Year	Overload line From Bus – To Bus	Length [m]	Replace Cost (PV) [£]
26	18	1 - 2	275	9522
26	18	13 - 15	50	1731
TOTAL:		2 lines	325	11253

There are totally 2 lines to be replaced, total length of which is 325m, and the present value of the replacement cost is about £11k (compare to Base Case: cost to reinforce 7 lines with over 10km was £387k, see Table 4-2). From the results presented, it can be concluded that for this network with Energy Storage (750kW, 3.7MWh) installed in Bus 29, network reinforcement may defer for about 14 years, whilst total costs saving is almost £374k.

Figure 4-15 explains the impact of storage location on voltage in the most distant bus (Bus 38): if storage (750kW, 3.7MWh) is installed in Bus 29, as suggested by optimization, no under-voltage occurs when load grows 25%. However, if storage is installed in Bus 27, there is under-voltage in Bus

38 during peak hours 5-6pm, as the inset in Figure 4-15 shows. This under-voltage is relatively small, but it can be demonstrated that the farther storage is installed from Bus 38, the higher the under-voltage in the bus. This is why storage cannot be placed in any bus closer to the supply point.

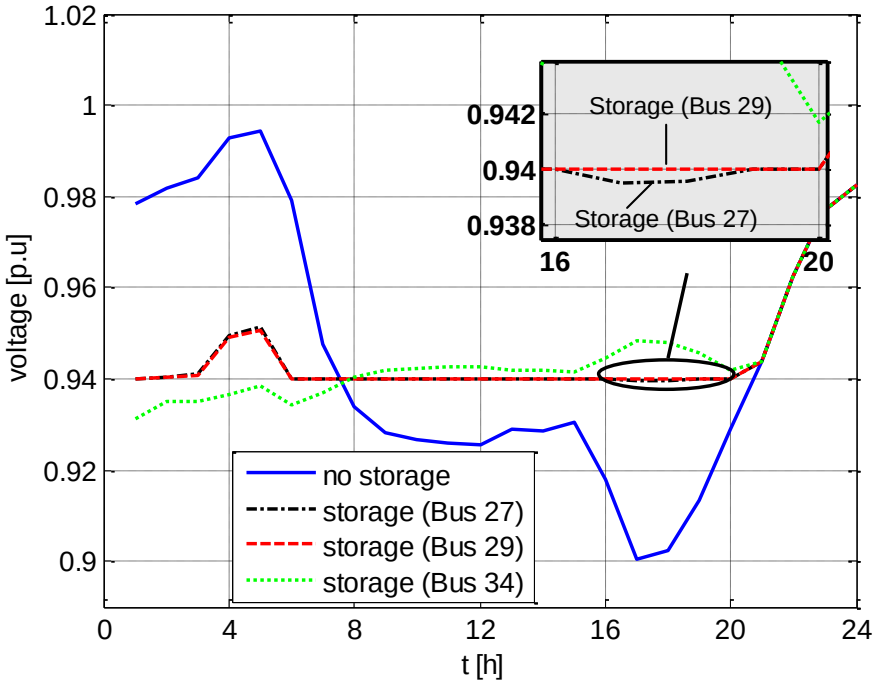


Figure 4-15: Voltage in Bus 38: voltage stays above low limit only if Storage is installed at Bus 29

Also because of the low voltage problem, storage cannot be placed in Bus 34, or any other bus towards the end of the feeder. Dotted line in Figure 4-15 clearly indicates that during storage charging (1-6am) voltage in Bus 38 falls below -6% of the nominal value if storage is installed in Bus 34. The voltage condition in the most distant bus (Bus 38) would worsen if storage was placed closer to the feeder end. Therefore, the optimal storage location amongst eligible buses is Bus 29.

4.5.5 Economic benefits of Demand Side Response and Energy Storage

In this section, a comparison of economic benefits between alternative methodologies is presented. For this analysis, it is assumed that economic benefits come from the savings in underground cables reinforcement costs. As the reinforcements should take place at different years in future, in order to get a fair estimation of the total expenditure, all the costs are referred to the current year, which is done by using present value calculations as described in Section 4.5.2, Equation (64).

Table 4-9 gives a summary of the results obtained in previous sections for each discussed approach. Tabulated are, apart from the present value of the replacement costs, some additional information such as when the first investment is necessary, the total number of lines to be replaced in the observed period and their total length.

Table 4-9: Comparison of economical benefits of DSR and Storage

		Methodology			
		Base Case	DSR	Storage 200kW	Storage 750kW
Year of 1st investment		4	13	9	18
Number of lines to replace		7	2	3	2
Total length	[m]	10,762	325	2,225	325
Total replacement cost (PV)	[£]	386,849	13,880	78,689	11,254
Replacement cost savings	[£]	-	372,969	308,160	375,595
Investment cost	[£]	-	21,600	200,000	750,000
Net benefit	[£]	-	351,369	108,160	-374,405

Based on the cost for replacement of 11kV underground cable of £82,900 [£/km] [90], total present value of replacement cost is calculated. Cost saving for each technology (DSR or Storage) is obtained when the replacement cost for that technology is subtracted from the replacement cost in base case.

The net benefit is calculated under certain assumptions. First of all, it is assumed that the storage investment cost is £1,000/kW [93]. It means that:

- investment in 200kW storage costs £200,000
- investment in 750kW storage costs £750,000

Investments related to DSR assume there are:

- mass deployment of smart appliances
- existence of smart meters in households
- existence of communication network between smart meters and central DNO dispatching centre
- investment cost per appliance is £4 [67], including the communication between smart meter and appliance
- estimated number of smart appliances in this network is 5,400, therefore the investment cost is $5{,}400 \cdot 4 = £21{,}600$

The net benefit is then calculated when the investment cost is deducted from the cost savings.

From Table 4-9 and obtained results, it can be concluded that Storage of 200kW is economically justified. However, storage of 750kW is still not economically justified, taking into account present cost of investment. DSR is economically justified under the above-mentioned assumptions. However,

note that in this analysis the only source of economic benefit comes from savings in replacement costs. Other stream of revenue for storage and DSR may also come from wind energy integration, ancillary system services provision, reduction in CO_2 emissions etc.

The value that storage brings to the system in order to postpone the network reinforcement may be defined as avoided costs in the network investments for the observed period:

$$V_{sto} = \frac{1}{PERIOD} \cdot \left(\frac{IC - IC_{STO}}{P_{storage}} \right) \tag{66}$$

where IC and IC_{STO} are network investment costs without and with storage, respectively. $PERIOD$ is observation period, in this case 20 years. The values for IC and IC_{STO} are taken from Table 4-9.

For storage 200kW, from Table 4-9 one obtains:

$$V_{sto,200kW} = \frac{1}{20} \cdot \frac{386849 - 78689}{200} = \frac{1540.8}{20} = 77$$

which says that value of storage for the total period of 20 years is 1541 £/kW, and annualized value is almost a 80 £/kW. For storage 750kW, value is:

$$V_{sto,750kW} = \frac{1}{20} \cdot \frac{386849 - 11254}{750} = \frac{500.8}{20} = 25$$

Value of 750kW storage is almost one-third of the 200kW storage. The results are in line with those obtained in CHAPTER 3.

Similarly, the value of smart appliances can be defined as avoided costs in the network investments for the observed period. Value per smart appliance (average value) is then:

$$V_{avg} = \frac{1}{PERIOD} \cdot \left(\frac{IC - IC_{SA}}{\sum N_i} \right) = \frac{1}{20} \cdot \frac{386849 - 13880}{5400} = \frac{69.1}{20} = 3.5$$

where $\mathrm{IC_{SA}}$ are network investment costs with smart appliances, that also may be found in Table 4-9. $\sum \mathrm{N_i}$ is total number of smart appliances on the network. Thus, the value that each smart appliance brings to the system for the whole observation period is about 70 £/device, and annualized value is around 3.5 £/device/year.

4.5.6 Network losses reduction with DSR and Storage

This section will discuss a phenomenon which has been discovered during testing the non-linear OPF model with DSR and Storage. Namely, as it was mentioned above, both DSR and Storage have a tendency to flatten the network voltage profiles: DSR shifts load to the periods of low demand and relatively high voltages, thus lowering the voltages in these periods. It also shifts load from the periods of higher demand and relatively low voltages, thus increasing voltage. This happens even in

case when voltage or line thermal capacity constraints are not infringed. As a result, voltage profiles will be less dynamic.

Similarly, storage is charged during low demand and relatively high voltages and discharged during higher demand and relatively low voltages. This results in reduced time-variation of voltages throughout the network. However, in contrast to DSR, which is exercised to flatten the voltages at all load levels, it was noticed that storage becomes active only when load grows over certain amount. During these tests the voltage constraints and line thermal capacity constraints were both disabled, so the constraints were not a trigger for storage activity. Since the principal difference, from the modelling point of view, between the shifting algorithm incorporated in DSR and storage, is that the former one has no losses and the latter one has losses due to efficiency of charging and discharging, the research was focused in that direction. When the storage efficiency was set to 100%, it started behaving alike to DSR.

The explanation for this behaviour of DSR and Storage lays in network losses: voltage in the network depends on load - the higher the load the lower the voltage. Apart from voltage, the losses in network lines also depend on load: losses are higher in periods of higher load. This is shown in Figure 4-16, which portrays total load (upper chart), total power losses in the network (middle chart) and voltage profile in Bus 38 (lower chart).

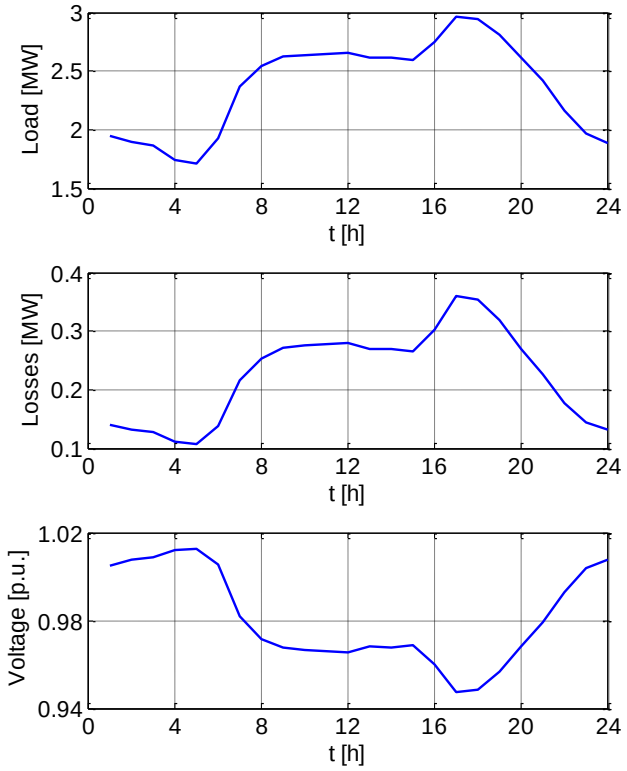


Figure 4-16: Dependence of total network losses (middle chart) and voltage (lower chart) on system load (upper chart)

The optimization tries to reduce the losses, as it will lead to the lower generation costs. In other words, it will try to reduce load whenever possible.

In case of DSR, since there are no losses associated with load shifting, DSR will shift load at all demand growth levels. This is shown in Figure 4-17, depicting the net DSR, for the case when there is no load increase and the case when load grows 20%. Negative values of net DSR mean load reduction, whilst positive values mean payback. It can be seen that for both load growth levels DSR is active. This has repercussions to total network losses as shown in Figure 4-18. Finally, Figure 4-19 depicts voltage in Bus 38.

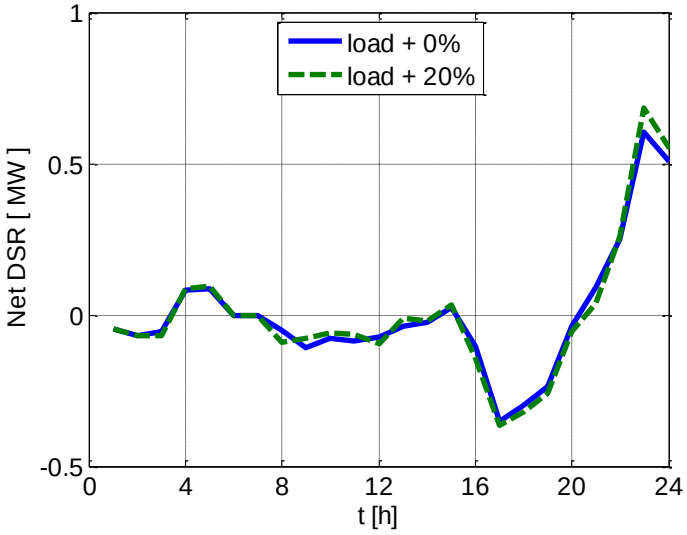


Figure 4-17: Net DSR activity

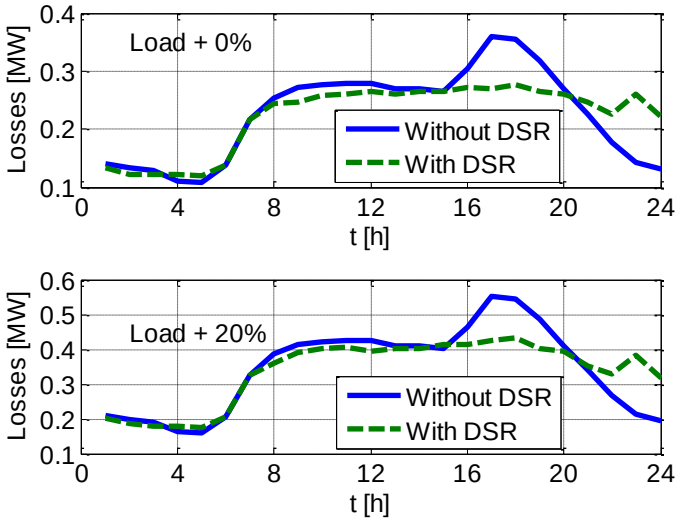


Figure 4-18: Total losses in the network with and without DSR when: there is no increase in load (upper chart) and load increases 20% (lower chart)

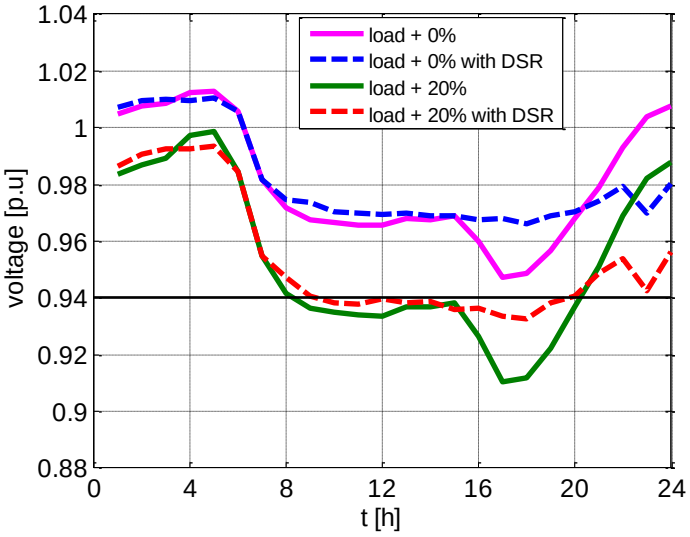


Figure 4-19: Voltage in Bus 38 with and without DSR, for no load increase and for load increase 20%

Even though losses are increased during payback periods (8-12pm), total network losses are reduced when DSR is applied, for any load level. Table 4-10 shows network losses, in addition to DSR reduced and payback energy for three demand levels: 0%, 10% and 20% growth.

Table 4-10: Total network losses are reduced due to DSR

Load	Network Losses [MWh]			DSR energy [MWh]		
	Without DSR (1)	With DSR (2)	Losses reduction (3) = (1) - (2)	Reduction (4)	Payback (5)	DSR Losses (6) = (4) - (5)
Load + 0%	5.4191	5.3351	0.084	4.1963	4.1963	0
Load +10%	6.7213	6.6122	0.1091	4.3272	4.3272	0
Load +20%	8.2108	8.0744	0.1364	4.3984	4.3984	0

Similar analysis is done with a storage (200kW, 1.2MWh, 83%) attached to Bus 38. Here the storage rated power, energy capacity size and the bus where it is attached does not play the role, since the constraints related to bus voltages and lines thermal capacity are disabled. The main parameter that affects optimizer selecting storage activity is storage efficiency, as will be shown in the following text.

Figure 4-20a shows storage activity, for the case when load grows 0%, 10% and 20%. One can see that storage is not active for load growth 0% and 10%. This is why losses in the network are the same without and with storage, Figure 4-20b – upper chart. The same applies to voltages, Figure 4-20c. However, in case of 20% load growth, storage is active (Figure 4-20a), which has impact on losses

(Figure 4-20b – lower chart) and voltages (Figure 4-20c). In this case, storage is charged during low load period (4-5am) and discharged during peak time (5-6pm). Note that charging and discharging power are about 50kW which is far below the storage rated power of 200kW.

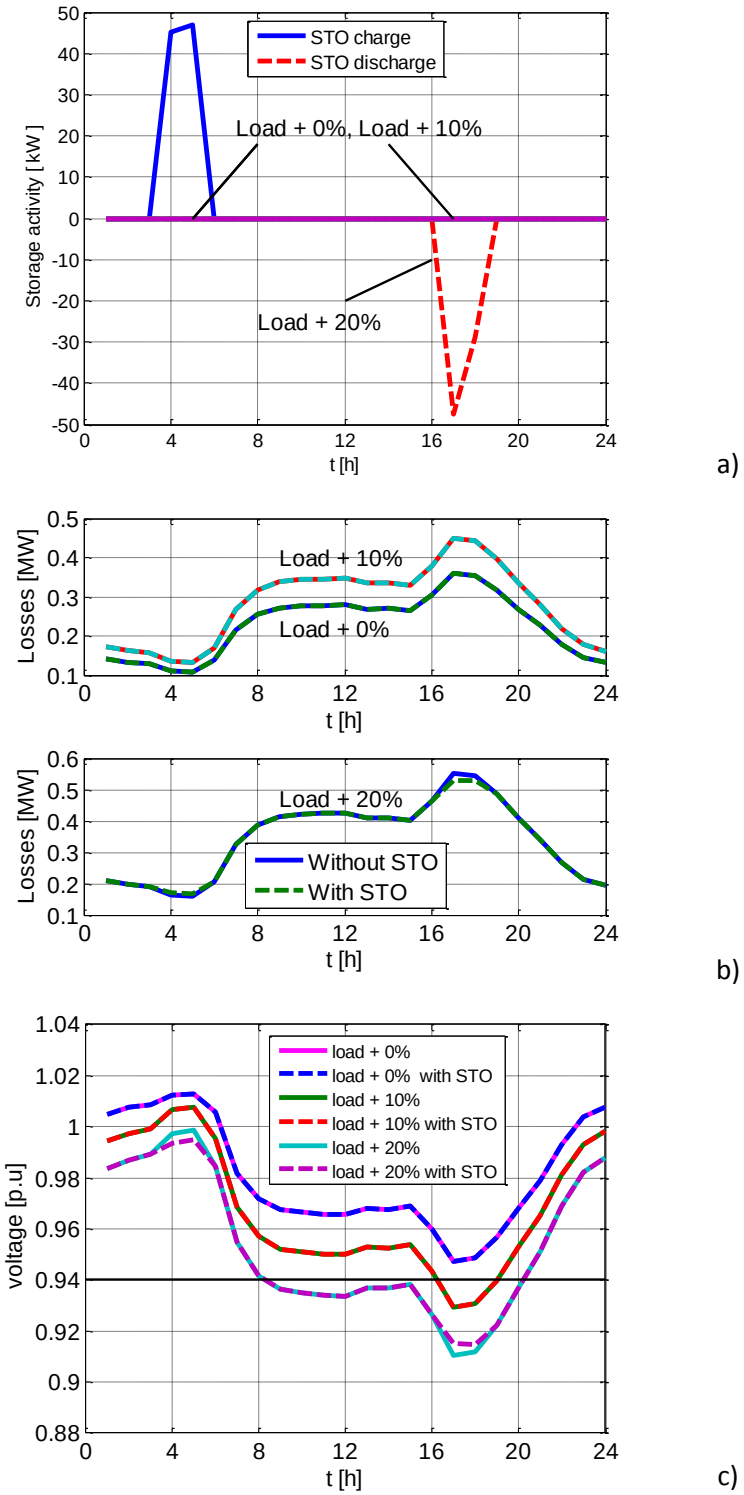


Figure 4-20: Storage (83% efficiency) activity (a); total losses in the network (b) and voltage in Bus 38 (c)

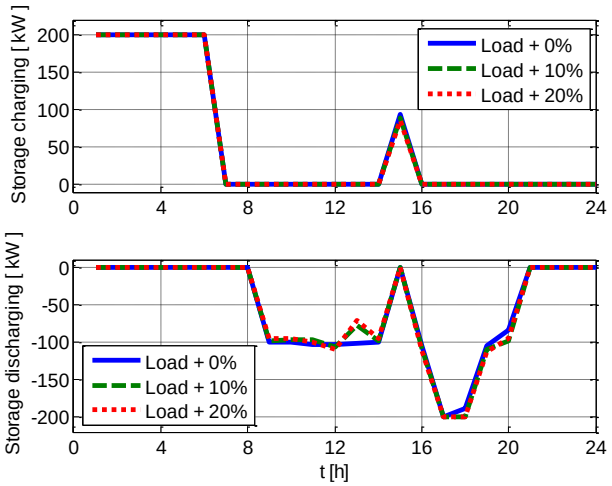
In order to explain this behaviour, tabulated in Table 4-11 are the network losses, losses reduction, storage charged and discharged energy as well as losses in storage due to its efficiency.

Table 4-11: Total network losses are reduced due to storage

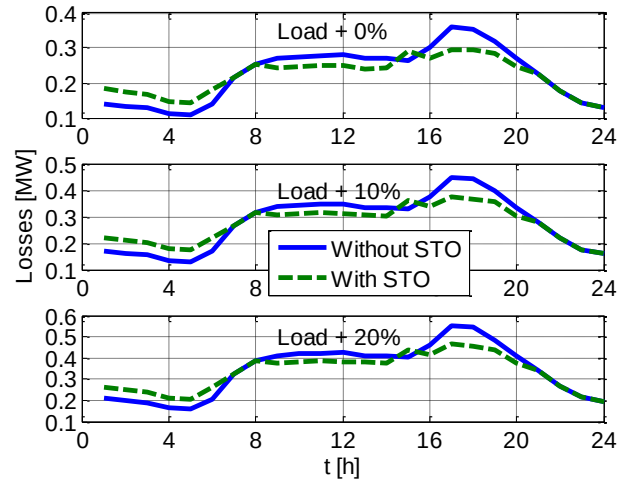
Load	Network Losses [MWh]			Storage energy [MWh]		
	Without Storage	With storage (Eff. 83%)	Losses reduction	Charge	Discharge	Storage Losses
	(1)	(2)	(3) = (1) - (2)	(4)	(5)	(6) = (4) - (5)
Load + 0%	5.4191	5.4191	0	0	0	0
Load +10%	6.7213	6.7213	0	0	0	0
Load +20%	8.2108	8.1947	0.0161	0.0919	0.0763	0.0156

In first two cases, 0% and 10% of load increase, storage is not active. When load grows 20%, storage becomes active. Total network losses in this case are reduced for 16.1kWh, due to storage. At the same time, losses in the storage are 15.6kWh, which is less than the network losses reduction. The total energy balance for this case indicates that 0.5kWh energy is saved. The storage is active only when the energy losses reduction in the network is greater than the losses in the storage.

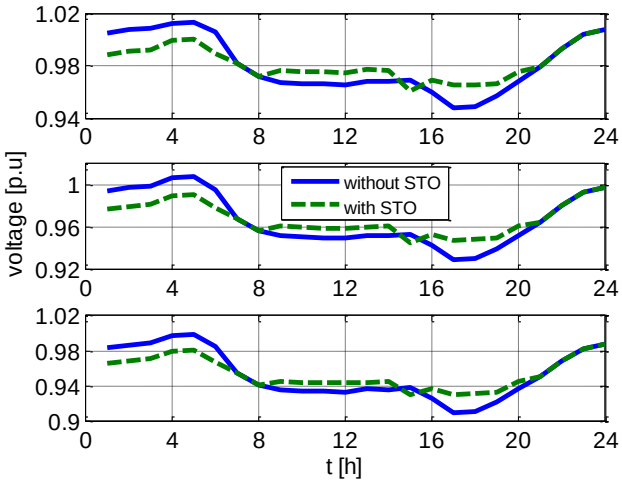
In order to prove this finding, storage efficiency is set to be 100% and the same analysis is repeated. Results are given in Figure 4-21 and Table 4-12.



a)



b)



c)

Figure 4-21: Storage (100% efficiency) activity (a); total losses in the network (b) and voltage in Bus 38 (c)

As expected, this time storage is active for all case of load growth, as demonstrated in Figure 4-21a. Storage is charged in period of low demand (1-6am and one hour in the afternoon – 3pm) and discharged when the load is higher: 8am-8pm (except 3pm). When the storage is charged, losses in the network increase, comparing to base case without storage (Figure 4-21b) and voltages reduce (Figure 4-21c). During discharge period, network losses are reduced and voltages boosted. Total reduction in network losses with this 100% efficient storage is greater than DSR case (compare with Table 4-10). Reason for this is higher storage flexibility comparing to DSR.

Table 4-12: Total network losses are reduced due to storage

Load	Network Losses [MWh]			Storage energy [MWh]		
	Without Storage	With storage (Eff. 100%)	Losses reduction	Charge	Discharge	Storage Losses
	(1)	(2)	(3) = (1) - (2)	(4)	(5)	(6) = (4) - (5)
Load + 0%	5.4191	5.3022	0.1169	1.2947	1.2947	0
Load +10%	6.7213	6.5793	0.1420	1.2921	1.2921	0
Load +20%	8.2108	8.0357	0.1751	1.2886	1.2886	0

This section may be concluded by saying that both DSR and Storage technologies, modelled to reduce system operation costs, have positive side effects. This means they will aim to reduce network losses, by reducing network branches loading during peak hours. However, it is not likely that storage will be used for network losses reduction only, since there are energy losses in the storage itself due to charging and discharging efficiency. Nevertheless, storage is intended to help congestions in the heavily loaded networks and thus it will implicitly reduce losses as well. On the other hand, as there are no losses associated with smart appliances' shifting, they could be used for network losses reduction as well.

4.6 Case Study 2

This case study shows an example of potential deployment of energy storage as a valid alternative to improve security of supply and instead of network reinforcement.

4.6.1 Analyzed test system and problem description

Leighton Buzzard substation consists of two 33/11kV/kV transformers, rated power 19MVA each (38MVA each in emergency regime), supplied from Sundon 132/33 kV/kV substation. Schematic diagram of the network is given in Figure 4-22a, showing the normal operation of the transformers. The branch supplying transformer T1 in Leighton Buzzard consists of the lines connecting the buses 1-2-3-4 and 5. This branch will be denoted as Branch 1. Similarly, the branch supplying transformer T2 consists of the lines connecting the buses 1'-2'-3'-4' and 5'. This branch will be denoted as Branch 2. The lengths of the lines are also shown in Figure 4-22a. The major difference between the two branches is that the parallel lines connecting Bus 3 and Bus 4 are 1.63 and 1.64km long, whilst the parallel lines, between Bus 3' and Bus 4' are 1.02 and 1.06km long. Thermal capacities, expressed in MVA, are given in the parenthesis next to each line.

Normal working condition assumes that transformers T1 and T2 in Leighton Buzzard substation are not operated in parallel. Both section breakers SB33 at 33kV and SB11 at 11kV in Leighton Buzzard substation are normally opened.

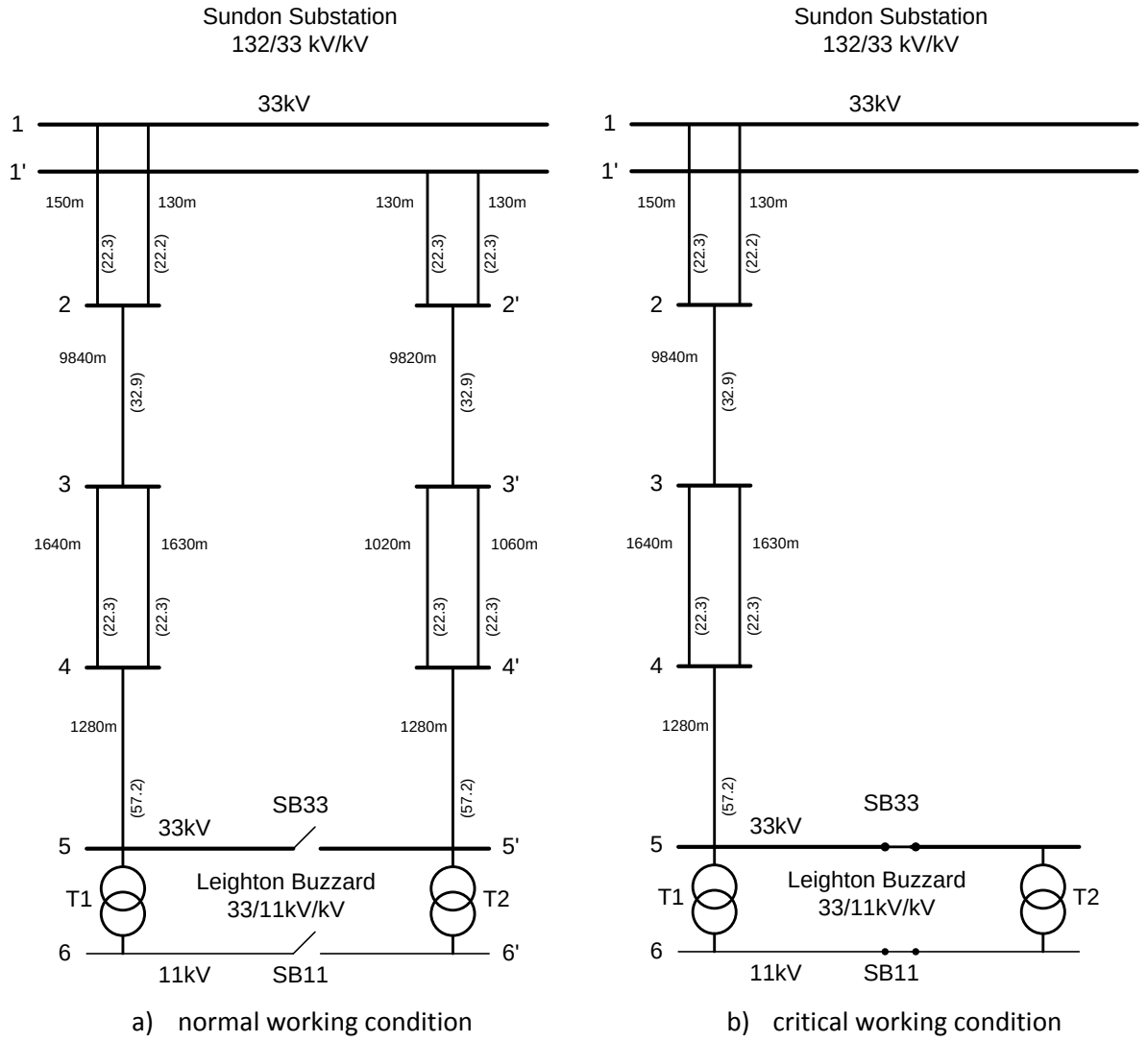


Figure 4-22: Schematic diagram of Leighton Buzzard 33/11 kV/kV substation

Circuit data is given in Table A. 4-4, APPENDIX 4, from which it can be noted that both branches supplying T1 and T2 have very similar parameters. Data about transformers T1 and T2 is given in Table A. 4-5, APPENDIX 4.

Of a particular interest for further analysis is a period of relatively high demand as it was, for example, in winter 2011. Figure 4-23 shows measured apparent powers flowing through each transformer as well as their sum for 12th and 13th January 2011. Peak is very sharp and occurs around 6pm each day, reaching 34MVA on 12th January.

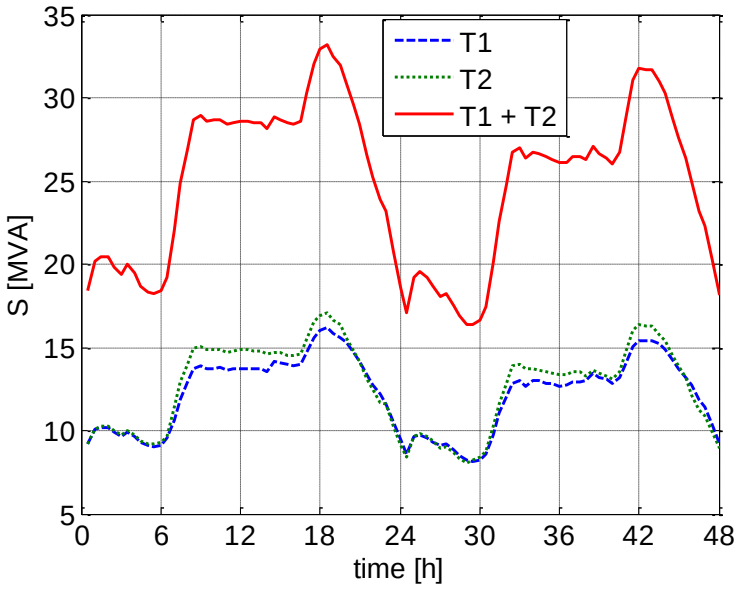


Figure 4-23: Loading of transformers T1 and T2 and total load

Under normal working conditions no line in the network experience overloading even during the peak time. This is demonstrated in the last column in Table A. 4-4, APPENDIX 4, where a snapshot of apparent power flows on 12th January 2011 at 18.00 is shown – apparent power in all the network lines are within thermal capacities. Assumed power factor for this case study is 0.96.

Voltage conditions in the network are also regular, with voltage magnitudes being in all buses in the range ±6% around nominal value. Network voltage profile for the peak time is shown in Figure 4-24.

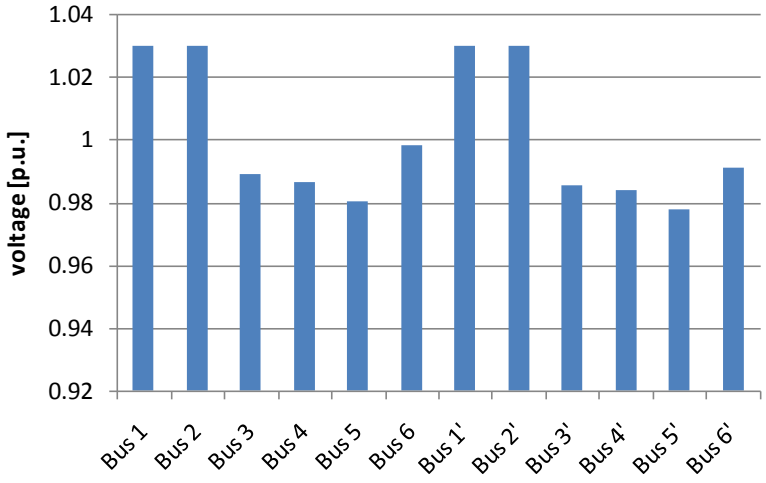


Figure 4-24: Network voltage profile during peak in normal working conditions (12th January 2011 at 18.00)

However, the problem arises when one of the branches that supply the transformers experiences an outage during high demand periods. In that case total load must be supplied from another branch.

In case of outage of Branch 1 supplying transformer T1, both transformers T1 and T2 are supplied from Branch 2 and line Bus 2' – Bus 3' becomes a bottleneck in case of heavy load conditions as experienced on 12-13 January 2011. Similarly, if Branch 2 supplying transformer T2 has a failure, both transformers are supplied from Branch 1 and line Bus 2 – Bus 3 becomes a bottleneck.

Due to symmetrical network topology, similar results are obtained in either branch failures. However, slightly more critical situation is the outage of Branch 2, which consists of somewhat shorter lines, in which case both transformers are to be supplied from Branch 1. This circumstance is presented in Figure 4-22b, and it will be further analyzed. This analysis assumes that during Branch 2 outage, load in Leighton Buzzard substation is supplied from both transformers T1 and T2. Otherwise, if supplied from only one transformer, that transformer would be slightly overloaded over its emergency rating.

Table A. 4-6, APPENDIX 4 shows apparent power snapshot during peak hour in case of Branch 2 outage, when total load in Leighton Buzzard substation is supplied from Branch 1, from which one can see that line Bus 3 – Bus 2 is overloaded. Time evolution of apparent power through this line is given in Figure 4-25. Straight horizontal line denotes the line thermal capacity limit.

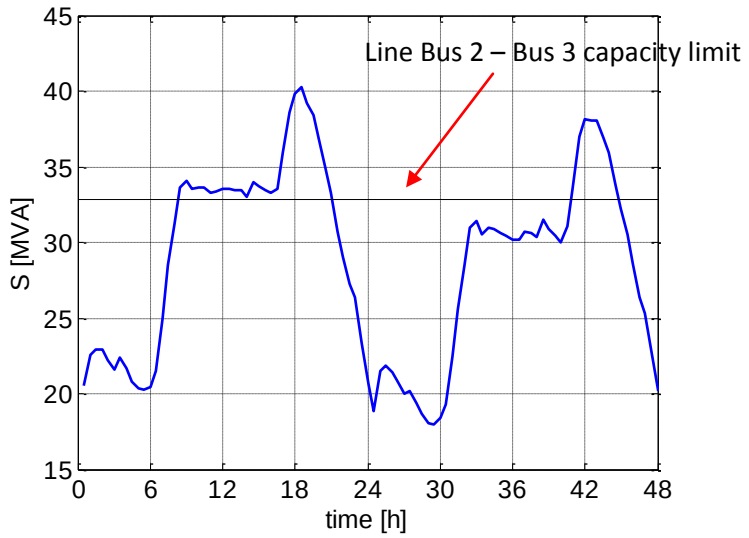


Figure 4-25: Apparent power through line Bus 2 – Bus 3 during outage of Branch 2

From Figure 4-25 it can be seen that this line is overloaded almost half of the day from 8am-9pm on 12th January 2011. On that day, around peak period, apparent power through the line reaches the maximal value over 40MVA.

In order to get a better insight on the network conditions during the peak, a detailed snapshot of the power flows through network lines is detailed in Table 4-13. Only the lines comprising Branch 1 and both transformers T1 and T2 are listed.

Table 4-13: Apparent power flows and active and reactive power losses in the network lines during peak, 12th January 2011 at 18.00 in case of Branch 2 outage

Power Flow						
Line No.	From Bus	To Bus	From Bus S (MVA)	To Bus S (MVA)	Loss P (MW)	Loss Q (Mvar)
1	1	2	15.31	-15.31	0.005	0.00
2	1	2	25.32	-25.33	0.006	0.01
3	4	5	36.69	-36.21	0.259	0.61
4	4	3	-18.30	18.33	0.091	0.06
5	4	3	-18.39	18.41	0.092	0.06
6	**3**	**2**	**-36.74**	**40.28**	**1.823**	**4.34**
7	5	6	18.19	-17.37	0.006	2.38
8	5	6	18.03	-17.22	0.006	2.36
				Total:	2.288	9.82

Table 4-13 shows significant losses of reactive power in the overloaded line (row 6 in Table 4-13, Bus 3 – Bus 2) as well as in the transformers, reaching almost 10Mvar during peak. Losses of active power are also relatively high in the overloaded line, reaching about 2MW.

Network voltage profile at peak time, in case of Branch 2 outage is shown in Figure 4-26. Voltage magnitude at 11kV (Bus 6 and Bus 6' in Figure 4-26) is kept near the nominal value as the transformers are equipped with tap changers. Transformer voltage at 33kV side (Bus 5) is just below the lower margin of -6%.

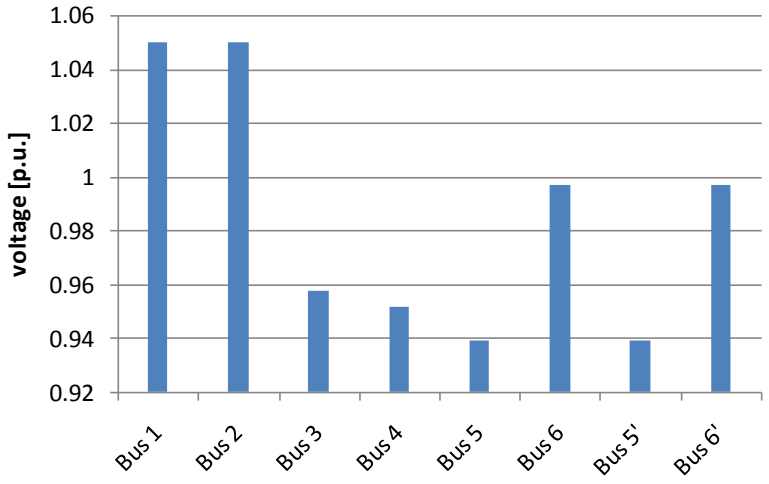


Figure 4-26: Network voltage profile during peak, in case of Branch 2 outage

4.6.2 Solutions to the problem

Network reinforcement

As we have seen from above analysis, if Branch 2 experiences an outage during heavy load conditions, line Bus 2 – Bus 3 will become overloaded. Similarly, if Branch 1 fails, line Bus 2' – Bus 3' becomes overloaded. Engineering recommendation P2/6 [91] requires both lines to be reinforced. Each of them are approximately 10km long, therefore in total 20km of the line should be reinforced. Taking into account that replacement cost for 33kV underground cable is £250,000/km [90], one gets the total replacement cost:

$$(9.84 + 9.82)\, km \cdot 250{,}000\, £/km = £4.9M$$

Therefore, total reinforcement cost of the congested lines is approximately £5M.

Utilization of Energy Storage

Instead of network reinforcement, distribution network operator (DNO) considers to install energy storage on 11kV side in Leighton Buzzard substation. Since the location is already proposed by DNO, the methodology explained in Section 4.3 is applied to determine the optimal size of the storage. Based on the load level as it was 12th of January 2011, when Branch 2 was out of order, the obtained results suggest installing storage with the following parameters:

Table 4-14: Required energy storage parameters for power flow control

Active Power	5.9 [MW]
Energy	22 [MWh]

Taking into account a rough price of storage technologies to be £1,000/kW, this would cost approximately £6M, which is higher than the network reinforcement.

Time evolution of apparent power through line Bus 2 – Bus 3 without and with storage is given in Figure 4-27 (upper chart). We can see that the line thermal capacity is not exceeded when storage is exercised. Figure 4-27 (lower chart) shows storage activity, charging and discharging. As expected, storage is charged during low load periods and discharged at full capacity during peak hour.

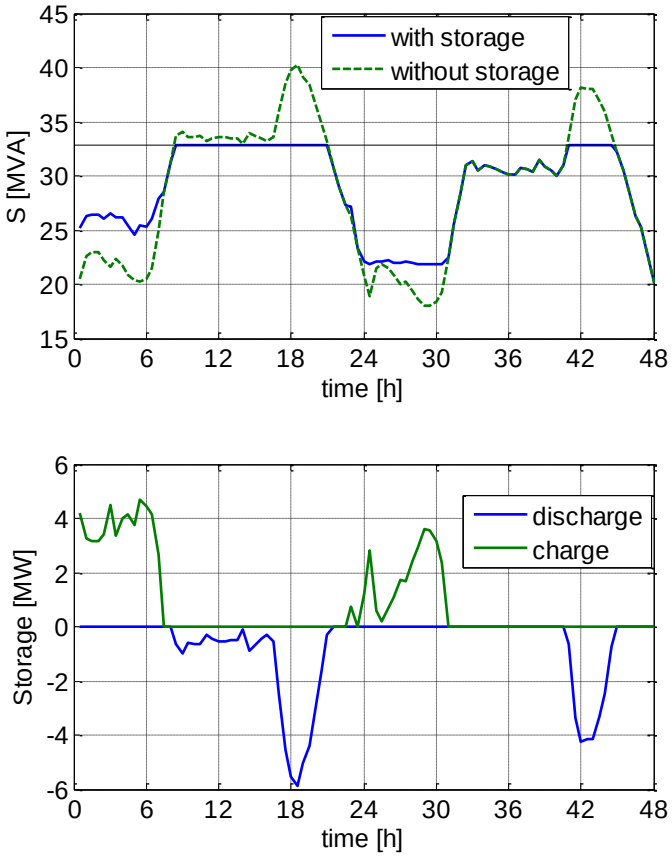


Figure 4-27: Apparent power through line Bus 2 – Bus 3 during outage of Branch 2 with and without storage (upper chart); lower chart shows storage activities

With support of storage, voltage conditions in the network are regular even during the abnormal working condition, with voltage magnitudes being in the range ±6% for all buses, as shown in Figure 4-28.

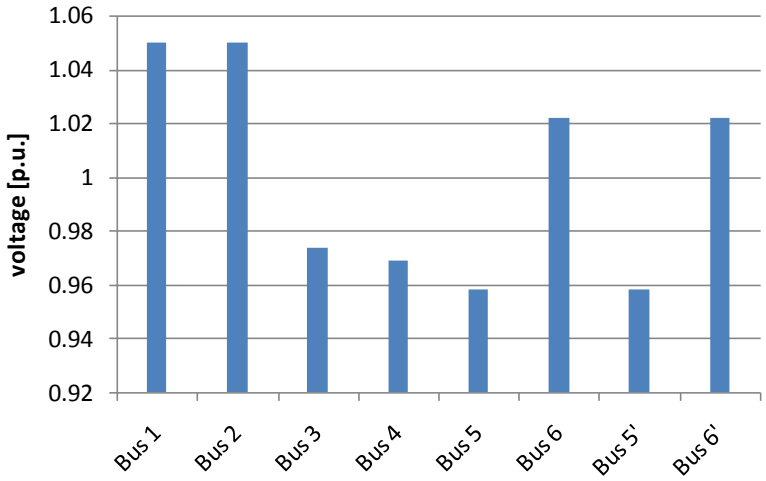


Figure 4-28: Network voltage profile during peak, in case of Branch 2 outage with support of storage

Energy Storage and Reactive Compensation

Careful examination of Table 4-13 discovers relatively high reactive power losses in the overloaded line and in the transformers during abnormal working conditions. This leads to the suggestion of combining and controlling reactive power compensation in addition to the active power output of the storage. Such systems are already commercially available, for example the one combining Static Var Compensator (SVC) with battery energy storage [89].

The methodology explained in Section 4.3 is expanded to involve reactive compensation control by adding a term in the objective function (**30**) that penalizes voltage deviations from the nominal value. As a result, the following optimal storage parameters are obtained:

Table 4-15: Required energy storage parameters for power flow control with reactive compensation

Active Power	2.55 MW
Reactive Power	9.60 Mvar
Energy	4.60 MWh

Comparing with the previous results (Table 4-14), when only the active power was controlled, one can see that the active power requirement is now almost halved, while the energy capacity requirements is reduced more than four times.

Using an educated guess that reactive power compensation costs about £50/kvar, total cost is approximately:

$$Cost = 50{,}000\frac{£}{Mvar} \cdot 9.6Mvar + 1{,}000{,}000\frac{£}{MW} \cdot 2.55MW \approx £3M$$

This leads to the conclusion that reactive compensation allows significant reduction in storage capacity and consequently in the storage costs.

Time evolution of apparent power through line Bus 2– Bus 3 in base case (without storage) as well as with storage and reactive power control is given in the upper chart in Figure 4-29, while middle chart shows storage activity: charging and discharging. Finally, lower chart in Figure 4-29 shows reactive power provided by storage.

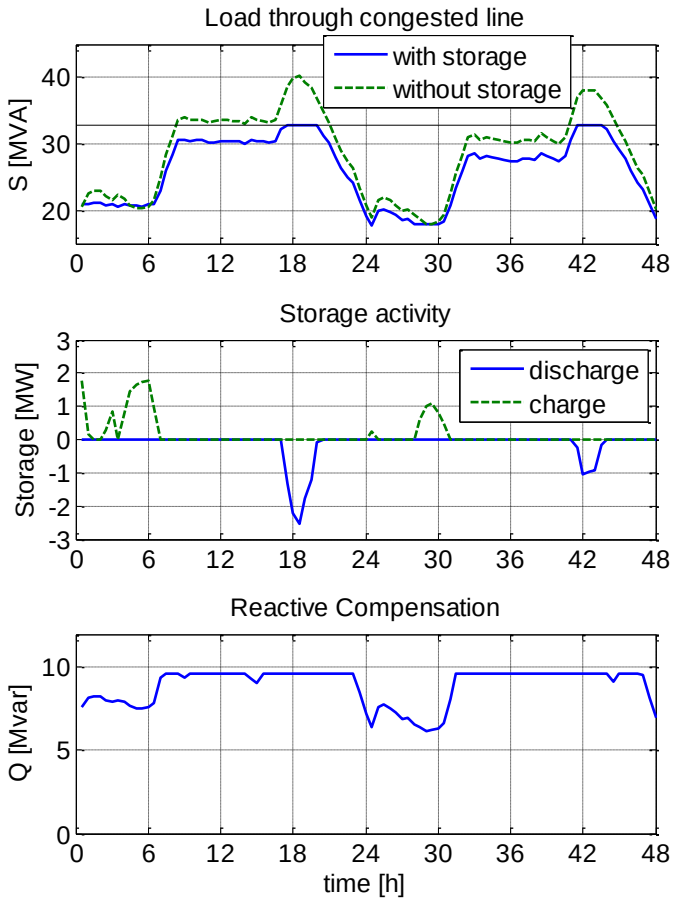


Figure 4-29: Apparent power through line Bus 2– Bus 3 during outage of Branch 2 with and without storage (upper chart); storage active power charging and discharging (middle chart); and reactive power compensation (lower chart)

Voltage conditions in the network are also regular, with voltage magnitudes being in the range ±6% in all buses. Figure 4-30 shows distribution of voltages throughout the network during the peak.

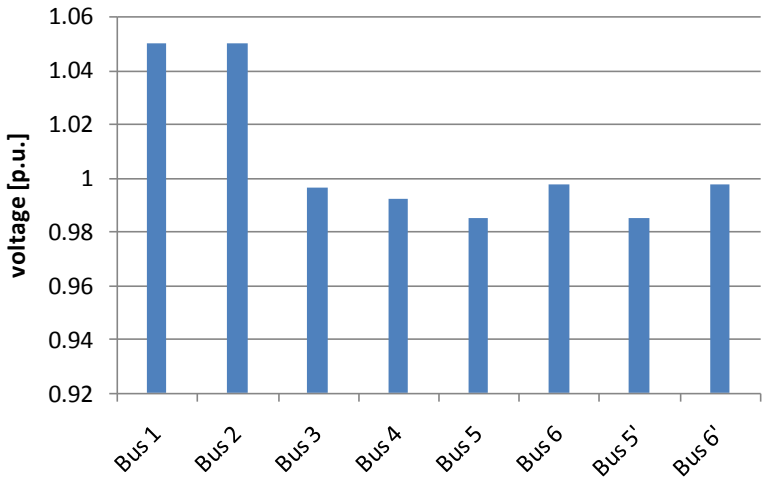


Figure 4-30: Network voltage profiles during peak time, in case of Branch 2 outage with storage and reactive power compensation

Reactive power control leads to the reduced variance of the network voltages. In case of active power control only and no voltage control the voltage variance is 0.0014pu, while in case with reactive compensation and voltage control the variance is reduced to 0.0009pu.

4.7 Conclusions

In this chapter, a methodology to support distribution network operation using demand side response and storage technologies is developed and successfully employed to control the voltages and power flows in the network, bringing the benefits to the network operator. The methodology is applied to two case studies:

- 11kV distribution network feeder where the problems related to the lack of network capacity and under-voltages in distant buses emerge.
- 33/11 kV/kV substation where the security of supply of the load is at risk when one of the upstream supplying branches is not in operation during high demand periods. Utilization of storage was explored as an alternative to network reinforcement.

In both cases it was demonstrated that the proposed approach with enabling technologies facilitates active network management in terms of:

- optimizing the existing network capacity utilization
- deferring network reinforcement
- reducing network losses

- improving power quality and
- improving security of supply

A model that optimizes sizing and location of the storage is presented and tested. DSR and storage location models in AC networks are non-linear mixed integer optimization problems whose dimension depends on network size. Sequential Linear programming approach is used within commercial optimization software.

In the first case study, the benefits that smart appliances and storage bring to the network in terms of reinforcement costs savings are quantified using cost avoidance criteria considering a period of 20 years. Present value method is used to refer all the costs to the current year.

For this particular system, reinforcement may be postponed for about 9 years by utilization of DSR. The length of replaced underground cables during this period is reduced from 10,762m (with no DSR) to 325m (with DSR), which brings the net benefit of about £351k to the system if the investment in the communication infrastructure and hardware requirements are taken into account. Value per device is found to be around £70 for the whole period. Annualized value is about 3.5 £/device/year.

With a specific storage device (200kW, 1.2MWh) attached to the most distant bus relative to the supply point, the first network reinforcement was necessary in Year 9, which is 5 years deferment compared to the base case. It was shown that in this case, storage rated power was insufficient to stop line overloading in Year 9. With this particular storage, there is requirement to reinforce three lines of total length 2225m during the period of 20 years, comparing to seven lines and more than 10km without storage. Net benefit to the system is around £108k, and the value of storage is almost £80/kW/year.

The next question answered in this chapter was related to optimal storage sizing (capacity and power) and location to maximally postpone investment in network reinforcement. It was found that storage 750kW, 3.7MWh located in Bus 29 would defer network reinforcement for about 14 years. However, it was shown that this storage would not be economically justified with present cost of battery technology.

Analysis of storage and DSR impact on network losses is also performed. It was shown that both DSR and Storage tend to reduce network losses. However, storage is used in this purpose only when the energy losses reduction in the network is greater than the energy losses in the storage.

Second case study summarises thinking by which energy storage can form a valid alternative in future for traditional circuit and transformer reinforcement options. It demonstrates that a DNO can operate a storage device with sufficient reliability to meet P2/6 security recommendations.

Network reinforcement to accommodate the peaks during the abnormal working conditions in case of an outage of the upstream network to the supply point would require replacement of 20km long 33 kV circuit that would cost approximately £5M. An alternative to the network reinforcement is instalment of energy storage, and there are two options for this:

- storage with active power control only: this approach requires a storage of about 6MW and 22MWh, which would cost around £6M
- storage with active power and reactive compensation: this would need a combination of SVC and battery energy storage, required to deliver 2.6MW and 9.6Mvar at peak time. The required energy capacity for this storage is about 4.6MWh, which is approximately 2h of work at rated power. This solution would halve the costs to around £3M.

Both case studies show that Storage and DSR may be used for network assets investments deferral, thus more efficiently using the existing network capacity. Both technologies have advantages and drawbacks and the benefits they bring to the network operation are very system-specific. DSR is distributed throughout the network, but requires communication infrastructure and is less flexible than storage. Storage is more beneficial to the network operation due to higher flexibility. On the other side, it has inherent energy losses and requires space and maintenance. Also, it is usually set in one node on the feeder and this location should be carefully chosen as it was recognized to be one of the key drivers for the value of storage, apart from storage size and efficiency. It was also shown that reactive power compensation can significantly reduce required storage sizing.

CHAPTER 5. Electrical Vehicles in Electricity Networks

5.1 Introduction

As explained in CHAPTER 1 a large-scale electrification of the transport sector is expected in next few decades, which will require significant investments in generation and network capacity in order to overcome problems related with high peaks and network congestion, if vehicles' battery charging is to be performed without any control (Business as Usual). However, due to low diversity of EV demand, this will lead to an inefficient utilisation of generation and network assets. In this chapter a novel methodology is presented for optimal charging of the electric vehicles to support network operation, reduce peak and help the utilization of renewable energy. The methodology is implemented in a multi-period DC OPF where the network and EV constraints are modelled as a part of problem formulation. By this, considered are the real life driving statistics of the light/medium size vehicles (according to the vehicle licensing data [113], more than 92% of total UK fleet consists of light/medium size vehicles). The statistics are based on the UK driving patterns [111]. Light/medium size vehicles are characterized with short journey times and relatively small distances driven, being off road on average 90% of the time [115]. In order to support this type of driving patterns, the upcoming electric vehicles will feature relatively modest amount of energy and relatively high power ratings of the on board batteries. These characteristics will make EV particularly suitable for network operation support, as they offer very flexible charging time. This can provide significant benefits, not only to the efficient utilisation of generation capacity, but also to the operation of distribution and transmission networks. Presented work considers a grid-to-vehicle concept (G2V), where the electric power flows one-way from grid to the batteries in the vehicles. Vehicle-to-grid applications (V2G), where the batteries can be discharged to support network operation, are not considered in this work. Thus, conservative estimates will be obtained for the benefits of incorporating EV demand response to assist with real time network control. This work does not consider any specific battery technologies and related battery costs, duty (charge-discharge) cycles, durability, life expectancy, etc.

This chapter is organized as follows: Section 5.2 describes essential UK transport characteristics for the small/medium size vehicles, based on which several important conclusions will be derived, such as driving patterns, number of journeys per day, start/end times of the journeys, daily travelled distances and their distributions, as well as probability of a car being stationary. Also, the energy required for each type of the journey will be estimated. Section 5.3 explains how driving distance is reduced into three basic groups: short, medium and long. The number of vehicles for each journey type, their start and end times and the energy required are also determined in Section 5.3. Different

charging strategies and their formulation are described in Section 5.4. Testing the algorithm is given in Section 5.5. Finally, Section 5.6 brings some conclusions.

5.2 Basic UK Transport Characteristics

Annual transport statistics data representing light/medium size vehicles may be found in the National Travel Survey (NTS) database [111]. The information refers to individual journeys made by the entire vehicle fleet, and is ordered according to journey start and end times, as well as distances travelled. An illustrative sample of the data is shown in Table 5-1.

Table 5-1: Sample of original data from NTS database

Start time	End time	Distance band	No. of journeys (yearly)
00:00 – 00:59	00:00 – 00:59	Under 1 mile	2,526,441
00:00 – 00:59	00:00 – 00:59	1 to under 2 miles	5,835,213
00:00 – 00:59	00:00 – 00:59	2 to under 3 miles	5,419,649
…	…	…	…
00:00 – 00:59	01:00 – 01:59	2 to under 3 miles	465,936
00:00 – 00:59	01:00 – 01:59	3 to under 5 miles	1,802,352
00:00 – 00:59	01:00 – 01:59	5 to under 10 miles	1,171,135
…	…	…	…
00:00 – 00:59	02:00 – 02:59	50 to under 100 miles	173,152
00:00 – 00:59	03:00 – 03:59	100 to under 200 miles	179,448
00:00 – 00:59	04:00 – 04:59	200 miles and over	141,670
…	…	…	…
23:00 – 2359	23:00 – 23:59	25 to under 35 miles	2,828,670
23:00 – 2359	23:00 – 23:59	35 to under 50 miles	532,048
23:00 – 2359	23:00 – 23:59	50 to under 100 miles	336,859

For an individual journey type, the data in Table 5-1 specifies the journey start time, end time, and distance driven during the journey, as well as the total number of journeys falling into that type during a year. There are in total 854 entries in the table[9].

In order to obtain daily numbers of journeys, annual values are divided by 365, resulting in Table 5-2.

[9] Due to the size of the table, only a sample is shown.

Table 5-2: Daily numbers of journeys and distances (obtained from Table 5-1)

Start time	End time	Band limit [mile]	No. of journeys (daily)	Lower distance [km]	Higher distance [km]	Average distance [km]
00:00 – 00:59	00:00 – 00:59	< 1	6,922	11,137.11	11,137.11	11,137.11
00:00 – 00:59	00:00 – 00:59	1 - 2	15,987	25,722.90	51,445.80	38,584.35
00:00 – 00:59	00:00 – 00:59	2 - 3	14,848	47,782.00	71,673.00	59,727.50
…	…		…	…	…	…
00:00 – 00:59	01:00 – 01:59	2 - 3	1,277	4,107.89	6,161.84	5,134.87
00:00 – 00:59	01:00 – 01:59	3 - 5	4,938	23,835.49	39,725.81	31,780.65
00:00 – 00:59	01:00 – 01:59	5 - 10	3,209	25,813.11	51,626.21	38,719.66
…	…		…	…	…	…
00:00 – 00:59	02:00 – 02:59	50 - 100	474	38,164.54	76,329.08	57,246.81
00:00 – 00:59	03:00 – 03:59	100 - 200	492	79,104.68	158,209.36	118,657.02
00:00 – 00:59	04:00 – 04:59	> 200	388	124,902.12	149,882.55	137,392.3
…	…		…	…	…	
23:00 – 23:59	23:00 – 23:59	25 – 35	7,750	311,734.89	436,428.84	374,081.9
23:00 – 23:59	23:00 – 23:59	35 - 50	1,458	82,088.45	117,269.22	99,678.83
23:00 – 23:59	23:00 – 23:59	50 - 100	923	74,247.37	148,494.75	111,371.1

Data in Table 5-2 is obtained in the following way:

- *Number of daily journeys* is obtained by dividing the number of journeys per year (from Table 5-1) by 365.
- *Lower distance* represents the daily lower distance driven within a given journey category, and is calculated by multiplying the number of (daily) journeys by the lower limit in the distance band (Table 5-1) and by 1.609 (km/mile). Distances “Under 1 mile” are rounded to 1 mile.
- *Higher distance* represents the daily higher distance driven within a given journey category, and is calculated by multiplying the number of (daily) journeys by the higher limit in the distance band (Table 5-1) and by 1.609 (km/mile). Distances “200 miles and over” are calculated as 60 miles/h multiplied by duration of the journey in hours.
- *Average distance* is calculated as a mean of lower and higher distance.

Example calculation of an entry in Table 5-2: for journeys that started between 00:00 and 00:59, and that finished between 00:00 and 00:59, in the category “1 to under 2 miles”, the yearly number of journeys is 5,835,213 (from Table 5-1), which gives 5,835,213/365 = 15,987 journeys a day. The rest of the calculation is tabulated below:

(1)	(2) = (1)/365	(3)	(4)	(5) = 1.609×(2)×(3)	(6) = 1.609×(2)×(4)	(7) = ((5)+(6))/2
No. of journeys (yearly)	No. of journeys (daily)	Lower distance band limit [mile]	Higher distance band limit [mile]	Lower distance [km]	Higher distance [km]	Average Distance [km]
5,835,213	15,987	1	2	25,722.90	51,445.80	38,584.35

After processing all entries in the original database, the aggregate parameters for all journeys can be obtained in terms of total number of journeys per day, and lower and upper bounds on daily distances travelled. The results are shown in Table 5-3.

Table 5-3: Total daily number of journeys and associated distances (for all categories of journeys)

Total daily no. of journeys [millions]	Total daily lower distance [mil. km]	Total daily higher distance [mil. km]	Minimum daily energy [GWh]	Maximum daily energy [GWh]
67.4	738.8	1,262.3	110.8	189.3

Multiplying the total daily distances by 0.15kWh/km, which is the assumed average energy consumption for electric vehicles[10], yields an estimate of the lower and upper bound on daily energy required for transportation (far right columns in Table 5-3).

There are about 34.2 million light- to medium-size vehicles registered in the UK [113]. Based on this number, and the data in Table 5-3, certain car-usage indicators can be found, as represented in Table 5-4. One of the key findings is that, on average, each vehicle makes roughly two journeys per day (since there are 67.4 million journeys a day and 34.2 million vehicles).

Table 5-4: Basic statistics on the UK transportation (daily)

No. of vehicles (million)	34.2
Daily distance [million km]	738.8 – 1262.3
Average daily distance [km/vehicle]	22 - 37
Energy demand [GWh]	110.8 – 189.3
Energy demand (average) [GWh]	150
Average energy per vehicle [kWh/vehicle]	4.4

[10] In [112], specific energy consumption is 0.16 kWh/km, although the value of 0.11 kWh/km is also reported. Reference [114] uses 0.20 kWh/km. In this work, the consumption of 0.15 kWh/km is assumed.

5.2.1 Number of journeys distances, and start/end times

Table 5-2 allows us to tabulate the number of journeys starting in a specific hour of the day and ending in the same or another hour of the day. The summary results are given in Table 5-5 (zero elements are shaded).

Table 5-5: Number of journeys (in thousands) for given start and end times

End Time (hour of day)

Start time (hour of day)	0-1	1-2	2-3	3-4	4-5	5-6	6-7	7-8	8-9	9-10	10-11	11-12	12-13	13-14	14-15	15-16	16-17	17-18	18-19	19-20	20-21	21-22	22-23	23-24
0-1	119	27	0	0	0	0	0	0	0	0	0	0	0	0	0	0	0	0	0	0	0	0	0	0
1-2	0	57	13	0	0	0	0	0	0	0	0	0	0	0	0	0	0	0	0	0	0	0	0	0
2-3	0	0	36	8	0	2	0	0	0	0	0	0	0	0	0	0	0	0	0	0	0	0	0	0
3-4	0	0	0	30	15	0	0	1	0	0	0	0	0	0	0	0	0	0	0	0	0	0	0	0
4-5	0	0	0	0	79	40	1	1	1	1	0	0	0	0	0	0	0	0	0	0	0	0	0	0
5-6	0	0	0	0	0	299	174	22	5	3	3	0	0	0	1	0	0	0	0	0	0	0	0	0
6-7	0	0	0	0	0	0	686	493	42	14	6	2	1	1	0	0	0	0	0	0	0	0	0	0
7-8	0	0	0	0	0	0	0	2172	1463	67	12	3	1	2	0	2	0	1	0	0	0	0	0	0
8-9	0	0	0	0	0	0	0	0	4369	1409	52	14	5	3	2	0	0	1	1	0	0	0	0	0
9-10	0	0	0	0	0	0	0	0	0	3132	935	53	19	4	2	3	3	2	0	1	0	0	0	0
10-11	0	0	0	0	0	0	0	0	0	0	3431	918	56	20	3	5	2	1	0	0	0	0	0	0
11-12	0	0	0	0	0	0	0	0	0	0	0	3517	1067	46	16	8	4	2	0	2	0	0	0	0
12-13	0	0	0	0	0	0	0	0	0	0	0	0	3443	1025	42	18	7	4	3	1	0	0	0	0
13-14	0	0	0	0	0	0	0	0	0	0	0	0	0	3402	1007	41	13	6	2	2	0	0	0	0
14-15	0	0	0	0	0	0	0	0	0	0	0	0	0	0	3304	1086	59	20	5	1	2	1	0	0
15-16	0	0	0	0	0	0	0	0	0	0	0	0	0	0	0	4041	1220	72	18	8	3	1	1	0
16-17	0	0	0	0	0	0	0	0	0	0	0	0	0	0	0	0	3856	1545	81	21	8	3	1	0
17-18	0	0	0	0	0	0	0	0	0	0	0	0	0	0	0	0	0	4216	1458	73	10	3	2	1
18-19	0	0	0	0	0	0	0	0	0	0	0	0	0	0	0	0	0	0	3142	910	33	10	5	1
19-20	0	0	0	0	0	0	0	0	0	0	0	0	0	0	0	0	0	0	0	2499	535	23	9	1
20-21	1	0	0	0	0	0	0	0	0	0	0	0	0	0	0	0	0	0	0	0	1619	361	16	6
21-22	4	0	0	0	0	0	0	0	0	0	0	0	0	0	0	0	0	0	0	0	0	1208	277	9
22-23	5	2	0	0	0	0	0	0	0	0	0	0	0	0	0	0	0	0	0	0	0	0	823	175
23-24	123	3	1	0	0	0	0	0	0	0	0	0	0	0	0	0	0	0	0	0	0	0	0	455

Similar tables can be compiled for minimum/maximum journey distances and the corresponding energies. The results are given in APPENDIX 5, Table A. 5-1 - Table A. 5-4.

Table 5-5 shows the number of trips for every pair of start and end times. The chart in Figure 5-1 shows trip profiles within one day. These profiles are important from the power system perspective because the system-wide impact of electric vehicles will be highly dependent on the time that vehicles are charged, which is directly linked to the time that EV trips occur.

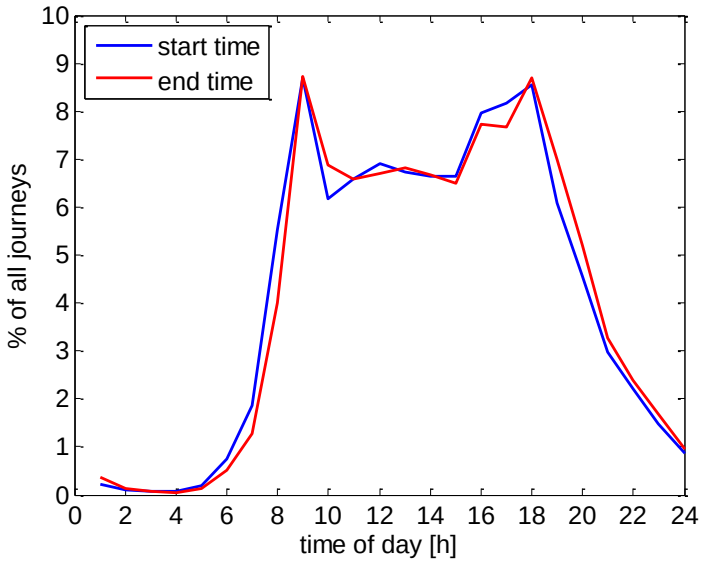


Figure 5-1: Daily journey profiles

Figure 5-1 demonstrates that the highest proportion (about 9%) of all journeys occurs in the morning hour between 8 and 9am, and in the evening/afternoon hour between 5 and 6pm, which clearly reflects commuting transport patterns. Note also that during these peaks, "start time" and "end time" curves almost coincide, suggesting that most of these trips last for a relatively short time (one hour or less).

A useful insight into the journey statistics can also be obtained by determining the cumulative distributions of the number of journeys per day and distance driven. For a given journey distance, these distributions give percentages of all journeys and total daily mileage that are contributed by vehicles travelling that distance or less. To illustrate this, higher daily driven distances are used (upper band limits from Table 5-1 and "Higher distance" column from Table 5-2), and the results are shown in Figure 5-2.

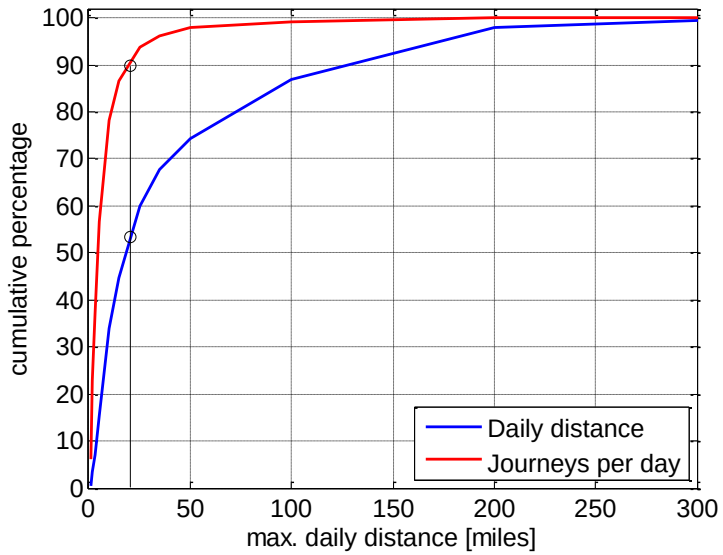


Figure 5-2: Cumulative percentage of number of journeys and total (maximum) daily mileage

Figure 5-2 shows that 90% of all journeys made during a day are below 20 miles (32 km); however, only 55% of total daily mileage results from these trips. The results also imply that about 75% of all miles could be driven by EVs with a 50 mile (80 km) range. Another conclusion following from the above figure is that if EVs were assumed to be completely carbon-neutral, the driving range of EV should be at least 70 miles (100 km) to generate an 80% reduction in CO_2 emissions from light and medium-size vehicles.

Figure 5-3 shows the distribution of aggregated distance (higher values) across distance ranges, while Figure 5-4 represents the distribution of the number of journeys. The figures suggest that 18%

of total driven distance and about 21% of all journeys correspond to the trips being in the range of 5-10 miles.

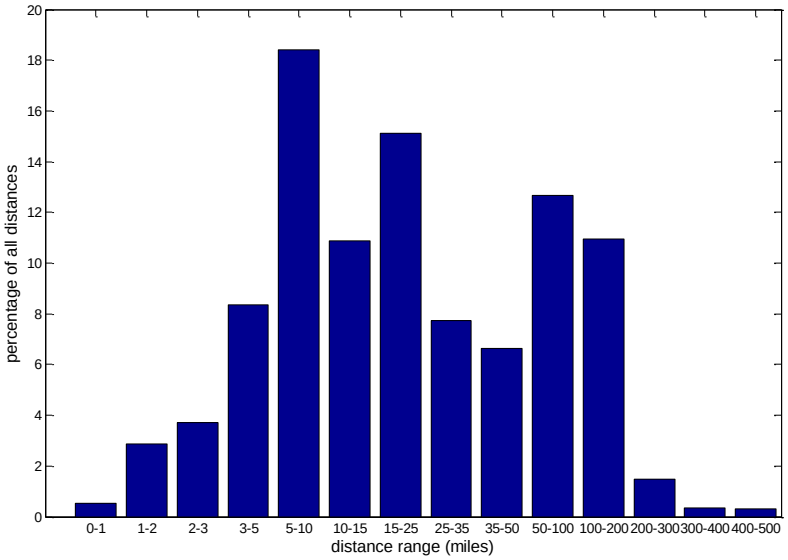


Figure 5-3: Distribution of aggregated daily distance (upper band limit) vs. distance range

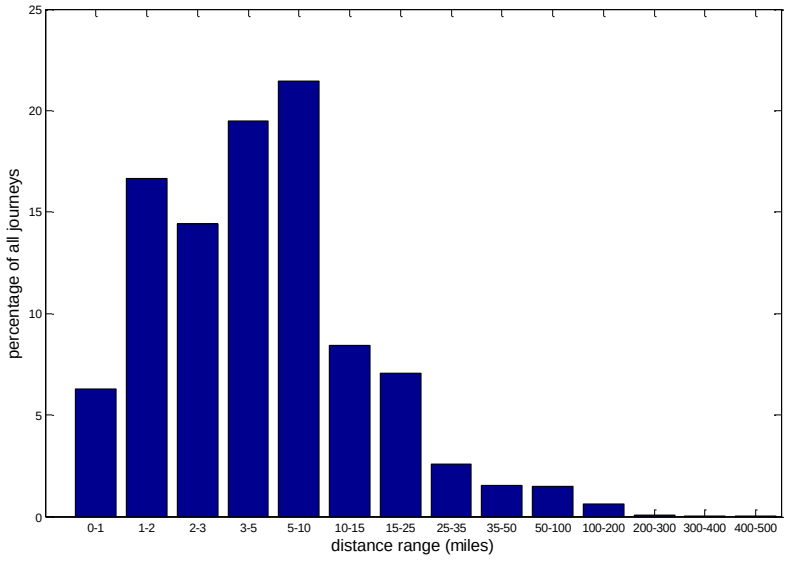


Figure 5-4: Distribution of number of journeys vs. distance range

From the perspective of an electrical power system with a high penetration of electric vehicles, it is crucial to know the probability of a vehicle being parked for each hour of the day, as these off-road (parked) vehicles are potentially available for charging. Calculation of this probability is based on the number of journeys and their start/end times (Table 5-5). The number $N_{journey}(t)$ of journeys for each hour of the day is calculated as a sum of:

1. total number of journeys starting at specific hour t
2. total number of journeys that started before hour t and which have not completed before hour t

Then, for each hour of the day it is possible to estimate probability of a journey, by dividing $N_{journey}(t)$ with the total number of journeys during a day:

$$P_{journey}(t) = \frac{N_{journey}(t)}{N_{journey}^{total}}$$

Probability that there will be no journeys during hour t, which is equivalent to the probability that a car will be available for charging, is then:

$$P_{available}(t) = 1 - P_{journey}(t) = 1 - \frac{N_{journey}(t)}{N_{journey}^{total}} \quad (67)$$

The results are graphically presented in Figure 5-5.

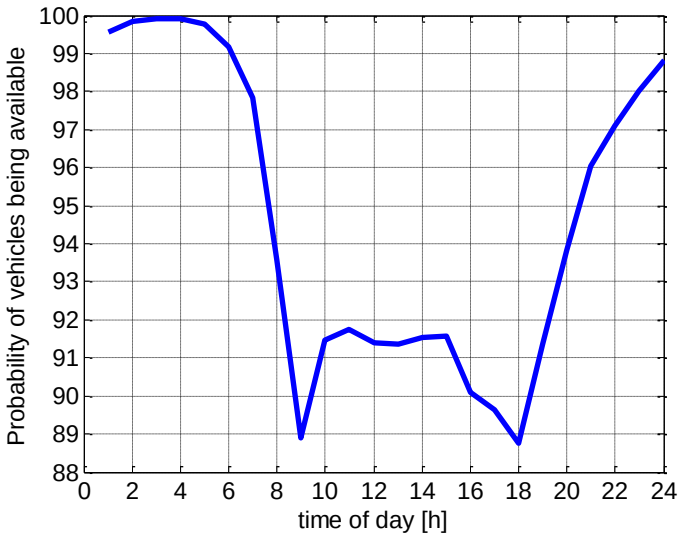


Figure 5-5: Probability of cars being off-road during the day

Figure 5-5 suggests that even during the rush-hour, a very large proportion of cars (89%) are still parked. The explanation for this is that the input data contains not only the vehicles for commuting, but also the vehicles for other purposes, the usage of which is randomly spread over the day. The data is in good correspondence with the findings in [115] where the number of parked cars was estimated to be around 90%.

5.3 Distance bands aggregation

The original NTS data (the excerpt of which is given in Table 5-1) is classified into 12 distance bands: under 1 mile, 1-2 miles, 2-3 miles, 3-5 miles, 5-10 miles, 10-15 miles, 15-25 miles, 25-35 miles, 35-50 miles, 50 -100 miles, 100-200 miles, and 200 miles and above.

This relatively large number of categories is impractical to handle and analyse. For that reason, the 12 distance bands are grouped into three clusters: Short, Medium and Long, as specified in Table 5-6. Instead of working with lower and higher distances, the average distance is used (see Table 5-2).

Table 5-6: Distance band clusters and equivalent distances

Journey type	Distance band [mile]	Equivalent distance [mile]
Short	≤ 15	9
Medium	$15 \div 50$	20
Long	≥ 50	100

For all the journeys belonging to the same type (Short, Medium or Long), with the same start and end times, all the average distances (from Table 5-2) are summed-up together. The results are presented in APPENDIX 5, Table A. 5-5 - Table A. 5-7.

The energies required to perform the journeys are again obtained by multiplying the distances with the average energy consumption of 0.15kWh/km. The results are shown in APPENDIX 5, Table A. 5-8 - Table A. 5-10.

After allocating distances and energies, the number of journeys in each category (Short, Medium or Long) needs to be assessed. For this purpose, the concept of “equivalent distance” is introduced in Table 5-6. The equivalent distance represents the average distance driven within a particular type of journey. For example, it is assumed that drivers who only drive short distances can travel any mileage between 0 and 15 miles, but on average they travel 9 miles. Similarly, the values of 20 and 100 miles are assumed as the average values for Medium and Long journeys, respectively. These values have been calibrated to ensure that the total number of journeys remain similar to those of the original vehicle fleet.

With equivalent distances defined, the number of journeys can be found by dividing the daily driven distances (given in APPENDIX 5, Table A. 5-5 - Table A. 5-7) by the equivalent distances. The results for short journeys are presented in Table 5-7, and for medium and long journeys are given in APPENDIX 5, Table A. 5-11 and Table A. 5-12.

Table 5-7: Number of short journeys defined by the start and end times (in 1,000)

Start time (hour of a day) \ End Time (hour of a day)	0-1	1-2	2-3	3-4	4-5	5-6	6-7	7-8	8-9	9-10	10-11	11-12	12-13	13-14	14-15	15-16	16-17	17-18	18-19	19-20	20-21	21-22	22-23	23-24
0-1	100.57	16.740	0	0	0	0	0	0	0	0	0	0	0	0	0	0	0	0	0	0	0	0	0	0
1-2	0	43.066	13.272	0	0	0	0	0	0	0	0	0	0	0	0	0	0	0	0	0	0	0	0	0
2-3	0	0	33.050	5.4667	0	0	0	0	0	0	0	0	0	0	0	0	0	0	0	0	0	0	0	0
3-4	0	0	0	21.889	14.832	0	0	0	0	0	0	0	0	0	0	0	0	0	0	0	0	0	0	0
4-5	0	0	0	0	76.722	26.357	0	0	0	0	0	0	0	0	0	0	0	0	0	0	0	0	0	0
5-6	0	0	0	0	0	258.75	123.43	0	0	0	0	0	0	0	0	0	0	0	0	0	0	0	0	0
6-7	0	0	0	0	0	0	598.07	372.86	1.8716	0	1.0023	0.9444	0	0	0	0	0	0	0	0	0	0	0	0
7-8	0	0	0	0	0	0	0	1766.1	1112.5	5.8534	0	0	0	0	0	1.6769	0	0	0	0	0	0	0	0
8-9	0	0	0	0	0	0	0	0	3169.8	1106.6	5.8615	1.1275	0	1.9660	0	0	0	0	0	0	0	0	0	0
9-10	0	0	0	0	0	0	0	0	0	2167.3	726.87	5.5010	1.7077	1.2972	0	1.5246	2.4683	0	0	0	0	0	0	0
10-11	0	0	0	0	0	0	0	0	0	0	2375.4	715.11	3.5304	0.7902	0.5609	0	0.8288	0	0	0	0	0	0	0
11-12	0	0	0	0	0	0	0	0	0	0	0	2450.7	853.87	10.065	0	0	0	0	0	0	0	0	0	0
12-13	0	0	0	0	0	0	0	0	0	0	0	0	2449.9	852.16	8.4671	0.8037	0	0	0	0	0	0	0	0
13-14	0	0	0	0	0	0	0	0	0	0	0	0	0	2489.0	811.22	10.815	0	0	0	0	0	0	0	0
14-15	0	0	0	0	0	0	0	0	0	0	0	0	0	0	2438.7	885.76	6.0107	0.9348	0	0	0	0	0	0
15-16	0	0	0	0	0	0	0	0	0	0	0	0	0	0	0	2712.5	988.18	6.1737	1.9564	0	0	0	0	0
16-17	0	0	0	0	0	0	0	0	0	0	0	0	0	0	0	0	2946.6	1213.6	7.4883	0	0	0	0	0
17-18	0	0	0	0	0	0	0	0	0	0	0	0	0	0	0	0	0	3265.5	1140.0	7.2666	0	0	0	0
18-19	0	0	0	0	0	0	0	0	0	0	0	0	0	0	0	0	0	0	2321.1	735.43	5.1414	0.4683	0	0
19-20	0	0	0	0	0	0	0	0	0	0	0	0	0	0	0	0	0	0	0	1794.5	394.00	1.6503	0	0
20-21	0	0	0	0	0	0	0	0	0	0	0	0	0	0	0	0	0	0	0	0	1188.3	294.66	0	0
21-22	0	0	0	0	0	0	0	0	0	0	0	0	0	0	0	0	0	0	0	0	0	929.04	214.30	0
22-23	0	0	0	0	0	0	0	0	0	0	0	0	0	0	0	0	0	0	0	0	0	0	648.70	144.57
23-24	84.071	0	0	0	0	0	0	0	0	0	0	0	0	0	0	0	0	0	0	0	0	0	0	372.01

5.3.1 Combinations of two journeys a day

As noted above, one of the fundamental findings that emerges from the NTS data is that each vehicle on average makes two journeys a day[11]. This means that all possible combinations of two journeys have to be taken into account: some cars will make two short journeys a day, some of them will make one short and one medium journey, and so on, ending with vehicles that make two long journeys. For each combination of two journeys the following information is required:

- the number of vehicles involved,
- start and end times of each journey and
- the energy needed for each journey.

This information is necessary for the optimization procedure: start and end times of journeys define when the vehicle is on-road; the rest of the time the vehicle is parked and thus available for power management (through charging or even discharging – the latter concept is discussed in [112]). Energy required for making the journeys is also an essential input into the optimization procedure. This energy need to be expanded to account for efficiency losses incurred during battery charging i.e. using AC/DC rectifiers, as well as other on-board consumption such as air conditioning etc.

The required input data is tabulated in Table 5-8.

[11] This is intuitively acceptable, since most vehicles are used for commuting, i.e. making journeys from home to workplace and back every day.

Table 5-8: Data required for optimization

Journey type		Journey 1		Journey 2		No. of vehicles	E1	E2
Journey 1	Journey 2	Start time	End time	Start time	End time		[kWh]	[kWh]

The first step in pre-processing this data is to determine which journey combinations are allowed with respect to their start/end times: since two journeys are physically taken by a single car, they cannot overlap. In other words, a journey cannot begin during another journey. Figure 5-6 shows graphical representation of feasible combinations of journeys, within a time horizon of 24 h.

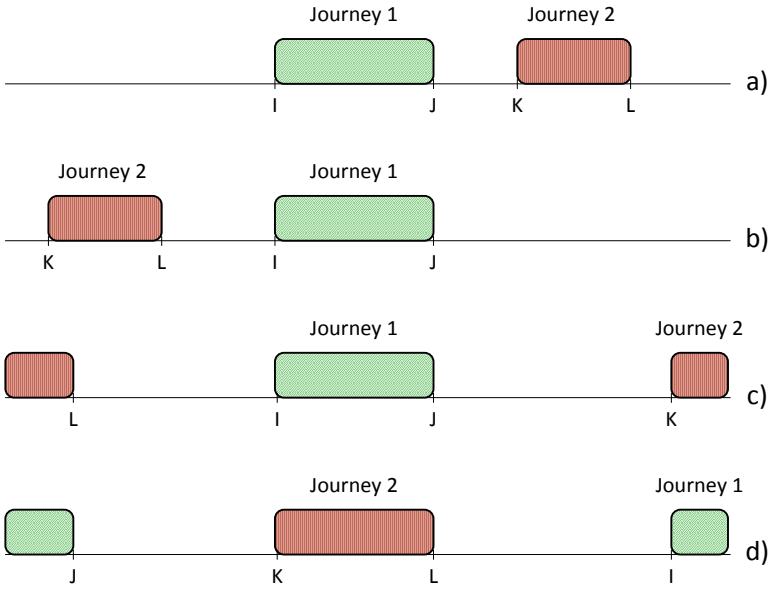


Figure 5-6: Allowed combination of journeys

Labels in Figure 5-6 have the following meaning:

- I – start time step of Journey 1 (in this case one time step corresponds to one hour)
- J – end time step of Journey 1
- K – start time step of Journey 2
- L – end time step of Journey 2

Case a) in Figure 5-6 describes the situation where Journey 2 starts after Journey 1 has finished, and both journeys are completed within one day (i.e. within 24 h). Case b) depicts a similar situation, the only difference being that Journey 2 precedes Journey 1. Case c) refers to the combination where Journey 2 starts after Journey 1 has finished, but it does not finish within the same day; the duration of Journey 2 extends until hour L in the next day. Finally, case d) describes a situation similar to the previous one, but this time Journey 1 finishes on the following day. All of these journey pairs are allowed (feasible) since there is no overlapping.

An illustrative example of allowed combinations of two *short journeys* can be made using data from Table 5-7. For this data (short journeys only), if Journey 1 starts in hour 8-9 and finishes in hour 11-12, then the eligible start/end times for Journey 2 are represented by the shaded cells in Figure 5-7. The shaded cells contain the numbers of eligible journeys. Non-shaded elements either represent journeys (i.e. start/end time combinations) that do not exist in Table 5-7, or journeys that are not allowed due to overlapping. The figure demonstrates that eligible second journeys can start in hour 0-1 and finish in hour 0-1, start in 0-1 and finish in 1-2 and so on, and start in 7-8 and finish in 7-8. All journeys starting between hours 8-9 and 11-12 are not allowed for Journey 2, since they would overlap with Journey 1. In this example, the next eligible journey can only start in hour 12-13, after Journey 1 has finished. Note that the shaded cells (eligible journeys) will change with different selections of start/end times for Journey 1 (different selections of green cell in Figure 5-7 will give different patterns of orange cells).

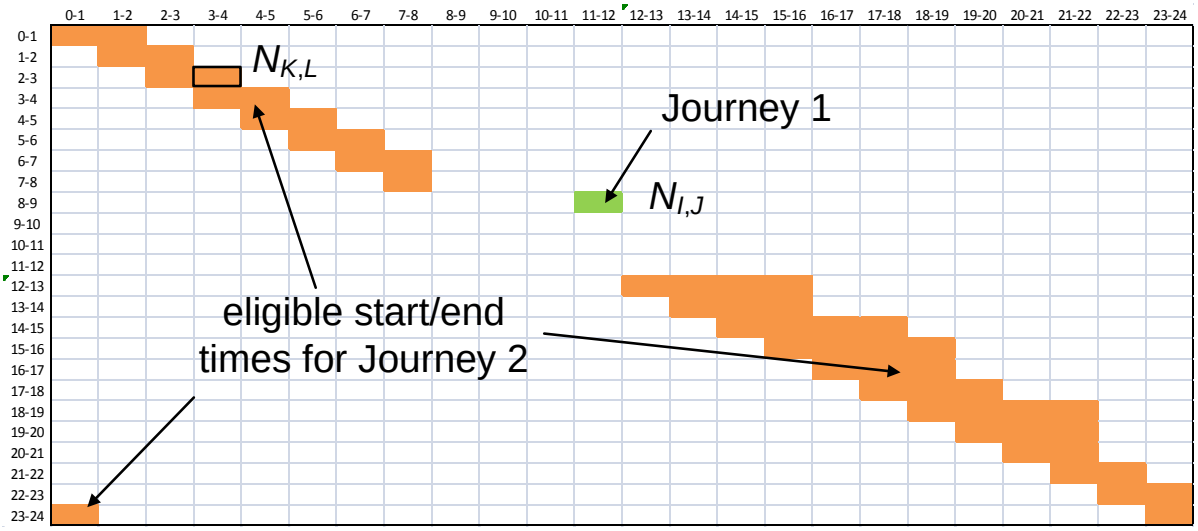


Figure 5-7: An example of eligible combinations of two short journeys

Once the eligible journeys (i.e. their start/end times, numbers and energies) have been identified, it is possible to calculate and fill in the entries in Table 5-8.

In a short and mathematically less rigorous way, the problem can be described in the following three steps:

1. **Task 1: Find the share of number $N_{I,J}$ from the green cell in Figure 5-7 (Journey 1) that correspond to any of the shaded cells $N_{K,L}$ (eligible journeys).**

   Solution: It is reasonable to assume that this share is directly proportional to the numbers in shaded cells (eligible for Journey 2), i.e. the proportion is equal to the number in each of the shaded cell divided by the sum of all shaded cells:

   $N_{I,J}^{K,L} = N_{I,J} \cdot \left[N_{K,L} / \sum N_{K,L}\right]$

2. **Task 2: Find the energy E_1 that $N_{I,J}^{K,L}$ vehicles (calculated in Task 1) will require for Journey 1.**

   Solution: The part of Journey 1 energy that is assigned to $N_{I,J}^{K,L}$ vehicles can be calculated by multiplying the specific energy for Journey 1 (the energy per vehicle) by the number of vehicles: $E_1 = N_{I,J}^{K,L} \cdot E_{I,J}/N_{I,J}$.

3. **Task 3: Find the energy E_2 that $N_{I,J}^{K,L}$ vehicles (calculated in Task 1) will require for Journey 2.**

   Solution: The part of Journey 2 energy consumption that is assigned to $N_{I,J}^{K,L}$ vehicles can be calculated in a similar manner as above by multiplying the specific energy for Journey 2 by $N_{I,J}^{K,L}$: $E_2 = N_{I,J}^{K,L} \cdot E_{K,L}/N_{K,L}$.

The same steps need to be followed for each possible combination of journey types: beside Short-Short (example of which is given above), this also has to be repeated for Short-Medium, Short-Long, etc. combinations of journeys. In general, eligible start/end times for Journey 2 for each of the combinations may differ from those indicated in Figure 5-7.

A more rigorous problem formulation follows where, for the reasons of conciseness, we adopt the following notation for journey types:

Table 5-9: Journey types definition

Journey type definition		
Type	1	Short
	2	Medium
	3	Long

For each journey of type T_1 starting at I and finishing at J ("Journey 1"), it is necessary to determine the share of the number of vehicles that corresponds to any other journey of type T_2 occurring between K and L ("Journey 2")$(I, J, K, L \in \{1, \dots, 24\},\ T_1, T_2 \in \{1,2,3\})$[12]. Let N_{I,J,T_1} denote the number of T_1 type journeys that start at I and finish at J, and Ne_{I,J,T_1}^{K,L,T_2} denote the number of corresponding eligible journeys of type T_2 lasting between K and L. This number depends not only on indices K, L and T_2, but also on the starting point (I, J, T_1), and this is why the latter are included in the superscript of Ne. The dependence on (I, J, T_1) is justified by the fact that each selection of Journey 1 will deliver a different set of eligible start/end times for Journey 2. Let S_e^{I,J,T_1} denote the sum of all eligible journeys for a given Journey 1:

[12] Compare with Task 1 above

$$S_e^{I,J,T_1} = \sum_{T_2=1}^{3} \sum_{K=1}^{24} \sum_{L=1}^{24} Ne_{I,J,T_1}^{K,L,T_2} \tag{68}$$

$$I, J \in \{1, \dots, 24\}, \quad T_1 \in \{1,2,3\}$$

Then the number N_{I,J,T_1}^{K,L,T_2} of vehicles that make one journey of type T_1 between I and J, and another journey of type T_2 between K and L is found as:

$$N_{I,J,T_1}^{K,L,T_2} = N_{I,J,T_1} \cdot \frac{Ne_{I,J,T_1}^{K,L,T_2}}{S_e^{I,J,T_1}}, \quad I, J, K, L \in \{1, \dots, 24\}, \quad T_1, T_2 \in \{1,2,3\} \tag{69}$$

Next, the energy that N_{I,J,T_1}^{K,L,T_2} number of vehicles require for Journey 1 (a journey of type T_1 that lasts between I and J) has to be found. One way to determine this energy is to assume that all vehicles have the same fuel consumption per kilometre driven. This assumption allows calculating the specific energy consumption per vehicle for each triplet (I, J, T_1). Then, the energy that corresponds to N_{I,J,T_1}^{K,L,T_2} number of vehicles is simply obtained by multiplying this number of vehicles by the specific energy[13]:

$$E1_{I,J,T_1}^{K,L,T_2} = N_{I,J,T_1}^{K,L,T_2} \cdot \frac{E_{I,J,T_1}}{N_{I,J,T_1}}, \quad I, J, K, L \in \{1, \dots, 24\}, \quad T_1, T_2 \in \{1,2,3\} \tag{70}$$

Energy E_{I,J,T_1} is the total energy that will be consumed by all the vehicles that make type T_1 journey, starting at I and finishing at J. Energy $E1_{I,J,T_1}^{K,L,T_2}$ is the part of energy E_{I,J,T_1} that corresponds only to those vehicles that will make another journey of type T_2 between K and L.

Finally, the energy that N_{I,J,T_1}^{K,L,T_2} number of vehicles need for Journey 2 (a journey of type T_2 that lasts between K and L) needs to be determined. Again, assuming that all vehicles have the same fuel consumption per kilometre, the specific energy consumption per vehicle can be calculated for each triplet (K, L, T_2). Now the required energy is[14]:

$$E2_{K,L,T_2}^{I,J,T_1} = N_{I,J,T_1}^{K,L,T_2} \cdot \frac{E_{K,L,T_2}}{N_{K,L,T_2}}, \quad I, J, K, L \in \{1, \dots, 24\}, \quad T_1, T_2 \in \{1,2,3\} \tag{71}$$

Energy E_{K,L,T_2} is the total energy that will be consumed by all the vehicles that make type T_2 journey starting at K and finishing at L. Energy $E2_{K,L,T_2}^{I,J,T_1}$ is the part of energy E_{K,L,T_2} that corresponds only to those vehicles whose Journey 1 is of type T_1 and occur between hours I and J.

[13] Compare with Task 2 above
[14] Compare with Task 3 above

The values determined using Equations (69)-(71) are used to populate Table 5-8. An excerpt from the table is given in APPENDIX 5, Table A. 5-13.

5.4 Charging strategies

Given the assumption that a vehicle makes on average two journeys a day, there are many possible charging patterns. In this work, we will focus on the following five charging strategies:

1. Charging after the first journey finished
2. Charging after the second journey finished
3. Charging after each journey
4. Charging all available time with minimum power
5. Optimal charging

All these charging patterns implicitly assume that the vehicle will be charged in the same electricity network. In other words, it is assumed that vehicle will make a journey from place A to place B, whereas both A and B are supplied from the same distribution network. This assumption makes sense if the network considered covers a certain region. However, if a feeder or low voltage level network is considered, then it is reasonable to believe that a vehicle, starting a journey from that network, will end the journey in another network, and this should be taken into account when modelling such relatively small networks.

5.4.1 Charging after the first journey finished

In this case, it is assumed that total energy required for both journeys will be supplied only after the first journey is finished. It is illustrated in Figure 5-8.

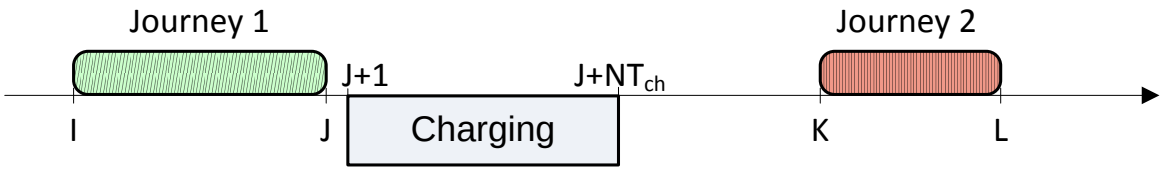


Figure 5-8: Charging after 1st journey

Charging starts immediately after the first journey finishes. It is also assumed that charging is performed at the maximal available power P_{ch}^{max} that the charger can provide. For example, in the UK, a vast majority of households are connected to 0.4kV level distribution network via a single-phase link, with a limit of electric current of 13A, which gives the maximum possible power of 3kW. In this case it is assumed that the charging process will be at $P_{ch}^{max} = 3$kW. In contrast to this, in the continental part of Europe many houses have 3-phase connection to the distribution network

enabling them to pull higher power from the network. For simplicity, it is assumed that all the vehicles on the network have the same charging power.

For a vehicle having one journey of type T_1 between hours I and J, and another journey of type T_2 between hours K and L, the number of time steps needed to charge the battery can be estimated from the following formula:

$$NT_{ch} = \frac{E1_{I,J,T_1}^{K,L,T_2}(b) + E2_{K,L,T_2}^{I,J,T_1}(b)}{N_{I,J,T_1}^{K,L,T_2}(b) \cdot P_{ch}^{max} \eta_{ch} \Delta t} \quad I,J,K,L \in \{1,\dots,24\}, \quad T_1,T_2 \in \{1,2,3\}, \quad b \in \mathbf{L_{bus}} \tag{72}$$

Here, index b designates the bus in the network. The expression $\frac{E1_{I,J,T_1}^{K,L,T_2}(b)+E2_{K,L,T_2}^{I,J,T_1}(b)}{N_{I,J,T_1}^{K,L,T_2}(b)}$ represents the total energy required per car in bus b to make a first journey of type T_1 between hour I and hour J, and to make a second journey of type T_2 between hour K and hour L. This energy must be increased by factor $\frac{1}{\eta_{ch}}$ to account for energy losses in battery and charger, so the energy seen by the network is obtained. Dividing this energy per car by P_{ch}^{max} gives total number of hours required for charging. If time resolution differs from one hour, number of time steps required for charging is calculated by dividing with Δt.

In this strategy, charging starts at time step $J+1$, immediately after first journey finishes, and lasts for next NT_{ch} hours, as indicated in Figure 5-8. However, if the time span between the first and second journey is not long enough to charge the battery, charging is interrupted during the second journey and continued immediately after the second journey.

The charging power of all vehicles in bus b that make one journey of type T_1 between I and J, and another journey of type T_2 between K and L, during each hour ct of charging period is then

$$Pch_{I,J,T_1}^{K,L,T_2}(ct,b) = P_{ch}^{max} \cdot N_{I,J,T_1}^{K,L,T_2}(b) \qquad ct \in \{J+1,\dots J+NT_{ch}\} \; b \in \mathbf{L_{bus}}$$
$$I,J,K,L \in \{1,\dots,24\}, \quad T_1,T_2 \in \{1,2,3\} \tag{73}$$

Total charging power in bus b at hour t is then obtained as a sum of all possible combinations of charging with respect to types of journeys and their start and end times:

$$P_{ch}^{sum}(t,b) = \sum_{T_1}\sum_{T_2}\sum_{I}\sum_{J}\sum_{K}\sum_{L} Pch_{I,J,T_1}^{K,L,T_2}(t,b) \qquad t \in \boldsymbol{T_{24}}, \quad b \in \mathbf{L_{bus}} \tag{74}$$

$\boldsymbol{T_{24}}$ is time horizon of interest, usually one day (24 hours) and $\mathbf{L_{bus}}$ is the set of load buses. This power has to be added to the power of base load already existing in the bus.

5.4.2 Charging after the second journey finished

In this case, charging starts immediately after the second journey, as shown in Figure 5-9. Again, it is assumed that charging is performed at the maximal available power $\boldsymbol{P_{ch}^{max}}$ that the charger can provide.

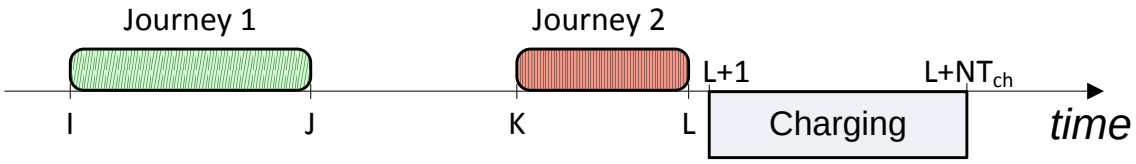


Figure 5-9: Charging after 2nd journey

The number of time steps needed to charge the battery for both Journey 1 and Journey 2 can be estimated using equation (72).

Charging starts at time step $\boldsymbol{L+1}$, immediately after the second journey finishes, and lasts for the next $\boldsymbol{NT_{ch}}$ hours (see Figure 5-9). If charging does not finish by the end of the current day, it continues on the following day and it can last until the beginning of the first journey (next day). If the time span between the end of the second journey and the beginning of the first journey on the next day is not long enough to charge the battery, charging is interrupted when the first journey starts and continued immediately after it finishes.

Charging power of all vehicles in bus b with this driving pattern (one journey of type T_1 between I and J, and another journey of type T_2 between K and L), for each hour ct of charging period is given by

$$Pch_{I,J,T_1}^{K,L,T_2}(ct,b) = P_{ch}^{max} \cdot N_{I,J,T_1}^{K,L,T_2}(b)$$
$$I,J,K,L \in \{1,\dots,24\}, \quad T_1,T_2 \in \{1,2,3\}, \quad ct \in \{L+1,\dots L+NT_{ch}\} \; b \in \mathbf{L_{bus}} \tag{75}$$

Now the charging period starts from hour $L+1$. Total charging power in bus b at hour t for all possible combinations of driving patterns is determined by expression (74).

5.4.3 Charging after each journey

This strategy is illustrated in Figure 5-10. Energy required for the first journey is supplied to the vehicle immediately after journey 1 finishes. Similarly, energy required for the second journey is supplied to the vehicle immediately after this journey finishes.

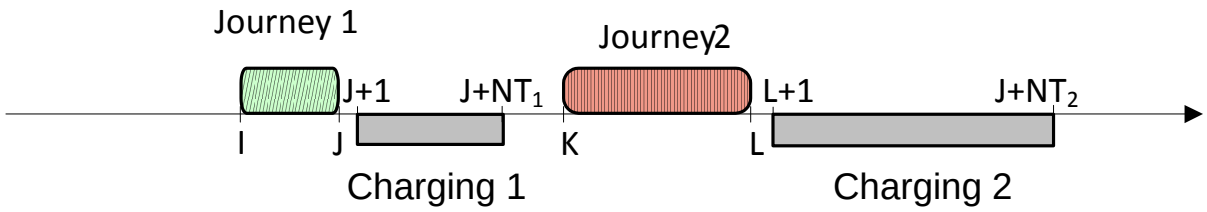


Figure 5-10: Charging after each journey

The duration of charging period for journey 1 (henceforth it will be referred to as 'charging period 1'), expressed in time steps is:

$$NT_1 = \frac{E1_{I,J,T_1}^{K,L,T_2}(b)}{N_{I,J,T_1}^{K,L,T_2}(b) \cdot P_{ch}^{max} \eta_{ch} \Delta t} \tag{76}$$

$$I, J, K, L \in \{1, \dots, 24\}, \quad T_1, T_2 \in \{1,2,3\}, \quad b \in \mathbf{L_{bus}}$$

Similarly, the duration of charging period for journey 2 ("charging period 2") is:

$$NT_2 = \frac{E2_{K,L,T_2}^{I,J,T_1}(b)}{N_{I,J,T_1}^{K,L,T_2}(b) \cdot P_{ch}^{max} \eta_{ch} \Delta t} \tag{77}$$

$$I, J, K, L \in \{1, \dots, 24\}, \quad T_1, T_2 \in \{1,2,3\}, \quad b \in \mathbf{L_{bus}}$$

The charging power in bus b of all vehicles that make one journey of type T_1 between I and J, and another journey of type T_2 between K and L, during both charging periods is then

$$Pch_{I,J,T_1}^{K,L,T_2}(ct, b) = P_{ch}^{max} \cdot N_{I,J,T_1}^{K,L,T_2}(b)$$

$$I, J, K, L \in \{1, \dots, 24\}, \quad T_1, T_2 \in \{1,2,3\}, ct \in \{J+1, \dots J+NT_1\} \cup \{L+1, \dots L+NT_2\}, \tag{78}$$

$$b \in \mathbf{L_{bus}}$$

The total charging power in bus b at hour t for all possible combinations of driving patterns is determined by expression (74).

It is also necessary to address the situation where the time span between journeys is shorter than the required charging times. In general, there are three such possibilities:

1. Periods required for charging are longer than the time spans between journeys: time between first and second journey is shorter than time NT_1 required to charge the battery for journey 1, and at the same time, period between second and first journey (on the following day) is shorter than the time NT_2 required to charge the battery for journey 2.

In this case, the required energy cannot be supplied to the battery and the problem is considered infeasible.

2. Charging period 1 is longer than the time span between the first and second journey: in this case, charging the energy for journey 1 starts immediately after journey 1 finishes, and lasts until journey 2. It is then interrupted. During this charging, a portion of energy required for journey 1 is supplied to the battery. Charging continues after journey 2 and lasts until the total required energy for both journeys is supplied to the battery.
3. Charging period 2 is longer than the time span between the second and first journey: in this case, charging the energy for journey 2 starts immediately after journey 2 finishes, and lasts until journey 1 (on the next day). It is then interrupted. Charging continues after journey 1 and lasts until the total required energy for both journeys is supplied to the battery.

5.4.4 Charging all available time with minimum power

In this case, vehicles are charged all the time they are off road with minimal possible power, as illustrated in Figure 5-11. The advantage of this type of charging is minimum network capacity deployment.

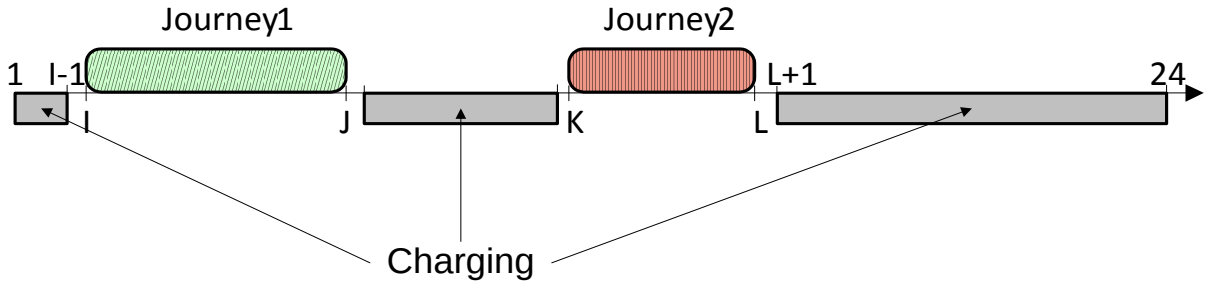


Figure 5-11: Charging all the standing time with minimum power

Time available for charging is the entire time horizon (usually one day, 24h) less journey time. For the vehicle that has one journey of type T_1 between I and J, and another journey of type T_2 between K and L, the number of time steps available to charge the battery is:

$$NT_{ch} = \|\mathbf{T_{24}}\| - [(J - I) + (L - K)] \quad (79)$$

$\|\mathbf{T_{24}}\|$ is the number of time steps within the optimization horizon. Charging power for all such vehicles in bus b during each time step ct of charging depends on the required energy for both journeys:

$$Pch_{I,J,T_1}^{K,L,T_2}(ct,b) = \frac{E1_{I,J,T_1}^{K,L,T_2}(b) + E2_{K,L,T_2}^{I,J,T_1}(b)}{NT_{ch} \cdot \eta_{ch}} \tag{80}$$

$$I,J,K,L \in \{1,\dots,24\}, \quad T_1,T_2 \in \{1,2,3\}, ct \in \boldsymbol{T_{24}} \backslash (\{I,\dots,J\} \cup \{K,\dots,L\}), b \in \mathbf{L_{bus}}$$

The total charging power in bus b at hour t for all possible combinations of driving patterns is determined by expression (74).

5.4.5 Optimal charging

In contrast to the charging strategies described above, the optimal charging denotes a way of storing the energy to a battery at different rates (different power) and at the times when it is the most beneficial to the system. Eligible time for charging periods may be anytime when the vehicle is off road. Charging may start, then continue with variable or constant power, or stop and continue later on. This gives tremendous flexibility which can be exploited to increase the utilization of intermittent sources such as wind, shift load to minimize the system peak or to manage network congestion.

The following is the mathematical formulation of optimal charging.

Charging power is a decision variable in the optimization problem. For all vehicles in bus b that make one journey of type T_1 between hour I and J, and another journey of type T_2 between hour K and L, charging power must be zero during the journeys:

$$Pch_{I,J,T_1}^{K,L,T_2}(t,b) = 0$$
$$I,J,K,L \in \{1,\dots,24\}, \quad T_1,T_2 \in \{1,2,3\}, t \in \{I,\dots J\} \cup \{K \dots L\}, b \in \mathbf{L_{bus}} \tag{81}$$

The rest of the time, whenever the vehicles are parked, charging power may take any value between zero and the maximal available power P_{ch}^{max}:

$$0 \le Pch_{I,J,T_1}^{K,L,T_2}(ct,b) \le P_{ch}^{max} \cdot N_{I,J,T_1}^{K,L,T_2}(b)$$
$$I,J,K,L \in \{1,\dots,24\}, \quad T_1,T_2 \in \{1,2,3\}, ct \in \boldsymbol{T_{24}} \backslash (\{I,\dots,J\} \cup \{K,\dots,L\}), b \in \mathbf{L_{bus}} \tag{82}$$

The energy charged into the batteries must be at least the required energy for both journeys:

$$\sum_{t \in \boldsymbol{T_{24}}} Pch_{I,J,T_1}^{K,L,T_2}(t,b)\,\Delta t \ge \frac{E1_{I,J,T_1}^{K,L,T_2}(b) + E2_{K,L,T_2}^{I,J,T_1}(b)}{\eta_{ch}} \tag{83}$$
$$I,J,K,L \in \{1,\dots,24\}, \quad T_1,T_2 \in \{1,2,3\}, b \in \mathbf{L_{bus}}$$

As before, total charging power in bus b at hour t is then obtained as a sum of all possible combinations of charging with respect to types of journeys and their start and end times, Equation (74). This power has to be added to the power of base load existing on the bus.

5.4.6 Proposed Optimization Problem Formulation

The approach of incorporating developed electric vehicles charging models into an OPF formulation is similar to the procedure shown in CHAPTER 3, where the detailed description of constraints and objective function is given. Since the methodology is based on a DC OPF, and developed car charging models are also linear, the overall optimization problem remains linear.

Most of the constraints described in CHAPTER 3 remain intact; thus they will be listed here with only the differences highlighted.

Power Balance Constraints (see CHAPTER 3, Section 3.2.1, Eq. (10) and (11)): As before, nodal power balance constraints must be written for each bus in the network. As contrary to DSR where flexible demand was a part of total load, now the total load consists of base load and charging power. This is described with the two first terms on the right hand side of equation (84).

$$\sum_{g \in \mathbf{NG_b}} P_g(t) + charge_shed_b(t) + load_shed_b(t) = \\ = Pd_b(t) + P_{ch}^{sum}(t,b) + P_b^{EX}(t) + over_slack_b(t) \\ t \in \mathbf{T_{24}}, b \in \mathbf{N_{BUS}} \tag{84}$$

where $charge_shed_b$ is curtailed charging power. Charging power $P_{ch}^{sum}(t,b)$ may be non-optimized, as described in sections 5.4.1-5.4.4, or optimized, Section 5.4.5.

Electric vehicles constraints are defined in sections 5.4.1-5.4.5, taking into account vehicles' availability for charging, maximal charging power, charging efficiency, energy consumption etc.

Network constraints (see CHAPTER 3, Section 3.2.2, Eq. (12)) limit the power flows over branches.

Generator constraints: In contrast to the generator model given in CHAPTER 3, where the generation cost was a linear function of power, in this model the quadratic cost function is used [72]:

$$C_g(P_g) = a_{1,g} + a_{2,g}P_g + a_{3,g}P_g^2, \quad g \in \mathbf{G} \tag{85}$$

where P_g is generator output power, $a_{1,g}$ [£] represent no-load cost, $a_{2,g}$ [£/MW] is linear cost coefficient and $a_{3,g}$ [£/MW^2] is quadratic cost coefficient.

By doing this, minimization of total generation costs will at the same time lead to flattening load profiles [116]. However, to keep the model linear, the quadratic function is approximated with linear segments, as shown in Figure 5-12.

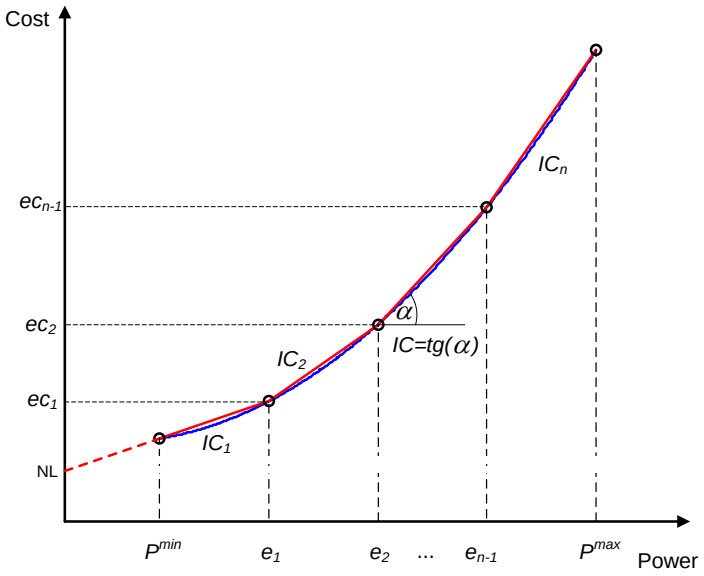


Figure 5-12: Piece-wise linearization of quadratic generation cost curve

For a given number $N_{s,g}$ of segments $(N_{s,g} \geq 1)$ for generator g, the range between minimum and maximum power of the generator is divided into sub-ranges separated by elbows (see Figure 5-12). The elbows points are:

$$e_{s,g} = P_{g,\min} + s \cdot \frac{P_{g,\max} - P_{g,\min}}{N_{s,g}} \qquad s \in 0 \cup \mathbf{NS}_g, \qquad g \in \mathbf{G} \tag{86}$$

where $\mathbf{NS}_g$ is a set of integers $\mathbf{NS}_g = \{1, \dots, N_{s,g}\}$ specified to denote segments for generator g. The costs at elbows points for each generator g are obtained using (**85**):

$$ec_{s,g} = a_{1,g} + a_{2,g} e_{s,g} + a_{3,g} e_{s,g}^2 \qquad s \in 0 \cup \mathbf{NS}_g, \qquad g \in \mathbf{G} \tag{87}$$

Each segment has a slope which is called incremental cost. Incremental costs are calculated as:

$$IC_{s,g} = \frac{ec_{s,g} - ec_{(s-1),g}}{e_{s,g} - e_{(s-1),g}} \qquad s \in \mathbf{NS}_g, \qquad g \in \mathbf{G} \tag{88}$$

If the first segment is extrapolated towards zero (dashed line in Figure 5-12), it intersects the cost-axis (vertical axis) at the No-Load Cost point (NL):

$$NL_g = ec_{0,g} - IC_{1,g} \cdot P_{g,\min} \qquad g \in \mathbf{G} \tag{89}$$

Power associated with each segment is a decision variable and it is limited by the surrounding elbows:

$$0 \le Pseg_{s,g}(t) \le e_{s,g} - e_{(s-1),g} \qquad s \in \mathbf{NS}_g, \quad t \in \mathbf{T_{24}}, \quad g \in \mathbf{G} \tag{90}$$

Total generator output power is then a sum of the powers of individual segments

$$P_g(t) = P_{g,\min} + \sum_{s=1}^{N_{s,g}} Pseg_{s,g}(t) \qquad t \in \mathbf{T_{24}}, \quad g \in \mathbf{G} \tag{91}$$

Objective function minimizes the total cost:

$$\begin{aligned} COST = & \sum_{t \in \mathbf{T_{24}}} \sum_{s \in \mathbf{NS}_g} \sum_{g \in \mathbf{G}} IC_{s,g} Pseg_{s,g}(t) + \sum_{t \in \mathbf{T_{24}}} \sum_{b \in \mathbf{L_{BUS}}} r_{LS} \cdot c_{LS} \cdot charge_shed_b(t) \\ & + \sum_{t \in \mathbf{T_{24}}} \sum_{b \in \mathbf{L_{BUS}}} c_{LS} \cdot load_shed_b(t) + \sum_{t \in \mathbf{T_{24}}} \sum_{b \in \mathbf{G_{BUS}}} c_{OS} \cdot Over_slack_b(t) \end{aligned} \tag{92}$$

The cost of the curtailed charging power is multiplied with r_{LS}, where $r_{LS} < 1$ making the cost of the curtailed charging power smaller than the cost of involuntary load shedding of base demand. In this way, in the case when there are not enough generation or network capacities to supply the entire load, electric vehicles will stop charging first, until the network conditions improve.

5.5 Case study

The algorithm is tested on the IEEE 30 bus test system. The electrical representation of the system is shown in Figure 5-13. The main system characteristics are given in Table 5-10.

Table 5-10: System data

Number of buses	30
Number of branches	41
Number of load buses	21
Peak Load [MW]	283.4

Figure 5-13 shows a snapshot of the system operating at peak time, without electric vehicles (only base load).

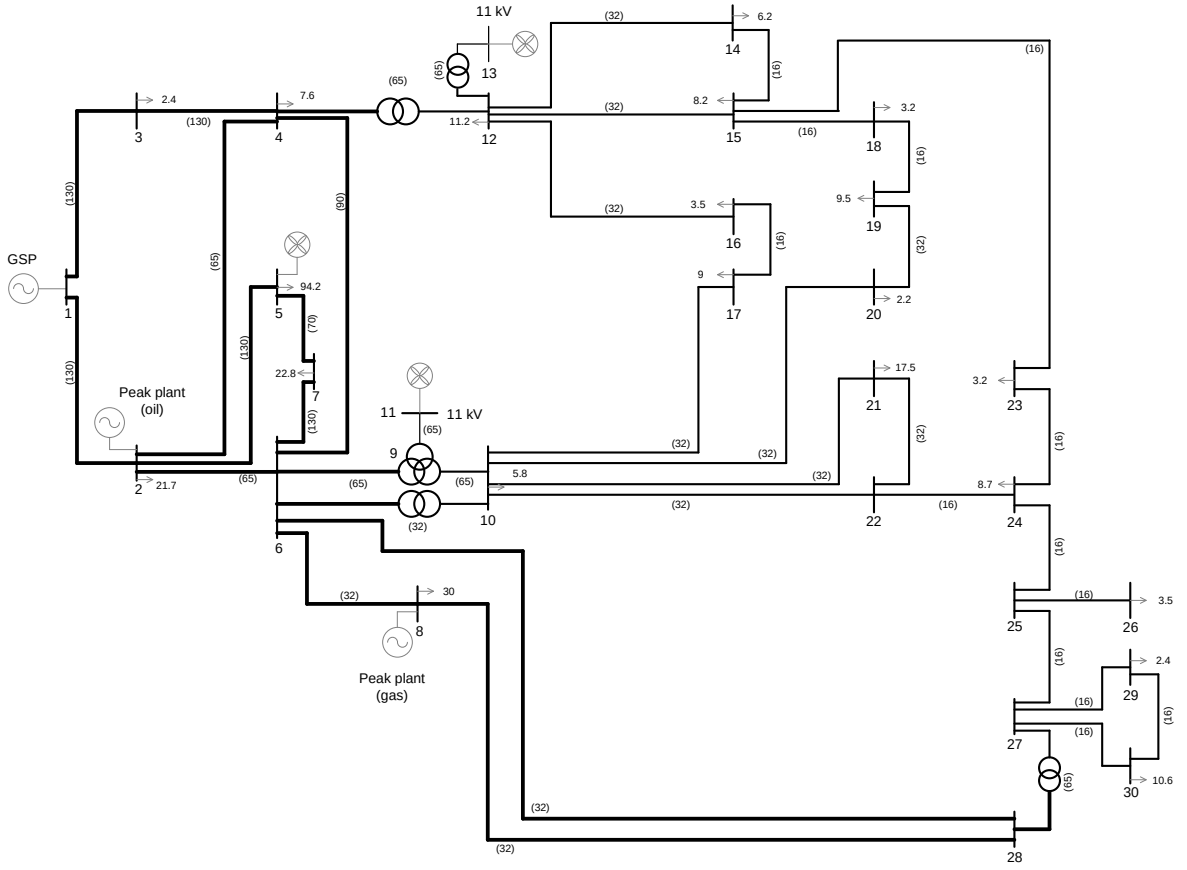


Figure 5-13: IEEE 30 bus test system

Base load peak for each bus is shown in the same figure next to the corresponding bus, indicated by an arrow. Given only the base load, no overloaded branches are detected. However, when electric vehicle charging is added to base load, overloading occurs. Numbers in parentheses show the line's thermal capacity. Thicker lines represent 132kV lines, whilst tinnier ones represent 33kV network. Beside the energy source at the General Supply Point (GSP), there are peak-plants attached at bus 2 and 8. Wind generators are planned to be attached at buses 5, 11 and 13 and their impact on network operation is to be investigated. Installed generation capacity as well as production costs are summarized in Table 5-11.

Table 5-11: Generator data

Bus	Type	Inst. Cap.	a_1	a_2	a_3
		[MW]	[£]	[£/MWh]	[£/(MW)^{2}h]
1	GSP	250	1000	16.19	0.00048
2	Oil	80	370	22.26	0.00712
5	Wind	20	0	0	0
8	Gas	40	670	27.79	0.00173
11	Wind	20	0	0	0
13	Wind	20	0	0	0

Note that there is a zero production cost associated to all wind generators in order to prioritize the usage of wind energy.

Number of vehicles present on the network is estimated based on statistical data for the UK [113], where it is found that there are approximately 1.5 vehicles per household. The number of households is in turn estimated with the assumption that the diversified load profile for household has a peak demand of 1kW. Since the peak load of the network is 283.4MW (Table 5-10), estimated number of households is

$$N_{household} = \frac{283400\ kW}{1\ kW/household} = 283400\ households$$

Then, the estimated number of vehicles is

$$N_{vehicles} = 283400\ households\ \cdot 1.5 \frac{vehicle}{household} = 425100\ vehicles$$

As mentioned above, the table of all possible combinations of journeys contains in total 44,161 entries. It is impractical to deal with this large quantity of data, and also, as it can be seen from APPENDIX 5 Table A. 5-13, there are many entries where the involved number of vehicles is relatively low, for example, around one. From these reasons a reduction of the data set is desirable. This is why all entries with the number of vehicles less than a specified value are removed. However, during this process of elimination, the total energy must be conserved. It means the energy associated with the eliminated journeys should be distributed amongst the remaining ones. This is done in the following steps:

- Extract from the table all the entries where the number of vehicles is less than a specified number N_{min}.
- For all such entries, sum the energies of the first journeys that end at time t and distribute it amongst the remaining entries where the first journey also ends at time t. This distribution is done in proportion to the amount of the energy of each of the remaining first journeys. The same is done for the second journey.

For example, if $N_{min} = 10$ then the table shrinks to 18,866 entries. This is less than half from the original table, but still, it is a relatively high number to get a tractable solution in multi-bus networks. This is why a further reduction is needed, which is achieved as follows:

It is assumed that the number N_{veh}^{bus} of vehicles in each bus is proportional to the peak of the bus. This follows the same logic that was used to estimate the total number of vehicles on the network. Profiles are then randomly assigned to the buses paying attention that sum of all vehicles in all profiles in one bus is equal to N_{veh}^{bus}. Next, the profiles are sorted with respect to the number of vehicles and only a specified number of profiles with highest numbers of vehicles is taken. The rest of the profiles are truncated. Finally, the number of vehicles in the remained profiles (that are not been truncated) is increased by the ratio between the sum of the number of vehicles in all profiles (before elimination) and the sum of the number of vehicles in remaining profiles. The same is done with the energy of the first and second journey. In this way, the number of vehicles in each bus, as well as their energies, remains intact. For this case, the number of 2,000 profiles is selected.

As mentioned above, four different charging strategies with non intelligent charging are examined, assuming there are two journeys a day:

- Charging after first journey
- Charging after second journey
- Charging after both journeys
- Charging all available time with min. power

Figure 5-14 shows the base load for the whole network, and above it, electric vehicle load, for each charging strategy.

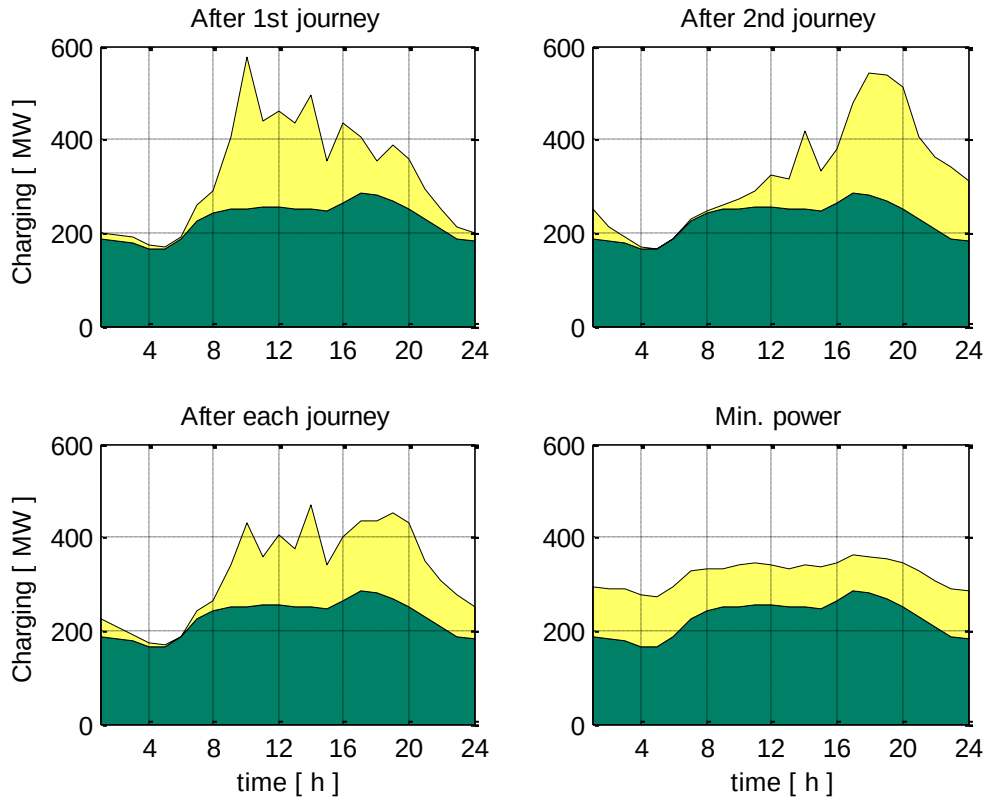


Figure 5-14: Total network load with different charging strategies

From Figure 5-14 it is obvious that both charging strategies after the first journey and after the second journey represent the worst charging strategies from the point of view of system peak (see below Table 5-12) and the number of overloaded branches (see Table A. 5-14 in APPENDIX 5). For these two strategies, system peak doubles. A better situation is obtained if the charging is done after each journey, where system peak is increased by 65%. Much better network conditions are experienced when vehicles are charged at all available times with minimal power – in this case, system peak increases by 30%. The least increase of peak, only 15%, is obtained in the case of optimal charging, which is shown in Figure 5-15.

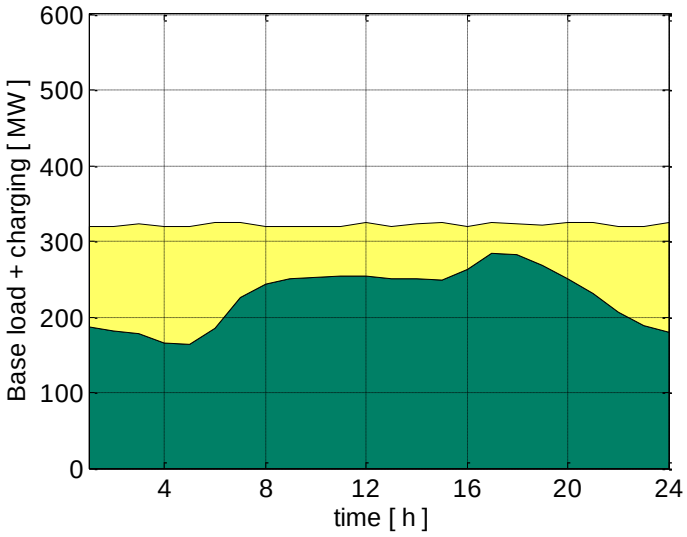


Figure 5-15: Optimal charging – load is almost flat, and peak is increased about 15% comparing to base load

Table 5-12 details the values of system peak and its relative increase comparing to base load peak, for each charging strategy.

Table 5-12: System peak for different charging strategies

Charging Strategy	System peak [MW]	Increase of system peak [% of base load]
After 1	577.8	203.9
After 2	541.0	190.9
After both	468.9	165.5
Min. power	363.7	128.3
Optimal	324.7	114.6

Table A. 5-14 in APPENDIX 5 shows line lengths, replacement prices, line capacities and maximal power flowing through the lines for each charging strategy. The bottom row in Table A. 5-14 gives the total number of overloaded elements (transformers and lines).

Summary of overloaded elements, their replacement costs and total replacement cost for each charging strategy type are given in Table 5-13. From the number of overloaded branches point of view, the worst case is charging after the second journey, which results in total of 15 overloaded elements. This is also the worst case regarding total replacement costs. The reason for this lies in the fact that the end of the second journey mostly coincides with the afternoon peak, when the network is already most highly loaded. The second worst case is charging after first journey. Charging after

each journey and charging with minimal power lead to overloading of five and one elements, respectively. Again, optimal charging does not cause overloading of network branches.

Table 5-13: Summary of replacement costs

Charging strategy	REPLACEMENT COST									
	Transformer		OHL 132kV			UG Cables 33kV			TOTAL	
	units	[£]	units	[km]	[£]	units	[km]	[£]	units	[£]
After 1	2	2037400	9	414.78	34053438	3	22	5649600	**14**	**41,740,438**
After 2	2	2037400	9	414.78	34053438	4	27.68	7108224	**15**	**43,199,062**
After both	1	1018700	4	206.26	16933946	0	0	0	**5**	**17,952,646**
Min. power	0	0	1	25.05	2056605	0	0	0	**1**	**2,056,605**
Optimal	0	0	0	0	0	0	0	0	**0**	**0**

From Table 5-13 the importance of offering the drivers an opportunity to charge the vehicles after each journey can be observed. For this particular network, the total replacement costs are more than halved compared to the case of single charging. Charging with minimum power induces even less replacement costs, while optimal charging requires no replacements and therefore no cost.

Due to lack of network capacities (for charging strategies 'after first journey', 'after second journey' and 'after both journeys' there is also lack of generation capacity), not all the vehicles could be charged as required. It means, charging of some vehicles must be curtailed. Figure 5-16 shows for each bus of the network and for each hour of the day the estimated number of vehicles that are not able to fully charge for strategy 'after first journey'. It can be noted that most of the charging curtailment occurred in buses 2, 5, 7 and 8. Electric vehicles are distributed in proportion to the load, and these buses supply the largest loads. Charging curtailment mostly occurs between 9am and 4pm since in that time most of the vehicles are expected to charge their batteries. After 4pm the number of curtailed vehicles drops since, around that time, the second journey starts.

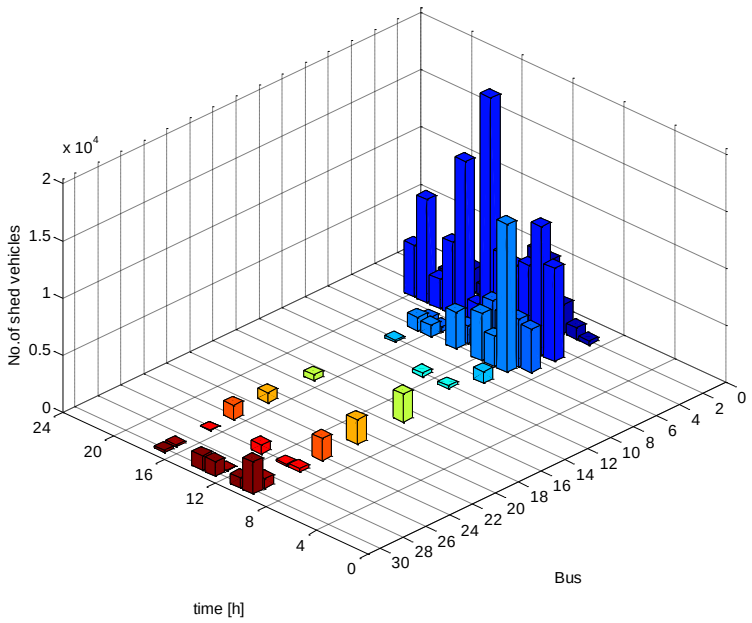


Figure 5-16: Estimated number of vehicles that could not be charged for strategy "charging after first journey"

Similar results are obtained for the other types of fixed charging. For example, for the charging strategy 'after second journey', the number of the curtailed vehicles is, as a function of time of the day and the network bus, given in Figure A. 5-1 in APPENDIX 5. The shift in time of the curtailed vehicles towards the end of the day is obvious: most vehicles are curtailed between 6pm and 9pm. This is due to a fact that second journey for most vehicles ends around 6pm (see also Figure 5-1).

It is interesting to estimate the maximum number of vehicles that could be maintained on system with the given network constraints, without any charging curtailment. The results of such analysis are given in Table 5-14. In this table, the total number of vehicles (absolute number and a percentage of the estimated number of vehicles which is for this system 425,100) that can be connected to the network without overloading any of the lines is given for each charging strategy.

Table 5-14: Maximum number of vehicles that could be connected to the network

STRATEGY	Max No. of EV that can be charged	
	No.	[%]
After first journey	93522	22
After second journey	68016	16
After both journeys	114777	27
Min. Power	216801	51
Optimal	437853	103

As it can be seen from Table 5-14, charging strategy 'after second journey' leads to the least number of vehicles that can be connected to the network without overloading of the network assets, which is the most prominent. In this case, only 16% of vehicles in this network may be served. About 6% more of vehicles can be connected to the network if the charging strategy is only after the first journey. The next lowest are charging after both journeys ('twofold') and charging all the time when the vehicle is off road at minimum power, with 27% and 51% of vehicles, respectively. However, with the optimal charging strategy, all the existing vehicles on the network may be charged without jeopardizing network assets. In addition, there is enough network capacity to accommodate 3% more of the estimated number of vehicles.

Optimal charging strategy not only allows all the existing vehicles to be charged, but also enables the best utilization of intermittent resources, such as wind generation. To investigate this, three wind generators are connected to the network at buses 5, 11, 13 (see Table 5-11). For three different wind profiles, total wind generation and total load (base load + optimal electric vehicles charging) are shown in Figure 5-17.

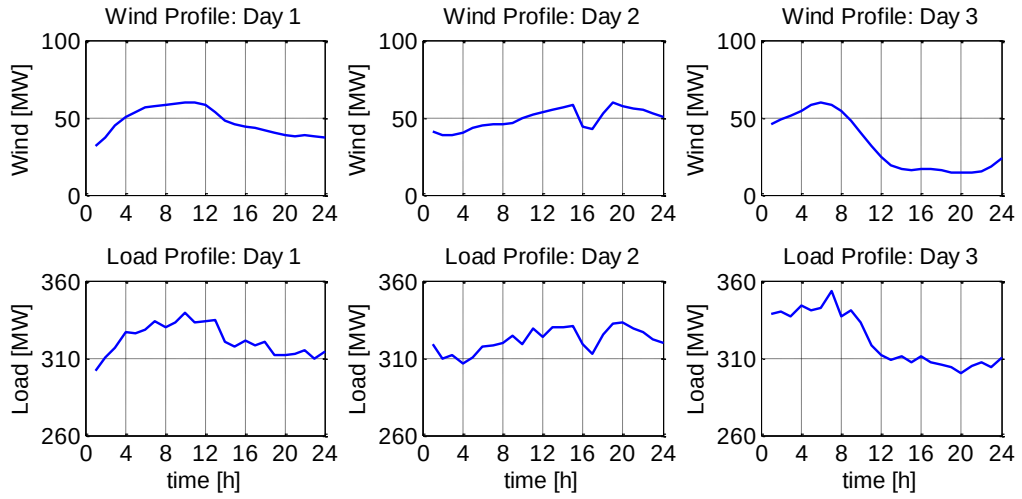
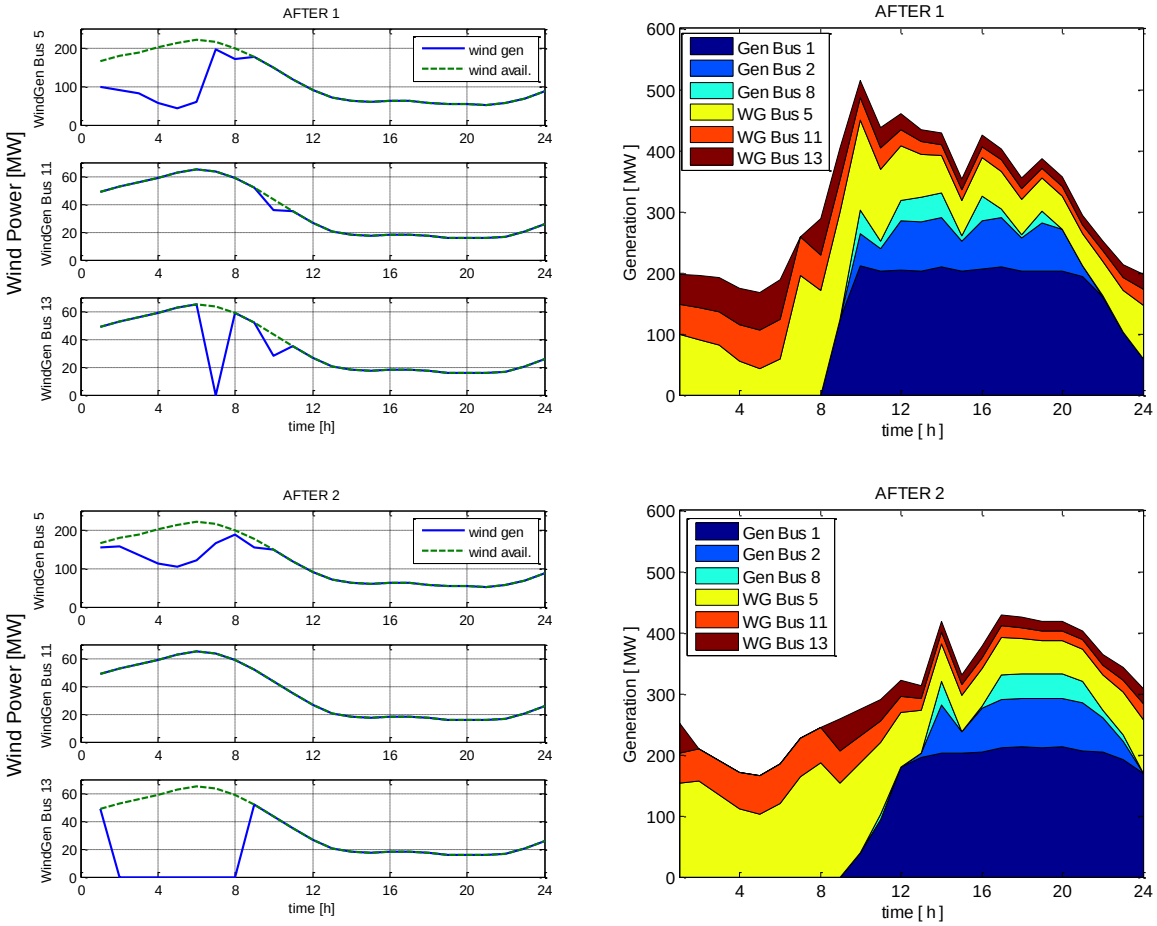


Figure 5-17: Total load (base load + EV) follows the wind (three different days with different wind profiles)

Wind following is the direct consequence of the assumed zero cost of wind generation. Thus a cost-driven signal is generated and sent to the customers, so the most vehicles will be charged during the low-cost periods. This can be generalized in the sense that the system operator can synthesize such a signal in different parts of the network at different times, in order to reduce congestions in the network.

In order to better illustrate the impact of flexible charging on wind utilization, the installed capacity of wind generators is increased to match the capacity of the lines that connect them to the network. For example, wind generators in buses 11 and 13 are connected to the network via 65MW transformers, and their capacity is increased to be 65MW. Bus 5, where another wind generator is placed, is connected to the network via two lines of capacities 130MW and 70MW. However, in bus 5 there is significant load, so the total wind generation in bus 5 is set to be 220MW, which is 10% more than the sum of lines capacity incident on bus 5. By choosing these values for wind generators, it is expected that there is no wind curtailment due to lack of connection capacity.

Figure 5-18 shows wind utilization (left charts) and each generator output (right charts) for each charging strategy.



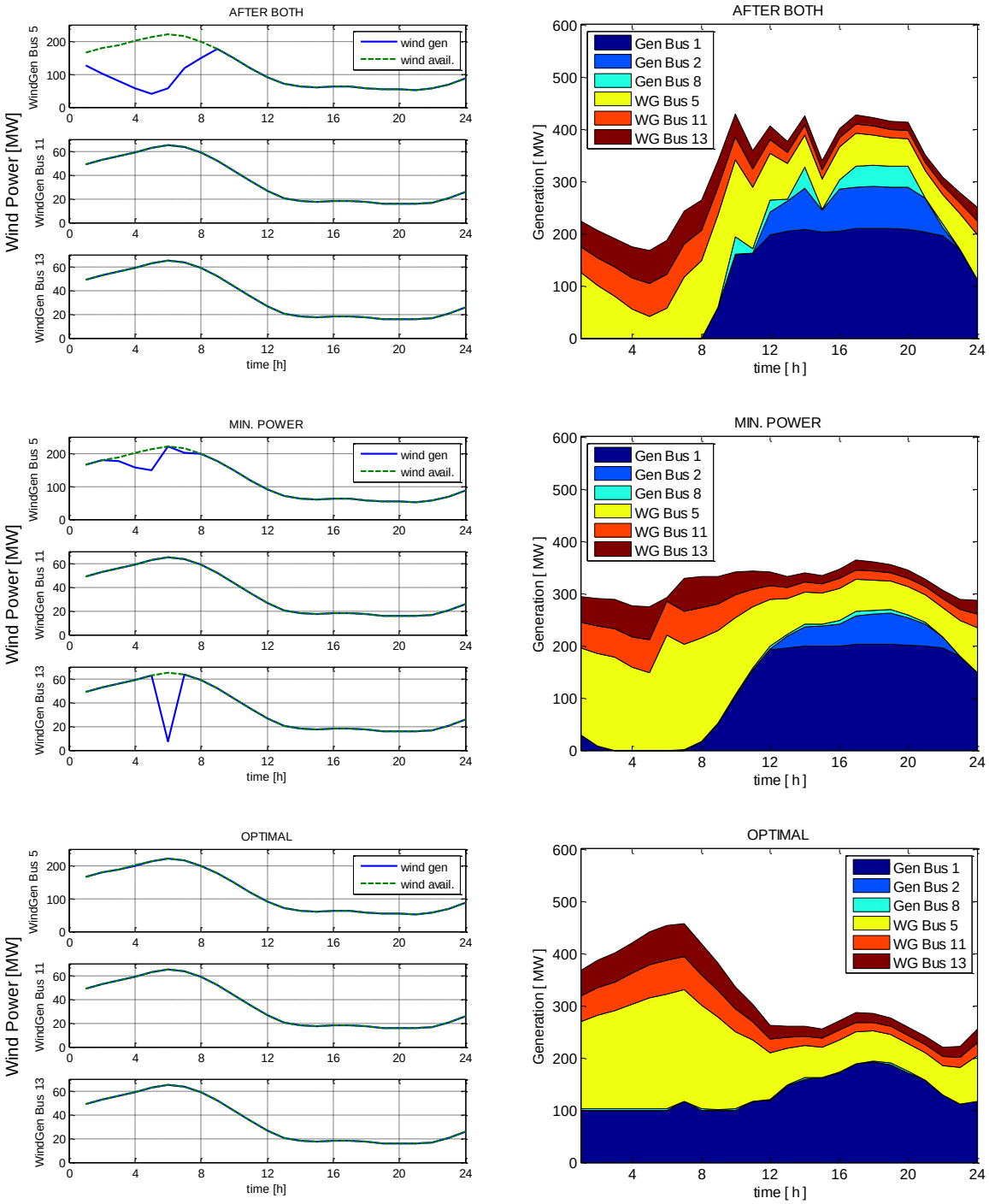


Figure 5-18: Wind utilization and total generation by technology

Figure 5-18 clearly shows that charging strategies after first journey, after second journey and after both journeys lead to wind curtailment and utilization of the expensive peak generators in buses 2 and 8. These are notably reduced if charging is performed with minimal power, and completely removed in the case of optimal charging.

Figure 5-19 explains how, when added together, different charging patterns in different buses give smoother curve. Figure 5-19 (upper chart) shows the optimal charging patterns in three buses with

relatively large load: bus 5, 8, and 21. Load in buses 5 and 21 have uneven shape between hour 0 and 12. However, their sum is a relatively smooth line because these two charging patterns complement each other: when one of them is low, another one is high and vice versa. In contrast to them, charging pattern in Bus 8 is almost flat throughout the day.

Figure 5-19 (lower chart) demonstrates that the effect of smoothing is emphasized when all network buses are taken into account. In the same figure, available wind is represented by the blue line. From the figure, it is obvious that charging patterns for the whole network closely follow the shape of the wind.

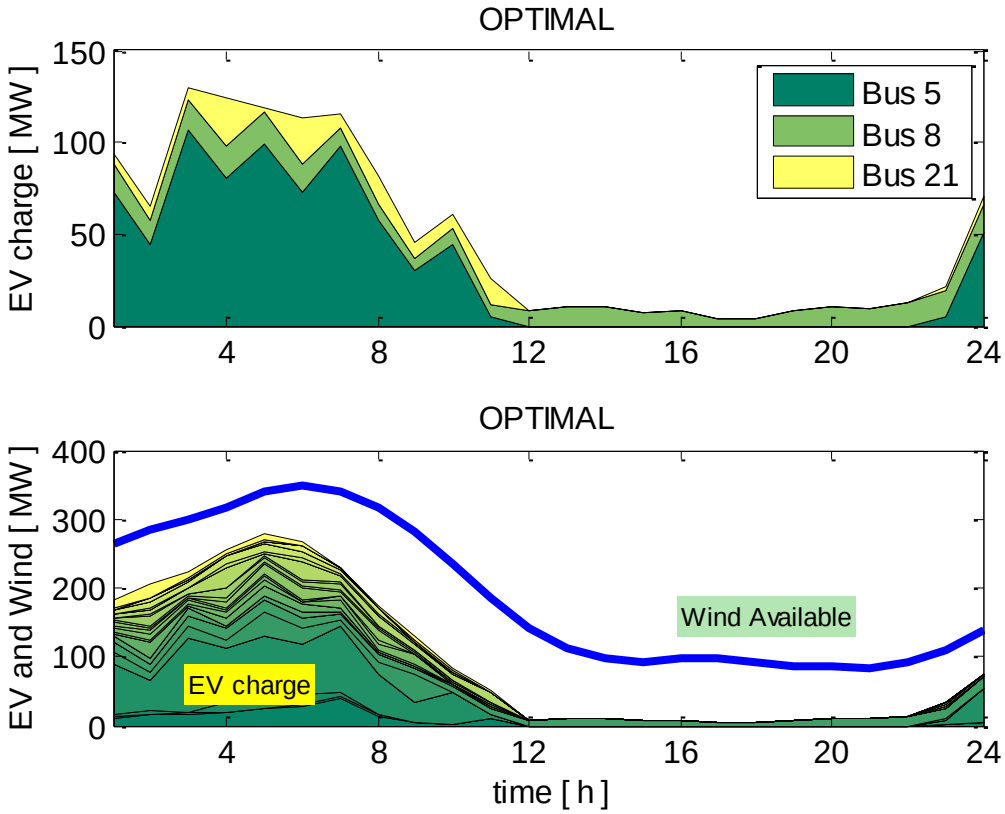


Figure 5-19: Complementarities of charging: selected buses (upper chart) and all the busses (lower chart)

5.6 Conclusion

In this chapter, a potential impact of driving patterns associated with commuting in the morning and making return journeys in the evening is analysed. Driving patterns are based on the UK driving statistics. If the charging is not performed in an intelligent manner, it will lead to more concentrated

EV charging in the morning hours, between 8am and 9am and evening charging between 6pm and 8pm.

Five charging strategies are modelled:

- charging the after first journey,
- charging after second journey,
- charging after both journeys,
- charging with minimum power all available time, and
- optimal charging.

The model is incorporated in multi-bus network and an optimization problem is formulated to minimize the total operation cost, while preserving all the system and EV constraints.

The model was tested on the 132/33kV IEEE 30 bus network. Again, the results are very system specific. It was shown that the charging strategy after the second journey, between 6pm and 8pm, exhibited the worst performance, since it coincides with system peak. From the results shown, it can be concluded that non intelligent charging of electric vehicles in this specific network is related with the following problems:

- system peak is doubled (the exception is charging with minimum power all available time)
- estimated cost of the required reinforcement of the network assets is more than £40M if the charging is made once a day
- if charging is made twice a day (after each journey) the estimated reinforcement cost halves to approximately £18M
- not all envisioned electric vehicles can be supplied – in the worst case (charging after second journey), only 16% of total fleet could be supplied from the network. In the best case (charging with minimum power) around 50% of the vehicles could be supplied
- wind curtailment

However, prudent charging strategies, lead to:

- increase peak of 14%
- no overloading of network assets, therefore no reinforcement cost
- all envisioned vehicles are integrated and there is room for 3% more vehicles
- no wind curtailment (optimal charging pattern follows the wind profile)
- smoothing the load profile

From the above, it may be concluded that EV loads are well suited to support network operation due to:

- their relatively modest amount of energy required
- short distances and consequently short driving times generally associated with small passenger vehicles
- batteries have relatively high power ratings
- considerable flexibility regarding the time when the vehicles are available for charging

The methodology described in this chapter is based on the real UK driving pattern data, derived from a survey with large enough sample to represent the national-level driving statistics of light/medium size vehicles. The methodology itself employs a deterministic approach. Whilst this approach is appropriate at the UK system-level, it is not likely that it will realistically represent driving patterns in the smaller size distribution networks. In order to improve the methodology to deal with these cases as well, a probabilistic approach is required, which may be a part of future work.

CHAPTER 6. General conclusions and discussions

Main objective of this work is to investigate the potential benefits of utilization of Storage, DSR and EV as alternative means for enhancing the performance of electricity networks. To this end, a novel demand response and storage models are developed and incorporated in the existing OPF algorithms to estimate a magnitude of order of the potential value of these enabling technologies for alternative future development of the electricity system. One of the goals of this research is also to identify the key factors that drive the value of these technologies for network applications.

In this context, the developed models are validated through the systematic testing of the relevant transmission and distribution networks operation. It was demonstrated that the proposed models could be successfully applied to mitigate network congestion problems, improve the utilization of the existing network capacity, and maximize the system capability to employ renewable energy sources in systems with constrained capacities.

DSR model used in this work is based on a batch of shiftable appliances composed of washing machines, dish washers, and washing machines with tumble-dryer. The approach can be readily extended to other appliances as well. The selection of the appliances is based on their flexibility which in turn depends on consumer acceptance and willingness to participate in DSR. Household appliances form a significant part of the UK electricity consumption, with 10% of the total annual energy and with a peak of almost 14GW, making them a considerable potential to provide demand response.

6.1 Enhancement of transmission network performance

A novel methodology for the quantification of benefits of DSR and Storage in managing network congestion is presented. The methodology is supported by an algorithm where DSR and Storage are fully integrated into the network operation optimization, based on a multi-period OPF. The inter-temporal link between the demand reduction and demand recovery periods (for DSR) and energy charging and discharging (for Storage) is taken into account in the overall optimization process.

The methodology is applied to the GB transmission network, using a set of case studies to quantify the benefits of smart appliances and storage. Smart appliances are modelled based on data from appliance research work and available results from consumer surveys. The Storage model is a generic one and is not dependent on a specific technology. Technology specific characteristics and performance parameters can be relatively easily implemented as required.

The results obtained demonstrate that DSR contributes to reducing network congestion and facilitates the integration of wind generation to an existing network. The key drivers for the value of DSR are shown to be the amount of wind penetration to the network and the congestion levels. In addition, the penetration of controllable appliances and their specific characteristics, such as flexibility and energy consumption per cycle, play an important role on their value. This shows that the technology potential is highly dependent on consumer attitude. The results of the shifting algorithm presented are based on the diversified curves (profiles) obtained from a survey, reflecting the time of use for each type of device and which is used in the algorithm. However, the questions on the stochastic behaviour of the profiles, for example, what the consequences might be if the estimates were not accurate, as well as the questions on the responsibility of providing this data, collecting or aggregating the data, data reliability, whether the customers can get their control back, are not in scope of this work. The results obtained also suggest that the potential use of DSR is system-specific and depends on the load location, which restricts its capability to reduce the wind curtailment.

Similarly, the key drivers for the value of Storage are storage size and efficiency. The optimization model suggests the optimal location for storages, in order to achieve optimal operation cost.

The value of smart appliances and storage is the highest in the systems with no wind capacity installed. In such systems, the generation from expensive marginal gas generators is displaced with the production from less expensive coal generators. However, this replacement also means that carbon emissions are increased, since coal generators are greater emitters of CO_2 than gas generators. For the UK network, the capitalized value of DSR for no wind case is about £20 per appliance and about £400/MW to £700/MW of installed storage capacity. When there is wind generation installed in the system, the value of smart appliances drops to £10 to £15 per appliance and about £350/MW to £600/MW for Storage, whilst CO_2 emissions is reduced. With present values of the required hardware, infrastructure and maintenance costs of £(2-4)/appliance/year [67], investment in smart appliances for transmission network congestion management only is not economically viable. However, since it is high likely that these enabling technologies will not be used for congestion management only, but also for system balancing and other ancillary services, their instalment will be economically justified [67]. Similar conclusion applies to storage.

It was also shown that demand growth has a positive impact on the value of DSR and Storage. On the contrary for load growth, the flexibility of conventional generators has negative impact on the value of both DSR and Storage. This result is expected, since DSR and Storage flatten demand. With flexible generation, there is no need for such a service and the value of these facilities reduces. Both

DSR and Storage change demand profile in such a way to follow the wind. Storage is charged during periods of high wind and low demand. However, a possible conflict situations are identified when there is charging during peak demand. At transmission level this does not produce severe problems since transmission networks have relatively large capacity, but it might cause problems at distribution levels and this is a fact that must be taken into account when planning distribution networks. It was also noted that in the buses with large amount of wind generation installed and with relatively small load (in the case of GB network, such buses are located in the north) storage activity is mostly driven by wind. In contrast, in buses characterized with high demand (southern part of the GB network), storage activity is driven by both load and wind. Storage at busses with diverse generation mix facilitates reduction in generation of higher cost marginal generators and increase generation from lower cost generators. In northern and central part of the GB network the role of storage is focused on maximizing the utilization of the wind energy. The main conclusion is that the value per appliance for DSR and value per MW of Storage decrease as the number of appliances or installed storage capacity grows.

In general, storage exhibits several times better performances than DSR in all the parameters considered. There are two fundamental reasons for this: firstly, storage flexibility is much higher than the flexibility of smart appliances. Secondly, storage can be installed where it is needed whereas DSR is constrained to the demand centres. Direct comparison between smart appliances and storage is not performed as DSR penetration is defined by the number of appliances available for shifting, whilst storage is defined by MW of installed capacity.

6.2 Enhancement of distribution network performance

The developed storage and demand side response models are applied to provide distribution network support services, such as voltage and power flow control. It was demonstrated that the proposed approach facilitates active network management in terms of optimizing the existing network capacity utilization, deferring network reinforcement and improving power quality. Two storage optimization models are presented: in the first model, the storage size (energy capacity and power rating) and its location are specified. The second model optimizes size of storage and finds the best location for it. DSR and storage location models in AC networks are non-linear mixed integer optimization problems whose dimension depends on network size, and to get tractable solution commercial optimization software is used.

The developed methodology is applied to an 11kV feeder where the problems related to the lack of network capacity and under-voltages in distant buses emerge.

The benefits that smart appliances and storage bring to the network, as well as their value, are quantified using cost avoidance criteria. Compared are the network branches reinforcement costs without and with the enabling technologies in a period of 20 years. The analysis is made using present value method referring all the costs to the current year, in order to compare the costs that appear in different years in future. The obtained results suggest that the potential use of DSR and Storage is system-specific.

For this particular system, annualized value per device is found to be around 3.5 £/device/year which is comparable to the investment cost of £(2-4) £/device/year [67]. More flexible devices, in terms of shifting in time, exhibit higher DSR activity, as well as the devices with higher energy consumption per cycle. It was also shown that the number of actually shifted devices depends on their flexibility. This means, the higher the flexibility of a device, the higher the probability it would be used for managing network congestions.

As the under-voltage problems start from the most distant bus relative to the supplying point, the system is simulated with specified storage 200kW, 1.2MWh connected at that bus. This enables deferment in network assets investments for about five years, and the value of storage is almost £80/kW/year.

Optimal storage sizing (capacity and power) and location to maximally postpone investment in network reinforcement are also demonstrated. It is shown that storage can defer network reinforcement for about 14 years in this specific system, but this solution is not economically justified with present cost of battery technology.

Analysis of storage and DSR impact on network losses is also performed. It was shown that both Storage and DSR have beneficial impact on network losses. DSR tends to reduce network losses at all load levels, since in the presented shifting algorithm there are no losses associated with a device shifting. In contrast to DSR, storage exhibits network loss reduction only when load exceeds certain level. It was shown that storage will charge/discharge only when the energy losses reduction in the network is greater than the energy lost in the storage.

Another case study shows that reactive compensation, in addition to active power control significantly reduce sizing of the storage requirements and consequently the investment cost. This leads to the conclusion that energy storage can be a viable alternative for traditional network reinforcement options.

The general conclusions on storage and DSR can be summarized as follows:

- Both Storage and DSR may be successfully used to mitigate congestion problems in both transmission and distribution networks and for deferment of investments in network assets thus enhancing the utilization of the existing network capacity.
- Storage and DSR may successfully be employed to effectively control voltages and power flows in electricity networks, bringing benefits to the network operator.
- The value that DSR and storage bring to the system is very system-specific.
- DSR is relatively inexpensive per device and it is dispersed throughout the network, but also has drawbacks that it requires communication infrastructure and is less flexible than storage.
- Storage has more flexibility than DSR, but also has inherent energy losses and requires space and maintenance.
- The key driver for Storage value is, apart from storage size and efficiency, the location where storage is placed. In addition, with current cost of battery storage, the size of the storage must be carefully chosen.
- Reactive power compensation can significantly reduce required storage sizing in distribution networks.

6.3 Electric Vehicles

In this work a novel methodology for optimal charging of the electric vehicles to support network operation is presented. The methodology enables system peak reduction, enhanced network assets utilization and more efficient deployment of renewable energy resources. Real life driving statistics of the light/medium size vehicles is included in the EV driving patterns modelling. The network and EV constraints are modelled as a part of the multi-period DC OPF problem.

There is considerable flexibility regarding the time when light/medium size vehicles are available for charging and this can provide significant benefits to the operation of both distribution and transmission networks. This work does not explicitly consider vehicle-to-grid (V2G) applications (discharging car batteries to support the grid). By excluding explicit V2G concepts, the analysis provides conservative estimates regarding the benefits of incorporating EV demand response for real time network control.

In the analysis it was assumed that average driving patterns observed at the national level are statistically similar to those at the local level. From the national statistics data, it is concluded that there are on average two journeys a day. This is why the potential impact of driving patterns characterized with extensive commuting in the morning and making return journeys in the evening was analyzed. Based on that, five charging strategies are introduced and modelled:

- charging after first journey (in the morning),
- charging after second journey (in the afternoon),
- charging after both journeys (in the morning and in the afternoon),
- charging with minimum power all available time (all day except journey time),
- Optimal charging.

The model was tested on the IEEE 30 bus network. The obtained results confirm that the migration of the transport sector into electricity one will cause large problems in overloading network assets if the charging of electric vehicles is not performed in an intelligent way, since large peaks are observed.

In the case of non optimal charging this specific network has insufficient capacity to accommodate all envisioned electric vehicles. For each charging strategy, the number of vehicles that may be connected without jeopardizing network assets was calculated. It was demonstrated that with the prudent charging strategy it is possible to accommodate a much higher portion of the envisioned fleet without network assets reinforcements comparing to the non-intelligent strategies (in this specific example, smart charging enables to connect 3% more vehicles than envisioned).

When the wind generators were introduced to the network it was noticed that the optimal charging pattern followed the wind profile. This result is expected, considering the assumed zero cost of wind generation. In the case of non-optimal charging strategies, it was noted that wind curtailment and higher utilization of expensive peak generators resulted.

This work shows that if the transport sector is to be electrified, prudent charging schemes must be developed, or else the existing networks have to be significantly reinforced. This transfer from using vehicles with internal combustion engines to immense deployment of electric vehicles will not be abrupt. Therefore, it leaves enough time to develop wise charging strategies and implement them in the upcoming electric vehicle models. The work presented in this thesis exhibits an effort in this direction. However, massive uptake of EV into electricity sector will be unlikely without establishing appropriate ICT infrastructure facilitated with smart meters.

6.4 Future work

Some possible directions regarding future work are as follows:

Thermal demand modelling: As mentioned above, a large scale electrification of the heat sector is expected in near future. Hence, the work to be done in this area includes thermal load modelling, such as heat pumps, ventilation and air conditioning. The prospective model must be accurate

enough to capture thermodynamics of the buildings as well as interactions between heat source, building and environment. Such models are described with differential equations of higher orders and as such are not suitable for applications in network operation models. Thus the trade-off between the thermal models complexity and tractability of the solution in network control and investment optimisation algorithms must be achieved, which will be the main effort of the future research. Modelling of heat storage would also be a part of this work.

Modelling the uncertainty – stochastic programming: The major challenge in this area is to model the uncertainty in various driving parameters such as energy prices, demand profiles and wind availability in the context of real time optimisation of active distribution networks. Such a problem is of huge complexity and the approach should exploit variance reduction methods to achieve acceptable tractability of the solution.

Development of distribution planning methodology taking into account DSR and storage: The main challenge is to coordinate long-term investment strategy in network assets and short-term operational decisions in the context of real time network control. The methods must be capable to determine optimal size, location and operating strategy of storage technologies to enhance the utilisation of existing distribution network capacity and to minimise future network reinforcement. The network security considerations are required in this kind of analysis, making the problem complex and large. To this end, alternative decomposition concepts such as Benders decomposition must be explored.

Literature

1. **The UK Renewable Energy Strategy**, Secretary of State for Energy and Climate Change, www.decc.gov.uk
2. **Benefits of Advanced Smart Metering for Demand Response based Control of Distribution Networks**, Summary Report, Imperial College London, March 2010.
3. J.Matevosyan: **Wind power integration in power systems with transmission bottlenecks**, IEEE Power Engineering Society (PES) General Meeting, Tampa, Florida, 2007.
4. Uhlen,K. et al.: **A Probabilistic Security Criterion for Determination of Power Limits in a Deregulated Environment**, CIGRE Sessions, Paris, France, 2000.
5. O.Breidablik et al.: **Innovative Measures to Increase the Utilization of Norwegian Transmission**, IEEE Power Tech Conference, Bologna, Italy, 2003.
6. D.Douglas: **Can Utilities Squeeze More Capacity out of the Grid?**, Transmission and Distribution World, 2003, pp. 38-43, available at: www.tdworld.com
7. J.Matevosyan and L.Soder: **Short-term Hydropower Planning Coordinated with Wind Power in Areas with Congestion**, Wind Energy, 10(3), 2007, pp. 44-47.
8. G.Ault et al.: **Calculation of Economic Transmission Connection Capacity for Wind Generation**, IET Renewable Power Generation, 1(1), pp. 61 - 69, 2007.
9. A.Shafiu et al.: **Active management and protection of distribution networks with distributed generation**, IEEE Power Engineering Society (PES) General Meeting, pp.1098-1103 Vol.1, June 2004
10. P.Djapic et al.: **Taking an Active Approach**, IEEE Power and Energy, Magazine, July/August 2007, pp. 68-77
11. **The Power to Choose – Demand Response in liberalised electricity markets**, International Energy Agency (IEA) Publications, 2003
12. **Demand Management Activities Applicable to Electricity Networks**, a report for Demand Management and Planning Project, by NSW Department of Infrastructure, Planning and Natural Resources, EnergyAustralia and TransGrid, February 2004.
13. **Modern Grid Benefits**, National Energy Technology Laboratory report for the U.S. Department of Energy, Office of Electricity Delivery and Energy Reliability, August 2007.
14. A.G.Martins: **Energy-conscious Urban Planning and Development - lessons from a case-study**, Proc. of the 1999 European Council for an Energy-Efficient Economy (ECEEE) Summer Study, Mandelieu, France, panel IV,07, June, 1999.

15. S.H.Lee, C.L.Wilkins: **A practical approach to appliance load control analysis: a water heater case study**, IEEE Trans. on Power Apparatus and Systems, Vol. PAS-102, No.4, April 1983, pp. 1007-1013
16. C.N.Kurucz, et al.: **A linear programming model for reducing system peak through customer load control program**, IEEE Trans. on Power Systems, Vol. 11, No. 4, Nov. 1996, pp. 1817-1824
17. J.Chen at al.: **Scheduling direct load control to minimize system operational cost**, IEEE Trans. on Power Systems, Vol. 10, No. 4, November 1995, pp. 1994-2001
18. W.Chen Chu at al.: **Scheduling of direct load control to minimize load reduction for utility suffering from generation shortage**, IEEE Trans. on Power Systems, Vol. 8, No. 4, November 1993, pp. 1525-1530
19. K.H.Ng, G.Sheble: **Direct load control – a profit-based load management using linear programming**, IEEE Trans. on Power Systems, Vol. 13, No. 2, pp. 688-694, May 1998
20. B.Fox et al.: **Scheduling of radio-controlled heating load**, Generation, Transmission and Distribution, IEE Proceedings, vol.145, no.6, pp.641-646, Nov 1998
21. A.I.McCartney: **Load management using radio teleswitches within NIE**, Power Engineering Journal , vol.7, no.4, pp.163-169, Aug 1993
22. G.Heffner: **Independent Review of Estimated Load Reductions for the PJM's Small Customer Load Response Pilot Project**, Ernest Orlando Lawrence Berkley National Laboratory, May 2004
23. M.L.Chan: **Interrelation of distribution automation and demand-side management**, Rural Electric Power Conference, pp.B1/1-B1/6, 28-30 Apr 1991
24. H.L.Smith: **DA/DSR directions. An overview of distribution automation and demand-side management with implications of future trends**, Computer Applications in Power, IEEE , vol.7, no.4, pp.23-25, Oct. 1994
25. D.Westermann, A.John: **Demand Matching Wind Power Generation With Wide-Area Measurement and Demand-Side Management**, IEEE Transactions on Energy Conversion, vol.22, no.1, pp.145-149, March 2007
26. E.Veldman et al.: **Technical benefits of distributed storage and load management in distribution grids**, IEEE PowerTech, Bucharest, pp.1-8, 2009
27. V.Stanojevic et al.: **Application of Storage and Demand Side Management to Support the Integration of Intermittent Distributed Generation**, 20th International Conference on Electricity Distribution (CIRED), Prague, June 2009

28. V.Silva et al.: **Storage and DSR Benefits in Transmission Congestion Management in Systems with High Wind Penetration**, 7th International Workshop on Large Scale Integration of Wind Power and on Transmission Network for Offshore Wind farms, Madrid, 2008
29. E.Shayesteh et al.: **A demand side approach for congestion management in competitive environment,** European Transaction on Electric Power, vol. 20, pp. 470–490, May 2010
30. C.Ibars et al.: **Distributed Demand Management in Smart Grid with a Congestion Game**, 1st IEEE International Conference on Smart Grid Communications (SmartGridComm), pp.495-500, October 2010
31. International Hydropower Association, www.hydropower.org
32. **Energy storage - Packing some power**, The Economist, 03 March 2011
33. http://en.wikipedia.org/wiki/List_of_pumped-storage_hydroelectric_power_stations
34. H.Bindner, P.Lundsager: **Integration of wind power in the power system,** Industrial Electronics Society (IECON), IEEE 28th Annual Conference, pp. 3309- 3316 vol.4, 5-8 Nov. 2002
35. M. Black, G.Strbac: **Value of Bulk Energy Storage for Managing Wind Power Fluctuations**, IEEE Transactions on Energy Conversion, Vol.22, No.1, pp. 197-205, March 2007
36. S.Derk: **Compressed Air Energy Storage in an Electricity System With Significant Wind Power Generation**, IEEE Transactions on Energy Conversion, vol.22, no.1, pp.95-102, March 2007
37. M. Black et al.: **The role of storage in integrating wind energy**, Future Power Systems Conference, Amsterdam, 2005
38. D.Rastler: **Electricity Energy Storage Technology Options: A White Paper Primer on Applications, Costs and Benefits**, Electric Power Research Institute (EPRI), Palo Alto, California, 2010
39. M.S.Habibi: **Model for impact of storage on spinning reserve requirements and distributed generation**, 33rd South-eastern Symposium on System Theory, pp.161-165, March 2001
40. M.W.Tsang, D.Sutanto: **Power system stability improvement using energy storage with fuzzy logic controller**, Advances in Power System Control, Operation and Management, (APSCOM 2000) International Conference, pp. 322-326 vol.2, Hong Kong, 2000

41. J.Svensson et al.: **Improved power system stability and reliability using innovative energy storage technologies**,, 8th IEE AC and DC Power Transmission, pp. 220-224, March 2006
42. N.Hatziargyriou et al.: **Impact of Energy Storage in the secure and economic operation of a small island**, Mediterranean Power Conference, Cyprus, Nov. 2004
43. M.Aktarujjaman et al.: **Black start with DFIG based distributed generation after major emergencies**, Power Electronics, Drives and Energy Systems Conference, (PEDES '06), pp.1-6, Dec. 2006
44. P.Denholm, R.Sioshansi: **The value of compressed air energy storage with wind in transmission-constrained electric power systems**, Energy Policy, Volume 37, Issue 8, pp. 3149-3158, August 2009
45. A.F.K.Kamga et al.: **Congestion management in transmission systems with large scale integration of wind energy**, Integration of Wide-Scale Renewable Resources Into the Power Delivery System, CIGRE/IEEE PES Joint Symposium, July 2009
46. G.Koeppel et al.: **Value of storage devices in congestion constrained distribution networks**, Power System Technology Conference (PowerCon) Vol.1, pp. 624-629, Singapore, Nov. 2004
47. G.Celli et al.: **Optimal integration of energy storage in distribution networks**, IEEE PowerTech Conference, pp. 1-7, Bucharest , 2009
48. **Smart Grid Technologies**, Pike Research report, December 2010
49. J.P.Voronov: **Upgrading of Power Grids as a real prospect of reviving industry in Russia**, (in Russian), EKO – Economical Journal, Novosibirsk, April 2001, http://econom.nsc.ru/eco/arhiv/ReadStatiy/2011_04/072Voronov2011_04.pdf
50. **Miami proposes to lead the nation in energy efficiency with $200 million Smart Grid initiative** – Mayor Manuel A. Diaz, News Release, available at: www.energysmartmiami.com
51. **GE Smart Meters Make UK Community More Energy Efficient**, Reuters, 02-06-2011, http://uk.reuters.com/article/2011/06/02/idUS122850+02-Jun-2011+BW20110602
52. **Swedish Utility to Install 90,000 GE Smart Meters**, Transmission and Distribution World, Jun 10, 2009.
53. **The Home Appliance Industry's Principles & Requirements for Achieving a Widely Accepted Smart Grid**, AHAM Smart Grid White Paper, Washington, December 2009.
54. **2010 Sustainability Report,** Whirlpool Corporation, 2010
55. www.smartgridnews.com, published on 9 March 2011

56. **GE Targets Net Zero Energy Homes by 2015**, published on 14 July 2009, available at: www.genewscenter.com
57. www.smart-energy-alliance.com
58. www.smartgridnews.com
59. www.abb.co.uk
60. www.london.gov.uk
61. Y.Makarov at al.: **Optimal size of energy storage to accommodate high penetration of renewable resources in WECC syste,**" Innovative Smart Grid Technologies (ISGT), pp.1-5, 19-21 Jan. 2010
62. I.Cobelo: **Active control of Distribution Networks**, PhD thesis, The University of Manchester, UK, 2005.
63. T.Gönen: **Electric Power Distribution System Engineering**, 2nd Edition, CRC Press, Boca Raton, Florida, 2008.
64. S.Gyamfi et al.: **Pattern Recognition Residential Demand Response: An Option for Critical Peak Demand Reduction in New Zealand**, Univ. of Canterbury Research Repository, New Zealand, 2010.
65. W.Mert et al.: **Consumer Acceptance of Smart Appliances**, European Communities, Brussels, 2008; available at: www.smart-a.org
66. R.Stamminger et al.: **Synergy Potential of Smart Appliances**, report for SMART-A project (Smart Domestic Appliances in Sustainable Energy Systems), University of Bonn, June 2007.
67. V.Silva: **Value of flexibility in systems with large wind penetration**, PhD Thesis, Imperial College London, 2010.
68. G. Strbac: **Demand side management: Benefits and challenges**, Energy Policy, vol. 36, no. 12, pp. 4419–4426, 2008.
69. A.Gomes et al.: **Physically-based load demand models for assessing electric load control actions**, PowerTech, 2009 IEEE Bucharest , pp.1-8, June 28 - July 2, 2009
70. V.Silva et al., **Value of Smart Domestic Appliances in Stressed Electricity Networks**, SMART-A report, Imperial College London and Univ. of Manchester, September 2009
71. D.P.Kothari, I.J.Nagrath: **Modern Power System Analysis**, 3rd Edition, Tata McGraw-Hill, New Delhi, 2003
72. A.Wood, B.Wollenberg: **Power Generation, operation and Control**, 2nd Edition, John Wiley and Sons, New York, 1996
73. **Great Britain Seven Year Statement**, National Grid, UK, NGET, 2007

74. Q.Zhou, P.Plumptre, **Annex to Section 2.3 of DTIM User Report**, National Grid, UK, 2009
75. F.Birol: **Power to the People**, International Atomic Energy Agency (IAEA), Bulletin 46/1, June 2004, pp. 9-12
76. **Digest of the United Kingdom Energy Statistics 2011**, Chapter 5: Electricity, Department of Energy and Climate Change (DECC), UK, 2011
77. G.Owen et al. : **GB Electricity Demand – realising the resource, Paper 1: GB Electricity Demand – Context and 2010 Baseline Data**, Sustainability First, UK, October 2011
78. J. Grainger, W. Stevenson: **Power System Analysis**, International Editions, McGraw-Hill, Singapore, 1994
79. D.Pudjianto: **Optimisation of Transmission System Investment and Operation Including Evaluation of VAr Support Contracts In Competitive Electricity Market**, PhD Thesis, The University of Manchester, 2003.
80. L.H. Walker: **Battery Storage Plants**, Wiley Encyclopedia of Electrical and Electronics Engineering, (Ed: J.G.Webster), Vol.2, pp. 233-250, John Wiley & Sons Inc., 1999.
81. A.A.Thatte, M.D.Ilic: **An assessment of reactive power/voltage control devices in distribution networks** Power Engineering Society General Meeting*, 2006.* doi: 10.1109/PES.2006.1709592
82. B.Kirby, E.Hirst: **Ancillary Service Details: Voltage Control**, Oak Ridge National Laboratory, Oak Ridge, Tennessee, Nov. 1997.
83. http://www.fico.com/en/Products/DMTools/Pages/FICO-Xpress-Optimization-Suite.aspx
84. **Xpress-SLP User Guide**, Version 1.12, May 2003, in PDF format, available from http://www.fico.com/en/Products/DMTools/Pages/FICO-Xpress-Optimization-Suite.aspx
85. **IFI/RPZ Annual Report**, April 2009 to March 2010 Inclusive, available at: http://www.ukpowernetworks.co.uk/wcmqs/products-services/networks/pdf/edfen_ifi_annual_report_2010_pdf.pdf
86. M.J. Heathcote: **The J & P Transformer Book: A practical Technology of the Power Transformer**, 12th edition, Newnes, Oxford, UK, 1998.
87. **National Grid: GB Seven Year Statement 2010**, Chapter 2, available at http://www.nationalgrid.com/uk/Electricity/SYS/archive/sys10
88. H.Lee Willis: **Power Distribution Planning Reference Book**, Marcel Dekker Inc., New York, 1997
89. **ABB launches SVC Light® with Energy Storage**, ABB Press Release, 29 April 2010,

90. **Electricity Distribution Price Control Review Final Proposals - Allowed revenue - Cost assessment appendix**, Ofgem, December 2009, available online at: www.ofgem.gov.uk
91. **Engineering Recommendation P2/6 – Security of supply**, Energy Networks Association (ENA), July 2006
92. **Load Profiles and Their Use in Electricity Settlement**, Elexon, 2011, available at: http://www.elexon.co.uk/wp-content/uploads/2012/01/load_profiles.pdf
93. D.Rastler: **Electricity Energy Storage Technology Options**, EPRI, Palo Alto, USA, 2010.
94. http://en.wikipedia.org/wiki/Government_incentives_for_plug-in_electric_vehicles
95. http://inventors.about.com/od/estartinventions/a/History-Of-Electric-Vehicles.htm
96. K.G. Høyer: **The history of alternative fuels in transportation: The case of electric and hybrid cars**, Utilities Policy, Vol. 16, No. 2., 2008, pp. 63-71
97. http://en.wikipedia.org/wiki/La_Jamais_Contente
98. http://en.wikipedia.org/wiki/Energy_crisis
99. H.Franssen: **Behind the Gas Pump, Implications of our Dependence on Mideast Oil U.S. Oil, Security, and National Energy Policy, Realities and Disconnects**, International Energy Associates, from a presentation at the University of Houston, 17 January, 2003.
100. S.Weart: **The discovery of global warming**, Harvard University Press, 2003.
101. R.Gorham: **Air Pollution from Ground Transportation: an assessment of causes, strategies and tactics, and proposed actions for the international community**, United Nations, Department of Economic and Social Affairs, Division for Sustainable Development, 2002
102. T. Soubbotina, K.Sheram: **Beyound Economic Growth – Meeting the Challenges of Global Development**, Chapter 10, The World Bank, Washington, USA, 2000.
103. **Technology Roadmap: Electric and plug-in hybrid electric vehicles**, International Energy Agency (IEA)/OECD, June 2011
104. J.Tomić, W.Kempton: **Using fleets of electric-drive vehicles for grid support**, Journal of Power Sources, Volume 168, Issue 2, Pages 459-468, June 2007
105. Y.Sugii et al.: **A genetic-algorithm based scheduling method of charging electric vehicles,** IEEE International Conference on Systems, Man, and Cybernetics (SMC '99), vol.4, pp.435-440, 1999
106. C.Hutson et al: **Intelligent Scheduling of Hybrid and Electric Vehicle Storage Capacity in a Parking Lot for Profit Maximization in Grid Power Transactions**," IEEE Energy 2030 Conference, , pp.1-8, Nov. 2008

107. **Investigation into the Scope for the Transport Sector to Switch to Electric Vehicles and Plugin Hybrid Vehicles**, Department for Business, Enterprise and Regulatory Reform (BERR) and Department for Transport (DfT), UK, 2008
108. P. Papadopoulos et al.: **Predicting Electric Vehicle impacts on residential distribution networks with Distributed Generation**, Vehicle Power and Propulsion Conference (VPPC), 2010 IEEE , pp.1-5, Sept. 2010
109. G.A.Putrus et al.: **Impact of electric vehicles on power distribution networks**, Vehicle Power and Propulsion Conference, 2009. VPPC '09. IEEE , pp.827-831, 7-10 Sept. 2009
110. S.Acha et al.: **Optimal charging strategies of electric vehicles in the UK power market**, Innovative Smart Grid Technologies (ISGT), IEEE PES, pp.1-8, Jan. 2011
111. **National Travel Survey Database 2008**, Department for Transport, UK, 2009
112. H.Lund, W.Kempton: **Integration of Renewable Energy into the Transport and Electricity Sectors through V2G**, Energy Policy (2008), doi:10.1016/j.enpol.2008.06.007
113. **Vehicle Licensing Statistics: 2008, National Statistics Bulletin**, Department for Transport, UK, 2009
114. **Strategies for the uptake of electric vehicles and associated infrastructure implications for The Committee on Climate Change**, Final Report October 2009, Element Energy Ltd, Cambridge, UK, 2009
115. W. Kempton et al.: **Vehicle-to-Grid Power: Battery, Hybrid, and Fuel Cell Vehicles as Resources for Distributed Electric Power in California**, Davis, CA. Institute for Transportation Studies Report # UCD-ITS-RR-01-03, June, 2001.
116. D.Gayme, U.Topcu: **Optimal power flow with distributed energy storage dynamics**, American Control Conference (ACC), 2011 , pp.1536-1542, June 29 -July 1, 2011

APPENDICES

APPENDIX 1. Node Power Injections

The complex vector of current injections for the whole network is given as:

$$\underline{\mathbf{I}} = [\underline{\mathbf{Y}}] \cdot \underline{\mathbf{V}} \tag{A1.1}$$

where:

$\underline{\mathbf{I}}$ - the complex vector of current injections into the nodes of the network

$[\underline{\mathbf{Y}}]$ - Y-bus matrix of the network (this matrix is the inverse of the Z-bus matrix)

$\underline{\mathbf{V}}$ - complex vector of nodes' voltages

Now, the power injection in node i can be calculated as $\underline{S_i} = \underline{V_i} \underline{I_i^*}$, or in the form which will be simpler to use:

$$\underline{S_i^*} = P_i - jQ_i = V_i^* \underline{I_i} \tag{A1.2}$$

Taking into the account previous matrix equation, one gets:

$$\underline{S_i^*} = V_i^* \underline{I_i} = \underline{V_i^*} \cdot \sum_{j \in \mathbf{N_G}} \underline{Y_{ij}} \underline{V_j} = \sum_{j \in \mathbf{N_G}} \underline{V_i^*} \underline{Y_{ij}} \underline{V_j} = \sum_{j \in \mathbf{N_G}} V_i V_j e^{-j\delta_{ij}} \left(G_{ij} + jB_{ij}\right) \tag{A1.3}$$

Transforming the Euler's notation of a complex number into trigonometric one, previous equation becomes:

$$\begin{aligned} \underline{S_i^*} &= \sum_{j \in \mathbf{N_G}} V_i V_j \left(\cos \delta_{ij} - j \cdot \sin \delta_{ij}\right)\left(G_{ij} + jB_{ij}\right) \\ &= P_i - jQ_i = \sum_{j \in \mathbf{N_G}} V_i V_j \left[\left(G_{ij} \cos \delta_{ij} + B_{ij} \sin \delta_{ij}\right) + j\left(B_{ij} \cos \delta_{ij} - G_{ij} \sin \delta_{ij}\right)\right] \end{aligned} \tag{A1.4}$$

Active and reactive injections are now obtained by separating real and imaginary parts of previous equation:

$$\begin{aligned} P_i &= \sum_{j \in \mathbf{N_G}} V_i V_j \left(G_{ij} \cos \delta_{ij} + B_{ij} \sin \delta_{ij}\right) \\ Q_i &= \sum_{j \in \mathbf{N_G}} V_i V_j \left(G_{ij} \sin \delta_{ij} - B_{ij} \cos \delta_{ij}\right) \end{aligned} \tag{A1.5}$$

APPENDIX 2. Diversified Curve Disaggregating

Equation (1) actually represents the system of linear equations which can be written in a compact matrix form. As an example, for a device having the operation cycle duration of 4 time steps, and for time horizon containing 24 time steps, the matrix form of (1) is given in Figure A. 2-1.

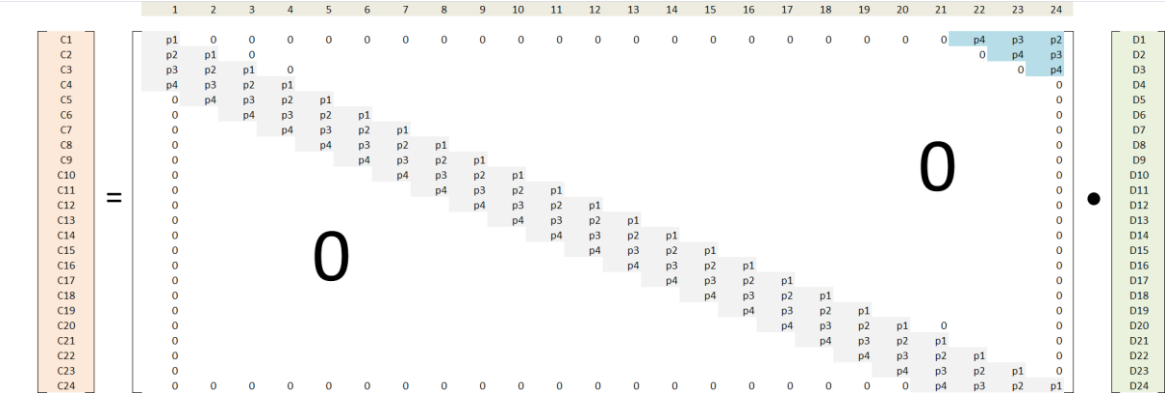


Figure A. 2-1: Matrix representation of the linear system equations (1)

On the left-hand side of the matrix equation, given in Figure A. 2-1, there is a vector-column of values $\boldsymbol{C_t}$ obtained from diversified curve (Figure 2-2, left-hand side charts). On the right-hand side there is a matrix product of the operation cycle matrix and the vector of unknown number of connected devices. The operation cycle matrix is a diagonal matrix with non-zero elements on the main diagonal and on the sub-main diagonals beneath it. The number of sub-main diagonals containing the consumption pattern data is defined by operation cycle duration. If diversified curve has a value different from 0 at the first time step, then the consumption pattern matrix will have values different from 0 in the upper right corner. It is shown by the shaded upper right corner of the matrix in Figure A. 2-1. It reflects the fact that the power consumed at the beginning of the day will consist of the power of the devices starting their consumption at the beginning of the day, and also of the devices which have started their consumption the day before, i.e. in the last time steps of the previous day. In this example, the consumption of all devices of this type at time step 1 is given by:

$$C_1 = D_1 \cdot p_1 + D_{24} \cdot p_2 + D_{23} \cdot p_3 + D_{22} \cdot p_4$$

where:

D_1 – number of devices starting their consumption at time step 1 of the present day

D_{24} – number of devices starting their consumption at time step 24 of the previous day

D_{23} – number of devices starting their consumption at time step 23 of the previous day

D_{22} – number of devices starting their consumption at time step 22 of the previous day

APPENDIX 3. 16 Bus GB Transmission System

A3.1. Generation installed capacity for GB 16 Bus System

Table A. 3-1: Distribution of generation installed capacity on network buses and generation types

Generation technology	Production cost	CO_2 emissions	Installed capacity [MW]																Total MW
			Bus number																
	£/MWh	kg/MWh	1	2	3	4	5	6	7	8	9	10	11	12	13	14	15	16	
wind[15]	0	0	5502	606	373	650	113	4933	2224	0	1008	2489	919	630	1182	0	1843	3626	26098
nuclear	20	0	0	0	0	0	0	1200	3613	0	0	0	0	1200	0	0	0	0	6013
marine	10	0	260	0	0	0	0	50	50	0	0	0	250	0	0	0	0	0	610
gas	30	390	0	1100	0	0	0	0	1020	0	1218	1100	2172	0	3385	905	1290	3005	15195
coal	35	700	0	0	0	0	1152	0	0	0	2000	6751	821	0	2478	0	3200	0	16402
other renewable	60	0	0	0	0	0	45	45	100	0	100	136	350	0	0	0	0	0	776
water	10	0	542	0	321	233	0	33	0	0	0	0	0	0	0	0	0	0	1129
marginal gas	90	390	10	436	0	0	123	120	2080	0	1285	3553	0	0	1108	0	2305	5905	16925
marginal coal	100	700	0	0	0	0	1152	0	0	0	0	1947	821	0	2478	0	0	0	6398
peakers	300	780	0	0	0	0	0	0	3229	0	665	168	81	0	519	140	1000	1030	6832
Total [MW]			6314	2142	694	883	2585	6381	12316	0	6276	16144	5414	1830	11150	1045	9638	13566	96378

[15] these values correspond to 20% of wind penetration

A3.2. Sensitivity regarding DSR Flexibility and Storage Efficiency

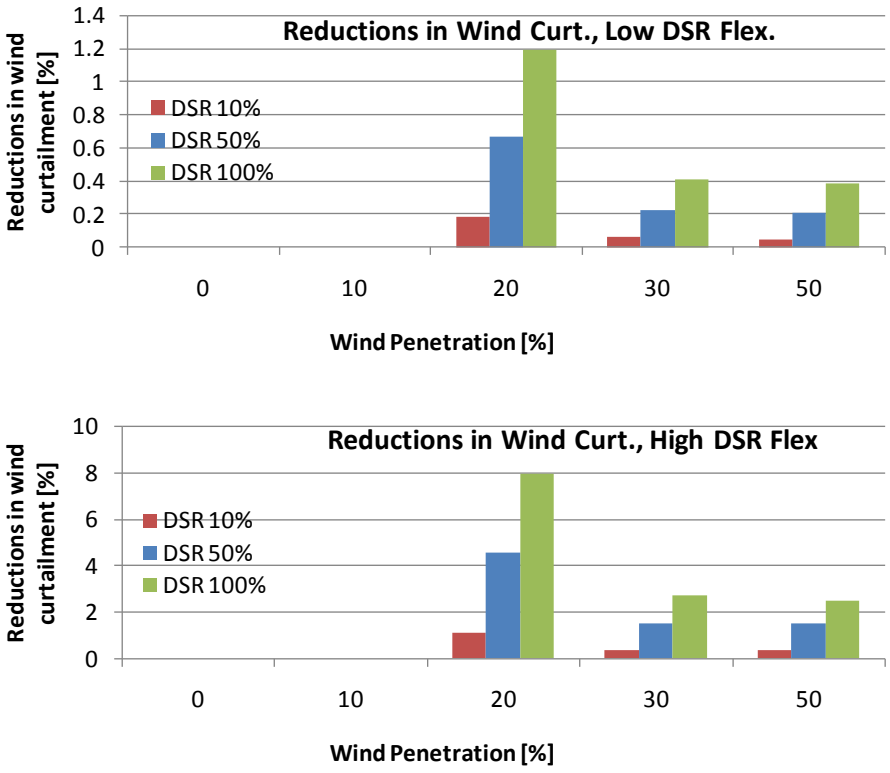


Figure A. 3-1: Effect of DSR flexibility on reduction in wind curtailment

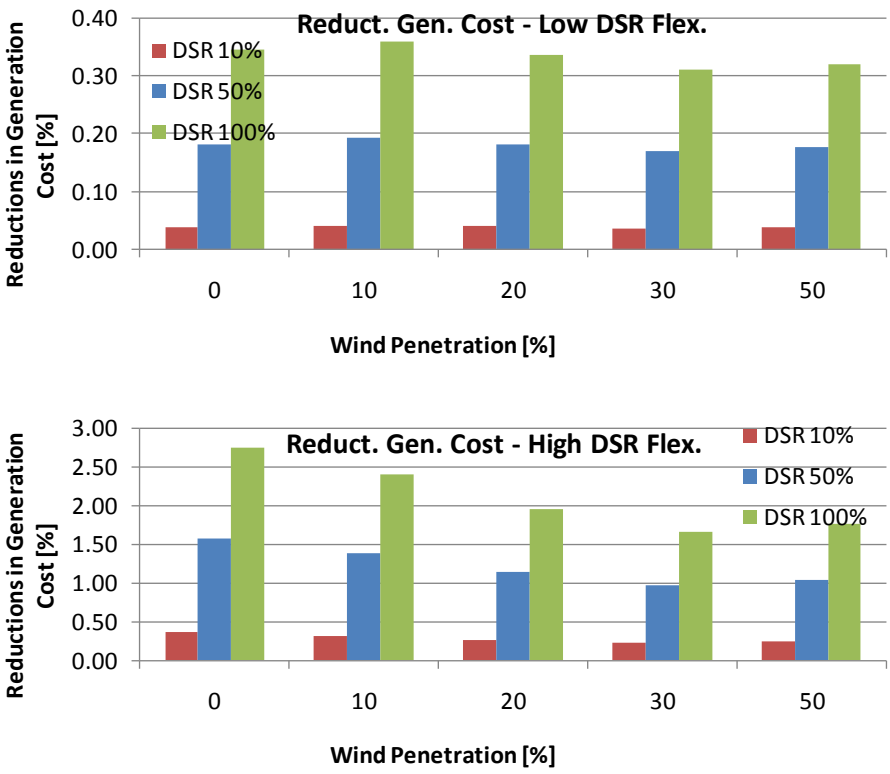


Figure A. 3-2: Effect of DSR flexibility on reduction in generation costs

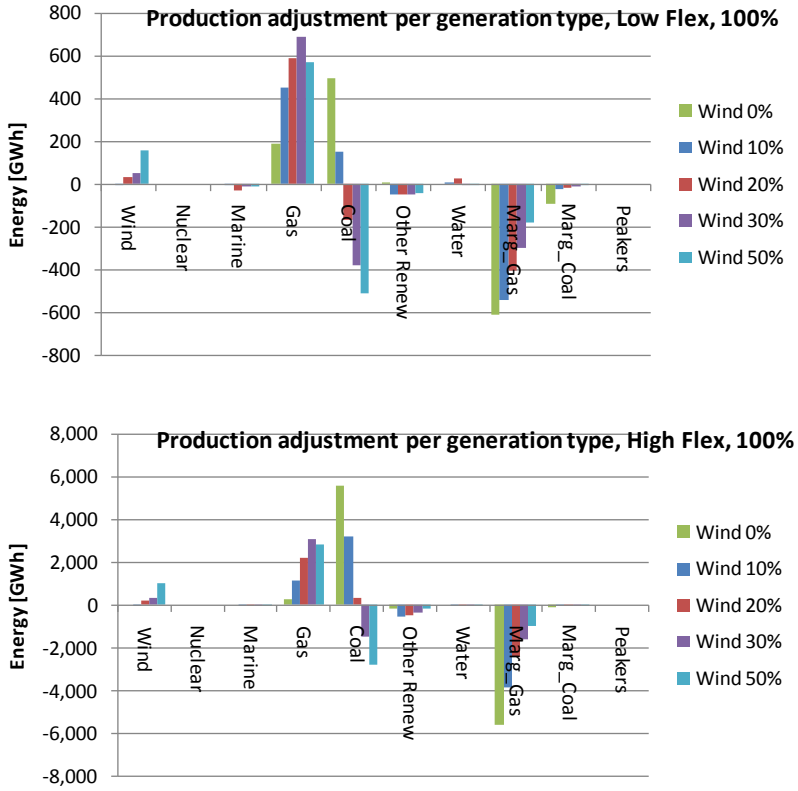


Figure A. 3-3: Effect of DSR flexibility on Generation adjustment

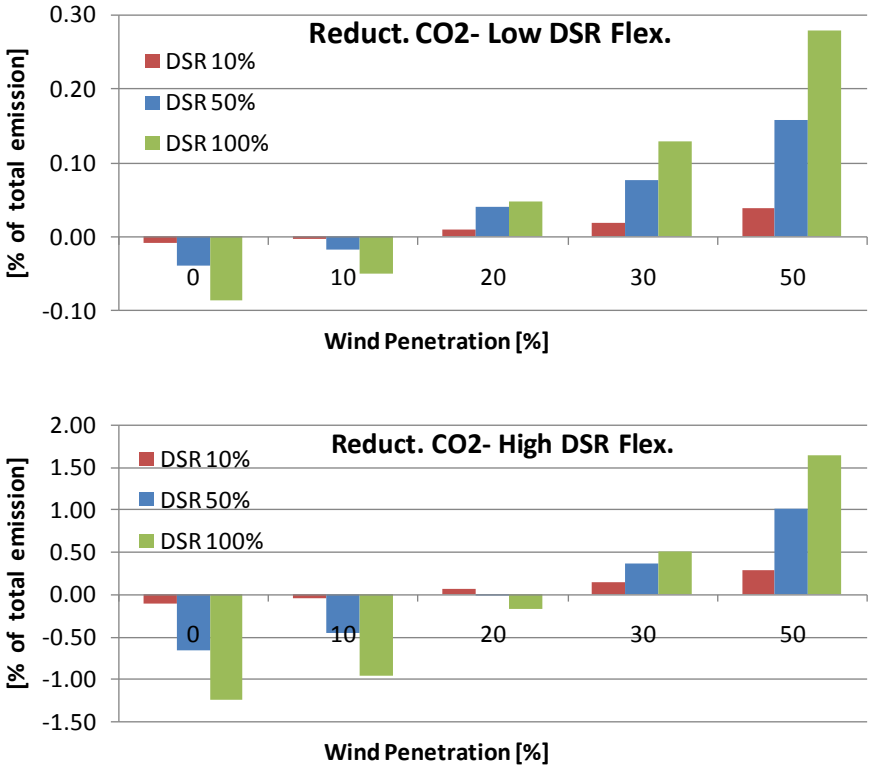


Figure A. 3-4: Effect of DSR flexibility on reduction in CO_2 emissions

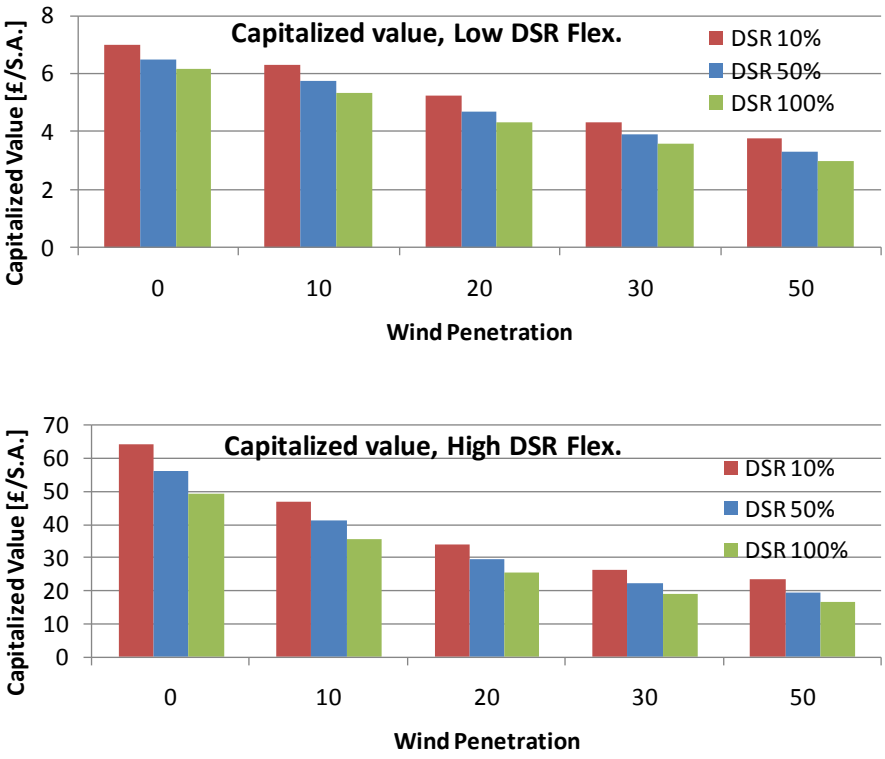


Figure A. 3-5: Effect of DSR flexibility on average capitalized value per appliance

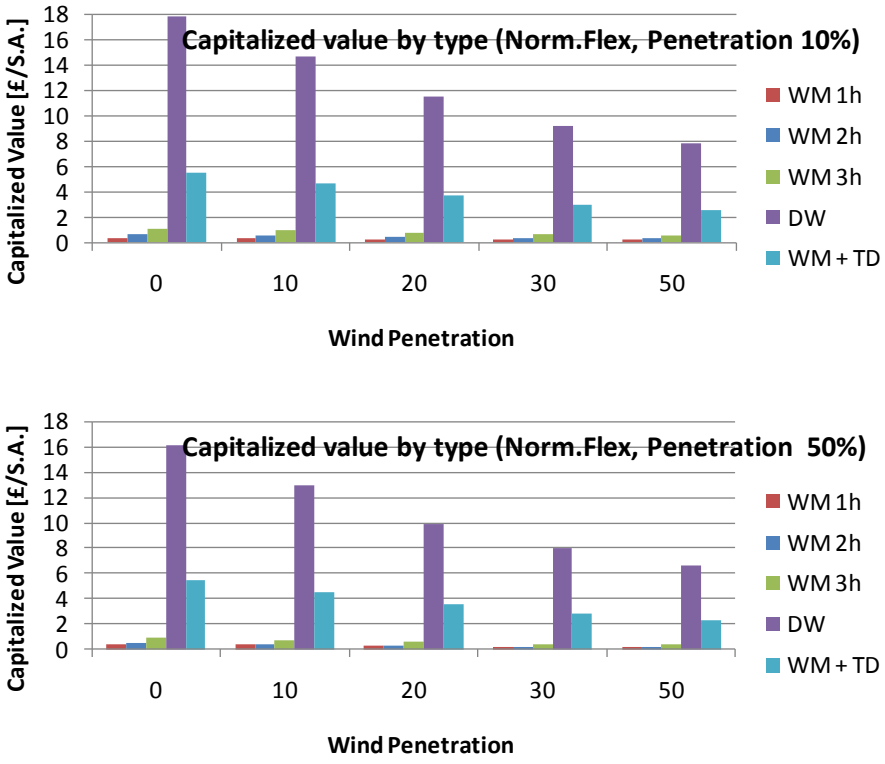


Figure A. 3-6: Effect of DSR flexibility on capitalized value per type of device

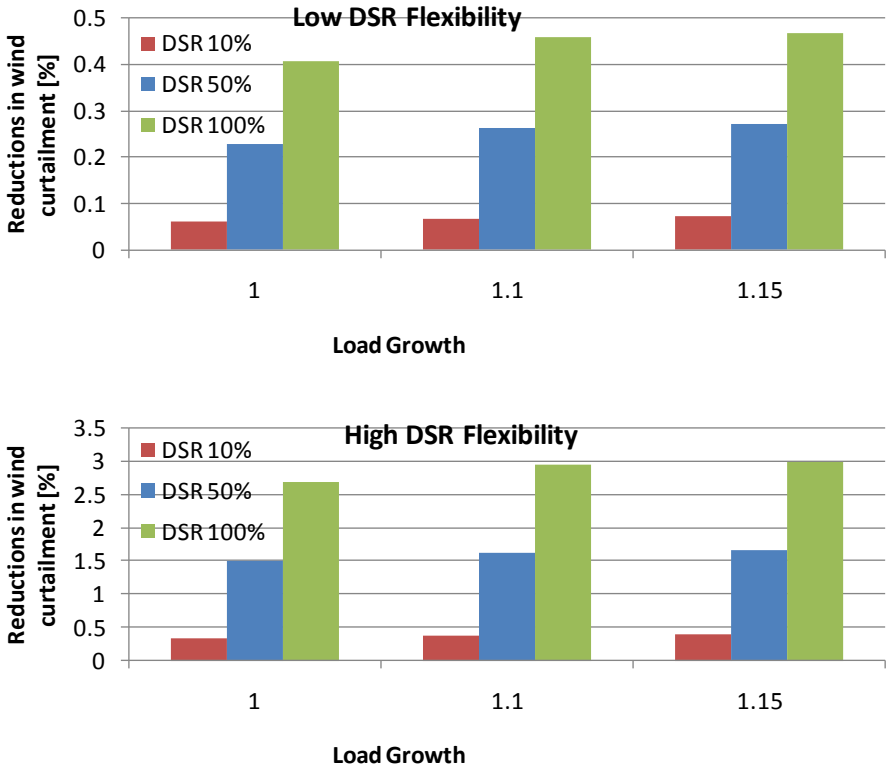


Figure A. 3-7: Effect of DSR flexibility on reduction in wind curtailment as load increases

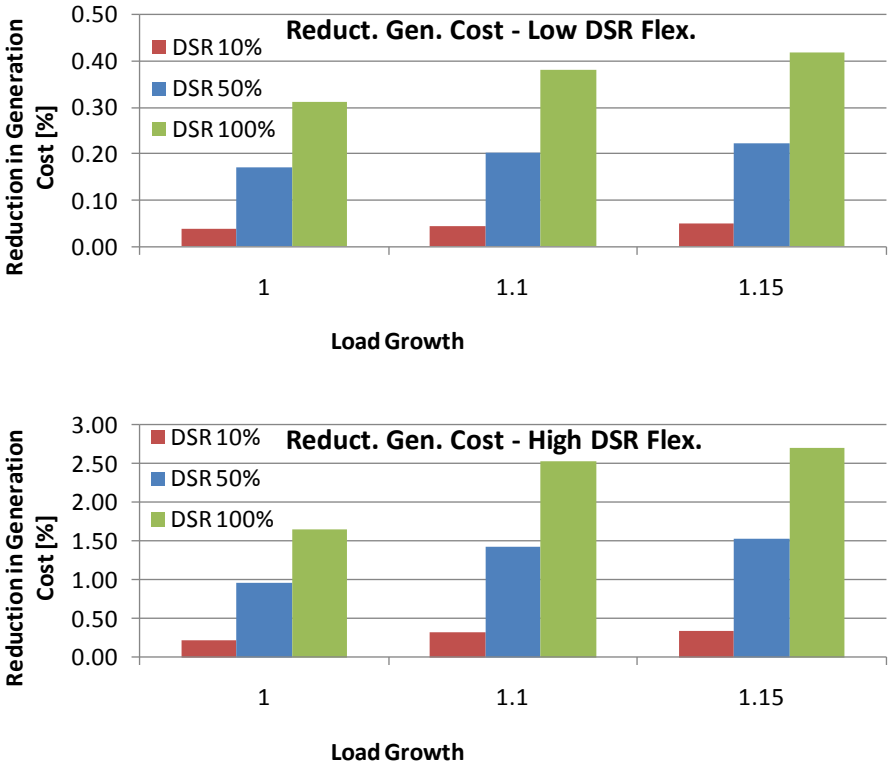


Figure A. 3-8: Effect of DSR flexibility on reduction in generation cost as load increases

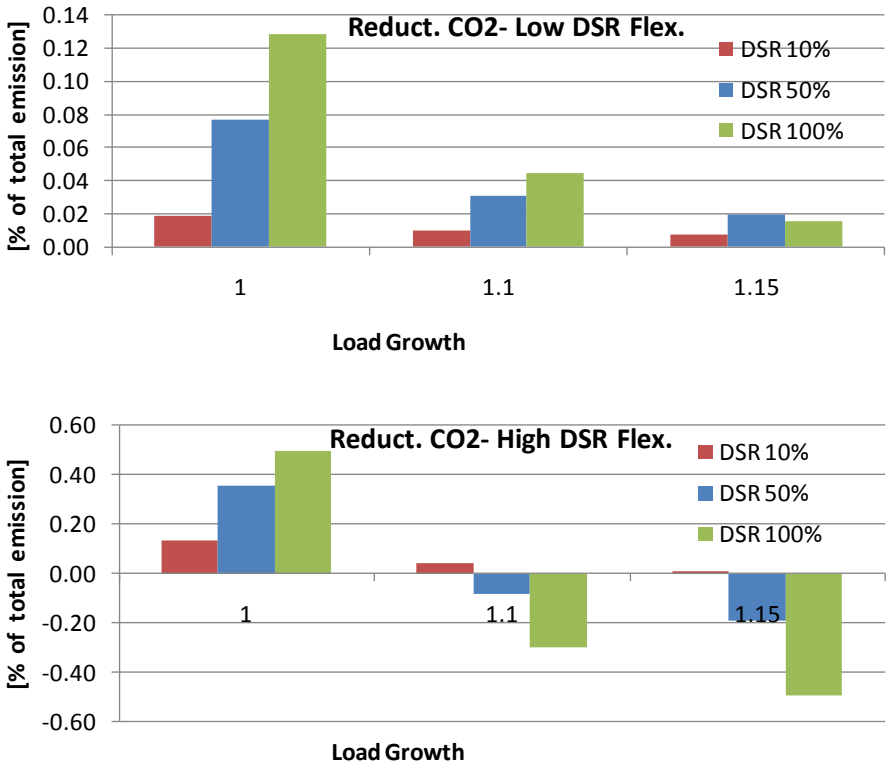


Figure A. 3-9: Effect of DSR flexibility on reduction in CO_2 emissions as load grows

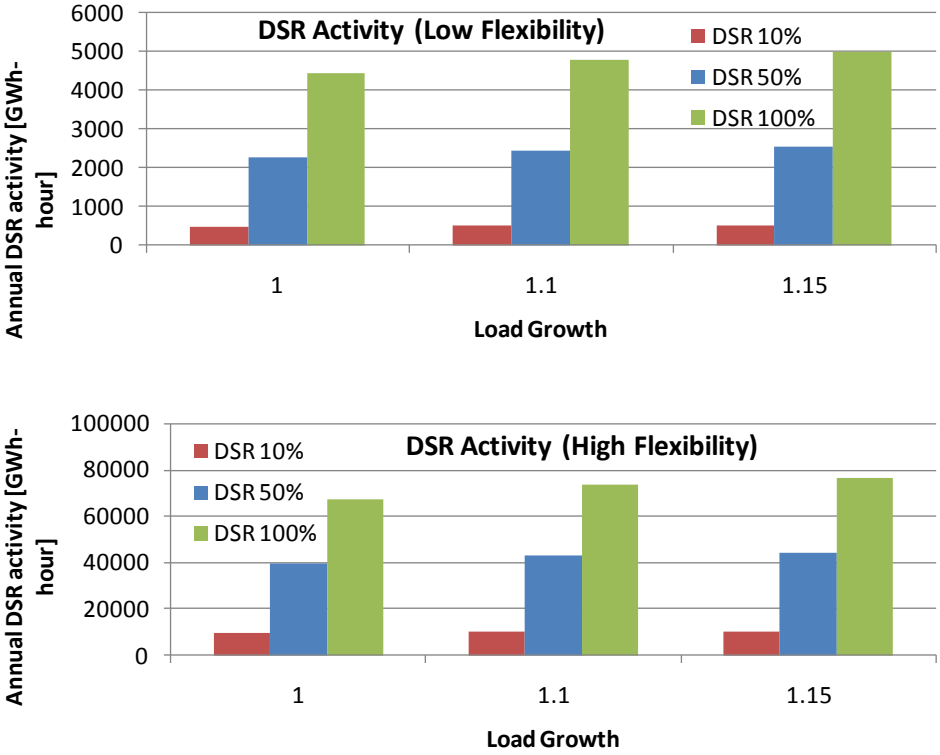


Figure A. 3-10: Effect of DSR flexibility on DSR activity as load grows

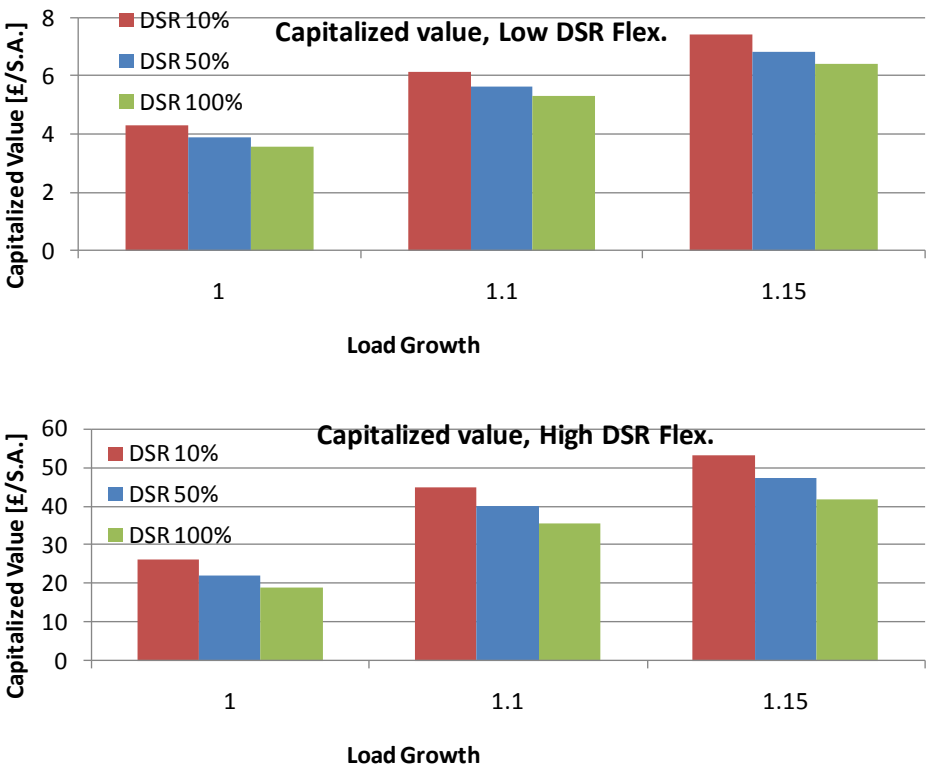


Figure A. 3-11: Effect of DSR flexibility on average capitalized value as load grows

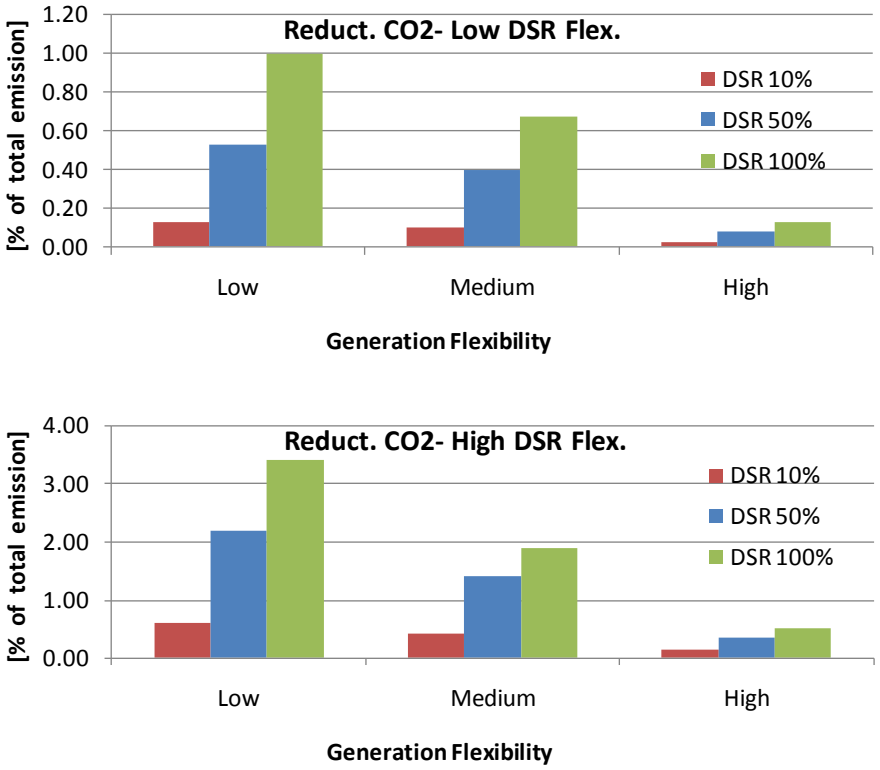


Figure A. 3-12: Effect of DSR flexibility on reductions in CO_2 emissions vs. generation flexibility

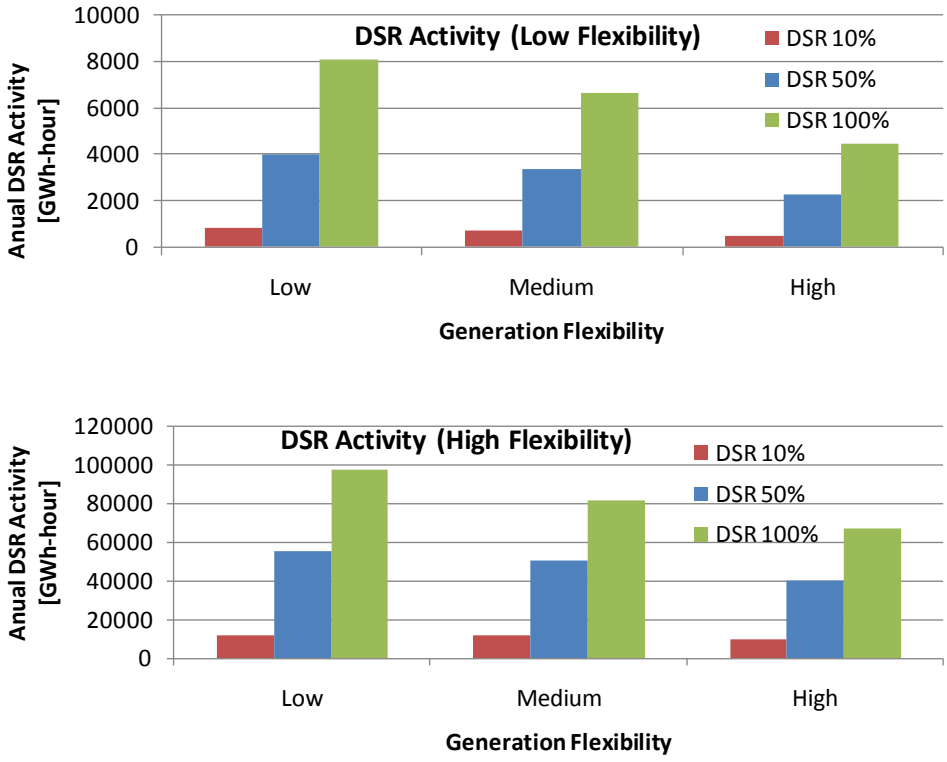


Figure A. 3-13: Effect of DSR flexibility on DSR activity vs. generation flexibility

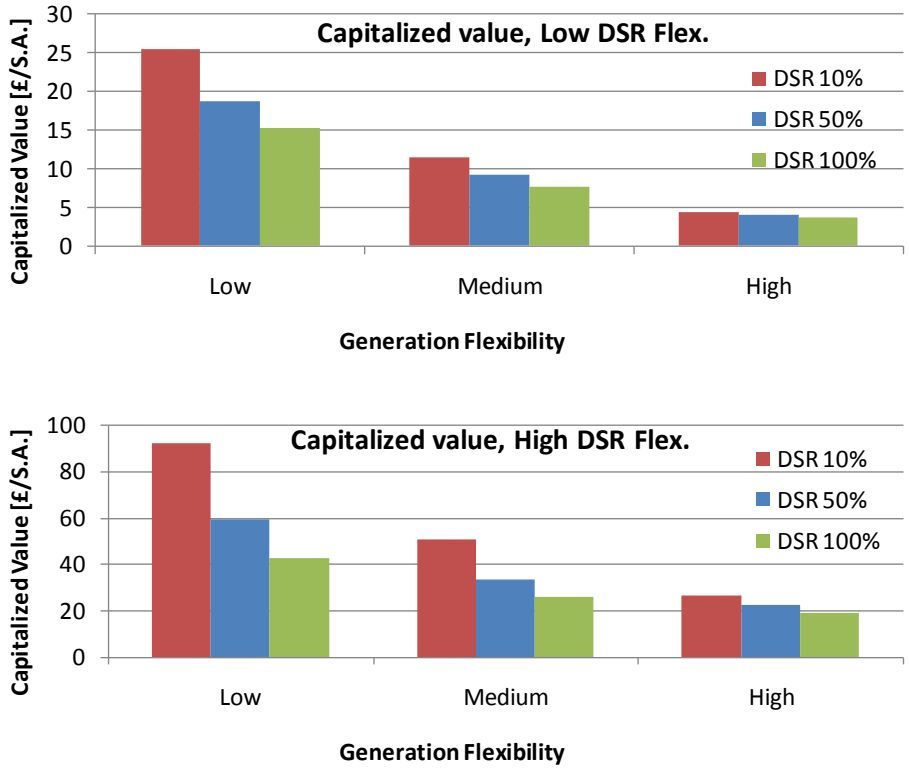


Figure A. 3-14: Effect of DSR flexibility on average capitalized value of DSR vs. generation flexibility

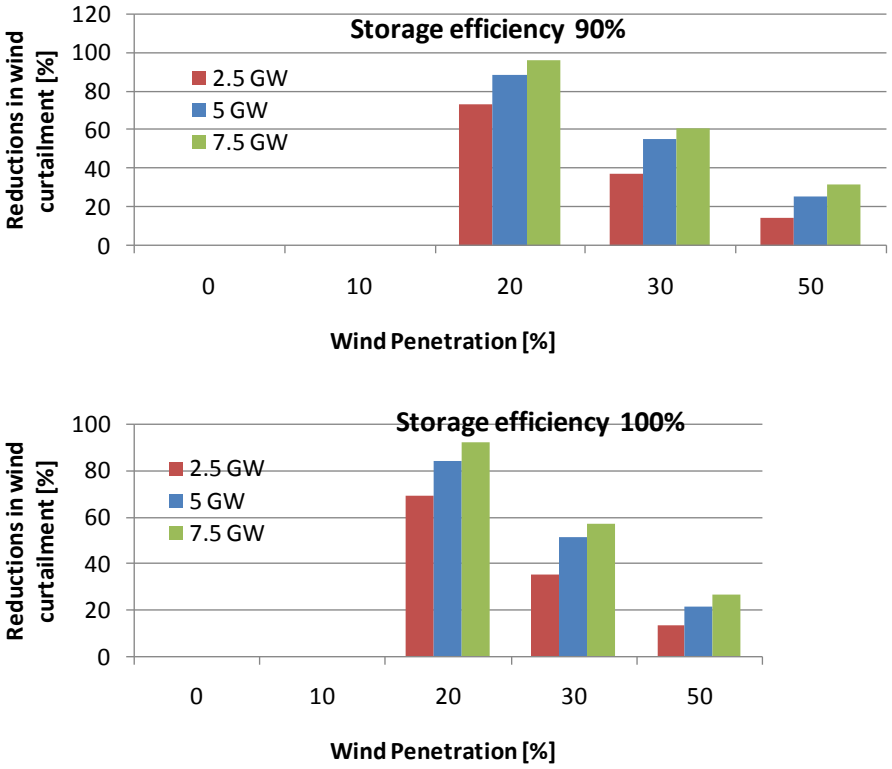


Figure A. 3-15: Effect of Storage efficiency on reduction in wind curtailment

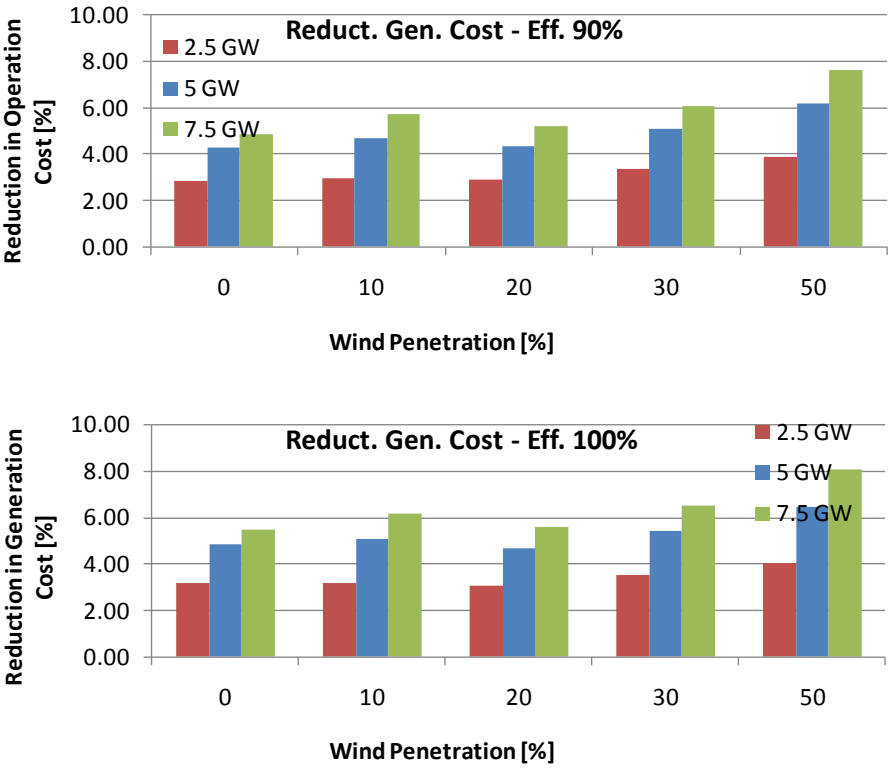


Figure A. 3-16: Effect of Storage efficiency on reduction in generation costs

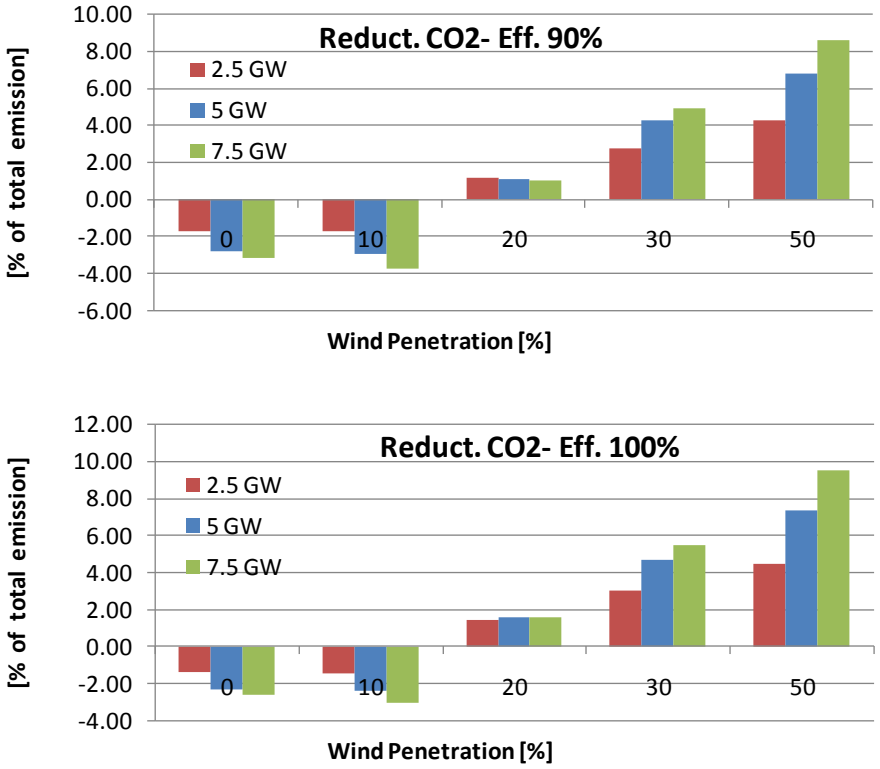


Figure A. 3-17: Effect of Storage efficiency on reduction in CO_2 emissions

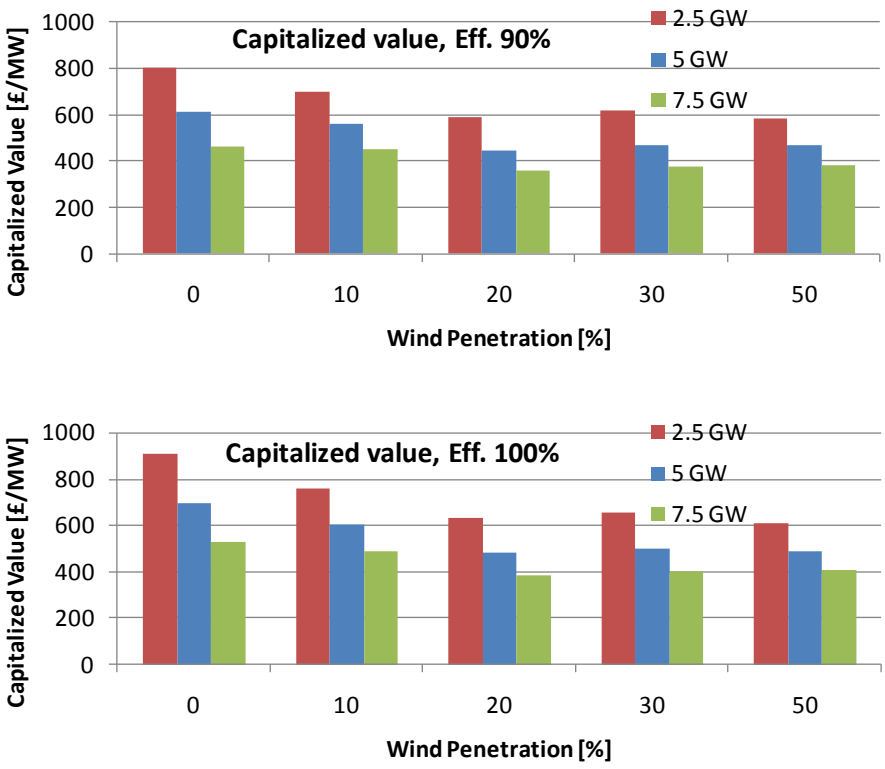


Figure A. 3-18: Effect of Storage efficiency on capitalized value of storage

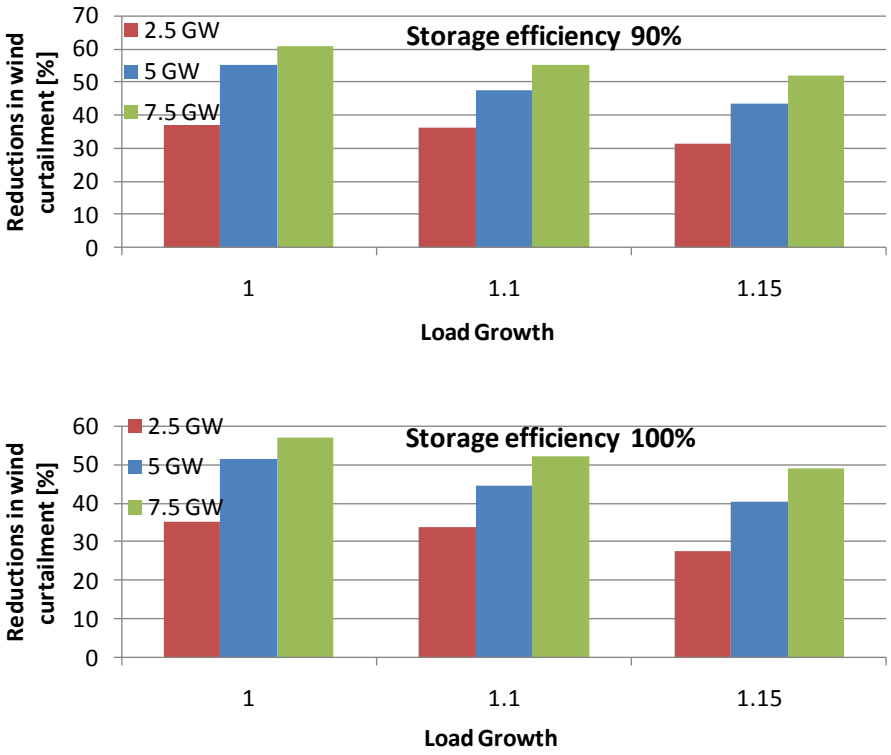


Figure A. 3-19: Effect of Storage efficiency on reduction in wind curtailment as load increases

Reduction in wind curtailed decreases with storage efficiency. The reason for that is as follows: with higher storage efficiency, in order to discharge the same energy required, less stored energy is needed. As this stored energy mostly comes from wind curtailed energy, there is detrimental effect of storage efficiency on reduction in wind energy curtailed.

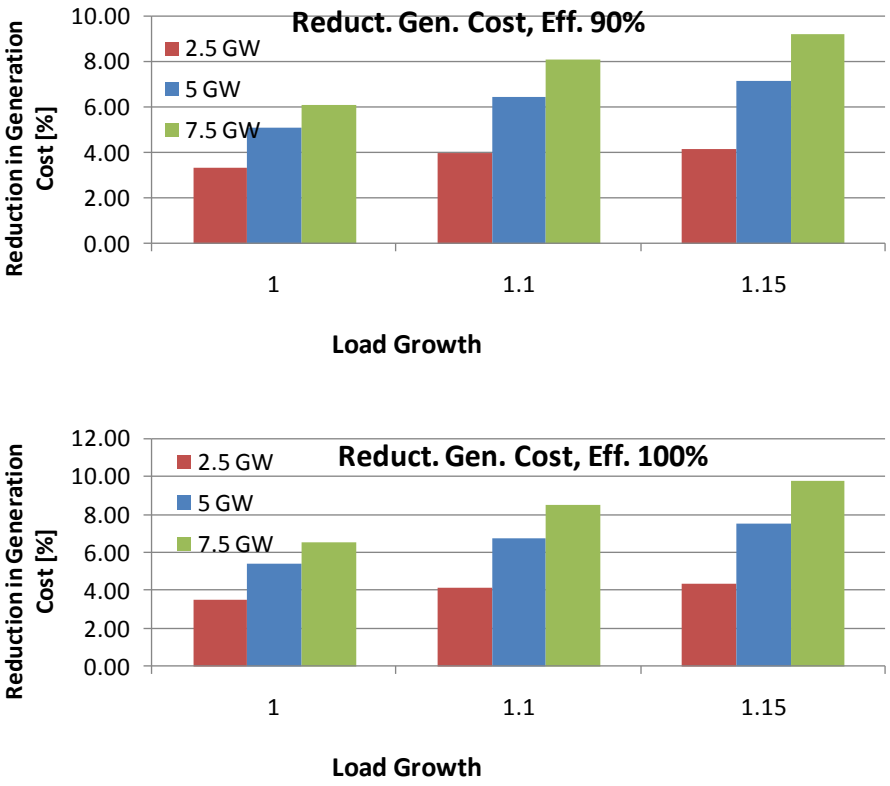


Figure A. 3-20: Effect of Storage efficiency on reduction in generation cost as load increases

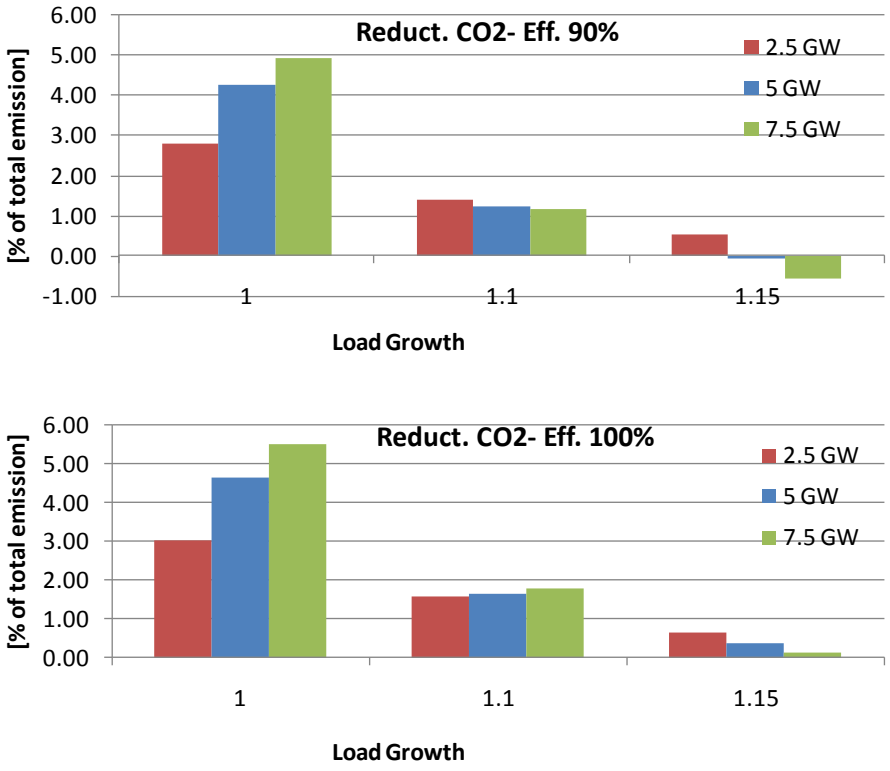


Figure A. 3-21: Effect of Storage efficiency on reduction in CO_2 emissions as load grows

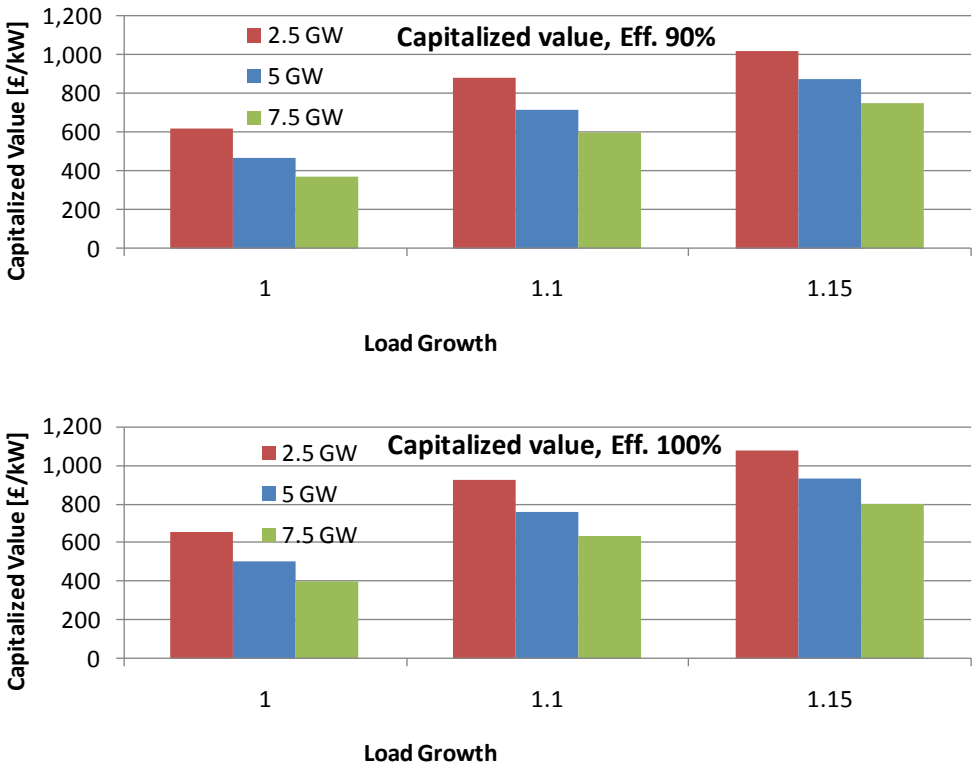


Figure A. 3-22: Effect of Storage efficiency on capitalized value of Storage vs. load growth

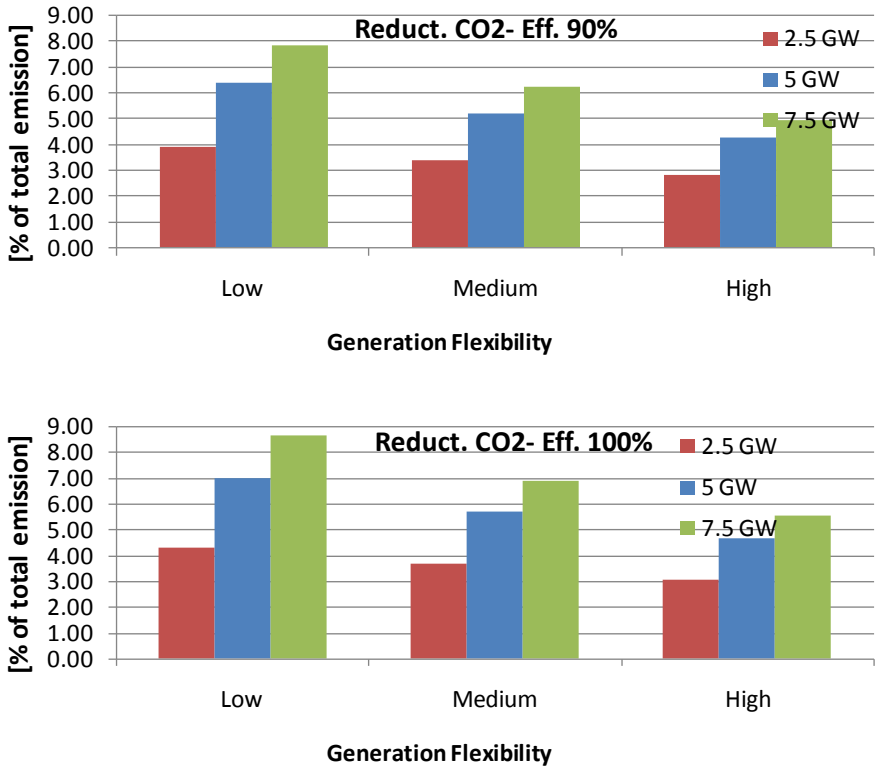


Figure A. 3-23: Effect of Storage efficiency on reduction in CO_2 emissions vs. generation flexibility

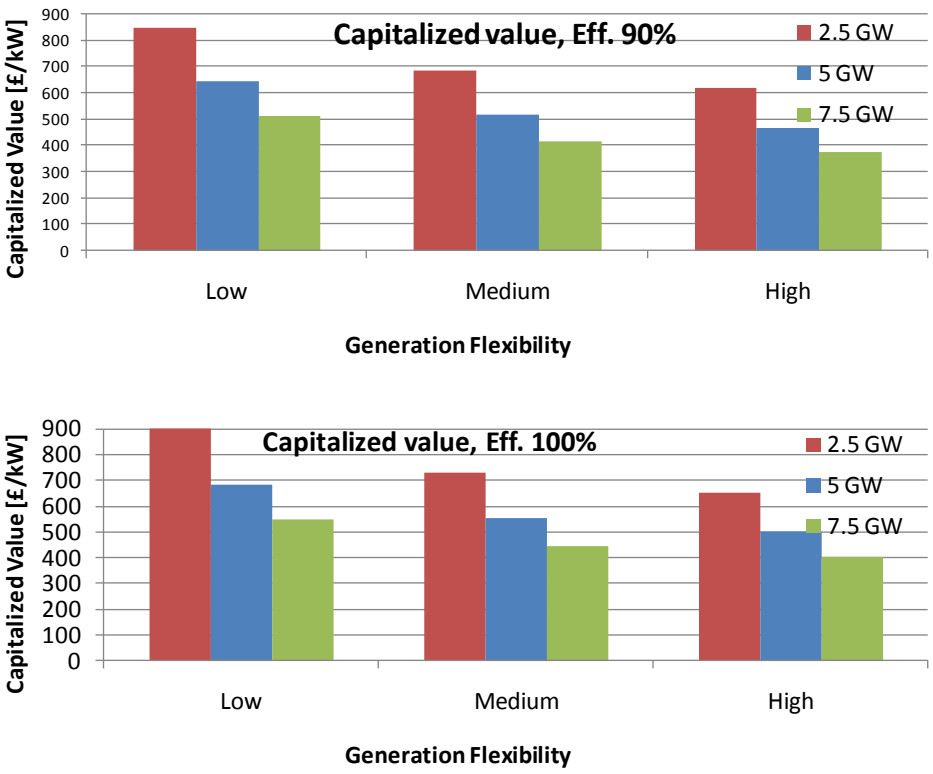


Figure A. 3-24: Effect of Storage efficiency on capitalized value of Storage vs. generation flexibility

A3.3. DSR activity

Information about shifted devices is kept tracked in a table whose just few excerpts are given below.

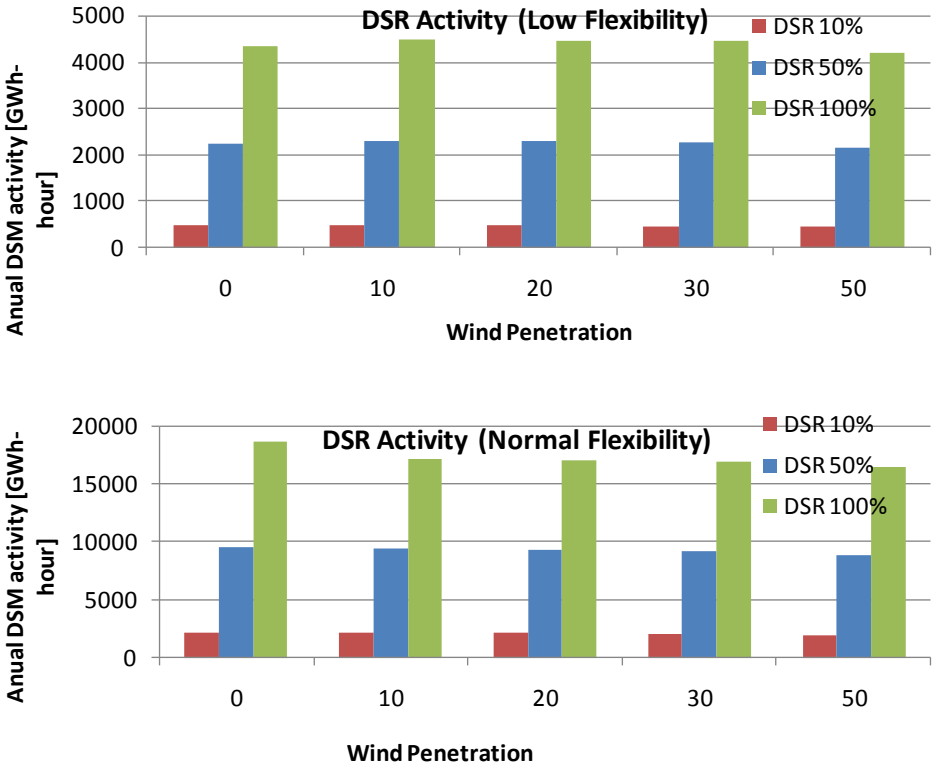
Table A. 3-2: Distribution of generation installed capacity on network buses and generation types

Device type	Bus	From time	To time	No. of devices
WM 1h	1	109	110	1930
WM 1h	1	110	111	2072
...				
WM 2h	16	113	115	103494
...				
WM+TD	10	8537	8539	54019
...				

First column in Table A. 3-2 refers to device type. Second column shows the bus number. Third and fourth column determine the hour of the year where the devices are shifted from and the hour where they are shifted to. Fifth column shows the number of devices shifted. For example, last

populated row in Table A. 3-2 says there are 54,019 of WM+TD in bus 10 being moved from hour 8537 to hour 8539. Although this device can be shifted for three hours, in this particular case it was shifted just for two hours. Note that the tables of this type can be rather lengthy.

Table A. 3-2 enables to determine DSR activity. DSR activity is defined as amount of shifted energy multiplied by the time difference between destination and origin time. For the example of WM+TD in Table A. 3-2, there are 54,019 devices shifted, each of them consuming 3347.5Wh (see Table 2-2), so the totally shifted energy in bus 10 by this type of device from hour 8537 to hour 8539 is about 181MWh. Now DSR activity is obtained when this energy is multiplied by 2h, which is difference between destination and origin time of shifting, giving in total about 362MWh-hour. Similar calculation is done for all entries in Table A. 3-2. Summed up for a specific device type it gives DSR activity for that type, and summed up for all entries in Table A. 3-2 gives total DSR activity for the whole network. Total DSR activity is shown in Figure A. 3-25.



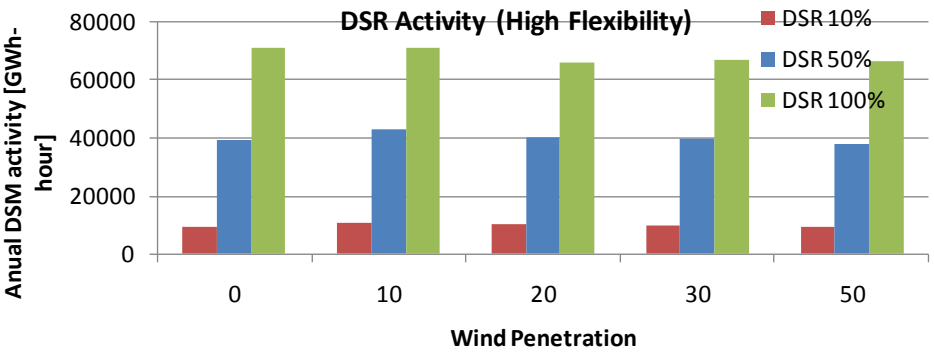
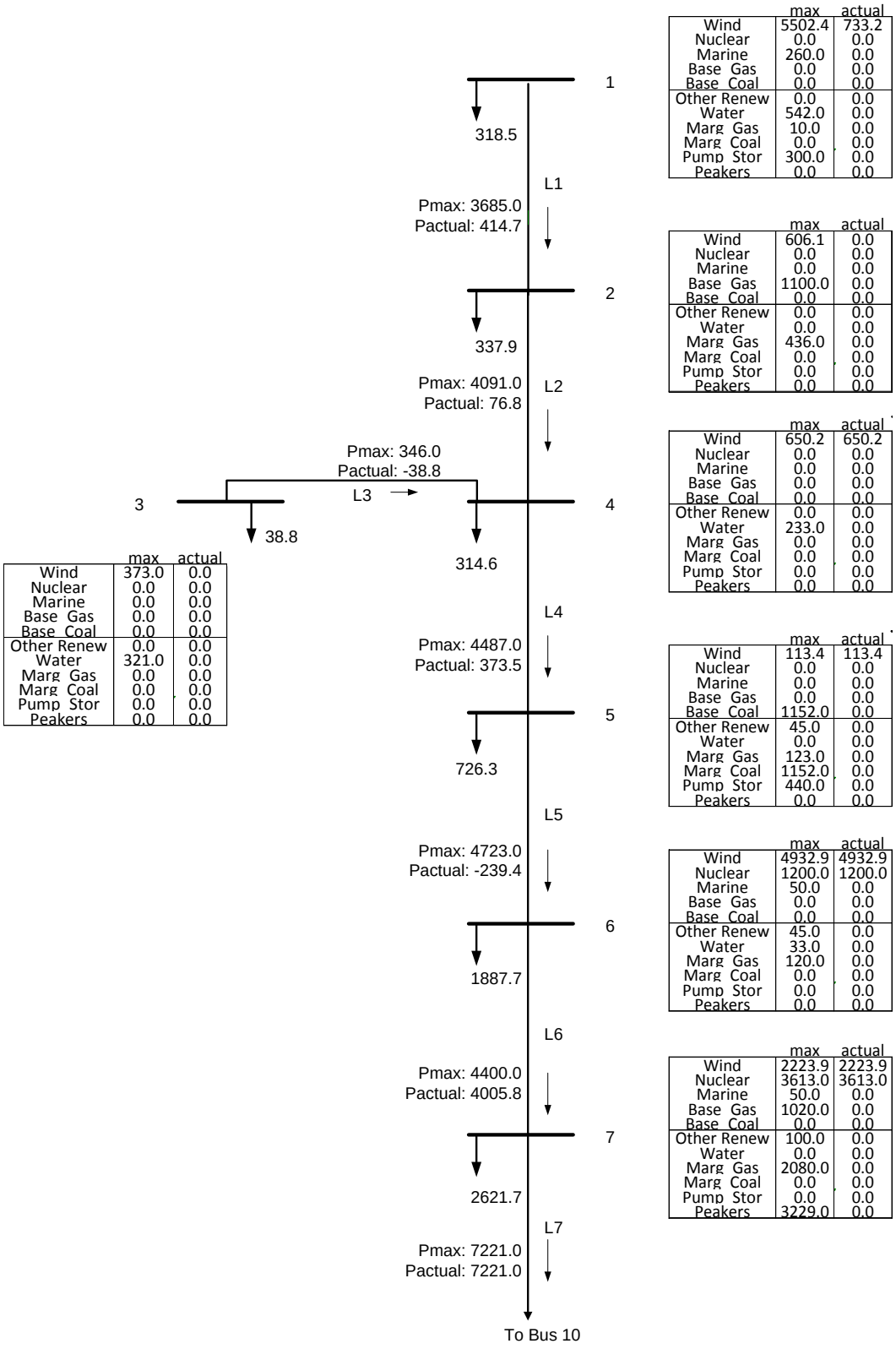


Figure A. 3-25: DSR activity

It can be noticed that DSR activity increases with penetration of flexible devices and with their flexibility. However, DSR activity practically does not depend on wind penetration. For all wind penetration levels, DSR activity is almost constant, which means that all DSR facility is used regardless the wind. It may be explained by no losses in DSR (energy paid back is equal to the energy being reduced), so in any condition, all available DSR capacity will be used.

A3.4. Snapshots



	max	actual
Wind	373.0	0.0
Nuclear	0.0	0.0
Marine	0.0	0.0
Base Gas	0.0	0.0
Base Coal	0.0	0.0
Other Renew	0.0	0.0
Water	321.0	0.0
Marg Gas	0.0	0.0
Marg Coal	0.0	0.0
Pump Stor	0.0	0.0
Peakers	0.0	0.0

	max	actual
Wind	5502.4	733.2
Nuclear	0.0	0.0
Marine	260.0	0.0
Base Gas	0.0	0.0
Base Coal	0.0	0.0
Other Renew	0.0	0.0
Water	542.0	0.0
Marg Gas	10.0	0.0
Marg Coal	0.0	0.0
Pump Stor	300.0	0.0
Peakers	0.0	0.0

	max	actual
Wind	606.1	0.0
Nuclear	0.0	0.0
Marine	0.0	0.0
Base Gas	1100.0	0.0
Base Coal	0.0	0.0
Other Renew	0.0	0.0
Water	0.0	0.0
Marg Gas	436.0	0.0
Marg Coal	0.0	0.0
Pump Stor	0.0	0.0
Peakers	0.0	0.0

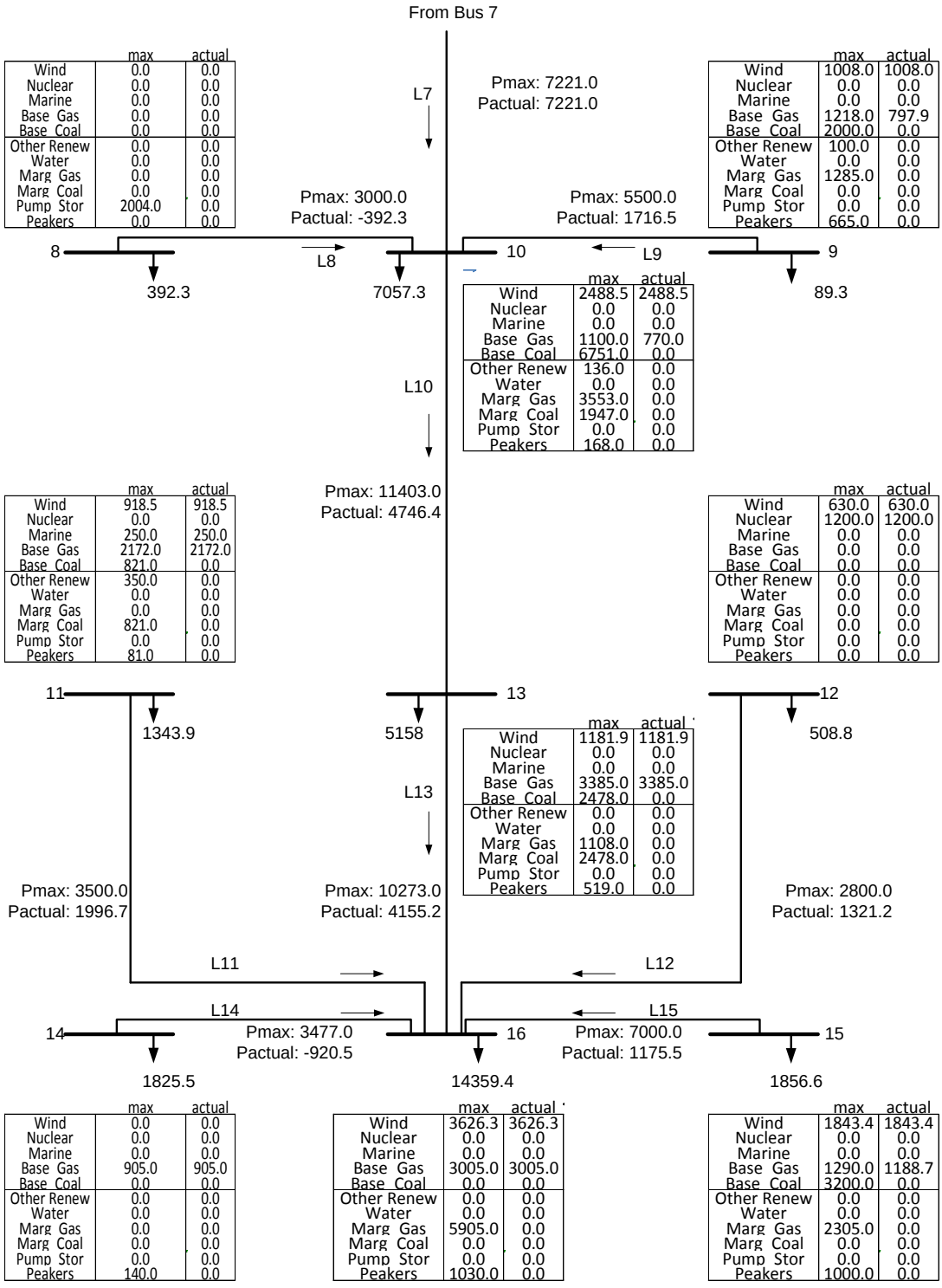
	max	actual
Wind	650.2	650.2
Nuclear	0.0	0.0
Marine	0.0	0.0
Base Gas	0.0	0.0
Base Coal	0.0	0.0
Other Renew	0.0	0.0
Water	233.0	0.0
Marg Gas	0.0	0.0
Marg Coal	0.0	0.0
Pump Stor	0.0	0.0
Peakers	0.0	0.0

	max	actual
Wind	113.4	113.4
Nuclear	0.0	0.0
Marine	0.0	0.0
Base Gas	0.0	0.0
Base Coal	1152.0	0.0
Other Renew	45.0	0.0
Water	0.0	0.0
Marg Gas	123.0	0.0
Marg Coal	1152.0	0.0
Pump Stor	440.0	0.0
Peakers	0.0	0.0

	max	actual
Wind	4932.9	4932.9
Nuclear	1200.0	1200.0
Marine	50.0	0.0
Base Gas	0.0	0.0
Base Coal	0.0	0.0
Other Renew	45.0	0.0
Water	33.0	0.0
Marg Gas	120.0	0.0
Marg Coal	0.0	0.0
Pump Stor	0.0	0.0
Peakers	0.0	0.0

	max	actual
Wind	2223.9	2223.9
Nuclear	3613.0	3613.0
Marine	50.0	0.0
Base Gas	1020.0	0.0
Base Coal	0.0	0.0
Other Renew	100.0	0.0
Water	0.0	0.0
Marg Gas	2080.0	0.0
Marg Coal	0.0	0.0
Pump Stor	0.0	0.0
Peakers	3229.0	0.0

(Continues on the next page)



	max	actual
Wind	0.0	0.0
Nuclear	0.0	0.0
Marine	0.0	0.0
Base Gas	0.0	0.0
Base Coal	0.0	0.0
Other Renew	0.0	0.0
Water	0.0	0.0
Marg Gas	0.0	0.0
Marg Coal	0.0	0.0
Pump Stor	2004.0	0.0
Peakers	0.0	0.0

	max	actual
Wind	1008.0	1008.0
Nuclear	0.0	0.0
Marine	0.0	0.0
Base Gas	1218.0	797.9
Base Coal	2000.0	0.0
Other Renew	100.0	0.0
Water	0.0	0.0
Marg Gas	1285.0	0.0
Marg Coal	0.0	0.0
Pump Stor	0.0	0.0
Peakers	665.0	0.0

	max	actual
Wind	2488.5	2488.5
Nuclear	0.0	0.0
Marine	0.0	0.0
Base Gas	1100.0	770.0
Base Coal	6751.0	0.0
Other Renew	136.0	0.0
Water	0.0	0.0
Marg Gas	3553.0	0.0
Marg Coal	1947.0	0.0
Pump Stor	0.0	0.0
Peakers	168.0	0.0

	max	actual
Wind	918.5	918.5
Nuclear	0.0	0.0
Marine	250.0	250.0
Base Gas	2172.0	2172.0
Base Coal	821.0	0.0
Other Renew	350.0	0.0
Water	0.0	0.0
Marg Gas	0.0	0.0
Marg Coal	821.0	0.0
Pump Stor	0.0	0.0
Peakers	81.0	0.0

	max	actual
Wind	630.0	630.0
Nuclear	1200.0	1200.0
Marine	0.0	0.0
Base Gas	0.0	0.0
Base Coal	0.0	0.0
Other Renew	0.0	0.0
Water	0.0	0.0
Marg Gas	0.0	0.0
Marg Coal	0.0	0.0
Pump Stor	0.0	0.0
Peakers	0.0	0.0

	max	actual
Wind	1181.9	1181.9
Nuclear	0.0	0.0
Marine	0.0	0.0
Base Gas	3385.0	3385.0
Base Coal	2478.0	0.0
Other Renew	0.0	0.0
Water	0.0	0.0
Marg Gas	1108.0	0.0
Marg Coal	2478.0	0.0
Pump Stor	0.0	0.0
Peakers	519.0	0.0

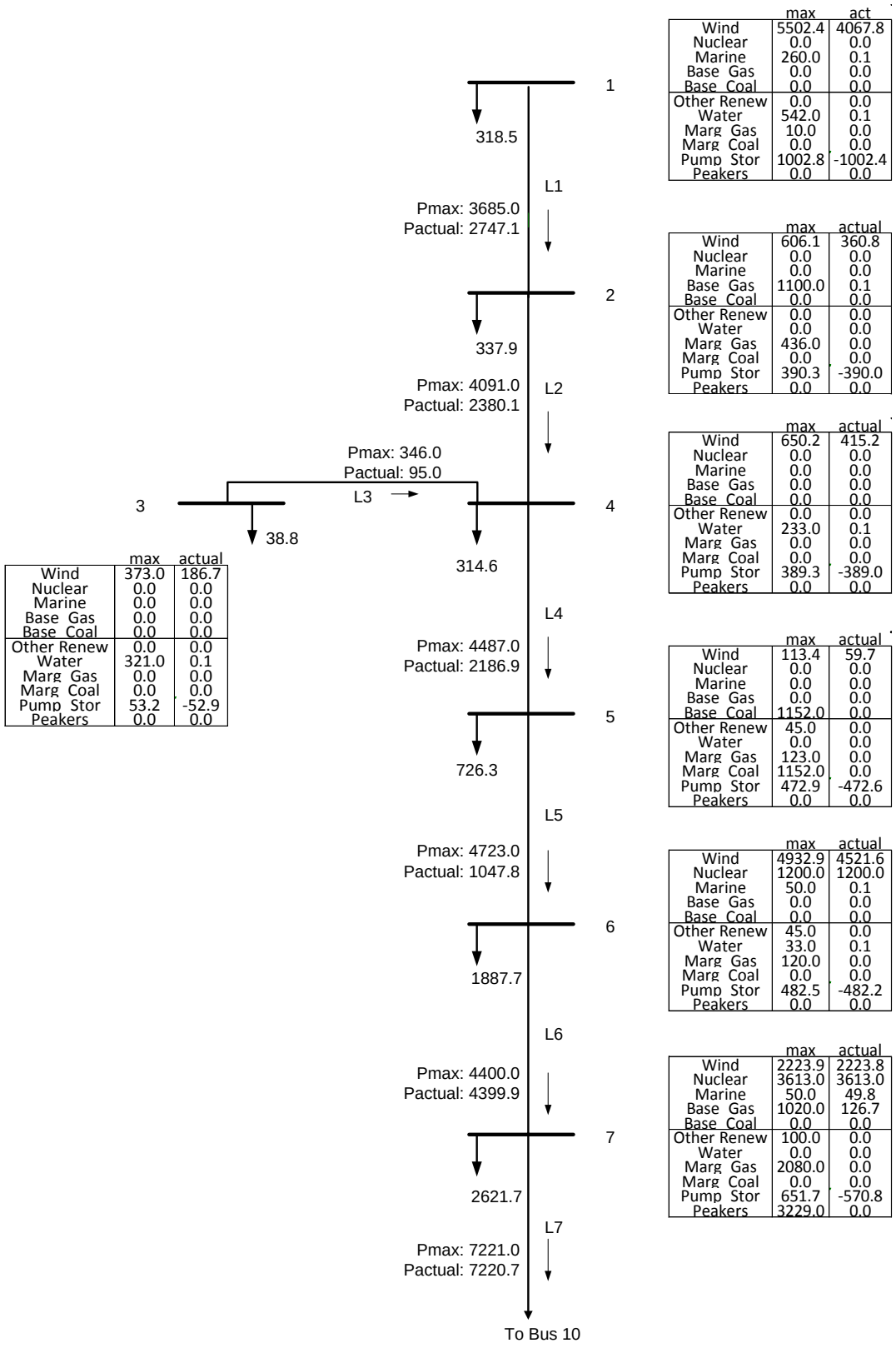
	max	actual
Wind	0.0	0.0
Nuclear	0.0	0.0
Marine	0.0	0.0
Base Gas	905.0	905.0
Base Coal	0.0	0.0
Other Renew	0.0	0.0
Water	0.0	0.0
Marg Gas	0.0	0.0
Marg Coal	0.0	0.0
Pump Stor	0.0	0.0
Peakers	140.0	0.0

	max	actual
Wind	3626.3	3626.3
Nuclear	0.0	0.0
Marine	0.0	0.0
Base Gas	3005.0	3005.0
Base Coal	0.0	0.0
Other Renew	0.0	0.0
Water	0.0	0.0
Marg Gas	5905.0	0.0
Marg Coal	0.0	0.0
Pump Stor	0.0	0.0
Peakers	1030.0	0.0

	max	actual
Wind	1843.4	1843.4
Nuclear	0.0	0.0
Marine	0.0	0.0
Base Gas	1290.0	1188.7
Base Coal	3200.0	0.0
Other Renew	0.0	0.0
Water	0.0	0.0
Marg Gas	2305.0	0.0
Marg Coal	0.0	0.0
Pump Stor	0.0	0.0
Peakers	1000.0	0.0

Figure A. 3-26: Snapshots during high wind (hour 6124), wind penetration 20%, base case

(Continued from previous page)



	max	act
Wind	5502.4	4067.8
Nuclear	0.0	0.0
Marine	260.0	0.1
Base Gas	0.0	0.0
Base Coal	0.0	0.0
Other Renew	0.0	0.0
Water	542.0	0.1
Marg Gas	10.0	0.0
Marg Coal	0.0	0.0
Pump Stor	1002.8	-1002.4
Peakers	0.0	0.0

	max	actual
Wind	606.1	360.8
Nuclear	0.0	0.0
Marine	0.0	0.0
Base Gas	1100.0	0.1
Base Coal	0.0	0.0
Other Renew	0.0	0.0
Water	0.0	0.0
Marg Gas	436.0	0.0
Marg Coal	0.0	0.0
Pump Stor	390.3	-390.0
Peakers	0.0	0.0

	max	actual
Wind	650.2	415.2
Nuclear	0.0	0.0
Marine	0.0	0.0
Base Gas	0.0	0.0
Base Coal	0.0	0.0
Other Renew	0.0	0.0
Water	233.0	0.1
Marg Gas	0.0	0.0
Marg Coal	0.0	0.0
Pump Stor	389.3	-389.0
Peakers	0.0	0.0

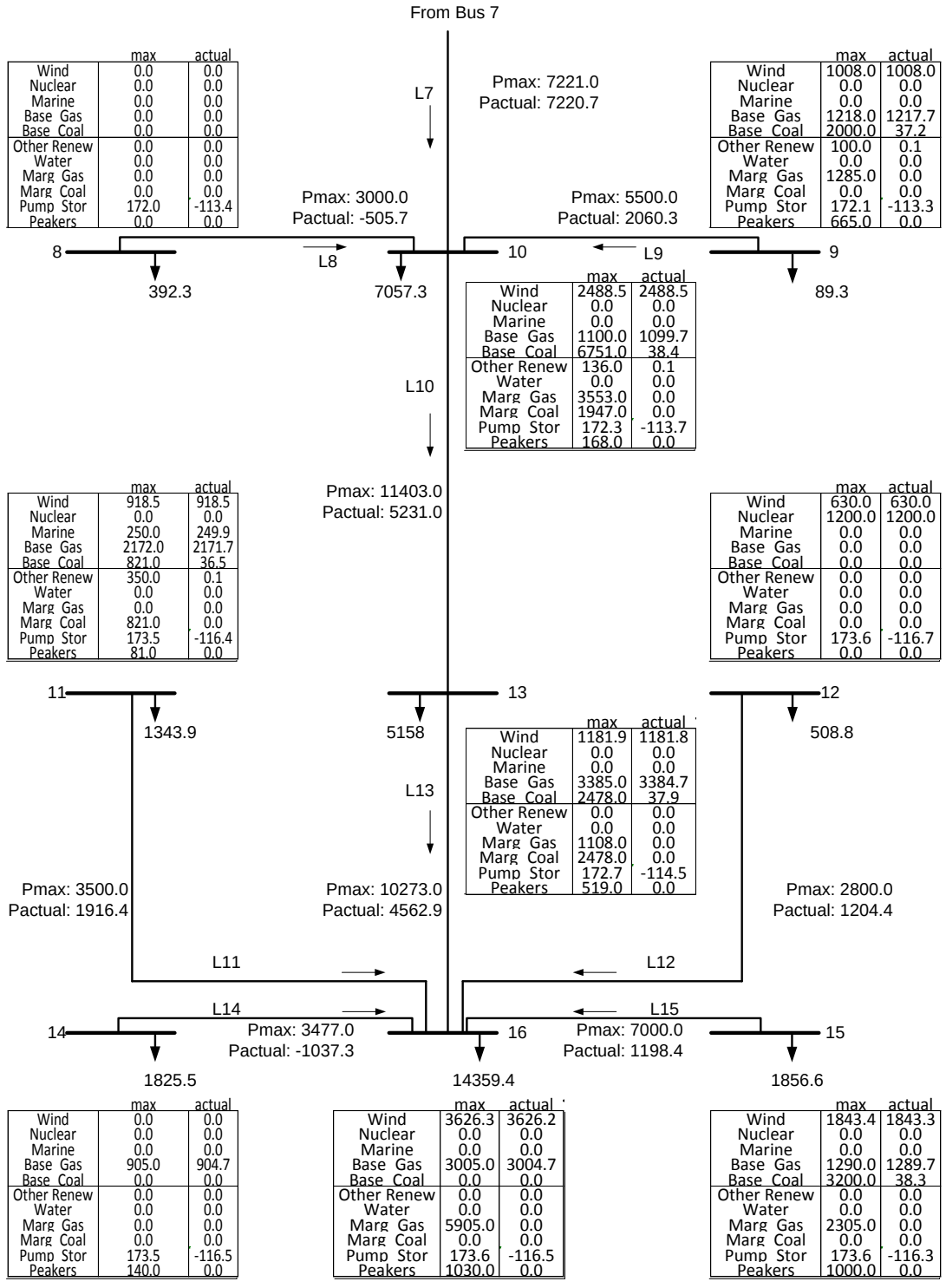
	max	actual
Wind	113.4	59.7
Nuclear	0.0	0.0
Marine	0.0	0.0
Base Gas	0.0	0.0
Base Coal	1152.0	0.0
Other Renew	45.0	0.0
Water	0.0	0.0
Marg Gas	123.0	0.0
Marg Coal	1152.0	0.0
Pump Stor	472.9	-472.6
Peakers	0.0	0.0

	max	actual
Wind	4932.9	4521.6
Nuclear	1200.0	1200.0
Marine	50.0	0.1
Base Gas	0.0	0.0
Base Coal	0.0	0.0
Other Renew	45.0	0.0
Water	33.0	0.1
Marg Gas	120.0	0.0
Marg Coal	0.0	0.0
Pump Stor	482.5	-482.2
Peakers	0.0	0.0

	max	actual
Wind	2223.9	2223.8
Nuclear	3613.0	3613.0
Marine	50.0	49.8
Base Gas	1020.0	126.7
Base Coal	0.0	0.0
Other Renew	100.0	0.0
Water	0.0	0.0
Marg Gas	2080.0	0.0
Marg Coal	0.0	0.0
Pump Stor	651.7	-570.8
Peakers	3229.0	0.0

	max	actual
Wind	373.0	186.7
Nuclear	0.0	0.0
Marine	0.0	0.0
Base Gas	0.0	0.0
Base Coal	0.0	0.0
Other Renew	0.0	0.0
Water	321.0	0.1
Marg Gas	0.0	0.0
Marg Coal	0.0	0.0
Pump Stor	53.2	-52.9
Peakers	0.0	0.0

(Continues on the next page)



	max	actual
Wind	0.0	0.0
Nuclear	0.0	0.0
Marine	0.0	0.0
Base Gas	0.0	0.0
Base Coal	0.0	0.0
Other Renew	0.0	0.0
Water	0.0	0.0
Marg Gas	0.0	0.0
Marg Coal	0.0	0.0
Pump Stor	172.0	-113.4
Peakers	0.0	0.0

	max	actual
Wind	1008.0	1008.0
Nuclear	0.0	0.0
Marine	0.0	0.0
Base Gas	1218.0	1217.7
Base Coal	2000.0	37.2
Other Renew	100.0	0.1
Water	0.0	0.0
Marg Gas	1285.0	0.0
Marg Coal	0.0	0.0
Pump Stor	172.1	-113.3
Peakers	665.0	0.0

	max	actual
Wind	2488.5	2488.5
Nuclear	0.0	0.0
Marine	0.0	0.0
Base Gas	1100.0	1099.7
Base Coal	6751.0	38.4
Other Renew	136.0	0.1
Water	0.0	0.0
Marg Gas	3553.0	0.0
Marg Coal	1947.0	0.0
Pump Stor	172.3	-113.7
Peakers	168.0	0.0

	max	actual
Wind	918.5	918.5
Nuclear	0.0	0.0
Marine	250.0	249.9
Base Gas	2172.0	2171.7
Base Coal	821.0	36.5
Other Renew	350.0	0.1
Water	0.0	0.0
Marg Gas	0.0	0.0
Marg Coal	821.0	0.0
Pump Stor	173.5	-116.4
Peakers	81.0	0.0

	max	actual
Wind	630.0	630.0
Nuclear	1200.0	1200.0
Marine	0.0	0.0
Base Gas	0.0	0.0
Base Coal	0.0	0.0
Other Renew	0.0	0.0
Water	0.0	0.0
Marg Gas	0.0	0.0
Marg Coal	0.0	0.0
Pump Stor	173.6	-116.7
Peakers	0.0	0.0

	max	actual
Wind	1181.9	1181.8
Nuclear	0.0	0.0
Marine	0.0	0.0
Base Gas	3385.0	3384.7
Base Coal	2478.0	37.9
Other Renew	0.0	0.0
Water	0.0	0.0
Marg Gas	1108.0	0.0
Marg Coal	2478.0	0.0
Pump Stor	172.7	-114.5
Peakers	519.0	0.0

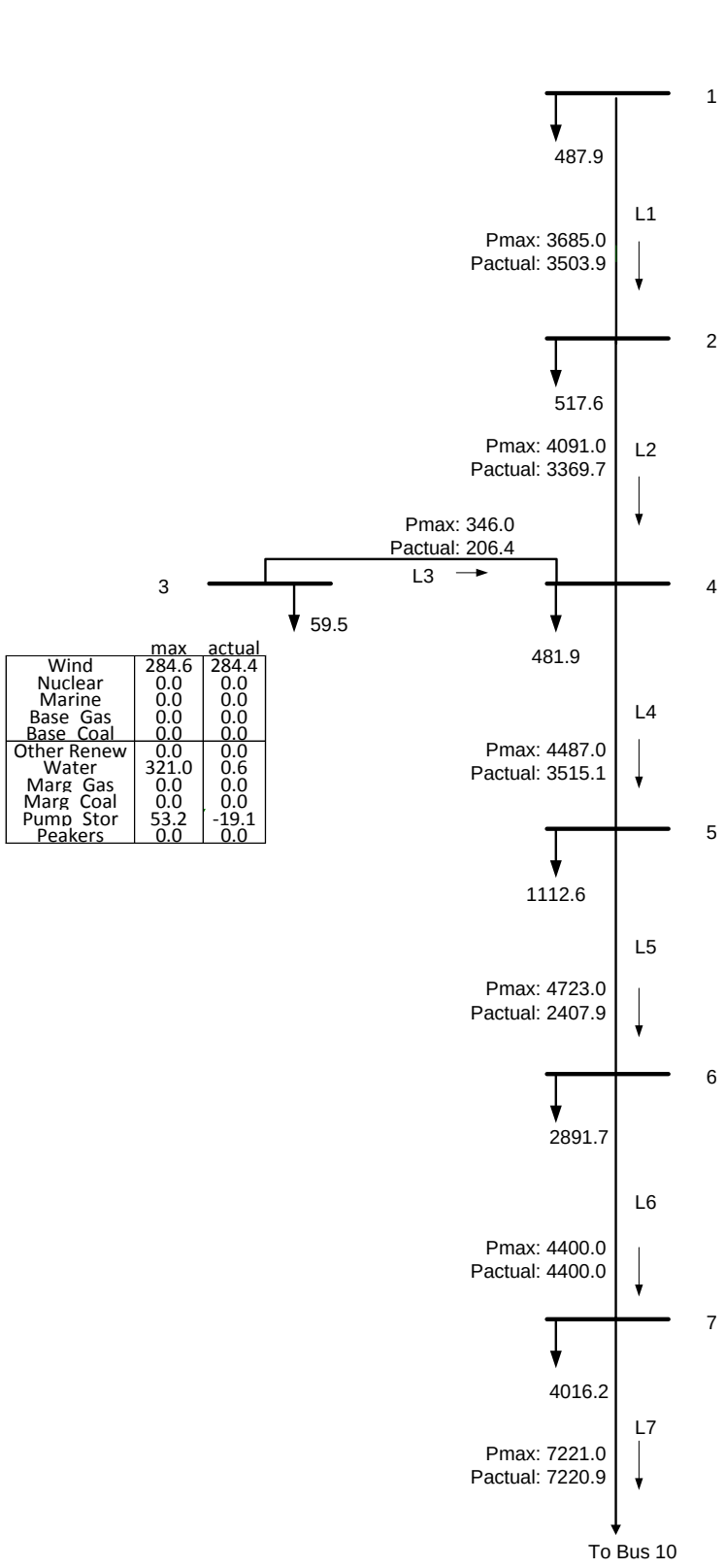
	max	actual
Wind	0.0	0.0
Nuclear	0.0	0.0
Marine	0.0	0.0
Base Gas	905.0	904.7
Base Coal	0.0	0.0
Other Renew	0.0	0.0
Water	0.0	0.0
Marg Gas	0.0	0.0
Marg Coal	0.0	0.0
Pump Stor	173.5	-116.5
Peakers	140.0	0.0

	max	actual
Wind	3626.3	3626.2
Nuclear	0.0	0.0
Marine	0.0	0.0
Base Gas	3005.0	3004.7
Base Coal	0.0	0.0
Other Renew	0.0	0.0
Water	0.0	0.0
Marg Gas	5905.0	0.0
Marg Coal	0.0	0.0
Pump Stor	173.6	-116.5
Peakers	1030.0	0.0

	max	actual
Wind	1843.4	1843.3
Nuclear	0.0	0.0
Marine	0.0	0.0
Base Gas	1290.0	1289.7
Base Coal	3200.0	38.3
Other Renew	0.0	0.0
Water	0.0	0.0
Marg Gas	2305.0	0.0
Marg Coal	0.0	0.0
Pump Stor	173.6	-116.3
Peakers	1000.0	0.0

Figure A. 3-27: Snapshots during high wind (hour 6124), with total installed storage capacity of 5GW, 80% efficiency, wind penetration 20%

(Continued from previous page)



	max	actual
Wind	284.6	284.4
Nuclear	0.0	0.0
Marine	0.0	0.0
Base Gas	0.0	0.0
Base Coal	0.0	0.0
Other Renew	0.0	0.0
Water	321.0	0.6
Marg Gas	0.0	0.0
Marg Coal	0.0	0.0
Pump Stor	53.2	-19.1
Peakers	0.0	0.0

	max	actual
Wind	4198.7	4198.4
Nuclear	0.0	0.0
Marine	260.0	0.6
Base Gas	0.0	0.0
Base Coal	0.0	0.0
Other Renew	0.0	0.0
Water	542.0	0.7
Marg Gas	10.0	0.0
Marg Coal	0.0	0.0
Pump Stor	1002.8	-207.9
Peakers	0.0	0.0

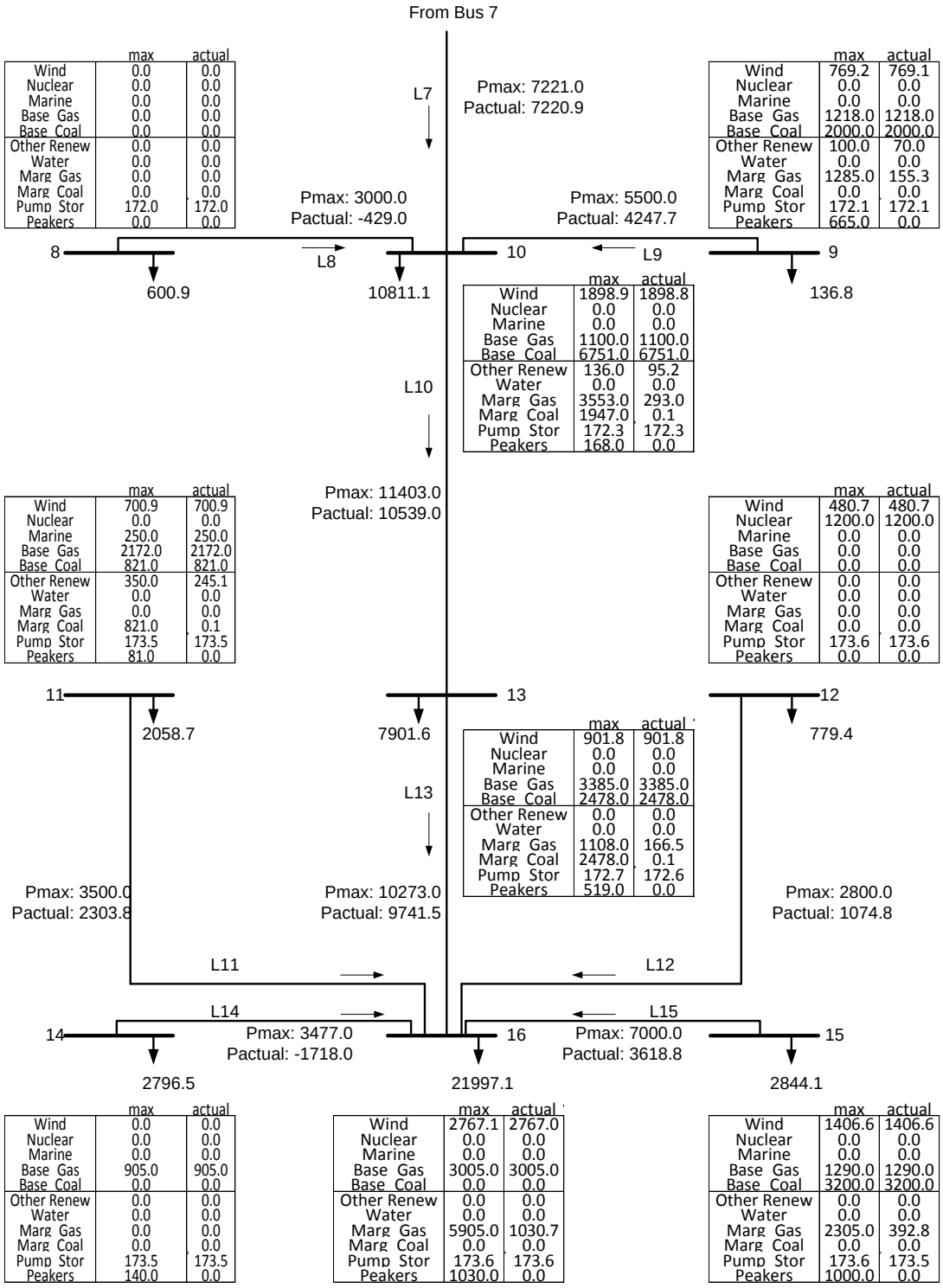
	max	actual
Wind	462.5	462.3
Nuclear	0.0	0.0
Marine	0.0	0.0
Base Gas	1100.0	0.1
Base Coal	0.0	0.0
Other Renew	0.0	0.0
Water	0.0	0.0
Marg Gas	436.0	0.0
Marg Coal	0.0	0.0
Pump Stor	390.3	-78.9
Peakers	0.0	0.0

	max	actual
Wind	496.1	495.9
Nuclear	0.0	0.0
Marine	0.0	0.0
Base Gas	0.0	0.0
Base Coal	0.0	0.0
Other Renew	0.0	0.0
Water	233.0	0.7
Marg Gas	0.0	0.0
Marg Coal	0.0	0.0
Pump Stor	389.3	-75.7
Peakers	0.0	0.0

	max	actual
Wind	86.5	86.4
Nuclear	0.0	0.0
Marine	0.0	0.0
Base Gas	0.0	0.0
Base Coal	1152.0	0.1
Other Renew	45.0	0.0
Water	0.0	0.0
Marg Gas	123.0	0.0
Marg Coal	1152.0	0.0
Pump Stor	472.9	-81.0
Peakers	0.0	0.0

	max	actual
Wind	3764.1	3763.9
Nuclear	1200.0	1200.0
Marine	50.0	0.6
Base Gas	0.0	0.0
Base Coal	0.0	0.0
Other Renew	45.0	0.0
Water	33.0	0.6
Marg Gas	120.0	0.0
Marg Coal	0.0	0.0
Pump Stor	482.5	-81.4
Peakers	0.0	0.0

	max	actual
Wind	1697.0	1696.9
Nuclear	3613.0	3613.0
Marine	50.0	50.0
Base Gas	1020.0	1019.8
Base Coal	0.0	0.0
Other Renew	100.0	0.3
Water	0.0	0.0
Marg Gas	2080.0	0.0
Marg Coal	0.0	0.0
Pump Stor	651.7	457.2
Peakers	3229.0	0.0



	max	actual
Wind	0.0	0.0
Nuclear	0.0	0.0
Marine	0.0	0.0
Base Gas	0.0	0.0
Base Coal	0.0	0.0
Other Renew	0.0	0.0
Water	0.0	0.0
Marg Gas	0.0	0.0
Marg Coal	0.0	0.0
Pump Stor	172.0	172.0
Peakers	0.0	0.0

	max	actual
Wind	769.2	769.1
Nuclear	0.0	0.0
Marine	0.0	0.0
Base Gas	1218.0	1218.0
Base Coal	2000.0	2000.0
Other Renew	100.0	70.0
Water	0.0	0.0
Marg Gas	1285.0	155.3
Marg Coal	0.0	0.0
Pump Stor	172.1	172.1
Peakers	665.0	0.0

	max	actual
Wind	1898.9	1898.8
Nuclear	0.0	0.0
Marine	0.0	0.0
Base Gas	1100.0	1100.0
Base Coal	6751.0	6751.0
Other Renew	136.0	95.2
Water	0.0	0.0
Marg Gas	3553.0	293.0
Marg Coal	1947.0	0.1
Pump Stor	172.3	172.3
Peakers	168.0	0.0

	max	actual
Wind	700.9	700.9
Nuclear	0.0	0.0
Marine	250.0	250.0
Base Gas	2172.0	2172.0
Base Coal	821.0	821.0
Other Renew	350.0	245.1
Water	0.0	0.0
Marg Gas	0.0	0.0
Marg Coal	821.0	0.1
Pump Stor	173.5	173.5
Peakers	81.0	0.0

	max	actual
Wind	480.7	480.7
Nuclear	1200.0	1200.0
Marine	0.0	0.0
Base Gas	0.0	0.0
Base Coal	0.0	0.0
Other Renew	0.0	0.0
Water	0.0	0.0
Marg Gas	0.0	0.0
Marg Coal	0.0	0.0
Pump Stor	173.6	173.6
Peakers	0.0	0.0

	max	actual
Wind	901.8	901.8
Nuclear	0.0	0.0
Marine	0.0	0.0
Base Gas	3385.0	3385.0
Base Coal	2478.0	2478.0
Other Renew	0.0	0.0
Water	0.0	0.0
Marg Gas	1108.0	166.5
Marg Coal	2478.0	0.1
Pump Stor	172.7	172.6
Peakers	519.0	0.0

	max	actual
Wind	0.0	0.0
Nuclear	0.0	0.0
Marine	0.0	0.0
Base Gas	905.0	905.0
Base Coal	0.0	0.0
Other Renew	0.0	0.0
Water	0.0	0.0
Marg Gas	0.0	0.0
Marg Coal	0.0	0.0
Pump Stor	173.5	173.5
Peakers	140.0	0.0

	max	actual
Wind	2767.1	2767.0
Nuclear	0.0	0.0
Marine	0.0	0.0
Base Gas	3005.0	3005.0
Base Coal	0.0	0.0
Other Renew	0.0	0.0
Water	0.0	0.0
Marg Gas	5905.0	1030.7
Marg Coal	0.0	0.0
Pump Stor	173.6	173.6
Peakers	1030.0	0.0

	max	actual
Wind	1406.6	1406.6
Nuclear	0.0	0.0
Marine	0.0	0.0
Base Gas	1290.0	1290.0
Base Coal	3200.0	3200.0
Other Renew	0.0	0.0
Water	0.0	0.0
Marg Gas	2305.0	392.8
Marg Coal	0.0	0.0
Pump Stor	173.6	173.5
Peakers	1000.0	0.0

Figure A. 3-28: Snapshots during peak demand and lower wind (hour 5923), with total installed storage capacity of 5GW, 80% efficiency, wind penetration 20%

APPENDIX 4. Distribution Networks

A4.1. Distribution Network 11kV 38 Bus

Load data is given in Table A. 4-1 as a time series. On the bottom of Table A. 4-1 shown are peak demand and daily energy consumption.

Table A. 4-1: Load time series data for case of load growth 0%, 10% and 20%

time	Load + 0%	Load + 10%	Load + 20%
[h]		[MW]	
1	1.9445	2.1390	2.3334
2	1.8958	2.0854	2.2750
3	1.8644	2.0508	2.2373
4	1.7369	1.9106	2.0843
5	1.7153	1.8868	2.0584
6	1.9308	2.1239	2.3170
7	2.3688	2.6057	2.8426
8	2.5470	2.8017	3.0564
9	2.6208	2.8829	3.1450
10	2.6401	2.9041	3.1681
11	2.6507	2.9158	3.1808
12	2.6561	2.9217	3.1873
13	2.6110	2.8721	3.1332
14	2.6169	2.8786	3.1403
15	2.5953	2.8548	3.1144
16	2.7523	3.0275	3.3028
17	2.9643	3.2607	3.5572
18	2.9450	3.2395	3.5340
19	2.8092	3.0901	3.3710
20	2.6110	2.8721	3.1332
21	2.4175	2.6593	2.9010
22	2.1647	2.3812	2.5976
23	1.9673	2.1640	2.3608
24	1.8841	2.0725	2.2609
Max.	2.9643	3.26073	3.55716
Energy [MWh]	56.9098	62.60078	68.29176

Table A. 4-2 below shows details on network branches: network topology (the nodes where the branch is connected to), branch length in meters, branch resistance and reactance in per unit (calculated with base power $S_B = 1MVA$) and thermal capacity limits. Last column in Table A. 4-2 shows the maximum flow through the branches for 0% load increase, in base case, i.e. when DSR and Storage facility are not exercised. Comparing last two columns in Table A. 4-2, it can be concluded that in the base case there are no overloaded branches in the network.

Table A. 4-2: Network branch data and power flows through the branches during peak hour for case 0% load growth

No.	From Bus	To Bus	Length	R	X	Thermal Capacity	Apparent Power
			[m]	p.u.		[MVA]	
1	1	2	275	0.024876	0.012217	3.553	3.3748
2	2	4	300	0.006387	0.001726	2.398	0.1071
3	2	3	1900	0.000131	6.42E-05	3.751	3.0653
4	3	6	223	0.008896	0.006189	4.884	0
5	3	5	326	0.011152	0.005483	3.751	2.8859
6	5	8	237	0.001306	0.000642	3.751	0
7	5	7	211	0.001098	0.000529	3.553	2.811
8	10	7	854	0.005256	0.001016	0.88	0.1071
9	7	9	7800	0.002195	0.001058	3.454	2.6966
10	9	11	193	0.002195	0.001058	3.553	2.3261
11	11	12	160	0.003712	0.002584	1.738	0.0714
12	11	13	10	0.000274	0.000132	3.553	2.2445
13	13	14	540	0.002917	0.000417	1.441	0.0892
14	13	15	50	0.005224	0.001392	2.453	2.1541
15	15	16	200	0.007835	0.002088	2.453	2.0266
16	16	17	185	0.01977	0.005536	2.651	0.215
17	17	18	10	0.007066	0.001978	2.651	0.1071
18	16	19	240	0.000137	6.61E-05	3.553	1.6055
19	19	20	145	0.008383	0.002265	2.398	0.1125
20	19	21	106	0.002195	0.001058	3.553	0.44
21	21	22	80	0.004472	0.002156	3.553	0.3272
22	22	23	100	0.004832	0.001288	2.453	0.2143
23	23	24	160	0.000412	0.000198	3.553	0.1071
24	24	26	80	0.001098	0.000529	3.553	0
25	24	25	20	0.000798	0.000216	2.398	0.1071
26	27	19	160	0.005625	0.002711	3.454	1.0527
27	27	28	315	0.000165	7.93E-05	3.454	0.1124
28	29	27	80	0.000494	0.000238	3.454	0.9346
29	29	30	30	0.013025	0.005891	1.738	0.0178
30	31	29	410	0.005439	0.001691	2.398	0.9164
31	32	31	12	0.007585	0.002049	2.398	0.8052
32	32	33	400	0.004626	0.001279	2.398	0.1125
33	34	32	36	0.003821	0.001068	2.398	0.6883
34	34	35	143	0.005309	0.001486	2.651	0.1125
35	36	34	285	0.005428	0.00251	3.168	0.5742
36	37	36	136	0.006426	0.002252	3.168	0.4654
37	38	37	30	0.005551	0.002043	2.651	0.1786

Table A. 4-3 lists the network buses and load distribution among buses. The load in each bus is defined as a percentage of total load which is given in Table A. 4-1. There are totally 23 load nodes in the network. Third and sixth column in Table A. 4-3 record the minimal voltages for 0% load increase, in base case, i.e. when DSR and Storage facility are not exercised. It can be seen that in the base case there are no buses experiencing under-voltages, i.e. voltage in all buses is over the lower limit of 0.94p.u.

Table A. 4-3: Load distribution among buses (in percent) and minimal voltages obtained during peak hour for case 0% load growth

Bus	Load %	Vmin [p.u.]	Bus	Load %	Vmin [p.u.]
1	0	1.0961	20	0.0375	0.9704
2	0	1.034	21	0.0375	0.9704
3	0.0596	1.0337	22	0.0375	0.9691
4	0.0358	1.0335	23	0.0358	0.9682
5	0	1.0069	24	0	0.9682
6	0	1.0337	25	0.0358	0.9681
7	0	1.0042	26	0	0.9682
8	0	1.0069	27	0	0.966
9	0.1192	0.9992	28	0.0375	0.966
10	0.0358	1.0038	29	0	0.9656
11	0	0.9948	30	0.006	0.9654
12	0.0238	0.9946	31	0.0358	0.9613
13	0	0.9943	32	0	0.956
14	0.0298	0.9941	33	0.0375	0.9555
15	0.0358	0.9848	34	0	0.9537
16	0.0596	0.9714	35	0.0375	0.9532
17	0.0358	0.9678	36	0.0358	0.9509
18	0.0358	0.9671	37	0.0954	0.9482
19	0	0.9712	38	0.0596	0.9474

A4.2. Leighton Buzzard Substation Data

Table A. 4-4 below shows details on circuit data supplying Leighton Buzzard Substation: network topology, branch length, resistance, reactance and susceptance as well as thermal capacity limits. Last column represents apparent power snapshot at peak time, in normal working conditions.

Table A. 4-4: Circuit data for Leighton Buzzard Substation network

No.	From Bus	To Bus	Length	R	X	Susceptance	Thermal Capacity	Apparent Power at Peak
			[km]	% on 100MVA base		p.u.	[MVA]	
1	1	2	0.15	0.23	0.14	0.02	22.29	6.95
2	1	2	0.13	0.11	0.12	0.02	29.15	11.51
3	1’	2’	0.13	0.17	0.13	0.01	22.29	9.99
4	1’	2’	0.13	0.19	0.12	0.02	22.29	9.51
5	4	5	1.28	1.74	4.08	0.01	57.16	17.71
6	4’	5’	1.28	1.74	4.08	0.01	57.16	18.75
7	4’	3’	1.02	1.55	0.95	0.14	22.29	9.51
8	4’	3’	1.06	1.60	0.98	0.15	22.29	9.21
9	4	3	1.64	2.48	1.52	0.22	22.29	8.81
10	4	3	1.63	2.47	1.51	0.22	22.29	8.85
11	2’	3’	9.82	12.35	29.4	0.04	32.87	19.49
12	3	2	9.84	12.38	29.47	0.04	32.87	18.30

Table A. 4-5 below shows that transformers T1 and T2 have all the parameters practically equal, except a small difference in reactance.

Table A. 4-5: Transformer data for Leighton Buzzard Substation

From Primary			LEIGHT BUZZ T1 (Bus 5)	LEIGHT BUZZ T2 (Bus 5’)
Voltage Primary [kV]			33	33
To Secondary S1			Leight Buzz 11 BB (Bus 6)	Leight Buzz 11 BB (Bus 6’)
Voltage Secondary [kV]			11	11
Vector Group			Dy11	Dy11
Primary	R	% on 100MVA base	0.10	0.10
	X		47.02	47.43
Secondary	R		0.10	0.10
	X		31.35	31.62
Minimum Tap %			-17.0	-17.0
Maximum Tap %			3.0	3.0
TX Nameplate Rating MVA			19/38	19/38
TX Rating type			ONAN/ Emergency	ONAN/ Emergency

Table A. 4-6 shows that during critical working conditions, line Bus 2 – Bus 3 becomes overloaded.

Table A. 4-6: Snapshot of power flows during peak, 12th January 2011 at 18.00 in case of Branch 2 outage (all the load supplied from Branch 1)

No.	From Bus	To Bus	Thermal Capacity	Apparent Power at Peak
			[MVA]	
1	1	2	22.29	15.32
2	1	2	29.15	25.33
3	1’	2’	22.29	0
4	1’	2’	22.29	0
5	4	5	57.16	36.70
6	4’	5’	57.16	0
7	4’	3’	22.29	0
8	4’	3’	22.29	0
9	4	3	22.29	18.37
10	4	3	22.29	18.46
11	2’	3’	32.87	0
12	**3**	**2**	**32.87**	**40.28**

APPENDIX 5. Electric Vehicles

Table A. 5-1: Daily driven minimal distances (in 1,000 km) for given start and end times

End Time (hour of a day)

Start time (hour of a day)	0-1	1-2	2-3	3-4	4-5	5-6	6-7	7-8	8-9	9-10	10-11	11-12	12-13	13-14	14-15	15-16	16-17	17-18	18-19	19-20	20-21	21-22	22-23	23-24
0-1	1005.3	743.0	38.2	79.1	124.9	0.0	0.0	0.0	138.8	0.0	0.0	0.0	0.0	0.0	0.0	0.0	0.0	0.0	0.0	0.0	0.0	0.0	0.0	0.0
1-2	0.0	516.9	259.5	39.2	0.0	0.0	0.0	0.0	0.0	0.0	0.0	0.0	0.0	0.0	0.0	0.0	0.0	0.0	0.0	0.0	0.0	0.0	0.0	0.0
2-3	0.0	0.0	331.4	172.8	0.0	287.3	70.1	0.0	0.0	0.0	0.0	0.0	0.0	0.0	0.0	0.0	0.0	0.0	0.0	0.0	0.0	0.0	0.0	0.0
3-4	0.0	0.0	0.0	317.4	346.7	67.3	54.8	222.7	0.0	0.0	0.0	0.0	0.0	0.0	0.0	0.0	0.0	0.0	0.0	0.0	0.0	0.0	0.0	0.0
4-5	0.0	0.0	0.0	0.0	753.4	812.4	114.1	104.4	166.5	412.2	0.0	0.0	0.0	0.0	0.0	0.0	0.0	0.0	0.0	0.0	0.0	0.0	0.0	0.0
5-6	0.0	0.0	0.0	0.0	0.0	2670.5	3818.5	2410.1	737.6	677.9	630.1	0.0	0.0	0.0	248.4	0.0	0.0	0.0	0.0	0.0	0.0	0.0	0.0	0.0
6-7	0.0	0.0	0.0	0.0	0.0	0.0	6255.2	11170.9	3263.6	1995.1	905.7	589.7	253.0	159.3	18.0	0.0	0.0	0.0	0.0	0.0	0.0	0.0	0.0	0.0
7-8	0.0	0.0	0.0	0.0	0.0	0.0	0.0	18797.2	27170.8	5060.9	1630.0	597.4	186.2	564.4	0.0	30.2	0.0	269.2	0.0	0.0	0.0	0.0	0.0	0.0
8-9	0.0	0.0	0.0	0.0	0.0	0.0	0.0	0.0	27573.2	20477.5	4432.1	1868.5	821.2	381.4	302.7	0.0	0.0	69.6	240.1	0.0	0.0	0.0	0.0	0.0
9-10	0.0	0.0	0.0	0.0	0.0	0.0	0.0	0.0	0.0	17913.5	15492.6	4771.6	2689.8	772.1	400.4	191.2	31.9	347.0	0.0	291.4	0.0	0.0	0.0	0.0
10-11	0.0	0.0	0.0	0.0	0.0	0.0	0.0	0.0	0.0	0.0	20466.4	15396.3	4449.5	2825.6	445.3	780.4	364.4	92.6	156.8	0.0	0.0	0.0	0.0	0.0
11-12	0.0	0.0	0.0	0.0	0.0	0.0	0.0	0.0	0.0	0.0	0.0	20379.6	17041.3	3807.5	2022.5	1888.8	955.5	526.0	0.0	544.0	0.0	0.0	0.0	0.0
12-13	0.0	0.0	0.0	0.0	0.0	0.0	0.0	0.0	0.0	0.0	0.0	0.0	20310.3	16236.7	3447.6	2452.0	1206.0	958.3	695.4	141.6	127.7	0.0	111.0	0.0
13-14	0.0	0.0	0.0	0.0	0.0	0.0	0.0	0.0	0.0	0.0	0.0	0.0	0.0	20789.4	16336.7	3045.4	1832.7	827.5	584.6	562.1	0.0	0.0	0.0	0.0
14-15	0.0	0.0	0.0	0.0	0.0	0.0	0.0	0.0	0.0	0.0	0.0	0.0	0.0	0.0	20994.2	16776.9	4645.4	2701.3	888.5	216.5	596.8	315.0	0.0	0.0
15-16	0.0	0.0	0.0	0.0	0.0	0.0	0.0	0.0	0.0	0.0	0.0	0.0	0.0	0.0	0.0	23119.5	19626.5	6085.6	2675.7	1552.3	1038.8	283.1	12.8	0.0
16-17	0.0	0.0	0.0	0.0	0.0	0.0	0.0	0.0	0.0	0.0	0.0	0.0	0.0	0.0	0.0	0.0	25795.5	28722.3	6426.5	3315.9	1555.2	504.6	277.6	0.0
17-18	113.8	0.0	0.0	0.0	0.0	0.0	0.0	0.0	0.0	0.0	0.0	0.0	0.0	0.0	0.0	0.0	0.0	29906.1	28034.1	5817.2	1505.7	508.6	607.9	381.6
18-19	0.0	0.0	0.0	0.0	0.0	0.0	0.0	0.0	0.0	0.0	0.0	0.0	0.0	0.0	0.0	0.0	0.0	0.0	21398.9	16582.5	2841.6	1446.3	1097.8	165.1
19-20	124.9	113.8	0.0	0.0	0.0	0.0	0.0	148.5	0.0	0.0	0.0	0.0	0.0	0.0	0.0	0.0	0.0	0.0	0.0	15572.4	9890.4	2309.0	1549.5	238.0
20-21	347.0	0.0	0.0	0.0	115.2	0.0	0.0	0.0	0.0	0.0	0.0	0.0	0.0	0.0	0.0	0.0	0.0	0.0	0.0	0.0	10526.2	6361.7	1723.0	1073.8
21-22	601.6	0.0	116.6	0.0	0.0	0.0	0.0	0.0	0.0	0.0	0.0	0.0	0.0	0.0	0.0	0.0	0.0	0.0	0.0	0.0	0.0	8032.6	4981.5	954.1
22-23	442.8	324.3	0.0	0.0	0.0	0.0	0.0	0.0	0.0	0.0	0.0	0.0	0.0	0.0	0.0	0.0	0.0	0.0	0.0	0.0	0.0	0.0	6129.2	3733.6
23-24	2549.0	291.1	125.9	0.0	0.0	0.0	0.0	0.0	0.0	0.0	0.0	0.0	0.0	0.0	0.0	0.0	0.0	0.0	0.0	0.0	0.0	0.0	0.0	3723.9

Table A. 5-2: Energy (in MWh) required for the minimum driven distances

End Time (hour of a day)

Start time (hour of a day)	0-1	1-2	2-3	3-4	4-5	5-6	6-7	7-8	8-9	9-10	10-11	11-12	12-13	13-14	14-15	15-16	16-17	17-18	18-19	19-20	20-21	21-22	22-23	23-24
0-1	150.8	111.5	5.7	11.9	18.7	0.0	0.0	0.0	20.8	0.0	0.0	0.0	0.0	0.0	0.0	0.0	0.0	0.0	0.0	0.0	0.0	0.0	0.0	0.0
1-2	0.0	77.5	38.9	5.9	0.0	0.0	0.0	0.0	0.0	0.0	0.0	0.0	0.0	0.0	0.0	0.0	0.0	0.0	0.0	0.0	0.0	0.0	0.0	0.0
2-3	0.0	0.0	49.7	25.9	0.0	43.1	10.5	0.0	0.0	0.0	0.0	0.0	0.0	0.0	0.0	0.0	0.0	0.0	0.0	0.0	0.0	0.0	0.0	0.0
3-4	0.0	0.0	0.0	47.6	52.0	10.1	8.2	33.4	0.0	0.0	0.0	0.0	0.0	0.0	0.0	0.0	0.0	0.0	0.0	0.0	0.0	0.0	0.0	0.0
4-5	0.0	0.0	0.0	0.0	113.0	121.9	17.1	15.7	25.0	61.8	0.0	0.0	0.0	0.0	0.0	0.0	0.0	0.0	0.0	0.0	0.0	0.0	0.0	0.0
5-6	0.0	0.0	0.0	0.0	0.0	400.6	572.8	361.5	110.6	101.7	94.5	0.0	0.0	0.0	37.3	0.0	0.0	0.0	0.0	0.0	0.0	0.0	0.0	0.0
6-7	0.0	0.0	0.0	0.0	0.0	0.0	938.3	1675.6	489.5	299.3	135.9	88.5	37.9	23.9	2.7	0.0	0.0	0.0	0.0	0.0	0.0	0.0	0.0	0.0
7-8	0.0	0.0	0.0	0.0	0.0	0.0	0.0	2819.6	4075.6	759.1	244.5	89.6	27.9	84.7	0.0	4.5	0.0	40.4	0.0	0.0	0.0	0.0	0.0	0.0
8-9	0.0	0.0	0.0	0.0	0.0	0.0	0.0	0.0	4136.0	3071.6	664.8	280.3	123.2	57.2	45.4	0.0	0.0	10.4	36.0	0.0	0.0	0.0	0.0	0.0
9-10	0.0	0.0	0.0	0.0	0.0	0.0	0.0	0.0	0.0	2687.0	2323.9	715.7	403.5	115.8	60.1	28.7	4.8	52.0	0.0	43.7	0.0	0.0	0.0	0.0
10-11	0.0	0.0	0.0	0.0	0.0	0.0	0.0	0.0	0.0	0.0	3070.0	2309.4	667.4	423.8	66.8	117.1	54.7	13.9	23.5	0.0	0.0	0.0	0.0	0.0
11-12	0.0	0.0	0.0	0.0	0.0	0.0	0.0	0.0	0.0	0.0	0.0	3056.9	2556.2	571.1	303.4	283.3	143.3	78.9	0.0	81.6	0.0	0.0	0.0	0.0
12-13	0.0	0.0	0.0	0.0	0.0	0.0	0.0	0.0	0.0	0.0	0.0	0.0	3046.5	2435.5	517.1	367.8	180.9	143.7	104.3	21.2	19.2	0.0	16.7	0.0
13-14	0.0	0.0	0.0	0.0	0.0	0.0	0.0	0.0	0.0	0.0	0.0	0.0	0.0	3118.4	2450.5	456.8	274.9	124.1	87.7	84.3	0.0	0.0	0.0	0.0
14-15	0.0	0.0	0.0	0.0	0.0	0.0	0.0	0.0	0.0	0.0	0.0	0.0	0.0	0.0	3149.1	2516.5	696.8	405.2	133.3	32.5	89.5	47.3	0.0	0.0
15-16	0.0	0.0	0.0	0.0	0.0	0.0	0.0	0.0	0.0	0.0	0.0	0.0	0.0	0.0	0.0	3467.9	2944.0	912.8	401.4	232.8	155.8	42.5	1.9	0.0
16-17	0.0	0.0	0.0	0.0	0.0	0.0	0.0	0.0	0.0	0.0	0.0	0.0	0.0	0.0	0.0	0.0	3869.3	4308.3	964.0	497.4	233.3	75.7	41.6	0.0
17-18	17.1	0.0	0.0	0.0	0.0	0.0	0.0	0.0	0.0	0.0	0.0	0.0	0.0	0.0	0.0	0.0	0.0	4485.9	4205.1	872.6	225.9	76.3	91.2	57.2
18-19	0.0	0.0	0.0	0.0	0.0	0.0	0.0	0.0	0.0	0.0	0.0	0.0	0.0	0.0	0.0	0.0	0.0	0.0	3209.8	2487.4	426.2	216.9	164.7	24.8
19-20	18.7	17.1	0.0	0.0	0.0	0.0	0.0	22.3	0.0	0.0	0.0	0.0	0.0	0.0	0.0	0.0	0.0	0.0	0.0	2335.9	1483.6	346.3	232.4	35.7
20-21	52.0	0.0	0.0	0.0	17.3	0.0	0.0	0.0	0.0	0.0	0.0	0.0	0.0	0.0	0.0	0.0	0.0	0.0	0.0	0.0	1578.9	954.3	258.4	161.1
21-22	90.2	0.0	17.5	0.0	0.0	0.0	0.0	0.0	0.0	0.0	0.0	0.0	0.0	0.0	0.0	0.0	0.0	0.0	0.0	0.0	0.0	1204.9	747.2	143.1
22-23	66.4	48.6	0.0	0.0	0.0	0.0	0.0	0.0	0.0	0.0	0.0	0.0	0.0	0.0	0.0	0.0	0.0	0.0	0.0	0.0	0.0	0.0	919.4	560.0
23-24	382.3	43.7	18.9	0.0	0.0	0.0	0.0	0.0	0.0	0.0	0.0	0.0	0.0	0.0	0.0	0.0	0.0	0.0	0.0	0.0	0.0	0.0	0.0	558.6

Table A. 5-3: Daily driven maximal distances (in 1,000 km) for given start and end times

End Time (hour of a day)

Start time (hour of a day)	0-1	1-2	2-3	3-4	4-5	5-6	6-7	7-8	8-9	9-10	10-11	11-12	12-13	13-14	14-15	15-16	16-17	17-18	18-19	19-20	20-21	21-22	22-23	23-24
0-1	1682.9	1221.0	76.329	158.20	149.88	0	0	0	333.07	0	0	0	0	0	0	0	0	0	0	0	0	0	0	0
1-2	0	876.80	436.72	78.410	0	0	0	0	0	0	0	0	0	0	0	0	0	0	0	0	0	0	0	0
2-3	0	0	549.27	281.04	0	574.54	140.16	0	0	0	0	0	0	0	0	0	0	0	0	0	0	0	0	0
3-4	0	0	0	528.51	575.93	134.61	109.63	340.01	0	0	0	0	0	0	0	0	0	0	0	0	0	0	0	0
4-5	0	0	0	0	1246.3	1281.7	228.29	208.86	199.84	618.26	0	0	0	0	0	0	0	0	0	0	0	0	0	0
5-6	0	0	0	0	0	4479.9	6076.8	4779.5	1303.8	1113.8	1039.4	0	0	0	670.72	0	0	0	0	0	0	0	0	0
6-7	0	0	0	0	0	0	10429.	18184.	6140.9	3813.8	1482.1	920.59	472.13	329.88	25.257	0	0	0	0	0	0	0	0	0
7-8	0	0	0	0	0	0	0	31488.	44634.	9549.0	3071.9	977.42	276.45	1008.3	0	48.295	0	807.70	0	0	0	0	0	0
8-9	0	0	0	0	0	0	0	0	46695.	33908.	8578.7	3725.5	1510.3	662.74	557.54	0	0	122.82	720.26	0	0	0	0	0
9-10	0	0	0	0	0	0	0	0	0	30458.	25689.	9306.7	4794.0	1184.7	662.67	349.10	51.626	791.04	0	874.31	0	0	0	0
10-11	0	0	0	0	0	0	0	0	0	0	34612.	25532.	8521.6	5480.4	762.77	1327.6	650.84	185.27	376.37	0	0	0	0	0
11-12	0	0	0	0	0	0	0	0	0	0	0	34692.	28426.	7313.8	3845.1	2808.3	1539.0	946.75	0	1278.9	0	0	0	0
12-13	0	0	0	0	0	0	0	0	0	0	0	0	34599.	27072.	6618.9	4638.3	1971.7	1548.0	1254.6	283.11	306.42	0	333.07	0
13-14	0	0	0	0	0	0	0	0	0	0	0	0	0	35423.	26915.	5797.6	3362.7	1506.4	908.80	1011.7	0	0	0	0
14-15	0	0	0	0	0	0	0	0	0	0	0	0	0	0	35649.	27797.	8788.0	5109.6	1533.9	324.74	1081.0	661.56	0	0
15-16	0	0	0	0	0	0	0	0	0	0	0	0	0	0	0	39138.	32166.	11712.	4838.9	2520.5	1594.5	509.60	21.337	0
16-17	0	0	0	0	0	0	0	0	0	0	0	0	0	0	0	0	43792.	47438.	12167.	5690.5	2512.4	801.28	499.60	0
17-18	238.97	0	0	0	0	0	0	0	0	0	0	0	0	0	0	0	0	50578.	45840.	11036.	2676.0	857.17	999.21	686.96
18-19	0	0	0	0	0	0	0	0	0	0	0	0	0	0	0	0	0	0	36268.	27906.	5455.3	2753.7	1643.7	247.72
19-20	187.35	204.83	0	0	0	0	0	534.58	0	0	0	0	0	0	0	0	0	0	0	26479.	16631.	4516.9	2789.1	343.89
20-21	520.42	0	0	0	276.45	0	0	0	0	0	0	0	0	0	0	0	0	0	0	0	17850.	10692.	3369.2	1864.1
21-22	1203.2	0	174.86	0	0	0	0	0	0	0	0	0	0	0	0	0	0	0	0	0	0	13633.	8374.0	1838.5
22-23	880.90	645.50	0	0	0	0	0	0	0	0	0	0	0	0	0	0	0	0	0	0	0	0	10413.	6155.9
23-24	4341.3	564.10	251.88	0	0	0	0	0	0	0	0	0	0	0	0	0	0	0	0	0	0	0	0	6329.4

Table A. 5-4: Energy (in MWh) required for the maximum driven distances

Start time (hour of a day) \ End Time (hour of a day)	0-1	1-2	2-3	3-4	4-5	5-6	6-7	7-8	8-9	9-10	10-11	11-12	12-13	13-14	14-15	15-16	16-17	17-18	18-19	19-20	20-21	21-22	22-23	23-24
0-1	252.4	183.2	11.4	23.7	22.5	0.0	0.0	0.0	50.0	0.0	0.0	0.0	0.0	0.0	0.0	0.0	0.0	0.0	0.0	0.0	0.0	0.0	0.0	0.0
1-2	0.0	131.5	65.5	11.8	0.0	0.0	0.0	0.0	0.0	0.0	0.0	0.0	0.0	0.0	0.0	0.0	0.0	0.0	0.0	0.0	0.0	0.0	0.0	0.0
2-3	0.0	0.0	82.4	42.2	0.0	86.2	21.0	0.0	0.0	0.0	0.0	0.0	0.0	0.0	0.0	0.0	0.0	0.0	0.0	0.0	0.0	0.0	0.0	0.0
3-4	0.0	0.0	0.0	79.3	86.4	20.2	16.4	51.0	0.0	0.0	0.0	0.0	0.0	0.0	0.0	0.0	0.0	0.0	0.0	0.0	0.0	0.0	0.0	0.0
4-5	0.0	0.0	0.0	0.0	187.0	192.3	34.2	31.3	30.0	92.7	0.0	0.0	0.0	0.0	0.0	0.0	0.0	0.0	0.0	0.0	0.0	0.0	0.0	0.0
5-6	0.0	0.0	0.0	0.0	0.0	672.0	911.5	716.9	195.6	167.1	155.9	0.0	0.0	0.0	100.6	0.0	0.0	0.0	0.0	0.0	0.0	0.0	0.0	0.0
6-7	0.0	0.0	0.0	0.0	0.0	0.0	1564.4	2727.7	921.1	572.1	222.3	138.1	70.8	49.5	3.8	0.0	0.0	0.0	0.0	0.0	0.0	0.0	0.0	0.0
7-8	0.0	0.0	0.0	0.0	0.0	0.0	0.0	4723.2	6695.2	1432.4	460.8	146.6	41.5	151.3	0.0	7.2	0.0	121.2	0.0	0.0	0.0	0.0	0.0	0.0
8-9	0.0	0.0	0.0	0.0	0.0	0.0	0.0	0.0	7004.3	5086.3	1286.8	558.8	226.6	99.4	83.6	0.0	0.0	18.4	108.0	0.0	0.0	0.0	0.0	0.0
9-10	0.0	0.0	0.0	0.0	0.0	0.0	0.0	0.0	0.0	4568.8	3853.5	1396.0	719.1	177.7	99.4	52.4	7.7	118.7	0.0	131.1	0.0	0.0	0.0	0.0
10-11	0.0	0.0	0.0	0.0	0.0	0.0	0.0	0.0	0.0	0.0	5191.8	3829.9	1278.2	822.1	114.4	199.1	97.6	27.8	56.5	0.0	0.0	0.0	0.0	0.0
11-12	0.0	0.0	0.0	0.0	0.0	0.0	0.0	0.0	0.0	0.0	0.0	5203.9	4264.0	1097.1	576.8	421.3	230.9	142.0	0.0	191.8	0.0	0.0	0.0	0.0
12-13	0.0	0.0	0.0	0.0	0.0	0.0	0.0	0.0	0.0	0.0	0.0	0.0	5190.0	4060.9	992.8	695.7	295.8	232.2	188.2	42.5	46.0	0.0	50.0	0.0
13-14	0.0	0.0	0.0	0.0	0.0	0.0	0.0	0.0	0.0	0.0	0.0	0.0	0.0	5313.5	4037.3	869.7	504.4	226.0	136.3	151.8	0.0	0.0	0.0	0.0
14-15	0.0	0.0	0.0	0.0	0.0	0.0	0.0	0.0	0.0	0.0	0.0	0.0	0.0	0.0	5347.4	4169.7	1318.2	766.4	230.1	48.7	162.2	99.2	0.0	0.0
15-16	0.0	0.0	0.0	0.0	0.0	0.0	0.0	0.0	0.0	0.0	0.0	0.0	0.0	0.0	0.0	5870.8	4825.0	1756.9	725.8	378.1	239.2	76.4	3.2	0.0
16-17	0.0	0.0	0.0	0.0	0.0	0.0	0.0	0.0	0.0	0.0	0.0	0.0	0.0	0.0	0.0	0.0	6568.8	7115.8	1825.1	853.6	376.9	120.2	74.9	0.0
17-18	35.8	0.0	0.0	0.0	0.0	0.0	0.0	0.0	0.0	0.0	0.0	0.0	0.0	0.0	0.0	0.0	0.0	7586.8	6876.0	1655.4	401.4	128.6	149.9	103.0
18-19	0.0	0.0	0.0	0.0	0.0	0.0	0.0	0.0	0.0	0.0	0.0	0.0	0.0	0.0	0.0	0.0	0.0	0.0	5440.3	4186.0	818.3	413.1	246.6	37.2
19-20	28.1	30.7	0.0	0.0	0.0	0.0	0.0	80.2	0.0	0.0	0.0	0.0	0.0	0.0	0.0	0.0	0.0	0.0	0.0	3972.0	2494.7	677.5	418.4	51.6
20-21	78.1	0.0	0.0	0.0	41.5	0.0	0.0	0.0	0.0	0.0	0.0	0.0	0.0	0.0	0.0	0.0	0.0	0.0	0.0	0.0	2677.5	1603.9	505.4	279.6
21-22	180.5	0.0	26.2	0.0	0.0	0.0	0.0	0.0	0.0	0.0	0.0	0.0	0.0	0.0	0.0	0.0	0.0	0.0	0.0	0.0	0.0	2045.1	1256.1	275.8
22-23	132.1	96.8	0.0	0.0	0.0	0.0	0.0	0.0	0.0	0.0	0.0	0.0	0.0	0.0	0.0	0.0	0.0	0.0	0.0	0.0	0.0	0.0	1562.0	923.4
23-24	651.2	84.6	37.8	0.0	0.0	0.0	0.0	0.0	0.0	0.0	0.0	0.0	0.0	0.0	0.0	0.0	0.0	0.0	0.0	0.0	0.0	0.0	0.0	949.4

Table A. 5-5: Daily driven short distances (≤ 15 miles) defined with start time and end time (in 1,000 km)

Start time (hour of a day) \ End Time (hour of a day)	0-1	1-2	2-3	3-4	4-5	5-6	6-7	7-8	8-9	9-10	10-11	11-12	12-13	13-14	14-15	15-16	16-17	17-18	18-19	19-20	20-21	21-22	22-23	23-24
0-1	905.18	150.66	0	0	0	0	0	0	0	0	0	0	0	0	0	0	0	0	0	0	0	0	0	0
1-2	0	387.60	119.44	0	0	0	0	0	0	0	0	0	0	0	0	0	0	0	0	0	0	0	0	0
2-3	0	0	297.45	49.201	0	0	0	0	0	0	0	0	0	0	0	0	0	0	0	0	0	0	0	0
3-4	0	0	0	197.00	133.49	0	0	0	0	0	0	0	0	0	0	0	0	0	0	0	0	0	0	0
4-5	0	0	0	0	690.50	237.22	0	0	0	0	0	0	0	0	0	0	0	0	0	0	0	0	0	0
5-6	0	0	0	0	0	2328.8	1110.9	0	0	0	0	0	0	0	0	0	0	0	0	0	0	0	0	0
6-7	0	0	0	0	0	0	5382.7	3355.7	16.844	0	9.0207	8.5002	0	0	0	0	0	0	0	0	0	0	0	0
7-8	0	0	0	0	0	0	0	15895.	10012.	52.680	0	0	0	0	0	15.092	0	0	0	0	0	0	0	0
8-9	0	0	0	0	0	0	0	0	28528.	9960.1	52.753	10.148	0	17.694	0	0	0	0	0	0	0	0	0	0
9-10	0	0	0	0	0	0	0	0	0	19506.	6541.8	49.509	15.369	11.674	0	13.721	22.215	0	0	0	0	0	0	0
10-11	0	0	0	0	0	0	0	0	0	0	21378.	6436.0	31.773	7.1124	5.0481	0	7.4594	0	0	0	0	0	0	0
11-12	0	0	0	0	0	0	0	0	0	0	0	22056.	7684.8	90.588	0	0	0	0	0	0	0	0	0	0
12-13	0	0	0	0	0	0	0	0	0	0	0	0	22049.	7669.4	76.204	7.2339	0	0	0	0	0	0	0	0
13-14	0	0	0	0	0	0	0	0	0	0	0	0	0	22401.	7301.0	97.340	0	0	0	0	0	0	0	0
14-15	0	0	0	0	0	0	0	0	0	0	0	0	0	0	21948.	7971.8	54.096	8.4135	0	0	0	0	0	0
15-16	0	0	0	0	0	0	0	0	0	0	0	0	0	0	0	24412.	8893.7	55.564	17.607	0	0	0	0	0
16-17	0	0	0	0	0	0	0	0	0	0	0	0	0	0	0	0	26520.	10922.	67.395	0	0	0	0	0
17-18	0	0	0	0	0	0	0	0	0	0	0	0	0	0	0	0	0	29389.	10260.	65.400	0	0	0	0
18-19	0	0	0	0	0	0	0	0	0	0	0	0	0	0	0	0	0	0	20890.	6618.9	46.272	4.2154	0	0
19-20	0	0	0	0	0	0	0	0	0	0	0	0	0	0	0	0	0	0	0	16151.	3546.0	14.852	0	0
20-21	0	0	0	0	0	0	0	0	0	0	0	0	0	0	0	0	0	0	0	0	10695.	2651.9	0	0
21-22	0	0	0	0	0	0	0	0	0	0	0	0	0	0	0	0	0	0	0	0	0	8361.3	1928.7	0
22-23	0	0	0	0	0	0	0	0	0	0	0	0	0	0	0	0	0	0	0	0	0	0	5838.3	1301.1
23-24	756.63	0	0	0	0	0	0	0	0	0	0	0	0	0	0	0	0	0	0	0	0	0	0	3348.0

Table A. 5-6: Daily driven medium distances (15 ÷ 50 miles) defined with start time and end time (in 1,000 km)

Start time (hour of a day) \ End Time (hour of a day)	0-1	1-2	2-3	3-4	4-5	5-6	6-7	7-8	8-9	9-10	10-11	11-12	12-13	13-14	14-15	15-16	16-17	17-18	18-19	19-20	20-21	21-22	22-23	23-24
0-1	392.07	534.21	0	0	0	0	0	0	0	0	0	0	0	0	0	0	0	0	0	0	0	0	0	0
1-2	0	254.59	128.73	0	0	0	0	0	0	0	0	0	0	0	0	0	0	0	0	0	0	0	0	0
2-3	0	0	142.87	123.06	0	0	0	0	0	0	0	0	0	0	0	0	0	0	0	0	0	0	0	0
3-4	0	0	0	225.93	233.13	0	0	0	0	0	0	0	0	0	0	0	0	0	0	0	0	0	0	0
4-5	0	0	0	0	246.95	741.17	0	0	0	0	0	0	0	0	0	0	0	0	0	0	0	0	0	0
5-6	0	0	0	0	0	1246.3	3155.5	86.113	0	0	0	0	0	0	0	0	0	0	0	0	0	0	0	0
6-7	0	0	0	0	0	0	2849.1	8363.4	801.00	75.201	48.573	0	14.433	14.433	21.649	0	0	0	0	0	0	0	0	0
7-8	0	0	0	0	0	0	0	9182.8	20592.	1227.3	38.702	17.486	42.258	24.772	0	24.147	0	0	0	0	0	0	0	0
8-9	0	0	0	0	0	0	0	0	8547.8	13094.	592.14	28.102	0	14.155	14.155	0	0	34.799	0	0	0	0	0	0
9-10	0	0	0	0	0	0	0	0	0	4629.8	9981.6	479.67	109.06	0	0	69.077	19.568	0	0	0	0	0	0	0
10-11	0	0	0	0	0	0	0	0	0	0	6002.2	9853.0	805.60	80.214	13.739	55.147	39.986	0	0	0	0	0	0	0
11-12	0	0	0	0	0	0	0	0	0	0	0	5368.8	10611.	618.69	107.36	0	0	0	0	0	0	0	0	0
12-13	0	0	0	0	0	0	0	0	0	0	0	0	5405.2	10064.	556.36	42.796	47.879	0	32.144	0	0	0	0	0
13-14	0	0	0	0	0	0	0	0	0	0	0	0	0	5704.5	10945	589.12	63.110	29.976	25.396	0	0	0	0	0
14-15	0	0	0	0	0	0	0	0	0	0	0	0	0	0	6219.3	10543.	1067.4	91.161	0	0	0	0	0	0
15-16	0	0	0	0	0	0	0	0	0	0	0	0	0	0	0	6716.1	13506.	990.36	19.359	0	0	0	17.069	0
16-17	0	0	0	0	0	0	0	0	0	0	0	0	0	0	0	0	8211.2	20139.	1470.6	67.377	27.131	27.062	0	0
17-18	0	0	0	0	0	0	0	0	0	0	0	0	0	0	0	0	0	10754.	20321.	1314.6	52.458	28.606	0	0
18-19	0	0	0	0	0	0	0	0	0	0	0	0	0	0	0	0	0	0	7535.2	9935.2	460.76	45.710	0	0
19-20	0	0	0	0	0	0	0	0	0	0	0	0	0	0	0	0	0	0	0	4764.6	6197.7	209.97	0	0
20-21	0	0	0	0	0	0	0	0	0	0	0	0	0	0	0	0	0	0	0	0	3347.9	3973.1	161.50	0
21-22	0	0	0	0	0	0	0	0	0	0	0	0	0	0	0	0	0	0	0	0	0	2417.1	3119.1	143.67
22-23	18.596	12.351	0	0	0	0	0	0	0	0	0	0	0	0	0	0	0	0	0	0	0	0	2373.0	2493.9
23-24	1652.8	37.262	0	0	0	0	0	0	0	0	0	0	0	0	0	0	0	0	0	0	0	0	0	1567.2

Table A. 5-7: Daily driven long distances (50+ miles) defined with start time and end time (in 1,000 km)

End Time (hour of a day)

Start time (hour of a day)	0-1	1-2	2-3	3-4	4-5	5-6	6-7	7-8	8-9	9-10	10-11	11-12	12-13	13-14	14-15	15-16	16-17	17-18	18-19	19-20	20-21	21-22	22-23	23-24
0-1	46.838	297.16	57.246	118.65	0	0	0	0	0	0	0	0	0	0	0	0	0	0	0	0	0	0	0	0
1-2	0	54.644	99.921	58.808	0	0	0	0	0	0	0	0	0	0	0	0	0	0	0	0	0	0	0	0
2-3	0	0	0	54.644	0	430.91	105.12	0	0	0	0	0	0	0	0	0	0	0	0	0	0	0	0	0
3-4	0	0	0	0	94.717	100.96	82.227	136.35	0	0	0	0	0	0	0	0	0	0	0	0	0	0	0	0
4-5	0	0	0	0	62.451	68.696	171.22	156.64	0	0	0	0	0	0	0	0	0	0	0	0	0	0	0	0
5-6	0	0	0	0	0	0	681.23	3508.7	835.80	563.10	283.11	0	0	0	0	0	0	0	0	0	0	0	0	0
6-7	0	0	0	0	0	0	110.33	2958.6	3884.4	2677.0	711.94	108.24	136.35	0	0	0	0	0	0	0	0	0	0	0
7-8	0	0	0	0	0	0	0	64.012	5296.8	6024.9	2125.9	482.95	0	0	0	0	0	0	0	0	0	0	0	0
8-9	0	0	0	0	0	0	0	0	58.287	4138.9	5860.5	2758.7	984.12	266.45	105.12	0	0	61.410	0	0	0	0	0	0
9-10	0	0	0	0	0	0	0	0	0	49.960	4067.6	6510.0	3041.3	476.70	186.31	187.35	0	156.12	0	0	0	0	0	0
10-11	0	0	0	0	0	0	0	0	0	0	158.20	4175.3	5648.1	3917.7	414.25	466.30	46.317	138.95	0	0	0	0	0	0
11-12	0	0	0	0	0	0	0	0	0	0	0	110.33	4437.1	4851.4	2661.4	1015.8	317.45	0	0	99.921	0	0	0	0
12-13	0	0	0	0	0	0	0	0	0	0	0	0	0	3920.8	4400.7	3227.6	968.51	332.03	95.758	212.33	0	0	0	0
13-14	0	0	0	0	0	0	0	0	0	0	0	0	0	0	3380.1	3735.0	2237.3	949.25	102.00	0	0	0	0	0
14-15	0	0	0	0	0	0	0	0	0	0	0	0	0	0	154.04	3772.0	5595.0	3534.2	876.91	0	52.042	0	0	0
15-16	0	0	0	0	0	0	0	0	0	0	0	0	0	0	0	0	3496.2	7853.2	3185.5	1233.4	109.28	0	0	0
16-17	0	0	0	0	0	0	0	0	0	0	0	0	0	0	0	0	62.451	7017.9	7759.0	3451.4	1202.1	122.82	0	0
17-18	0	0	0	0	0	0	0	0	0	0	0	0	0	0	0	0	0	98.360	6355.9	7046.5	1701.2	452.77	262.29	0
18-19	0	0	0	0	0	0	0	0	0	0	0	0	0	0	0	0	0	0	408.01	5690.3	3641.4	1923.4	612.02	0
19-20	0	0	0	0	0	0	0	0	0	0	0	0	0	0	0	0	0	0	0	110.33	3517.0	3188.1	1835.0	109.28
20-21	0	0	0	0	0	0	0	0	0	0	0	0	0	0	0	0	0	0	0	145.19	1902.1	2384.5	1163.1	
21-22	902.41	0	0	0	0	0	0	0	0	0	0	0	0	0	0	0	0	0	0	0	0	54.644	1629.9	1252.6
22-23	643.24	472.54	0	0	0	0	0	0	0	0	0	0	0	0	0	0	0	0	0	0	0	0	59.848	1149.6
23-24	1035.6	390.31	188.91	0	0	0	0	0	0	0	0	0	0	0	0	0	0	0	0	0	0	0	0	111.37

Table A. 5-8: Energy required for short distances (in MWh)

End Time (hour of a day)

Start time (hour of a day)	0-1	1-2	2-3	3-4	4-5	5-6	6-7	7-8	8-9	9-10	10-11	11-12	12-13	13-14	14-15	15-16	16-17	17-18	18-19	19-20	20-21	21-22	22-23	23-24
0-1	135.77	22.599	0	0	0	0	0	0	0	0	0	0	0	0	0	0	0	0	0	0	0	0	0	0
1-2	0	58.140	17.917	0	0	0	0	0	0	0	0	0	0	0	0	0	0	0	0	0	0	0	0	0
2-3	0	0	44.617	7.3801	0	0	0	0	0	0	0	0	0	0	0	0	0	0	0	0	0	0	0	0
3-4	0	0	0	29.550	20.023	0	0	0	0	0	0	0	0	0	0	0	0	0	0	0	0	0	0	0
4-5	0	0	0	0	103.57	35.583	0	0	0	0	0	0	0	0	0	0	0	0	0	0	0	0	0	0
5-6	0	0	0	0	0	349.32	166.63	0	0	0	0	0	0	0	0	0	0	0	0	0	0	0	0	0
6-7	0	0	0	0	0	0	807.40	503.36	2.5266	0	1.3531	1.2750	0	0	0	0	0	0	0	0	0	0	0	0
7-8	0	0	0	0	0	0	0	2384.3	1501.9	7.9021	0	0	0	0	0	2.2638	0	0	0	0	0	0	0	0
8-9	0	0	0	0	0	0	0	0	4279.2	1494.0	7.9130	1.5222	0	2.6541	0	0	0	0	0	0	0	0	0	0
9-10	0	0	0	0	0	0	0	0	0	2925.9	981.27	7.4264	2.3054	1.7512	0	2.0582	3.3322	0	0	0	0	0	0	0
10-11	0	0	0	0	0	0	0	0	0	0	3206.8	965.41	4.7660	1.0668	0.7572	0	1.1189	0	0	0	0	0	0	0
11-12	0	0	0	0	0	0	0	0	0	0	0	3308.5	1152.7	13.588	0	0	0	0	0	0	0	0	0	0
12-13	0	0	0	0	0	0	0	0	0	0	0	0	3307.4	1150.4	11.430	1.0850	0	0	0	0	0	0	0	0
13-14	0	0	0	0	0	0	0	0	0	0	0	0	0	3360.2	1095.1	14.601	0	0	0	0	0	0	0	0
14-15	0	0	0	0	0	0	0	0	0	0	0	0	0	0	3292.2	1195.7	8.1144	1.2620	0	0	0	0	0	0
15-16	0	0	0	0	0	0	0	0	0	0	0	0	0	0	0	3661.9	1334.0	8.3346	2.6411	0	0	0	0	0
16-17	0	0	0	0	0	0	0	0	0	0	0	0	0	0	0	0	3978.0	1638.4	10.109	0	0	0	0	0
17-18	0	0	0	0	0	0	0	0	0	0	0	0	0	0	0	0	0	4408.4	1539.0	9.8100	0	0	0	0
18-19	0	0	0	0	0	0	0	0	0	0	0	0	0	0	0	0	0	0	3133.5	992.83	6.9409	0.6323	0	0
19-20	0	0	0	0	0	0	0	0	0	0	0	0	0	0	0	0	0	0	0	2422.6	531.90	2.2279	0	0
20-21	0	0	0	0	0	0	0	0	0	0	0	0	0	0	0	0	0	0	0	0	1604.2	397.79	0	0
21-22	0	0	0	0	0	0	0	0	0	0	0	0	0	0	0	0	0	0	0	0	0	1254.2	289.30	0
22-23	0	0	0	0	0	0	0	0	0	0	0	0	0	0	0	0	0	0	0	0	0	0	875.75	195.17
23-24	113.49	0	0	0	0	0	0	0	0	0	0	0	0	0	0	0	0	0	0	0	0	0	0	502.21

Table A. 5-9: Energy required for medium distances (in MWh)

End Time (hour of a day)

Start time (hour of a day)	0-1	1-2	2-3	3-4	4-5	5-6	6-7	7-8	8-9	9-10	10-11	11-12	12-13	13-14	14-15	15-16	16-17	17-18	18-19	19-20	20-21	21-22	22-23	23-24
0-1	58.810	80.132	0	0	0	0	0	0	0	0	0	0	0	0	0	0	0	0	0	0	0	0	0	0
1-2	0	38.188	19.310	0	0	0	0	0	0	0	0	0	0	0	0	0	0	0	0	0	0	0	0	0
2-3	0	0	21.431	18.459	0	0	0	0	0	0	0	0	0	0	0	0	0	0	0	0	0	0	0	0
3-4	0	0	0	33.890	34.969	0	0	0	0	0	0	0	0	0	0	0	0	0	0	0	0	0	0	0
4-5	0	0	0	0	37.043	111.17	0	0	0	0	0	0	0	0	0	0	0	0	0	0	0	0	0	0
5-6	0	0	0	0	0	186.95	473.32	12.916	0	0	0	0	0	0	0	0	0	0	0	0	0	0	0	0
6-7	0	0	0	0	0	0	427.36	1254.5	120.15	11.280	7.2859	0	2.1649	2.1649	3.2474	0	0	0	0	0	0	0	0	0
7-8	0	0	0	0	0	0	0	1377.4	3088.9	184.09	5.8053	2.6229	6.3387	3.7158	0	3.6221	0	0	0	0	0	0	0	0
8-9	0	0	0	0	0	0	0	0	1282.1	1964.1	88.821	4.2154	0	2.1233	2.1233	0	0	5.2198	0	0	0	0	0	0
9-10	0	0	0	0	0	0	0	0	0	694.47	1497.2	71.951	16.359	0	0	10.361	2.9352	0	0	0	0	0	0	0
10-11	0	0	0	0	0	0	0	0	0	0	900.33	1477.9	120.84	12.032	2.0608	8.2721	5.9979	0	0	0	0	0	0	0
11-12	0	0	0	0	0	0	0	0	0	0	0	805.32	1591.7	92.804	16.104	0	0	0	0	0	0	0	0	0
12-13	0	0	0	0	0	0	0	0	0	0	0	0	810.78	1509.6	83.455	6.4194	7.1818	0	4.8217	0	0	0	0	0
13-14	0	0	0	0	0	0	0	0	0	0	0	0	0	855.67	1641.7	88.368	9.4665	4.4964	3.8095	0	0	0	0	0
14-15	0	0	0	0	0	0	0	0	0	0	0	0	0	0	932.90	1581.5	160.12	13.674	0	0	0	0	0	0
15-16	0	0	0	0	0	0	0	0	0	0	0	0	0	0	0	1007.4	2025.9	148.55	2.9039	0	0	0	2.5604	0
16-17	0	0	0	0	0	0	0	0	0	0	0	0	0	0	0	0	1231.6	3020.9	220.59	10.106	4.0697	4.0593	0	0
17-18	0	0	0	0	0	0	0	0	0	0	0	0	0	0	0	0	0	1613.1	3048.1	197.20	7.8688	4.2909	0	0
18-19	0	0	0	0	0	0	0	0	0	0	0	0	0	0	0	0	0	0	1130.2	1490.2	69.115	6.8566	0	0
19-20	0	0	0	0	0	0	0	0	0	0	0	0	0	0	0	0	0	0	0	714.69	929.65	31.496	0	0
20-21	0	0	0	0	0	0	0	0	0	0	0	0	0	0	0	0	0	0	0	0	502.18	595.96	24.225	0
21-22	0	0	0	0	0	0	0	0	0	0	0	0	0	0	0	0	0	0	0	0	0	362.57	467.86	21.550
22-23	2.7894	1.8527	0	0	0	0	0	0	0	0	0	0	0	0	0	0	0	0	0	0	0	0	355.96	374.09
23-24	247.92	5.5893	0	0	0	0	0	0	0	0	0	0	0	0	0	0	0	0	0	0	0	0	0	235.08

Table A. 5-10: Energy required for long distances (in MWh)

End Time (hour of a day)

Start time (hour of a day)	0-1	1-2	2-3	3-4	4-5	5-6	6-7	7-8	8-9	9-10	10-11	11-12	12-13	13-14	14-15	15-16	16-17	17-18	18-19	19-20	20-21	21-22	22-23	23-24
0-1	7.0257	44.574	8.5870	17.798	0	0	0	0	0	0	0	0	0	0	0	0	0	0	0	0	0	0	0	0
1-2	0	8.1967	14.988	8.8212	0	0	0	0	0	0	0	0	0	0	0	0	0	0	0	0	0	0	0	0
2-3	0	0	0	8.1967	0	64.636	15.768	0	0	0	0	0	0	0	0	0	0	0	0	0	0	0	0	0
3-4	0	0	0	0	14.207	15.144	12.334	20.452	0	0	0	0	0	0	0	0	0	0	0	0	0	0	0	0
4-5	0	0	0	0	9.3676	10.304	25.683	23.497	0	0	0	0	0	0	0	0	0	0	0	0	0	0	0	0
5-6	0	0	0	0	0	0	102.18	526.30	125.37	84.465	42.466	0	0	0	0	0	0	0	0	0	0	0	0	0
6-7	0	0	0	0	0	0	16.549	443.79	582.66	401.56	106.79	16.237	20.452	0	0	0	0	0	0	0	0	0	0	0
7-8	0	0	0	0	0	0	0	9.6018	794.53	903.74	318.89	72.443	0	0	0	0	0	0	0	0	0	0	0	0
8-9	0	0	0	0	0	0	0	0	8.7431	620.84	879.07	413.81	147.61	39.968	15.768	0	0	9.2115	0	0	0	0	0	0
9-10	0	0	0	0	0	0	0	0	0	7.4941	610.14	976.50	456.20	71.506	27.946	28.102	0	23.419	0	0	0	0	0	0
10-11	0	0	0	0	0	0	0	0	0	0	23.731	626.30	847.22	587.66	62.138	69.945	6.9476	20.843	0	0	0	0	0	0
11-12	0	0	0	0	0	0	0	0	0	0	0	16.549	665.57	727.71	399.21	152.38	47.618	0	0	14.988	0	0	0	0
12-13	0	0	0	0	0	0	0	0	0	0	0	0	0	588.13	660.10	484.15	145.27	49.804	14.363	31.850	0	0	0	0
13-14	0	0	0	0	0	0	0	0	0	0	0	0	0	0	507.02	560.26	335.59	142.38	15.300	0	0	0	0	0
14-15	0	0	0	0	0	0	0	0	0	0	0	0	0	0	23.106	565.80	839.26	530.13	131.53	0	7.8063	0	0	0
15-16	0	0	0	0	0	0	0	0	0	0	0	0	0	0	0	0	524.43	1177.9	477.82	185.01	16.393	0	0	0
16-17	0	0	0	0	0	0	0	0	0	0	0	0	0	0	0	0	9.3676	1052.6	1163.8	517.71	180.32	18.423	0	0
17-18	0	0	0	0	0	0	0	0	0	0	0	0	0	0	0	0	0	14.754	953.39	1056.9	255.19	67.915	39.344	0
18-19	0	0	0	0	0	0	0	0	0	0	0	0	0	0	0	0	0	0	61.202	853.54	546.21	288.52	91.803	0
19-20	0	0	0	0	0	0	0	0	0	0	0	0	0	0	0	0	0	0	0	16.549	527.55	478.21	275.25	16.393
20-21	0	0	0	0	0	0	0	0	0	0	0	0	0	0	0	0	0	0	0	0	21.779	285.32	357.68	174.47
21-22	135.36	0	0	0	0	0	0	0	0	0	0	0	0	0	0	0	0	0	0	0	0	8.1967	244.49	187.89
22-23	96.486	70.881	0	0	0	0	0	0	0	0	0	0	0	0	0	0	0	0	0	0	0	0	8.9773	172.44
23-24	155.34	58.547	28.337	0	0	0	0	0	0	0	0	0	0	0	0	0	0	0	0	0	0	0	0	16.705

Table A. 5-11: Number of medium journeys defined by the start and end times (in 1,000)

End Time (hour of a day)

Start time (hour of a day)	0-1	1-2	2-3	3-4	4-5	5-6	6-7	7-8	8-9	9-10	10-11	11-12	12-13	13-14	14-15	15-16	16-17	17-18	18-19	19-20	20-21	21-22	22-23	23-24
0-1	19.603	26.710	0	0	0	0	0	0	0	0	0	0	0	0	0	0	0	0	0	0	0	0	0	0
1-2	0	12.729	6.4367	0	0	0	0	0	0	0	0	0	0	0	0	0	0	0	0	0	0	0	0	0
2-3	0	0	7.1437	6.1531	0	0	0	0	0	0	0	0	0	0	0	0	0	0	0	0	0	0	0	0
3-4	0	0	0	11.296	11.656	0	0	0	0	0	0	0	0	0	0	0	0	0	0	0	0	0	0	0
4-5	0	0	0	0	12.347	37.058	0	0	0	0	0	0	0	0	0	0	0	0	0	0	0	0	0	0
5-6	0	0	0	0	0	62.318	157.77	4.3056	0	0	0	0	0	0	0	0	0	0	0	0	0	0	0	0
6-7	0	0	0	0	0	0	142.45	418.17	40.050	3.7600	2.4286	0	0.7216	0.7216	1.0824	0	0	0	0	0	0	0	0	0
7-8	0	0	0	0	0	0	0	459.14	1029.6	61.365	1.9351	0.8743	2.1129	1.2386	0	1.2073	0	0	0	0	0	0	0	0
8-9	0	0	0	0	0	0	0	0	427.39	654.70	29.607	1.4051	0	0.7077	0.7077	0	0	1.7399	0	0	0	0	0	0
9-10	0	0	0	0	0	0	0	0	0	231.49	499.08	23.983	5.4531	0	0	3.4538	0.9784	0	0	0	0	0	0	0
10-11	0	0	0	0	0	0	0	0	0	0	300.11	492.65	40.280	4.0107	0.6869	2.7573	1.9993	0	0	0	0	0	0	0
11-12	0	0	0	0	0	0	0	0	0	0	0	268.44	530.59	30.934	5.3681	0	0	0	0	0	0	0	0	0
12-13	0	0	0	0	0	0	0	0	0	0	0	0	270.26	503.21	27.818	2.1398	2.3939	0	1.6072	0	0	0	0	0
13-14	0	0	0	0	0	0	0	0	0	0	0	0	0	285.22	547.25	29.456	3.1555	1.4988	1.2698	0	0	0	0	0
14-15	0	0	0	0	0	0	0	0	0	0	0	0	0	0	310.96	527.17	53.374	4.5580	0	0	0	0	0	0
15-16	0	0	0	0	0	0	0	0	0	0	0	0	0	0	0	335.80	675.32	49.518	0.9679	0	0	0	0.8534	0
16-17	0	0	0	0	0	0	0	0	0	0	0	0	0	0	0	0	410.56	1006.9	73.531	3.3688	1.3565	1.3531	0	0
17-18	0	0	0	0	0	0	0	0	0	0	0	0	0	0	0	0	0	537.71	1016.0	65.734	2.6229	1.4303	0	0
18-19	0	0	0	0	0	0	0	0	0	0	0	0	0	0	0	0	0	0	376.76	496.76	23.038	2.2855	0	0
19-20	0	0	0	0	0	0	0	0	0	0	0	0	0	0	0	0	0	0	0	238.23	309.88	10.498	0	0
20-21	0	0	0	0	0	0	0	0	0	0	0	0	0	0	0	0	0	0	0	0	167.39	198.65	8.0752	0
21-22	0	0	0	0	0	0	0	0	0	0	0	0	0	0	0	0	0	0	0	0	0	120.85	155.95	7.1836
22-23	0.9298	0.6175	0	0	0	0	0	0	0	0	0	0	0	0	0	0	0	0	0	0	0	0	118.65	124.69
23-24	82.642	1.8631	0	0	0	0	0	0	0	0	0	0	0	0	0	0	0	0	0	0	0	0	0	78.360

Table A. 5-12: Number of long journeys defined by the start and end times (in 1,000)

End Time (hour of a day)

Start time (hour of a day)	0-1	1-2	2-3	3-4	4-5	5-6	6-7	7-8	8-9	9-10	10-11	11-12	12-13	13-14	14-15	15-16	16-17	17-18	18-19	19-20	20-21	21-22	22-23	23-24
0-1	0.4683	2.9716	0.5724	1.1865	0	0	0	0	0	0	0	0	0	0	0	0	0	0	0	0	0	0	0	0
1-2	0	0.5464	0.9992	0.5880	0	0	0	0	0	0	0	0	0	0	0	0	0	0	0	0	0	0	0	0
2-3	0	0	0	0.5464	0	4.3091	1.0512	0	0	0	0	0	0	0	0	0	0	0	0	0	0	0	0	0
3-4	0	0	0	0	0.9471	1.0096	0.8222	1.3635	0	0	0	0	0	0	0	0	0	0	0	0	0	0	0	0
4-5	0	0	0	0	0.6245	0.6869	1.7122	1.5664	0	0	0	0	0	0	0	0	0	0	0	0	0	0	0	0
5-6	0	0	0	0	0	0	6.8123	35.087	8.3580	5.6310	2.8311	0	0	0	0	0	0	0	0	0	0	0	0	0
6-7	0	0	0	0	0	0	1.1033	29.586	38.844	26.770	7.1194	1.0824	1.3635	0	0	0	0	0	0	0	0	0	0	0
7-8	0	0	0	0	0	0	0	0.6401	52.968	60.249	21.259	4.8295	0	0	0	0	0	0	0	0	0	0	0	0
8-9	0	0	0	0	0	0	0	0	0.5828	41.389	58.605	27.587	9.8412	2.6645	1.0512	0	0	0.6141	0	0	0	0	0	0
9-10	0	0	0	0	0	0	0	0	0	0.4996	40.676	65.100	30.413	4.7670	1.8631	1.8735	0	1.5612	0	0	0	0	0	0
10-11	0	0	0	0	0	0	0	0	0	0	1.5820	41.753	56.481	39.177	4.1425	4.6630	0.4631	1.3895	0	0	0	0	0	0
11-12	0	0	0	0	0	0	0	0	0	0	0	1.1033	44.371	48.514	26.614	10.158	3.1745	0	0	0.9992	0	0	0	0
12-13	0	0	0	0	0	0	0	0	0	0	0	0	0	39.208	44.007	32.276	9.6851	3.3203	0.9575	2.1233	0	0	0	0
13-14	0	0	0	0	0	0	0	0	0	0	0	0	0	0	33.801	37.350	22.373	9.4925	1.0200	0	0	0	0	0
14-15	0	0	0	0	0	0	0	0	0	0	0	0	0	0	1.5404	37.720	55.950	35.342	8.7691	0	0.5204	0	0	0
15-16	0	0	0	0	0	0	0	0	0	0	0	0	0	0	0	0	34.962	78.532	31.855	12.334	1.0928	0	0	0
16-17	0	0	0	0	0	0	0	0	0	0	0	0	0	0	0	0	0.6245	70.179	77.590	34.514	12.021	1.2282	0	0
17-18	0	0	0	0	0	0	0	0	0	0	0	0	0	0	0	0	0	0.9836	63.559	70.465	17.012	4.5277	2.6229	0
18-19	0	0	0	0	0	0	0	0	0	0	0	0	0	0	0	0	0	0	4.0801	56.903	36.414	19.234	6.1202	0
19-20	0	0	0	0	0	0	0	0	0	0	0	0	0	0	0	0	0	0	0	1.1033	35.170	31.881	18.350	1.0928
20-21	0	0	0	0	0	0	0	0	0	0	0	0	0	0	0	0	0	0	0	0	1.4519	19.021	23.845	11.631
21-22	9.0241	0	0	0	0	0	0	0	0	0	0	0	0	0	0	0	0	0	0	0	0	0.5464	16.299	12.526
22-23	6.4324	4.7254	0	0	0	0	0	0	0	0	0	0	0	0	0	0	0	0	0	0	0	0	0.5984	11.496
23-24	10.356	3.9031	1.8891	0	0	0	0	0	0	0	0	0	0	0	0	0	0	0	0	0	0	0	0	1.1137

Table A. 5-13: An example of data ready for optimization

Journey type		Journey 1		Journey 2		No. of veh.	E1	E2
Journey 1	Journey 2	Start time	End time	Start time	End time		[kWh]	[kWh]
1	1	0	1	1	2	64.93	87.881	88.456
1	1	0	1	1	3	20.01	27.082	27.473
1	1	0	1	2	3	49.83	67.441	68.413
1	1	1	2	0	1	64.70	87.348	87.349
…	…	…	…	…	…	…	…	…
1	2	0	1	1	3	9.71	13.135	29.609
1	2	0	1	2	3	10.77	14.578	32.861
1	2	0	1	2	4	9.28	12.556	28.317
…	…	…	…	…	…	…	…	…
1	3	0	1	1	3	1.51	2.039	22.982
1	3	0	1	2	6	6.5	8.793	97.967
1	3	0	1	2	7	1.58	2.145	23.952
…	…	…	…	…	…	…	…	…
3	3	15	20	22	2	1.41	21.156	21.338
3	3	15	20	22	24	3.43	51.474	51.517
3	3	15	20	23	1	3.09	46.37	46.457
…	…	…	…	…	…	…	…	…

Note that Table A. 5-13 is rather lengthy – it contains 71,302 entries (rows). However, some of the entries have to be removed since they refer to the same combination of journeys. As an example, compare Row 1 and Row 4 in; Row 1 describes a combination of two short journeys of which Journey 1 lasts between hours 0-1 and another Journey 2 between hours 1-2; Row 4 also describes a combination of two short journeys of which one lasts between hours 1-2 and another one between hours 0-1. In fact, it is the same combination of journeys, so one of those two rows has to be removed from the table. After removing all duplicated rows, the number of entries reduces to 44,161.

Table A. 5-14: Maximal flows through the lines

From bus	To bus	Length [km]	Replacement price [£, £/km]×10^3	Line capacity [MW]	Max. Power flow [MW]				
					After 1	After 2	After both	Min. power	Optimal
1	2	25.05	82.1	130	296.2	276.8	231.6	157.0	130.0
1	3	71.96	82.1	130	161.6	144.2	117.4	86.8	78.9
2	4	75.66	82.1	65	89.5	76.0	62.9	48.9	48.5
3	4	16.51	82.1	130	155.2	139.6	115.0	83.9	76.7
2	5	86.38	82.1	130	149.3	152.1	137.8	94.2	101.4
2	6	76.8	82.1	65	122.1	104.3	84.5	64.8	63.8
4	6	18.03	82.1	90	144.4	125.1	105.5	70.8	75.0
5	7	50.53	82.1	70	56.7	45.4	49.3	26.4	43.9
6	7	35.72	82.1	130	86.1	83.5	83.0	54.9	67.4
6	8	18.3	82.1	32	64.2	41.5	29.2	30.5	32.0
6	9	transformer	1018.7	65	63.3	59.3	48.1	36.0	41.2
6	10	transformer	1018.7	32	36.8	34.5	28.0	20.9	24.0
9	11	transformer	1018.7	65	0.0	0.0	0.0	0.0	0.0
9	10	transformer	1018.7	65	63.3	59.3	48.1	36.0	41.2
4	12	transformer	1018.7	65	88.0	87.8	71.3	52.9	55.8
12	13	transformer	1018.7	65	0.0	0.0	0.0	0.0	0.0
12	14	6.97	256.8	32	15.3	15.5	14.1	9.5	12.2
12	15	3.55	256.8	32	35.1	32.5	30.7	21.0	28.6
12	16	5.41	256.8	32	17.5	13.5	11.6	8.1	9.5
14	15	5.44	256.8	16	6.5	4.3	3.8	1.8	4.0
16	17	5.24	256.8	16	12.5	6.1	7.6	3.6	6.0
15	18	5.95	256.8	16	11.9	12.6	11.0	7.0	8.8
18	19	3.52	256.8	16	7.0	5.7	5.2	2.9	5.2
19	20	1.85	256.8	32	19.8	17.2	15.2	9.1	17.3
10	20	5.69	256.8	32	22.3	22.0	17.8	11.8	19.8
10	17	2.3	256.8	32	17.6	20.8	13.9	8.7	12.4
10	21	2.04	256.8	32	43.9	36.0	29.4	19.6	30.9
10	22	4.08	256.8	32	20.0	16.6	13.6	9.3	13.9
21	22	0.64	256.8	32	12.4	12.4	6.9	2.9	10.3
15	23	5.5	256.8	16	15.5	9.8	9.7	5.2	7.4
22	24	4.87	256.8	16	13.6	13.4	10.1	6.4	9.2
23	24	7.35	256.8	16	5.5	3.2	4.2	1.2	3.4
24	25	8.96	256.8	16	8.5	11.3	9.4	4.2	8.5
25	26	10.35	256.8	16	13.2	9.3	8.6	4.5	7.1
25	27	5.68	256.8	16	14.6	17.2	14.3	8.5	10.7
28	27	transformer	1018.7	65	44.6	39.0	34.1	24.9	28.7
27	29	11.31	256.8	16	16.0	15.1	12.9	7.7	11.1
27	30	16.41	256.8	16	17.5	17.5	14.5	8.8	14.3
29	30	12.34	256.8	16	8.7	9.4	7.8	4.6	9.0
8	28	87.12	82.1	32	7.6	7.9	6.7	5.3	6.9
6	28	26.09	82.1	32	44.7	36.7	30.7	19.9	23.0

Number of overloaded elements	14	15	5	1	0

Colour legend:

OHL	Transformer	UG cable

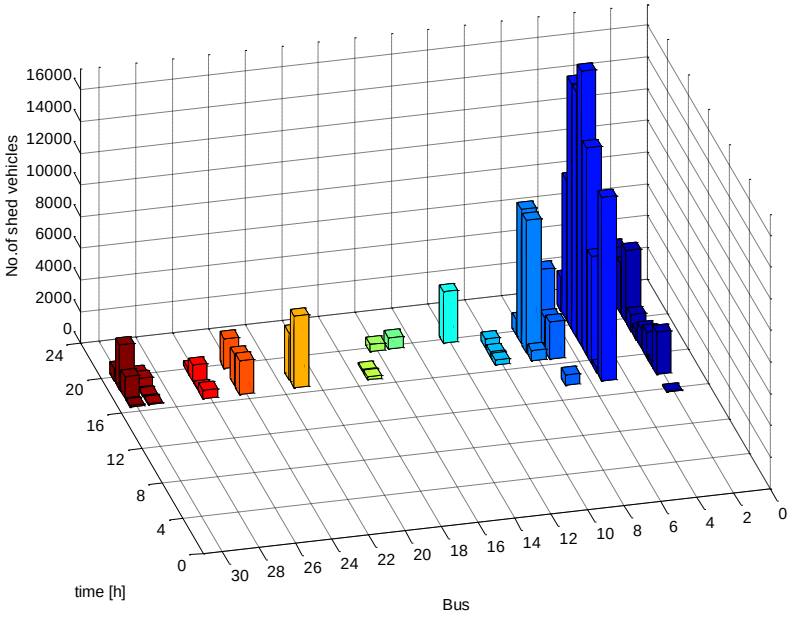


Figure A. 5-1: Estimated number of vehicles that could not be charged for strategy "charging after second journey"